Universidade do Minho
Escola de Engenharia

João Manuel Rainha Costa

Stepwise optimization of curcumin biosynthesis in *Saccharomyces cerevisiae* using synthetic biology approaches

June 2024

Stepwise optimization of curcumin biosynthesis in *Saccharomyces cerevisiae* using synthetic biology approaches
João Manuel Rainha Costa
UMinho | 2024

Universidade do Minho
Escola de Engenharia

João Manuel Rainha Costa

Stepwise optimization of curcumin biosynthesis in *Saccharomyces cerevisiae* using synthetic biology approaches

PhD thesis in Chemical and Biological Engineering

Work developed under supervision of
Professor Lígia Raquel Marona Rodrigues
Professor Joana Lúcia de Lima Correia Rodrigues

June 2024

Copyright and Terms of Use for Third Party Work

This dissertation reports on academic work that can be used by third parties as long as the internationally accepted standards and good practices are respected concerning copyright and related rights.

This work can thereafter be used under the terms established in the license below.

Readers needing authorization conditions not provided for in the indicated licensing should contact the author through the RepositóriUM of the University of Minho.

License granted to users of this work:



CC BY-NC-ND

https://creativecommons.org/licenses/by-nc-nd/4.0/

Acknowledgements

Gostaria de expressar os meus agradecimentos a todos que de alguma forma, direta ou indiretamente, contribuíram para a realização deste trabalho. Em primeiro lugar agradecer às minhas orientadoras: Professora Lígia Rodrigues, por toda a competência e profissionalismo na orientação deste trabalho; Professora Joana Rodrigues pelo permanente acompanhamento, por todos os conselhos, sugestões, revisões e lembretes durante todo o processo. Também gostaria de agradecer à Adelaide Braga pela ajuda nos ensaios em reator e por toda disponibilidade em ajudar e transmitir conhecimento. Agradecer também ao Bruno e ao Óscar pelas otimizações bioinformáticas. Pelas hidrólises em reator pressurizado agradecer ao Laboratório Tecnologias Limpas nomeadamente à Cristina Rocha e à Catarina Teixeira. Pelo apoio nas análises por HPLC gostava de agradecer às técnicas Maura e Raquel. A todos os colegas do LBBS e do grupo BioVal, Daniela, Débora, Márcia, Beatriz, Diana e todos que por cá passaram, por toda a ajuda e companhia. Gostaria de expressar os meus agradecimentos ao Centro de Engenharia Biológica por permitir o desenvolvimento deste trabalho.

Agradeço também à minha família, especialmente aos meus pais, por todo suporte e esforço durante esta jornada. À minha namorada, Alice, que sempre me acompanhou de perto durante todo o meu percurso.

This study was supported by the Portuguese Foundation for Science and Technology (FCT) under the scope of the strategic funding of UIDB/BIO/04469/2020 unit with DOI 10.54499/UIDB/04469/2020. I would also like to acknowledge FCT for funding the individual PhD scholarship SFRH/BD/138325/2018 and consequent extension COVID/BD/153247/2023.





Statement of Integrity

I hereby declare having conducted this academic work with integrity.

I confirm that I have not used plagiarism or any form of undue use of information or falsification of results along the process leading to its elaboration.

I further declare that I have fully acknowledged the Code of Ethical Conduct of the University of Minho.

University of Minho, Braga, 6th July 2024



João Manuel Rainha Costa

Abstract

Stepwise optimization of curcumin biosynthesis in *Saccharomyces cerevisiae* using synthetic biology approaches

Curcumin is the main active compound found in the rhizomes of turmeric (*Curcuma longa*). The reported biological activities of curcumin include anti-inflammatory, antioxidant, and anti-cancer. Hereupon, curcumin has seen a substantial market growth emerging as one of the most studied natural therapeutic products. However, curcumin extraction from turmeric remains challenging. Therefore, the microbial production emerges as a viable solution for curcumin production. The biosynthesis of curcumin starts with the phenylpropanoid pathway where tyrosine/phenylalanine are converted to ferulic acid. Ferulic acid is then activated through condensation with a CoA molecule and diketide-CoA synthase (DCS) and curcumin synthase (CURS), synthesize curcumin from two molecules of activated ferulic acid and one malonyl-CoA molecule. Metabolic engineering of microorganisms to produce curcumin was mainly achieved in *Escherichia coli*. Herein, we intend to synthesize curcumin in a genetic modified *Saccharomyces cerevisiae*. Firstly, the biosynthesis of curcumin from ferulic acid was evaluated in yeast using a plasmid system. The highest curcumin titers were obtained by expressing a feruloyl-CoA synthase (FerA) from *Pseudomonas paucimobilis* and DCS and CURS from *C. longa*. The deletion of ferulic acid decarboxylase improved curcumin production reaching 2.7 mg/L from 30 mg/L of ferulic acid. Next, the artificial pathway composed by FerA, DCS and CURS was integrated into yeast genome using a CRISPR-Cas9. To convert *p*-coumaric acid into curcumin, caffeic acid *O*-methyltransferase from *Arabidopsis thaliana* and 4-hydroxyphenylacetate 3-monooxygenase oxygenase from *Pseudomonas aeruginosa*, along with the reductase component from *Salmonella enterica* were introduced. The pathway was integrated into a *p*-coumaric acid overproducing strain leading to *de novo* curcumin biosynthesis. The enhancement of fluxes through the phenylpropanoid pathway led to the synthesis of 4.2 mg/L of curcumin with methionine supplementation. Bioreactor experiments significantly improved curcumin production relatively to flask experiments. Additionally, extracts from rice residues were used as substrates for curcumin production, surpassing the levels obtained with standard media. The curcumin levels reported in this study are the highest documented thus far in genetically engineered yeast. Overall, this thesis marks progress in advancing the development of an efficient *S. cerevisiae* cell factory for curcumin production.

Keywords: CRISPR-Cas9, Curcumin, Genetic Engineering, *Saccharomyces cerevisiae*, Rice Residues

Resumo

Otimização gradual da biossíntese de curcumina em *Saccharomyces cerevisiae* usando técnicas de biologia sintética

A curcumina é o principal composto ativo encontrado nos rizomas do açafrão (*Curcuma longa*). As atividades biológicas reportadas da curcumina incluem ação anti-inflamatória, antioxidante e anticancerígena. O mercado da curcumina tem aumentando substancialmente sendo atualmente um dos produtos terapêuticos naturais mais estudados. Contudo, a extração natural de curcumina tem limitações associadas. A produção microbiana surge como uma solução viável para a sua produção. A biossíntese da curcumina começa com a via dos fenilpropanóides, onde a tirosina/fenilalanina são convertidas em ácido ferúlico. Este é ativado através da condensação com uma molécula de CoA, e a dicetídeo-CoA sintase (DCS) e a curcumina sintase (CURS) sintetizam curcumina a partir de duas moléculas de ácido ferúlico ativado e uma de malonil-CoA. A modificação genética de microrganismos para produzir curcumina foi principalmente estudada em *Escherichia coli*. Neste trabalho, pretendemos sintetizar curcumina em *Saccharomyces cerevisiae*. Inicialmente, a biossíntese de curcumina em levedura foi avaliada a partir do ácido ferúlico usando um sistema em plasmídeo. As maiores concentrações de curcumina foram obtidas ao expressar a feruloyl-CoA sintase (FerA) de *Pseudomonas paucimobilis* e DCS e CURS de *C. longa*. A deleção da ácido ferúlico descarboxílase melhorou a produção de curcumina, atingindo 2,7 mg/L a partir de 30 mg/L de ácido ferúlico. Em seguida, a via artificial composta por FerA, DCS e CURS foi integrada no genoma de levedura usando CRISPR-Cas9. Para conversão de ácido cumárico em curcumina, foram introduzidas a ácido cafeico *O*-metiltransferase de *Arabidosis thaliana* e a 4-hidroxifenilacetato 3-monooxigenase de *Pseudomonas aeruginosa* juntamente com a componente redutase de *Salmonella enterica*. A via foi integrada numa estirpe produtora de ácido cumárico, alcançando a biossíntese de curcumina a partir de glucose. O aumento dos fluxos na via dos fenilpropanóides levou à produção de 4,2 mg/L de curcumina após suplementação de metionina. Os ensaios em reator aumentaram significativamente a produção de curcumina relativamente aos obtidos em frasco. Além disso, extratos de resíduos da indústria do arroz foram usados como substratos para produção de curcumina, tendo sido obtidos melhores resultados comparativamente com o meio tradicional. Os níveis de curcumina reportados aqui são os mais altos documentados até o momento em levedura geneticamente modificada. No geral, esta tese marca o progresso no desenvolvimento de uma fábrica celular para a produção de curcumina.

Palavras-chave: CRISPR-Cas9, Curcumina, Engenharia genética, *Saccharomyces cerevisiae*, Resíduos de arroz

Contents

CHAPTER 1 . General Introduction 1

1.1 Motivation and Context 2

1.2 Research Aims 3

1.3 Outline 4

CHAPTER 2 . Microbial Production of Curcumin 6

2.1 Curcumin 7

2.1.1 Chemistry 7

2.1.2 Extraction, purification and chemical synthesis 8

2.2 Curcumin Biological Activities 9

2.2.1 Anticancer Properties 9

2.2.2 Antioxidant and Anti-inflammatory Properties 10

2.2.3 Antibacterial, Antifungal, and Antiviral properties 11

2.2.4 Safety and Bioavailability 12

2.3 Curcumin Biosynthesis in *Curcuma longa* 12

2.3.1 The Phenylpropanoid Pathway 13

2.3.2 The Type III Polyketide Synthases Reactions 14

2.4 Curcumin Production in Microorganisms 15

2.4.1 Metabolic Engineering of *E. coli* to Produce Curcuminoids 15

2.4.1.1 Curcuminoid Production from a Fed Precursor in *E. coli* 20

2.4.1.2 *De Novo* Curcuminoid Production in *E. coli* 25

2.4.1.3 *E. coli* Chassis Optimization 28

2.4.2 Metabolic Engineering of Other Organisms to Produce Curcuminoids 31

2.5 Conclusions and Future Perspectives 34

CHAPTER 3 . *Saccharomyces cerevisiae* as Microbial Cell Factory 35

3.1 Genetic Engineering Tools for *Saccharomyces cerevisiae* 36
3.1.1 Homologous Recombination 36
3.1.2 CRISPR-Cas9 37
3.1.2.1 CRISPR-Cas9 Applications in *Saccharomyces cerevisiae* 38
3.1.2.1.1 Gene Knock-in and Gene Knock-out 38
3.1.2.1.2 Multiple Gene Deletion and Point-Mutations 39
3.1.2.1.3 Cell Factory Development 40
3.1.2.1.4 Innovative CRISPR Toolkits 42
3.1.2.2 CRISPR-Cas9: Key Messages 44
3.2 Heterologous Production of Polyphenols in *Saccharomyces cerevisiae* 45
3.2.1 Pathway Enzyme Selection and Engineering 45
3.2.2 Spatial Location of Heterologous Enzymes 50
3.2.3 Strain Optimization 50
3.2.3.1 Amino Acids Overproducing Strains 51
3.2.3.2 Extender and Cofactor Availability 52
3.2.4 Transporter Expression 54
3.3 Final Remarks 55
CHAPTER 4 . Curcumin Biosynthesis from Ferulic Acid by Engineered *Saccharomyces cerevisiae* 56
4.1 Introduction 57
4.2 Materials and Methods 59
4.2.1 Strains, Plasmids, and Genes 59
4.2.2 Plasmids and Strain Construction 60
4.2.3 Curcumin Production and Extraction 62
4.2.4 Curcumin Quantification 63
4.3 Results and Discussion 63

4.3.1 Curcumin Production using 4CL and CUS Enzymes 63
4.3.2 Curcumin Production using Rich Culture Medium 66
4.3.3 Curcumin Production using Type III PKS from *C. longa* 67
4.3.4 Suppressing FDC Activity in *S. cerevisiae* 67
4.3.5 Curcumin Production using Feruloyl-CoA Synthetase (FerA) 68
4.4 Conclusions 69
CHAPTER 5 . *De novo* Curcumin Production in *Saccharomyces cerevisiae* 70
5.1 Introduction 71
5.2 Materials and Methods 73
5.2.1 Genes, Plasmids and Strains 73
5.2.2 Strain Construction 74
5.2.3 Strain Cultivation and Curcumin Extraction 77
5.2.4 Metabolites Analysis 78
5.2.5 Bioinformatic Analysis 78
5.3 Results and Discussion 79
5.3.1 Curcumin Biosynthesis from Supplemented Substrates 79
5.3.2 *De novo* Curcumin Biosynthesis 82
5.3.3 Enhancing *p*-Coumaric Acid Conversion to Caffeic Acid 84
5.3.4 Methylation of Caffeic Acid to Ferulic Acid 87
5.3.5 Precursor Supply Enhancement 89
5.3.6 Increasing Flux through Ferulic Acid Biosynthesis 90
5.4 Conclusions 91
CHAPTER 6 . Operational Optimization of Curcumin Biosynthesis by Engineered Yeast 93
6.1 Introduction 94
6.2 Materials and Methods 95

6.2.1 Strains, Media and Cultivation 95
6.2.2 Experimental Design 96
6.2.3 Bioreactors Experiments 96
6.2.3.1 Inoculum Preparation 96
6.2.3.2 Bioreactor Settings and Operation 96
6.2.3.3 Fed-batch Experiments 97
6.2.4 Rice By-Products Characterization 97
6.2.5 Rice By-Products Hydrolysis 97
6.2.6 Carbon/Nitrogen Ratio 98
6.2.7 Analytical Methods 98
6.3 Results and Discussion 98
6.3.1 Optimization Culture Conditions using Experimental Design 98
6.3.2 Curcumin Production in Bioreactors using Genetic Modified Yeast 100
6.3.3 Bioreactor Fermentation of Strain JQ4 102
6.3.4 Enhancement of Curcumin Production using Ethanol Fed 104
6.3.5 Curcumin Production Using Residues 107
6.3.5.1 Characterization of Raw Materials 107
6.3.5.2 Acidic Hydrolysis of Residues 108
6.3.5.3 Hydrothermal Treatment in Pressurised Bioreactor 109
6.4 Conclusions 111
CHAPTER 7 . Conclusions and Perspectives 113
CHAPTER 8 . References 120
Appendix 148

List of Abbreviations

%DO: Dissolved oxygen percentage
4CL: 4-Coumarate-CoA ligase
5-FOA: 5-Fluoroorotic acid
ACC: Acetyl-CoA carboxylase
ACH: Acetyl-CoA hydrolase
ACS: Acetyl-CoA synthase
adhE: Aldehyde-alcohol dehydrogenase
AraE: Arabinose-H^+ transport protein
AroG: Phospho-2-dehydro-3-deoxyheptonate aldolase
ATP: Adenosine triphosphate
Bcl-2: B-cell lymphoma 2
BPCY: Biomass-product coupled yield
C/N: Carbon/Nitrogen ratio
C3'H: *p*-Coumaroyl shikimate-3′-hydroxylase
C3H: 4-Coumarate 3-hydroxylase
C3H3: *p*-Coumaroyl ester 3-hydroxylase
C4H: Cinnamate-4-hydroxylase
CAN1: Canavanine resistance
CCoAOMT: Caffeoyl-CoA *O*-methyltransferase
CHI: Chalcone isomerase
CHS: Chalcone synthase
CM: Chorismate mutase
CoA: Coenzyme A
COMT: Caffeic acid *O*-methyltransferase
COX-2: Cyclooxygenase-2
CPR: Cytochrome P450 reductase
CRISPR: Clustered regularly interspaced short palindromic repeats
CRISPR-Cas9: CRISPR associated Cas9
CRISPRi: CRISPR interference
crRNA: CRISPR RNA
CSE: Caffeoyl-shikimate esterase
CST: *p*-Coumaroyl shikimate transferase
CurA: Curcumin reductase
CURS: Curcumin synthase
CUS: Curcuminoid synthase
CYB5: Cytochrome b5
DAHPS: 3-Deoxy-D-arabino-heptulosonate-7-phosphate synthase
DCS: Diketide-CoA synthase
DNS: 3,5-Dinitrosalicylic acid
DSB: Double strand break
Ech: Enoyl-CoA hydratase
EtOH: Ethanol
F3H: Flavanone 3- hydroxylase
faaA: Palmitoyl-CoA ligase

FabD: S-Malonyltransferase (carrier protein)
FabF: 3-Oxoacyl synthase (carrier protein)
$FADH_2$: Flavin adenine dinucleotide
Fcs: Feruloyl/*p*-coumaroyl-CoA synthetase
FDA: Food and Drug Administration
FDC: Ferulic acid decarboxylase
FerA: Feruloyl-CoA synthetase
FOX1: Fatty-acyl coenzyme A oxidase
FVA: Flux variability analysis
GEM: Genetic engineered microorganisms
GRAS: Generally regarded as safe
gRNA: Guide RNA
HCT: Shikimate hydroxycinnamoyl transferase
HMF: Hydroxymethylfurfural
HpaB: 4-hydroxyphenylacetate 3-monooxygenase oxygenase component
HpaC: 4-hydroxyphenylacetate 3-monooxygenase reductase component
HPLC: High performance liquid chromatography
HR: Homologous recombination
ILV: Threonine deaminase
IPTG: Isopropil ß-D-1 thiogalactopyranoside
JEFCA: Joint FAO/WHO Expert Committee on Food Additives
KanMX: Kanamycin A resistance
LB: Lysogeny Broth
MAGE: Multiplex automatic genome engineering
MatB: Malonate synthetase
MatC: Malonate carrier protein
MET13: Methylenetetrahydrofolate reductase
Mgs: Monoglucosyldiacylglycerol synthase
MOMA: Minimization of metabolic adjustment
NADH: Nicotinamide adenine dinucleotide
NF- κ B: Nuclear factor kappa B
NHEJ: Non-homologous end joining
OD_{600nm}: Optical density at 600 nm
ORF: Open reading frame
PAD: Phenylacrylic acid decarboxylase
PAL: Phenylalanine ammonia lyase
PAM: Protospacer-adjacent motif
PCR: Polymerase chain reaction
PDC: Phenylpyruvate decarboxylase
PDH: Prephenate dehydrogenase
Pex10p: Peroxisome biogenesis factor
pFBA: Flux Balance Analysis
PheA: Prephenate dehydratase
PKS: Polyketide synthase
poxB: Pyruvate oxidase
RB: Rice bran
RBS: Ribosome binding site

RH: Rice husk
ROOM: Regulatory on/off minimization
ROS: Reactive oxygen species
SAH: *S*-adenosylhomocysteine
SAM: S-adenosylmethionine
SARS-Cov-2: Severe acute respiratory syndrome coronavirus 2
SCAP: SREBP cleavage-activating protein
scRNA: Scaffold RNA
SD: Synthetic defined
snfA: Serine protein kinase
SREBP: Sterol regulatory element-binding protein
srpB: Solvent resistance membrane pump
STAT3: Signal transducer and activator of transcription 3
STS: Stilbene synthase
TAL: Tyrosine ammonia lyase
TALEN: Transcription activator-like effector nucleases
TAT1: Tyrosine and tryptophan amino acid transporter
TB: Terrific broth
TCA: Tricarboxylic acid
TIR: Translation initiation rates
TN: Total nitrogen
TNF-α: Tumor necrosis factor alpha
TOC: Total organic carbon
tracrRNA: Auxiliary trans-activating crRNA
TSC13: Enoyl reductase
TyrA: Chorismate mutase-prephenate dehydrogenase
TyrR: Tyrosine repressor
UHPLC: Ultra high performance liquid chromatography
URA3: Orotidine-5'-phosphate decarboxylase
WYIELD: Weighted yield
YE: Yeast extract
YNB: Yeast nitrogen base
YPD: Yeast peptone dextrose
ZFN: Zinc finger nucleases

List of Figures

Figure 2.1: Structures of curcumin, bisdemethoxycurcumin, and demethoxycurcumin. 8

Figure 2.2: Curcuminoid biosynthetic pathway in *Curcuma longa*. 4CL: 4-coumarate-CoA ligase; C3H: 4-coumarate 3-hydroxylase; C4H: cinnamate-4-hydroxylase; COMT: caffeic acid *O*-methyltransferase; CURS: curcumin synthase; DCS: diketide-CoA synthase; PAL: phenylalanine ammonia lyase; TAL: tyrosine ammonia lyase. 13

Figure 3.1: The mechanism of action of clustered, regularly interspaced, short palindromic repeats–associated Cas9 (CRISPR-Cas9). The guide RNA (gRNA) molecule directs Cas9 protein to the target DNA and Cas9 cleaves genomic DNA 3–4 bp upstream of the PAM (protospacer-adjacent motif) site. 38

Figure 3.2: Strategies used to integrate DNA fragments using double-strand breaks (DSB) originated by clustered, regularly interspaced, short palindromic repeats–associated Cas9 (CRISPR-Cas9). The knock-out can be performed by providing a homologous repair fragment for gene integration (**a**) or knock-in (**b**). (**c**) Combination of *in vivo* recombination and fragment integration using a created DSB. The homologous repair fragment can be *in vivo* assembled using *Saccharomyces cerevisiae* machinery by providing the fragments with homologous ends. The assembled fragment is used to homology repair the DSB..... 40

Figure 3.3: Clustered, regularly interspaced, short palindromic repeats–associated Cas9 (CRISPR-Cas9) associated with delta (δ) integration. CRISPR-Cas9 system creates a double-strand break (DSB) at the repetitive δ sequences present in the *S. cerevisiae* genome allowing the multi-copy integration of a DNA fragment containing a gene or even a pathway..... 42

Figure 3.4: Pathways involved in the aromatic amino acids biosynthesis. CM: chorismate mutase; CS: chorismate synthase; DAHP: 3-deoxy-D-arabino-heptulosonate-7-phosphate; DAHPS: 3-deoxy-D-arabino-heptulosonate-7-phosphate synthase; DHQ: 3-dehydroquinate dehydratase; DHQS: 3-dehydroquinate synthase; E4P: D erythrose-4-phosphate; EPSPS: 5-enolpyruvylshikimate 3-phosphate synthase; HPP-AT: 4 hydroxyphenylpyruvate aminotransferase; PDC: phenylpyruvate decarboxylase; PDH: prephenate dehydrogenase; PDT: prephenate dehydratase; PEP: Phosphoenolpyruvic acid; PPY-AT: phenylpyruvate aminotransferase; SDH: shikimate dehydrogenase; SK: shikimate kinase. 53

Figure 4.1: Curcumin biosynthetic pathway. The names of enzymes are abbreviated as follows: 4CL: 4-coumarate-CoA ligase; FerA: feruloyl-CoA synthetase; DCS: diketide-CoA synthase; CURS: curcuminoid synthase; CUS: curcumin synthase. 58

Figure 4.2: Curcumin production in *Saccharomyces cerevisiae* after 72 h of growth. (**A**) Strain B4C (with 4-coumarate-CoA ligase (4CL) and curcumin synthase (CUS) genes) in shake flasks containing SD-URA with glucose. The precursor ferulic acid was added 24 h upon inoculation at a concentration of: 16 mg L−1 (0.08 mM) (Left flask); and 194 mg L−1 (1 mM) (Right flask). The yellow colour in the right flask indicates the presence of curcumin; (**B**) Curcumin was extracted with methanol from *S. cerevisiae* B4C cells. After extraction the solution turned yellow; (**C**) HPLC analysis of curcumin produced by the recombinant strain B4C. Upper chromatogram represents the curcumin standard. Note: The other peaks visualized in the standard correspond to other curcuminoids also present in the mixture (demethoxycurcumin and bisdemethoxycurcumin). Lower chromatogram represents one extract that contains curcumin produced by the recombinant S. cerevisiae B4C 65

Figure 4.3: *Saccharomyces cerevisiae* strain B4DC fermentation flasks. Left flask: No ferulic acid was added to the culture media; Right flask: 16 mg/L of ferulic acid were added to the media at 24 h of fermentation; the yellow colour formation in the culture media indicate the presence of curcumin. 67

Figure 5.1: Schematic representation of the artificial biosynthetic pathway constructed for de novo curcumin biosynthesis in *Saccharomyces cerevisiae*. Blue arrows indicate that the strain is overproducing aromatic amino acids. Enzymes names: PAL: Phenylalanine ammonia lyase; TAL: Tyrosine ammonia lyase; C4H: Trans-cinnamate 4-monooxygenase; HpaB/C: 4-hydroxyphenylacetate 3-monooxygenase oxygenase and reductase components; COMT: Caffeic acid O-methyl transferase; FerA: feruloyl-CoA synthetase; DCS: Diketide-CoA synthase, CURS1: Curcumin synthase 1..... 79

Figure 5.2: Metabolic profile and curcumin production of strain JG1 cultivated in YPD media with 20 g/L glucose. At 12h, 2% galactose and 30 mg/L ferulic acid were added to the media. Glu: Glucose, Gal: Galactose, EtOH: Ethanol, Fer: Ferulic acid. The presented average values ± standard deviations were derived from three independent biological replicates..... 82

Figure 5.3: **(a)** Curcumin production (yellow bars) and optical density at 600 nm (OD_{600nm}) (grey bars) obtained after 72 h fermentation by JQ1 strain in rich (RM) and minimal (MM) media. The presented average values ± standard deviations were derived from three independent biological replicates. (**b**) HPLC analysis of the curcuminoid standard (blue spectrum) and curcuminoid extract from JQ1 (purple spectrum). Identification of peaks stand for A: bisdemethoxycurcumin, B: demethoxycurcumin, C: curcumin. 83

Figure 5.4: Caffeic acid and *p*-coumaric production by strains JQCA1, JQCA2 and JQCA3 cultivated in rich media with 20 g/L glucose after 72 h of fermentation. The presented average values ± standard

deviations were derived from three independent biological replicates. *p*Cou: *p*-Coumaric acid, Caf: Caffeic acid. 85

Figure 5.5: (**a**) Metabolic profile and optical density at 600 nm (OD_{600nm}) of the strain JQ2 in rich media with 20 g/L glucose and (**b**) production of phenylpropanoids during fermentation. The presented average values ± standard deviations were derived from three independent biological replicates. *p*Cou: *p*-Coumaric acid, Caf: Caffeic acid and Fer: Ferulic acid..... 86

Figure 5.6: Strain JQ3 growth in solid minimal media (on the left) and biomass pellet after fermentation in rich media (on the right), exhibiting yellow biomass due to curcumin production. 87

Figure 5.7: *De novo* curcumin production and phenylpropanoid accumulation in JQ1, JQ2, JQ3, JQ4 *Saccharomyces cerevisiae* strains in rich media with 20 g/L of glucose after 72 h of fermentation. SeHpaC: 4-hydroxyphenylacetate 3-monooxygenase reductase component from *Salmonella enterica*; *At*COMT: Caffeic acid *O*-methyl transferase from Arabidopsis thaliana; *Pp*FerA: feruloyl-CoA synthetase from *Pseudomonas paucimobilis*; CIDCS: diketide-CoA synthase, CICURS1: curcumin synthase 1 from Curcuma longa; *Pa*HpaB: 4-hydroxyphenylacetate 3-monooxygenase oxygenase component; *Pa*HpaB (opt): *Pa*HpaB codon-optimized; pCou: *p*-coumaric acid; Caf: Caffeic acid; Fer: Ferulic acid. The presented average values ± standard deviations were derived from three independent biological replicates..... 88

Figure 5.8: Curcumin produced by strain JQ3 expressing plasmids harbouring different genes. ACC1: Acetyl-CoA carboxylase; FOX1: Fatty-acyl coenzyme A oxidase; MET13: methylenetetrahydrofolate reductase. The presented average values ± standard deviations were derived from three independent biological replicates. 90

Figure 6.1: (**a,c**) Metabolic profile and optical densities at 600 nm (OD_{600nm}) of JQ2 strain in rich media with 20 g/L glucose and (**b,d**) production of phenylpropanoids and curcumin during fermentation in batch 2-L bioreactor with pH control (**a,b**) by automatic fed of 2 M of NaOH and (**c,d**) with no pH control. The presented average values ± standard deviations were derived from two independent biological replicates. Cur: Curcumin; Cou: *p*-Coumaric acid; Caf: Caffeic acid; and Fer: Ferulic acid... 101

Figure 6.2: (**a**) Metabolic profile and optical density at 600 nm (OD_{600nm}) of JQ2 strain in rich media with 20 g/L glucose, (**b**) production of curcumin (**c**) and production of phenylpropanoids during fermentation in fed-batch bioreactor (feed: 250 g/L of glucose, 10 g/L yeast extract at a flowrate of 5 mL/h). The presented average values ± standard deviations were derived from two independent biological replicates. Cou: *p*-Coumaric acid; Caf: Caffeic acid; and Fer: Ferulic acid. 102

Figure 6.3: (**a**) Metabolic profile and optical density at 600 nm (OD_{600nm}) of the strain JQ4 in rich media with 20 g/L glucose and (**b**) production of phenylpropanoids and curcumin during fermentation in batch 2-L bioreactor. The presented average values ± standard deviations were derived from two independent biological replicates. Cur: Curcumin; Cou: *p*-Coumaric acid; Caf: Caffeic acid; and Fer: Ferulic acid...103

Figure 6.4: (**a,c**) Metabolic profiles and optical densities at 600 nm (OD_{600nm}) of JQ4 strain in rich media with 20 g/L glucose and (**b,d**) production of phenylpropanoids and curcumin during fermentation in 2-L bioreactor experiment with an ethanol pulse of 1 g/L (at 24 h and 48 h) (**a,b**) and in fed-batch experiment (**c,d**) by automatic fed of 4.3 g/L ethanol and 10 g/L of yeast extract at a flowrate of 4 mL/h - feed was initiated at 27 h of fermentation. The presented average values ± standard deviations were derived from two independent biological replicates. Cur: Curcumin; Cou: *p*-Coumaric acid; Caf: Caffeic acid; and Fer: Ferulic acid. 105

Figure 6.5: Dissolved oxygen levels (%DO) during a batch bioreactor experiment with JQ4 strain growing in YPD media with 20 g/L of glucose with an oxygen flowrate of 15 L/h. 107

List of Tables

Table 2.1: Identity and kinetic parameters of curcumin synthase (CURS) 1, 2 and 3 from *Curcuma longa.*.....14

Table 2.2: Production of curcumin in microorganisms. The host organism, substrate precursor, genes expressed, strategies applied, fermentation conditions, and titers obtained are presented.....16

Table 3.1: Developed toolkits for genetic engineering *S. cerevisiae* based on Clustered, regularly interspaced, short palindromic repeats–associated Cas9 (CRISPR-Cas9). dCas9: Cas9 defective in DNA cleavage; gRNA: guide RNA; nCas9: nicking Cas9. 43

Table 3.2: Production of hydroxycinnamic acids and polyphenols in *Saccharomyces cerevisiae*. Genes, genetic systems, chassis, chassis modifications, substrates, conditions and titers obtained. 47

Table 4.1: *Saccharomyces cerevisiae* strains used in this work. 59

Table 4.2: Plasmids used in this work. 60

Table 4.3: Primer pairs used to PCR-amplify DNA parts and for colony PCR (forward and reverse primers – FW and RV). Underlined sequence indicates the restriction site. Bold sequence indicates the synthetic terminator 27. 62

Table 4.4: Curcumin production by the different *Saccharomyces cerevisiae* strains harbouring the curcumin biosynthetic pathway. Ferulic acid (16 mg/L) was added to the culture medium at 24 h of fermentation. Colonies 1 to 5 were picked from the transformation plate. Connected lines represent cultures that exhibit statistically significant different curcumin production values (* student t-test, $p<0.05$). SD: synthetic defined media; YPD: yeast extract peptone dextrose media; 4CL: 4-coumarate-CoA ligase; FerA: feruloyl-CoA synthetase; DCS: diketide-CoA synthase; CURS: curcuminoid synthase; CUS: curcumin synthase..... 64

Table 4.5: Cell densities of the different *Saccharomyces cerevisiae* strains during the fermentations. The values represent the media of different transformants with the respective standard deviation. SD: Synthetic Defined media; YPD: Yeast Peptone Dextrose media; FA: Ferulic Acid; DCW: Dry Cell Weight. 66

Table 5.1: *Saccharomyces cerevisiae* strains used in this study.....74

Table 5.2: Primers used in this work. For gene amplification primers, the bold sequence represents the restriction enzyme sequence used to clone the gene, and the underlined sequence represents the

homology sequence for cloning via assembly cloning. For cassette amplification primers, the underlined sequence represents the 25-bp homology sequence for the corresponding homology arms. 75
Table 5.3: Plasmids used in this work. 77
Table 5.4: Curcumin production by different *Saccharomyces cerevisiae* strains after 72 h. Cur: curcumin, DMC: demethoxycurcumin, *Pp*FerA: feruloyl-CoA synthetase from *Pseudomonas paucimobillis*; *Cl*DCS: diketide-CoA synthase from *Curcuma longa*, *Cl*CURS1: curcumin synthase 1 from *C. longa*, *At*COMT: caffeic acid *O*-methyl transferase from *Arabidopsis thaliana*; *Pa*HpaB: 4-hydroxyphenylacetate 3-monooxygenase oxygenase subunit B from *Pseudomonas aeruginosa*, *Se*HpaC: 4-hydroxyphenylacetate 3-monooxygenase reductase subunit C from *Salmonella enterica*. The presented average values ± standard deviations were derived from three independent biological replicates. 80
Table 5.5: Phenylpropanoids produced during fermentation by engineered *Saccharomyces cerevisiae* strains for *de novo* curcumin production. The presented average values ± standard deviations were derived from three independent biological replicates. 84
Table 6.1: Strains used in this work..... 95
Table 6.2: Set of experiments conducted based on the experimental design framework and respective responses..... 99
Table 6.3: Phenylpropanoids and curcumin production by JQ3 strain in YPD media without and with ethanol (EtOH) supplementation (1 g/L of EtOH added at 24 h and 48 h) in 250 mL flasks. The presented average values ± standard deviations were derived from three independent biological replicates. Cur: Curcumin; Cou: *p*-Coumaric acid; Caf: Caffeic acid; and Fer: Ferulic acid. 104
Table 6.4: Chemical characterization of rice husk and rice bran raw materials. 108
Table 6.5: Chemical characterization of rice husk and rice bran extracts obtained after acidic hydrolysis. HMF: Hydroxymethylfurfural. 109
Table 6.6: Chemical characterization of rice husk and rice bran extracts obtained after hydrolysis in pressurized reactor followed by enzymatic digestion. HMF: Hydroxymethylfurfural. 110
Table 6.7: Curcumin production and intermediates accumulation after fermentation of JQ4 strain using extracts obtained by hydrolysis in pressurised reactor followed by enzymatic digestion without/with supplementation of 10 g/L of yeast extract. RH: rice husk; RB: rice bran; YE: yeast extract. The presented average values ± standard deviations were derived from three independent biological replicates..... 110

Scientific Output

Papers published in peer-reviewed journals

Rainha, J., Gomes, D., Rodrigues, L. R., Rodrigues, J. L. (2020). Synthetic biology approaches to engineer *Saccharomyces cerevisiae* towards the industrial production of valuable polyphenolic compounds. *Life*, *10*(5), 56.

Rainha, J., Rodrigues, J. L., Rodrigues, L. R. (2021). CRISPR-Cas9: A powerful tool to efficiently engineer *Saccharomyces cerevisiae*. *Life*, *11*(1), 13.

Rainha, J., Rodrigues, J. L., Faria, C., Rodrigues, L. R. (2022). Curcumin biosynthesis from ferulic acid by engineered *Saccharomyces cerevisiae*. *Biotechnology Journal*, *17*(3), 2100400.

Rainha, J., Rodrigues, J. L., Rodrigues, L. R. (2024). *De novo* biosynthesis of curcumin in *Saccharomyces cerevisiae. ACS Synthetic Biology.*

Papers in preparation for submission to peer reviewed journals

Rainha, J., Rodrigues, J. L., Rodrigues, L. R. Enhanced curcumin production in engineered yeast through operational optimization.

Book chapters

Gomes, D., **Rainha, J.**, Rodrigues, L. R., Rodrigues, J. L. (2022). Yeast synthetic biology approaches for the production of valuable polyphenolic compounds. In: Harzevili, F.D. (eds) *Synthetic biology of yeasts: Tools and applications* (pp. 119-156). Cham: Springer International Publishing.

Rainha, J., Rodrigues, L. R., Rodrigues, J. L. (2022). Microbial Production of Curcumin. In: Jafari, S.M., Harzevili, F.D. (eds) *Microbial Production of Food Bioactive Compounds* (pp. 1-35). Cham: Springer International Publishing.

Conference oral flash presentations

Rainha, J., Rodrigues, J. L., Rodrigues, L. R. "Exploring *Saccharomyces cerevisiae* as a curcumin producer". *Biotechnology to Build a Brighter Future: Food, Health and Environmental Applications.* 2021. March 10th, Online.

Rainha, J., Rodrigues, J. L., Rodrigues, L. R. "Rice industry wastes as substrate for curcumin production in engineered *Saccharomyces cerevisiae". Biotechnology for a circular Bioeconomy*. 2023. March 28-29th, Online.

Conference posters

Rainha, J., Gomes, D., Rodrigues, J. L., Rodrigues, L. R. "CRISPR-Cas9 based strategy to engineer *Saccharomyces cerevisiae* towards the production of curcumin from ferulic acid''. *Microbiotec'19*, 2019, December 5-7th. Coimbra, Portugal.

Rainha, J., Rodrigues, J. L., Rodrigues, L. R. ''Engineering *Saccharomyces cerevisiae* towards the production of curcumin''. *5th Applied Synthetic Biology in Europe*, 2020, November 2-4th. Online.

Rainha, J., Rodrigues, J. L., Rodrigues, L. R. "Towards the development of a *Saccharomyces cerevisiae* cell factory to produce the polyphenol curcumin''. *The 15th International Congress on Yeasts (ICY) and the 30th International Conference on Yeast Genetics and Molecular Biology (ICYGMB30),* 2021, August 23-27th, Online.

Rainha, J., Rodrigues, J. L., Rodrigues, L. R. "Metabolic engineering of curcumin production in *Saccharomyces cerevisiae*''. *The 2nd International BioDesign Research Conference*, 2021, December, 6-17th, Online.

Rainha, J., Rodrigues, J. L., Rodrigues, L. R. ''*De novo* curcumin biosynthesis by an engineered *Saccharomyces cerevisiae*''. *6th Applied Synthetic Biology in Europe*, 2022, November 2-4th, Edinburgh, Scotland.

Rainha, J., Rodrigues, J. L., Rodrigues, L. R. ''Engineered *Saccharomyces cerevisiae* for *de novo* biosynthesis of curcumin''. *ICYGMB31 - 31st International Conference on Yeast Genetics and Molecular Biology*. 2023, August 20-25th, Florence, Italy.

CHAPTER 1. General Introduction

ABSTRACT: In recent times, natural products derived from plants have received significant attention due to their diverse therapeutic properties and potential applications in various industries. Among these, curcumin, a polyphenolic compound found in turmeric, emerges as one of the most promising. Its known anti-inflammatory, antioxidant, and anticarcinogenic properties suggest considerable potential for application in the pharmaceutical industry. While curcumin pharmacological benefits are well-known, the traditional methods of extraction from turmeric are often limited by low yields and environmental concerns associated with agricultural practices. The development of microbial cell factories offers several advantages to produce compounds that are difficult to obtain naturally. *Saccharomyces cerevisiae*, as a well-established microbial host, has numerous advantages for the bio-based synthesis of valuable compounds. Hereupon, this thesis focuses on constructing a genetically engineered *S. cerevisiae* to be used as a microbial cell factory to produce curcumin from cheaper substrates.

1.1 Motivation and Context

In the last decades, the use genetic engineered microorganisms (GEM) emerged as a promising strategy for the synthesis of difficult or expensive to obtain natural compounds [1]. The main examples are the production of human insulin initially extracted from living animals [2] and the production of the anti-malarial drug artemisinin, an active compound of the plant *Artemisia annua* [3]. Besides pharmaceuticals, other compounds such as food ingredients are produced using GEMs, including vitamins (nearly 100% of the commercial riboflavin is produced from GEM [4]), colourants, sweeteners (such stevia extracts), nutritional proteins and enzymes used in food industry (e.g., lactases, amylases) [5]. Moreover, biofuels such as bioethanol have been produced by GEMs [6]. Hereupon, the use of GEMs, acknowledged for its eco-friendly attributes, animal welfare considerations, and cost-effectiveness, stands out as a sustainable and profitable method of production.

Numerous studies have established that curcumin holds the potential to be utilized as a therapeutic agent [7]. Currently, curcumin is extracted from turmeric rhizomes. However, conventional agricultural methods fall short in meeting the escalating demand for this compound. Furthermore, agricultural practices are linked with extensive land and resource utilization, substantial waste generation, climate dependency, slow growth, and inconsistent product yields. This has led to an exploration of alternative curcumin production platforms. In fact, curcumin can be chemically synthesized but the process requires the use of harsh chemicals and is very complex [8]. The use of GEMs as "cell factories" to produce curcumin appears as an ideal solution since it may allow its production in a more reliable, affordable, and eco-friendly way. Hereupon, the motivation of this thesis includes the following points:

1. **Biotechnological Innovation:** Curcumin has already been produced in engineered *Escherichia coli* but no reports were available at the beginning of this project addressing the heterologous production of curcumin using a genetically modified *S. cerevisiae*. The exploration of different host organisms adds depth to our understanding of the metabolic pathways involved in curcumin synthesis and opens new possibilities to enhance curcumin yields. *S. cerevisiae* is a model microorganism for biotechnological applications, with several molecular biology tools available to facilitate the development of yeast cell factories for industrial purposes. In addition, this microorganism has been extensively explored to produce other polyphenols. This work provides a solid foundation for future research in the area and

diversifies the platforms available to produce curcumin. Moreover, it contributes to the advancement of knowledge in the field of synthetic biology and metabolic engineering.

2. **Global Health Improvement:** Curcumin is known for its diverse therapeutic properties. The development of a yeast cell factory may facilitate its incorporation into pharmaceutical formulations. Extraction of curcumin from natural sources often yields impure products. Using yeast cell factories may enable the production of high-purity curcumin formulations. Moreover, *S. cerevisiae,* unlike *E. coli,* is considered safe for human consumption [9]. The use of yeast as a production host ensures biocompatibility and safety, meeting regulatory standards for health-related products. Additionally, it can be incorporated into novel drug delivery systems, enhancing the bioavailability and therapeutic efficacy of curcumin, or even to produce yeast fermented foods enriched with curcumin.
3. **Economic Impact:** The successful development of a bioprocess using a genetically modified yeast to produce curcumin has the potential to revolutionize the curcumin market. The economic feasibility of curcumin as a commercially viable product can be significantly enhanced, benefitting industries involved in pharmaceuticals, biomedical applications, or cosmetics.
4. **Sustainability and Circular Economy:** By engineering yeast strains to efficiently synthesize curcumin, this research contributes to the development of a sustainable and resource-efficient alternative to traditional curcumin extraction methods. In addition, by specifically engineering hosts to utilize industrial wastes or by-products as culture media, the work aims to close the loop on resource utilization. This approach not only addresses the environmental impact associated with waste generation, but also transforms waste materials into valuable resources, thereby contributing to the development of a circular economy within the context of curcumin production.

1.2 Research Aims

This thesis sought to genetically engineer *S. cerevisiae* with the overarching goal of facilitating the production of the polyphenol curcumin. The specific objectives of this research involved the stepwise development of an engineered strain capable of synthesizing curcumin from simpler and more cost-effective substrates. These objectives included:

1. Designing, constructing, and optimizing various enzymatic steps involved in the biosynthesis of curcumin in *S. cerevisiae*;
2. Establishing an engineered *S. cerevisiae* strain capable of *de novo* biosynthesis of curcumin;
3. Optimizing the engineered strain at both genetic and operational levels, including scalability considerations;
4. Investigating the use of industrial wastes as culture media for curcumin biosynthesis using the engineered yeast.

1.3 Outline

This dissertation comprises eight chapters that address the abovementioned objectives. The current section (**Chapter 1**) provides an overview of the context, motivation, and research aims, along with a delineation of the thesis structure.

Chapter 2 concerns a literature review with a general overview of curcumin biological properties, applications, and extraction methods. The curcumin biosynthetic pathway is presented and the heterologous production of curcuminoids was subsequently reviewed and discussed.

Chapter 3 focuses on the literature review related to the application of synthetic biology methodologies to produce polyphenolic compounds in genetically engineered *S. cerevisiae*. This chapter also includes a review on the use of clustered regularly interspaced short palindromic repeats (CRISPR) technologies for precise engineering of *S. cerevisiae*.

The Experimental Results are presented in Chapter 4 to Chapter 6. In each chapter, a brief introduction, materials and methods, results, discussion, and conclusions are provided.

In **Chapter 4** the results concerning curcumin production from ferulic acid in *S. cerevisiae* are reported. Genes from different sources were expressed in plasmids and different pathways constructed. The influence of an endogenous yeast gene responsible for ferulic acid degradation was also evaluated.

De novo curcumin production in *S. cerevisiae* is described in **Chapter 5**. At first, the pathway previously defined was integrated into *S. cerevisiae* genome using CRISPR-Cas9 technology. Subsequently, the synthesis of curcumin was evaluated from the upstream phenylpropanoids (caffeic acid and *p*-coumaric acid) by introducing the respective enzymatic steps. This defined pathway was integrated into a *p*-coumaric acid overproducing strain and *de novo* curcumin biosynthesis evaluated. To

enhance curcumin production levels, optimizations at genetic level were evaluated. Also, an *in silico* analysis was conducted to identify potential gene targets that could improve curcumin production.

Chapter 6 outlines the optimization efforts aimed at enhancing curcumin production at an operational level. Initially, the fermentation conditions were optimized and the scale-up of the process studied in batch and fed-batch operation modes. Secondly, rice industry residues were selected to use as culture media for curcumin production. The fermentable sugars were obtained using appropriate extraction methods. After characterization, the curcumin production using rice industry extracts was evaluated.

Final conclusions and future perspectives for further research are described in **Chapter 7**.

Finally, **Chapter 8** gathers all the key references used in this work.

CHAPTER 2. Microbial Production of Curcumin

ABSTRACT: The polyphenol curcumin produced in turmeric rhizomes has been extensively explored as a natural therapeutic agent. Several studies have demonstrated curcumin biological activities including its promising anticarcinogenic activity. New methodologies for curcumin production have been explored in the last decades. The development of microbial cell factories through genetic engineering of microorganisms is a common alternative for high-level production of scarce natural compounds. The scope of this chapter is to give an overview of the current developments regarding the microbial production of curcumin. Firstly, the curcumin chemistry, value, and extraction will be reviewed followed by its biological activities, relevance, and safety. Subsequently, the curcumin biosynthetic pathway in the plant will be elucidated. Finally, the studies regarding curcumin microbial production will be explored offering a complete description of the works available on the field.

The information presented in this chapter was partially published as a book chapter:

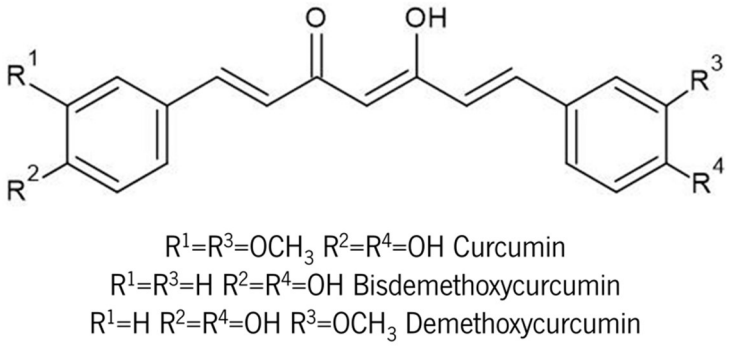
Rainha, J., Rodrigues, L. R., & Rodrigues, J. L. (2022). Microbial Production of Curcumin. In: Jafari, S.M., Harzevili, F.D. (eds) *Microbial Production of Food Bioactive Compounds* (pp. 1-35). Cham: Springer International Publishing.

2.1 Curcumin

Curcuminoids are polyphenolic compounds found in turmeric (*Curcuma longa*) rhizomes and represent the main active compounds of the plant, approximately 3% of its total chemical composition [10]. Since antiquity, rhizomes of this perennial herb have been used in culinary as spice and as natural yellow colouring agent for textiles and cosmetics. In addition, the curcuminoid-rich rhizome extract has been used in Asian traditional medicine, for example, for wound healing or in the treatment of respiratory or digestive disorders [11]. Moreover, it is known as a powerful antioxidant being also used as a preservative [11]. There are three major types of curcuminoids found in *C. longa* rhizomes: curcumin (±77%), demethoxycurcumin (±17%), and bisdemethoxycurcumin (±3%) [12]. The term curcumin is commonly used to designate a turmeric extract containing a curcuminoid mixture.

2.1.1 Chemistry

Curcuminoids consist in two phenolic groups connected by two α, β-unsaturated carbonyl groups, and these compounds are chemically classified as diarylheptanoids (**Figure 2.1**). The chemical structures of the three curcuminoids differ in the number of methoxy groups at ortho-positions of the phenol rings [8]. Curcumin has two methoxy groups while demethoxycurcumin has one and bisdemethoxycurcumin none. The molecular formula of the main curcuminoid, curcumin, is $C_{21}H_{20}O_6$, and it has a molecular weight of 368.37 g/mol. Crystallized curcumin [IUPAC name (1E, 6E)-1,7-bis-(4-hydroxy-3-methoxy-phenyl)-1,6-heptadien-3,5-dione; CAS number: 458-37-7] is an orange-yellow crystalline powder water insoluble. Curcumin solubility increases with pH; however, it quickly degrades in alkaline solution. Curcumin is soluble in organic solvents such as methanol, ethanol, or acetone and has two tautomeric forms, -keto and -enol [8]. The enol tautomer is exclusively observed in alkaline conditions, while the keto form is predominant both at acid and neutral pH values. Curcumin has three labile protons (at neutral pH), one enolic and the others phenolic corresponding to pKa1, pKa2, and pKa3 values of 7.8, 8.5, and 9.0, respectively [8]. Additionally, curcumin holds an excellent metal chelating capacity due to its central unsaturated diketone portion [8].



$R^1=R^3=OCH_3$ $R^2=R^4=OH$ Curcumin
$R^1=R^3=H$ $R^2=R^4=OH$ Bisdemethoxycurcumin
$R^1=H$ $R^2=R^4=OH$ $R^3=OCH_3$ Demethoxycurcumin

Figure 2.1: Structures of curcumin, bisdemethoxycurcumin, and demethoxycurcumin.

Curcumin was first isolated in 1815, but it was only after more than a hundred years that the first study of its effects against human disease was published (in 1937). Later, in 1949, its antibacterial activity was reported [13]. In the last decades, several studies have reported and confirmed curcumin biological activities. Curcumin has over 23,000 citations in PUBMED and over 320 clinical trials ongoing or closed (clinicaltrials.gov). Hereupon, curcumin appears as one of the most studied natural therapeutic products. The reported effects for human health include anti-inflammatory, antioxidant, anti-cancer, wound healing properties, antiviral, among others [11]. In addition, other reports showed that curcumin can attenuate debilitating effects of conventional therapeutics due to its hemoprotective, chemosensitive, radioprotective and radiosensitive properties [14]. Due to all these potential therapeutic effects, curcumin market size reached 85.77 million dollars in 2023 and is expected to reach 205.48 million dollars in 2032 (Fortune Business Insights, Market Research Report 2023 [15]). Currently, there are several curcumin formulations available in the market: Theracurcumin® (Integrative Therapeutics) [16], a highly bioavailable form of curcumin produced by surface-controlled colloidal dispersion; Meriva® (Thorne Research) [17], curcumin encapsulated with hydrophilic carriers; or C3 complex® (Sabinsa Corporation) [18], that combines curcumin with bioperine. All these formulations contain a mixture of the three curcuminoids extracted from the plants and increase their bioavailability that is usually very low as described in the following sections.

2.1.2 Extraction, purification and chemical synthesis

The curcuminoid content of *C. longa* rhizomes is variable depending on factors such as the geographical origin, the soil condition, or the weather [19]. Conventional curcumin extraction from plants and purification involves a solvent extraction followed by purification with column chromatography [8]. The organic solvents employed include methanol, ethyl acetate, ethanol, hexane, or acetone [8].

However, curcuminoids are susceptible to degradation via heat or light and their extraction must rely on methods that can be easily controlled [20]. Recently, more innovative methods have been employed for curcuminoid extraction. For example, carbon dioxide as supercritical antisolvent [21], microextraction based on eutectic solvents [22], microwave-assisted extraction [23] and supramolecular solvent-based extraction [24]. Some reports also concluded that the use of an enzyme-assisted pre-treatment of turmeric before the extraction increased the curcumin yields [25]. However, this strategy makes the process not profitable due to the high costs associated with purified enzymes. Pure curcumin can also be obtained from a curcuminoid mixture through column chromatography. The mixture is usually adsorbed in a silica gel using mixtures of solvents, for instance dichloromethane/acetic acid or methanol/chloroform, and three fractions containing the individual curcuminoids are obtained [26, 27]. However, the extraction of curcumin from turmeric rhizomes exhibits several drawbacks. First, the curcumin production is limited by the plant seasonality. Secondly, the geographical location can affect the curcuminoid content of the rhizome extracts, as previously stated [19]. In addition, plant crops require a lot of resources to be maintained. Moreover, as secondary metabolite, curcumin accumulates in low amounts making its extraction and purification difficult and expensive [8]. Overall, the production of curcumin by means of farming is unprofitable and consequently not appealing.

Pure curcumin can also be obtained by chemical synthesis. The synthesis method involves several steps and reagents and starts with acetylacetone and boron trioxide (B_2O_3) [28]. Chemical synthesis could be an alternative to overcome the limitations related to plant extraction, but it relies on the use of harsh and expensive chemicals, extreme conditions, and it is easily contaminated by undesired by-products [8]. To reduce the associated costs, the replacement of B_2O_3 by the less costly borontrifluoride has been proposed [29]. However, the large-scale chemical synthesis of curcumin remains a challenge due to its complexity [30]. Consequently, more simple, efficient, and environmentally friendly methods are necessary.

2.2 Curcumin Biological Activities

2.2.1 Anticancer Properties

The anticancer activity is one of the most reported biological effects of curcumin. The anticancer effects of this compound are diverse, targeting various levels of regulation during the various stages of carcinogenesis from DNA mutation to the metastasis and apoptosis [31]. The extensive elucidation of curcumin anticarcinogenic effects has already led to studies aiming to synthetically modify the

functional groups of the curcumin molecule (aromatic side chains, di-keto moiety, methylene site and carbon linker chain) to find structural analogues with relatively stronger pharmacological efficacy for cancer treatment [32].

The mechanism of action is still a matter of study since curcumin targets are diverse. A vast number of works showed that curcumin can effectively modulate several molecular targets in various cancer-associated signalling cascades and pathways [33]. The anti-cancer effects include the downregulation of transcription factors of proliferative pathways such as the nuclear factor kappa B (NF-κB) (highly activated in carcinogenic cells). The NF-κB inactivation downregulates the expression of carcinogenic-related genes including cyclin D1, cyclooxygenase-2 (COX-2), and B-cell lymphoma 2 (Bcl-2) [34–37]. Curcumin also showed to inhibit signal transducer and activator of transcription 3 (STAT3) phosphorylation that regulates the expression of several genes involved in cell proliferation and migration [38]. Moreover, curcumin decreases the expression levels of the downstream effectors in signalling pathways such as Wnt/β-catenin at the mRNA level [39]. Curcumin can modulate multiple pathways that eventually may lead to apoptosis induction [40, 41] through the suppression of p53 pathway [42]. Curcumin has also been reported as a potential hypomethylation agent preventing the DNA methylation and thus tumour formation [43].

2.2.2 Antioxidant and Anti-inflammatory Properties

Curcumin chemically possesses antioxidant properties due to its two Michael acceptors and two phenolic hydroxyl groups [8]. Hereupon, curcumin is a potent direct antioxidant being capable of scavenging hazardous oxidants rapidly. Furthermore, curcumin may also induce cytoprotective enzymes to ensure long-term physiological protection against the oxidative stress acting as an indirect antioxidant [44]. This compound showed capacity to increase the levels of some oxide protective enzymes, for instance, heme oxygenase-1, superoxide dismutase, or glutathione peroxidase [45].

The inflammation process is associated with several human illnesses including neurodegenerative diseases, such as Alzheimer's, Parkinson's, or multiple sclerosis, cardiovascular diseases, respiratory diseases (asthma and bronchitis), or arthritis, among others [46]. The inflammatory response is strictly correlated with oxidative stress since inflamed cells liberate reactive oxygen species (ROS) leading to oxidative stress [47]. On the other hand, ROS can activate intracellular signalling cascades that increase the expression of pro-inflammatory genes [48]. The principal mediator of inflammation is the tumour necrosis factor α (TNF-α) [49]. Curcumin can inhibit the production of TNF-α, as well as the

production of other inflammatory cytokines, such as interleukin family [50]. In addition, curcumin is capable of downregulating COX-2, lipoxygenase, and nitric oxide synthase, all enzymes involved in inflammatory response [51]. The downregulation of these enzymes is accomplished via suppression of the NF-κB activation [11].

2.2.3 Antibacterial, Antifungal, and Antiviral properties

The curcumin antibacterial activity has already been demonstrated against several pathogenic bacteria [52]. The mechanism of action involves blocking prokaryotic cell division [53]. Nowadays, due to the emergence of multi-resistant bacteria, there is intensive research focused on the discovery of novel antibacterial agents. The antimicrobial effect of curcumin has already been studied in combination with antibiotics such as ampicillin, oxacillin and norfloxacin [54, 55]. The administrated cocktails led to a synergistic effect with increased antibacterial activity. The development of curcumin cocktails may be very advantageous because it may result in a wider spectrum of activity and reduce side effects compared to the administration of conventional antibiotics.

Curcumin also demonstrated antifungal properties through the reduction of ergosterol synthesis and consequent ergosterol precursor accumulation which leads to cell death via generation of ROS [56]. The appearance of multi-resistant *Candida* species has become a problem mainly in hospital environment. Curcumin was found to be a potent fungicide against several *Candida* species [57]. Moreover, the synergistic effect with existing fungicides also resulted in a relative significant increase of antifungal activity [58].

Nowadays and more than ever, finding new effective antiviral compounds has become a main concern. The existing antiviral therapies are not always well-tolerated or quite effective and have high associated costs [52]. Numerous studies demonstrated a wide variety of antiviral effects attributed to curcumin. This phytochemical can act at several stages of viral infection from preventing viral entry, viral attachment, replication, protein expression, or acting as a viricide [59]. Curcumin showed antiviral properties against several types of viruses including RNA virus (e.g., human immunodeficiency viruses, Zika virus, Dengue, Influenza A, Norovirus, viral haemorrhagic septicaemia virus) and DNA virus (e.g., Herpes virus and Human Adenovirus) [60]. In addition, reports demonstrated curcumin antiviral activity against the novel SARS-Cov-2 virus by blocking direct viral infection [61].

2.2.4 Safety and Bioavailability

As a food ingredient, curcumin is recognized as "generally safe" by the Food and Drug Administration (FDA) [62] with an adequate daily intake value recommended of up to 3 mg per kg of body weight by Joint FAO-WHO Expert Committee Report on Food Additives (JEFCA) [63] and European Food Safety Authority (EFSA) (European Food Safety Authority). Other investigations reported that this compound is safe for humans up to 12 g/day without any side effects [64].

Although curcumin presents a wide range of therapeutic applications, its bioavailability is low due to its lack of water solubility, a relatively low absorption in intestine, rapid metabolism in liver, and fast elimination through the gallbladder if administered orally [65]. It is only significantly detected in plasma or in tissues after administration of high oral doses [66]. A study performed with healthy individuals revealed that curcumin is converted into glucuronide and sulphate conjugates and excreted without being properly absorbed [67]. For instance, the ingestion of 12 g of curcumin resulted in only 29.7 ng/mL detected in blood after 1 h of ingestion. This value is far below the effective concentrations reported in the *in vitro* studies [64].

To overcome the poor bioavailability, several synthetic curcumin derivatives have been developed. It was demonstrated that the glycosylation of the aromatic ring improves curcumin solubility and thus its kinetic stability leading to a better therapeutic response [68]. The curcumin kinetic stability can be enhanced by masking the 4-OH groups attached to the phenyl rings, thus avoiding conjugation reactions in the human body [69]. Other strategies employed include curcumin formulations with oils, polymers, or with natural products such as bioperine [31]. In addition, to increase the targeting and bioavailability of curcumin, different types of delivery systems have been developed based on nanoformulations including polymeric nanoparticles, liposomes, nanogels, peptide formulations, and cyclodextrin complexes [20].

2.3 Curcumin Biosynthesis in *Curcuma longa*

Curcuminoids are secondary metabolites produced by *C. longa*. The biosynthesis of these compounds starts with the phenylpropanoid pathway which channels the carbon fluxes from primary metabolism (amino acid metabolism) to different branches of the secondary metabolism including the synthesis of curcuminoids [70]. Curcuminoids consist of two phenylpropanoid units derived from phenylalanine

connected by a central carbon derived from malonyl-CoA [71]. Curcuminoid synthesis reactions are catalysed by an enzyme cluster called type III polyketide synthases (PKS) [72].

2.3.1 The Phenylpropanoid Pathway

The enzyme phenylalanine ammonia lyase (PAL) is the first enzyme of this pathway and catalyses the deamination of phenylalanine to form cinnamic acid (**Figure 2.2**). Cinnamic acid is then hydroxylated into *p*-coumaric acid by cinnamate-4-hydroxylase (C4H). At this point, there are two different ways for *p*-coumaric acid metabolization. First, it may be converted in other phenylpropanoid analogues namely ferulic acid by 4-coumarate 3-hydroxylase (C3H) and caffeic acid *O*-methyltransferase (COMT) having caffeic acid as intermediate, or it can be activated by condensation with coenzyme A (CoA) to form the corresponding hydroxycinnamoyl-CoA thioester [70]. This last reaction is catalysed by 4-coumarate-CoA ligase (4CL). 4CL can act in multiple substrates, also activating the *p*-coumaric acid analogues (ferulic or caffeic acids) [73]. Activated *p*-coumaric acid, *p*-coumaroyl-CoA, can as well be converted to the other activated analogues, caffeoyl-CoA and then feruloyl-CoA by a set of enzymes which include *p*-coumaroyl shikimate transferase (CST) and caffeoyl-CoA *O*-methyltransferase (CCoAOMT) [72].

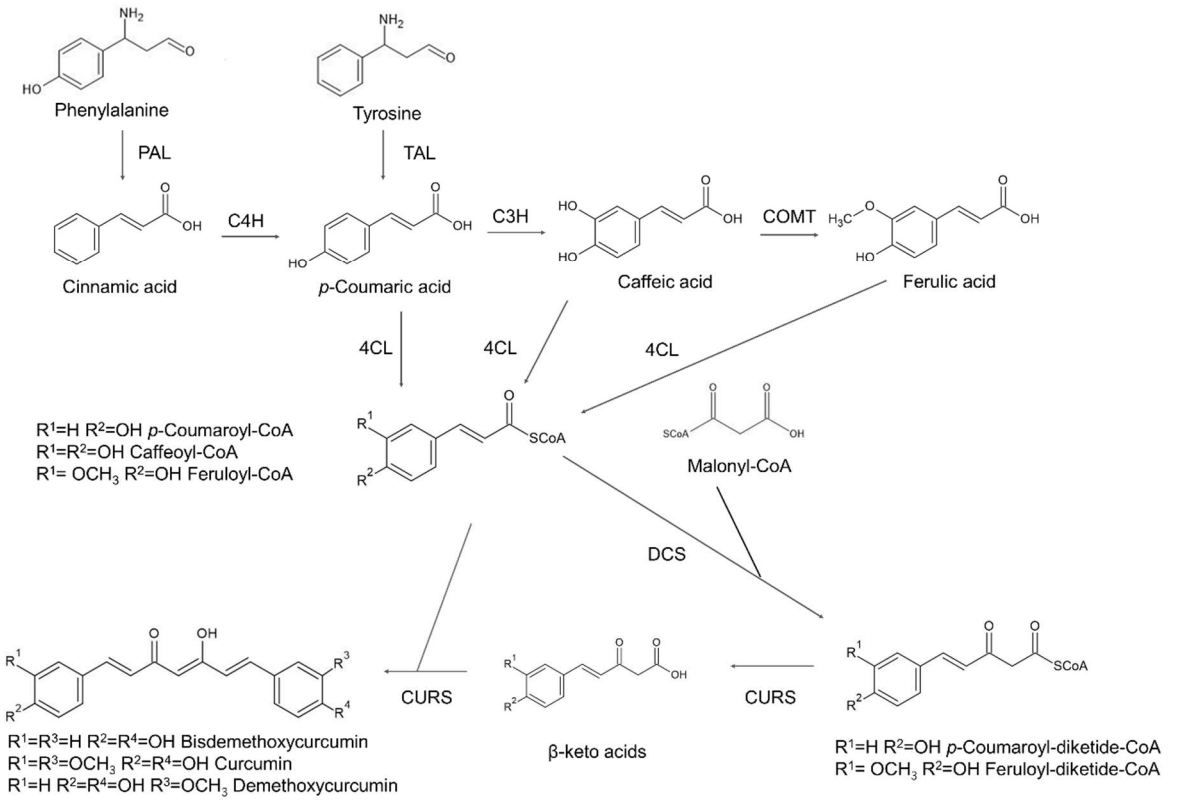


Figure 2.2: Curcuminoid biosynthetic pathway in *Curcuma longa*. 4CL: 4-coumarate-CoA ligase; C3H: 4-coumarate 3-hydroxylase; C4H: cinnamate-4-hydroxylase; COMT: caffeic acid *O*-methyltransferase; CURS: curcumin synthase; DCS: diketide-CoA synthase; PAL: phenylalanine ammonia lyase; TAL: tyrosine ammonia lyase.

2.3.2 The Type III Polyketide Synthases Reactions

The biosynthesis of curcuminoids is accomplished by the action of two type III PKS. The type of curcuminoid synthesized depends on the activated phenylpropanoids used as substrates. For instance, to synthesize curcumin, diketide-CoA synthase (DCS) (EC number: 2.3.1.218) catalyses the formation of feruloyl-diketide-CoA from feruloyl-CoA and malonyl-CoA. Afterwards, curcumin synthase (CURS) catalyses the hydrolysis of feruloyl-diketide-CoA to a β-keto acid and condensates it with another molecule of feruloyl-CoA forming curcumin. On the other hand, a combination of two *p*-coumaroyl-CoA molecules originates bisdemethoxycurcumin, and the combination of *p*-coumaroyl-CoA with feruloyl-CoA originates demethoxycurcumin [71]. Three different isoforms of curcumin synthase have been identified in *C. longa*, CURS1, 2, and 3. These enzymes have different substrate specificities (**Table 2.1**), which could be the reason to explain the distribution of the three curcuminoids in turmeric [74]. CURS1 prefers feruloyl-CoA but also uses *p*-coumaroyl-CoA with low efficiency. CURS2 also uses preferentially feruloyl-CoA while CURS3 uses both substrates almost equally. The substrate specificities of CURS suggest that CURS1 and CURS2 synthesize curcumin preferentially, while CURS3 synthesizes curcumin, demethoxycurcumin, and bisdemethoxycurcumin almost equally [74]. CURSs and DCS share a conserved Cys-His-Asn catalytic triad and more than 60% identity. Bioinformatic analysis revealed that CURS's secondary structure is mainly composed of α-helix and random coils. In addition, it was also predicted that CURSs are phosphorylated as a posttranslational modification. The predicted isoelectric points suggest a moderately acidic nature of the proteins [75].

Table 2.1: Identity and kinetic parameters of curcumin synthase (CURS) 1, 2 and 3 from *Curcuma longa.*

Enzyme	EC number	Substrate	K_{cat}/K_M ($s^{-1}M^{-1}$)	Molecular weight (kDa)	Isoelectric point	References
CURS1	2.3.1.217	Feruloyl-CoA	1001	21.1	4.93	[71, 75]
		p-Coumaroyl-CoA	75			
CURS2	2.3.1.219	Feruloyl-CoA	1622	20.3	5.28	[74, 75]
		p-Coumaroyl-CoA	176			
CURS3	2.3.1.219	Feruloyl-CoA	2017	20.6	4.96	
		p-Coumaroyl-CoA	1742			

2.4 Curcumin Production in Microorganisms

Attributable to its pharmacological potential, curcumin production and purification has been raising the attention of the scientific community. New extraction and purification methodologies have been evaluated aiming to obtain pure curcuminoids or pure curcumin extracts [76, 77]. However, as mentioned before, plant extraction and the chemical synthesis of curcumin is not ideal due to the associated costs and issues regarding the process sustainability. The microbial production appears as the third alternative to produce curcuminoids [70]. Microorganisms can grow in inexpensive substrates and have rapid production cycles surpassing the drawbacks of plant extraction [5]. In addition, the downstream processes are easier to implement in large-scale fermentations comparatively to rhizome extraction since microbes do not produce other compounds with similar structures that make the curcuminoids difficult to isolate. The metabolic engineering of microorganisms to produce curcumin was mainly implemented in *Escherichia coli*, a model host for genetic engineering purposes. However, other studies have reported the production of curcuminoids in less conventional hosts such as the bacteria *Pseudomonas putida*, or the eukaryotic fungi *Aspergillus oryzae* and the yeast *Yarrowia lipolytica* (**Table 2.2**).

2.4.1 Metabolic Engineering of *E. coli* to Produce Curcuminoids

Advances on metabolic engineering have allowed researchers to develop genetically modified microorganisms able to produce plant-derived compounds such as flavonoids, stilbenes, or curcuminoids [70, 93]. *E. coli* is the most notorious biological chassis for this kind of application because it is easy to manipulate and to handle. The biosynthesis of curcumin has been accomplished in this organism from multiple substrates including the phenylpropanoid precursors or the aromatic amino acids. To design an artificial curcumin biosynthetic pathway in *E. coli*, several enzymatic steps are required since *E. coli* naturally lacks the curcuminoid precursors. Moreover, the *de novo* biosynthesis of curcumin in *E. coli* to make the process simpler and more profitable has been reported [88]. The following sections highlight the advances on *E. coli* metabolic engineering to produce curcuminoids starting with the construction of microorganisms able of synthesizing curcumin from fed precursors. Next, the advances on the curcuminoid *de novo* biosynthesis will be reviewed. Finally, the endogenous chassis optimizations performed to improve curcuminoid biosynthesis will be presented.

Table 2.2: Production of curcumin in microorganisms. The host organism, substrate precursor, genes expressed, strategies applied, fermentation conditions, and titers obtained are presented.

Host organism	**Substrate precursor**	**Curcuminoid**	**Genes expressed** [1,2]	**Strategies applied** [3]	**Fermentation conditions** [4]	**Titer (mg/L)**	**Reference**
E. coli BLR (DE3)	*p*-Coumaric acid (1 mM)	Bisdemethoxycurcumin	*Le*4CL *Os*CUS *Cg*ACC	Heterologous genes expression controlled by IPTG inducible promoter. Increase MCoA pool by the expression of *Cg*ACC.	Flask fermentation LB + M9 100 mL 60 h	91	[78]
	Ferulic acid (1 mM)	Curcumin				113	
	Cinnamic acid (1 mM)	Dicinnamoylmethane				84	
E. coli BL21 (DE3)	Phenylalanine (3 mM)	Dicinnamoylmethane	*Tf*PAL1 *At*4CL1 *Os*CUS	Heterologous genes expression controlled by IPTG inducible promoter.	Flask fermentation LB 50 mL 72 h	360	[79]
E. coli K-12	Ferulic acid (2 mM)	Curcumin	*At*4CL1 *Cl*DCS *Cc*CURS1	Heterologous genes expression controlled by IPTG/aTc inducible promoters.	Flask fermentation LB 50 mL 63 h	70	[80]
	Tyrosine (3 mM)	Curcumin	*Rg*TAL *Se*C3H *Ms*CCoAOMT *At*4CL1 *Cl*DCS *Cc*CURS1			0.2	
E. coli BL21 (DE3)	Ferulic acid (2 mM)	Curcumin	*At*4CL1 *Cl*DCS *Cc*CURS1	Heterologous genes expression controlled by IPTG inducible promoter. Selection of the best *E. coli* strain to improve production. Optimization of induction parameters, carbon source and culture media.	Flask fermentation LB + M9 50 mL 63 h	353.4	[81]
					Flask fermentation TB 50 mL 63 h	301.2	

Table 2.2: *Continuation*

Host organism	Substrate precursor	Curcuminoid	Genes expressed [1,2]	Strategies applied [3]	Fermentation conditions [4]	Titer (mg/L)	Reference
E. coli BL21 (DE3)	Ferulic acid (3 mM)	Curcumin	*At*4CL1 *Cl*DCS *Cl*CURS1	Reduction of the number of plasmids	Flask fermentation LB +M9 50 mL 63 h	563	[82]
	Tyrosine (3 mM)	Curcumin	*Rg*TAL *Se*C3H *At*COMT *At*4CL1 *Cl*DCS *Cl*CURS1	Co-culture strategy was applied to reduce metabolic burden Reduction of the number of plasmids used in each module		15.8	
E. coli BL21 Star™ (DE3)	Glucose (10 g/L + 100 g)	Bisdemethoxycurcumin	*Rg*TAL *At*4CL *Os*CUS *Rh*MatB *Rh*MatC	Use of a tyrosine overproducing strain Co-culture strategy to reduce metabolic burden MatB and MatC overexpression to increase MCoA availability	Bioreactor fermentation AMM 3 L 22 h	6.28	[83]
E. coli BL21 (DE3)	Glucose (10 g/L)	Dicinnamoylmethane	*At*PAL *Os*4CL *Os*CUS	Use of tyrosine/phenylalanine overproducing strain	Flask fermentation LB + M9 24 h	6.95	[84]
		Bisdemethoxycurcumin	*Se*TAL *Os*4CL *Os*CUS			4.63	
E. coli BL21 (DE3)	Cinnamic acid (0.1 mM)	Diccinamoylmethane	*Pc*4CL *Os*CUS *Nt*ACC	Use of CRISPRi to silence genes of TCA cycle and fatty acid biosynthesis to increase MCoA availability Increase MCoA pool by the expression of *Nt*ACC	Bioreactor fermentation LB 3 L 48 h	11.6	[85]
E. coli C41(DE3)	Glucose (15 g/L)	Curcumin	*Se*TAL *Se*C3H *At*COMT *Nt*4CL2 *Cl*DCS *Cl*CURS2	Use of a tyrosine overproducing strain Optimization of the expression ratios of curcumin biosynthetic genes by random mutagenesis	Tube fermentation LB 3 mL 45 h	3.8	[86]

Table 2.2: *Continuation*

Host organism	Substrate precursor	Curcuminoid	Genes expressed [1,2]	Strategies applied [3]	Fermentation conditions [4]	Titer (mg/L)	Reference
E. coli BW25113	Ferulic acid (4 mM)	Curcumin	*At*4CL (mutant) *Os*CUS (mutant) *Af*mgs *Ec*ACS	Inactivation of fatty acid biosynthesis genes and ACS overexpression to increase pool of MCoA pool Deletion of the native *curA* to prevent curcumin degradation Use of medium copy plasmids and operon re-arrangement Construction of a mutant CUS by random mutagenesis Expression of *Af*mgs to optimize cell membrane morphology	Flask fermentation YM9 100 mL 48 h Oleic acid was added to media to improve production	537.8	[87]
E. coli C41(DE3)	Glucose (25 g/L) Glycerol (10 g/L)	Curcumin	*Fj*TAL HpaB/C *At*COMT *At*4CL *Cl*DCS *Cl*CURS *Pp*srpB	Use of a tyrosine overproduction strain Deletion of f*adR* and *mcrC* to increase MCoA pool Deletion of the native *curA* to prevent curcumin degradation Expression of *Pp*srpB to reduce ferulic acid toxicity	Flask fermentation LB 25 mL 12 h	137.5	[88]
					Fed-Batch Salt media Feed (600 g/L glycerol)	524.1	
A. oryzae RIB40 RkuptrP2-1	Feruloyl-NAC (Feruloyl-CoA analogue) (1.1 mg)	Curcumin	*Os*CUS *Ao*ACC	Increase MCoA pool by deletion of genes involved in the regulation of ergosterol biosynthesis and overexpression of native ACC	Mutants cultivated in agar plates PD 72 h	404.2 µg/plate	[89]
P. putida KT2440	*p*-Coumaric acid (5 mM)	Bisdemethoxycurcumin	*Os*CUS	*Ech* deletion to increase MCoA pool	Microplate fermentation MOPS 500 µL 48 h	2.15	[90]
Y. lipolytica PO1f	*p*-Coumaric acid (2 mM)	Bisdemethoxycurcumin	*Nt*4CL *Os*CUS *Yl*Pex10p *Yl*ACC	Overexpression of Pex10p and ACC to increase MCoA pool	Flask fermentation YNB 50 mL 168 h	0.17	[91]

Table 2.2: *Continuation*

Host organism	Substrate precursor	Curcuminoid	Genes expressed [1,2]	Strategies applied [3]	Fermentation conditions [4]	Titer (mg/L)	
S. cerevisiae BY4742	Glucose (20 g/L)	Curcumin	*At*PAL *At*4CL1 *At*C4H *Aa*CPR *At*HCT *At*CCoAOMT *At*C3'H *At*CSE *Cl*DCS *Cl*CURS	Replacement of TSC13 gene by *Md*ECR	Flask fermentation YNB 30 mL 72 h	1.5	[92]

[1]: *Aa: Artimisia annua; Ag: Aspergillus oryzae; Al: Acholeplasma laidlawii; At: Arabidopsis thaliana; Cg: Corynebacterium glutamicum; Cl: Curcuma longa; Ec: Escherichia coli; Le: Lithospermum erythrorhizon; Ms: Medicago sativa; Nf: Nocardia farcinica; Nt: Nicotiana tabacum; Os: Oryza sativa; Pc: Petroselinum crispum; Pp: Pseudomonas putida; Rg: Rhodotorula glutinis; Rl: Rhizobium leguminosarum; Se: Saccharothrix espanaensis; Tf: Trifolium pratense; Yl: Yarrowia lipolytica.*

[2]: 4CL: 4-coumarate-CoA ligase; ACC: acetyl-CoA carboxylase; C3'H: *p*-coumaroyl shikimate-3'-hydroxylase; C3H: 4-coumarate 3-hydroxylase; C4H: cinnamate-4-hydroxylase; CCoAOMT: caffeoyl-CoA *O*-methyltransferase; COMT: caffeic acid *O*-methyltransferase; CPR: cytochrome P450 reductase; CSE: caffeoyl-shikimate esterase; CURS: curcumin synthase; CUS: curcuminoid synthase; DCS: diketide-CoA synthase; HCT: shikimate hydroxycinnamoyl transferase; HpaB/C: 4-hydroxyphenylacetate 3-monooxygenase; MatB: malonate synthetase; MatC: malonate carrier protein; mgs: monoglucosyldiacylglycerol synthase; PAL: phenylalanine ammonia lyase; Pex10p: peroxisome biogenesis factor; srpB: solvent resistance membrane pump; TAL: tyrosine ammonia lyase.

[3]: aTc: anhydrotetracycline; *curA:* curcumin reductase gene; CRISPRi: Clustered Regularly Interspaced Short Palindromic Repeats interference*; Ech:* enoyl-CoA hydratase lyase gene; *Md*ECR: enoyl-CoA reductase gene from *Malus domestica;* IPTG: isopropyl β-d-1-thiogalactopyranoside; MCoA: malonyl-CoA TCA: tricarboxylic acid cycle.

[4]: AMM: Andrew's Magic media; LB: Lysogeny Broth; M9: M9 minimal media; MOPS: morpholinepropanesulfonic acid minimal media; PD: Polypeptone-Dextrin media; TB: Optimized terrific broth; YM9: Yeast extract M9 media.

2.4.1.1 Curcuminoid Production from a Fed Precursor in *E. coli*

The first proof-of-concept on the artificial curcuminoid biosynthesis by a microorganism was reported by Katsuyama et al. [78]. To achieve that, a plasmid containing PAL gene from *Rhodotorula rubra* (a multi-substrate enzyme that accepts phenylalanine and tyrosine to produce cinnamic acid and *p*-coumaric acid, respectively) and 4CL gene from *Lithospermum erythrorhizon* was constructed. Another plasmid containing curcuminoid synthase (CUS) gene from *Oryza sativa* (rice) and a third one containing acetyl-CoA carboxylase (ACC) from *Corynebacterium glutamicum* were also constructed. The three plasmids were then transformed into *E. coli* BLR DE3 strain. All the genes were placed under control of strong isopropyl β -D-1-thiogalactopyranoside (IPTG)-inducible T7 promoters that lead to a robust protein expression. ACC was expressed to increase the intracellular pool of the curcuminoid extender substrate malonyl-CoA as this previously proved to be important for the synthesis of other plant polyketides [94]. The enzyme CUS from *O. sativa* (NCBI accession number AK109558) used in this work is also a type III PKS, like DCS and CURS, and was identified by the same research group [95] before the discovery and characterization of DCS and CURS enzymes in *C. longa* [71]. This CUS enzyme is capable of synthesizing curcuminoids from two molecules of activated phenylpropanoids and one extender malonyl-CoA molecule in a single step catalysing the same reactions carried by DCS and CURS in *C. longa*. Contrary to DCS, CUS also accepts cinnamoyl-CoA acid as substrate to produce the curcuminoid dicinnamoylmethane, however it prefers *p*-coumaroyl-CoA over feruloyl-CoA and cinnamoyl-CoA [71, 95]. Morita et al. [96] studied the architecture of CUS active site and concluded that it contains a single downward-expanding active site capable of accommodating two activated *p*-coumaric acid molecules (*p*-coumaroyl-CoA), a malonyl-CoA and a putative H_2O molecule that forms hydrogen bond networks at the active centre. In the following year, Miyazono et al. [97] annotated the CUS crystal structure. It was found that CUS challenges the traditional model of head-to-tail polyketide assembling, catalysing only condensation reactions without performing cyclization. The use of "one-pot" CUS for curcuminoid biosynthesis represents a simpler system than the double enzyme DCS/CURS system since it is only required the expression of one enzyme thus reducing the metabolic charge for the cells. The engineered strain constructed by Katsuyama et al. [78] was grown in the presence of 3 mM of tyrosine or phenylalanine. The production of the correspondent curcuminoid was detected in both assays yielding 53.4 mg/L of bisdemethoxycurcumin (from tyrosine) and 107 mg/L of dicinnamoylmethane (from phenylalanine). When both phenylalanine and tyrosine (3 mM of each) were supplemented to the media, dicinnamoylmethane was produced in higher amounts over bisdemethoxycurcumin, although

CUS prefers *p*-coumaroyl-CoA over cinnamoyl-CoA. The authors hypothesized that these differences may be due to the distinct incorporation rates of tyrosine and phenylalanine or *p*-coumaric and cinnamic acids by the multi-substrate enzymes PAL and 4CL. In addition, despite being reported as cytotoxic agents, the produced curcuminoids did not cause inhibitory effects on cellular growth at the reported concentrations. Next, to improve the curcuminoids titers, the hydroxycinnamic acids were directly supplied to the culture media. For that purpose, the PAL step was removed, and the engineered *E. coli* harboured only the 4CL, CUS, and ACC genes. Precursors were fed to the culture media at a lower concentration of 1 mM. The engineered *E. coli* strain produced 91 mg/L of bisdemethoxycurcumin from *p*-coumaric acid, 84 mg/L of dicinnamoylmethane from cinnamic acid and 113 mg/L of curcumin from ferulic acid. Additionally, 57 mg/L of curcumin were produced from rice bran pitch, a ferulic acid-rich industrial waste resulting from rice bran. In another study using the same pathway (4CL, CUS, and ACC), Katsuyama et al. [98] produced 15 asymmetric curcuminoids, 9 of these unnatural, by adding *p*-coumaric acid analogues to the medium. This was only possible due to the wide range of substrate specificities of the enzymes involved, an interesting feature to the discovery of novel drug candidates.

In the subsequent years, a curcuminoid producing engineered *E. coli* reporter strain was developed for the screening of novel PAL enzyme efficiency [79]. The pathway was composed of different PALs, 4CL1 from *Arabidopsis thaliana*, and CUS from *O. sativa*. Three PALs from *Trifolium pratense* were screened (PAL1, PAL3, and PAL4). The best results were obtained using PAL1. The curcuminoids production reached 360 mg/L dicinnamoylmethane from 3 mM of phenylalanine, 3.4 times more than in Katsuyama's work [78]. In this case, ACC was not overexpressed, demonstrating that the natural endogenous malonyl-CoA concentration was enough to ensure the production of these levels of curcuminoids.

The first report addressing the use of the DCS/CURS system from *C. longa* to heterologously produce curcumin in *E. coli* was published by Rodrigues et al. [80]. At first, Rodrigues et al. constructed two different biosynthetic pathways: (1) composed by 4CL1 from *A. thaliana* and *O. sativa* CUS; and (2) harbouring the same 4CL but in combination with DCS and CURS1 from *C. longa*. CURS1 was selected over the other CURS isoenzymes since it has the highest turnover rate towards feruloyl-CoA. All genes were expressed under the control of T7 promoter. The *E. coli* K-12 strains expressing DCS and CURS1 enzymes produced 28-fold more curcumin (70 mg/L) than the ones expressing CUS (2.5 mg/L) when 2 mM of ferulic acid were fed to the culture media. Therefore, the two-enzyme system pathway (2) was found to be more efficient than the CUS pathway (1) to synthesize curcumin. Interestingly, when *p*-

coumaric acid was supplemented, the amount of bisdemethoxycurcumin was very low compared to curcumin for both pathways. However, *in vitro* experiments reported that *A. thaliana* 4CL1 and CUS exhibit a higher preference for *p*-coumaric acid and *p*-coumaroyl-CoA, respectively [73, 95]. In another assay performed by Rodrigues et al. [80], the two carboxylic acids (*p*-coumaric acid and ferulic acid) were both directly supplemented to the culture media, which resulted in the production of the three curcuminoids bisdemethoxycurcumin, demethoxycurcumin, and curcumin. The curcumin titer was higher, as expected, due to CURS1 preference for feruloyl-CoA. Moreover, in the same study, to produce curcumin from tyrosine, a new pathway was designed that enables the synthesis of caffeic acid as intermediate. The enzymes TAL (conversion of tyrosine to *p*-coumaric acid) from *Rhodotorula glutinis*, C3H (*p*-coumaric acid to caffeic acid) from *Saccharothrix espanaensis* and CCoAOMT (caffeoyl-CoA to feruloyl-CoA) from *Medicago sativa* were expressed together with 4CL1, DCS, and CURS1. The curcumin production was tested using *p*-coumaric acid or tyrosine as precursors. As expected, the production was higher when *p*-coumaric acid was used since the number of intermediates is lower, resulting in a lower loss of product over the pathway reactions. Interestingly, bisdemethoxycurcumin was the curcuminoid produced in higher amounts when *p*-coumaric acid was supplemented to the media besides CURS1 preference for feruloyl-CoA possible due to high accumulation of *p*-coumaroyl-CoA. Using tyrosine as substrate, the *p*-coumaric acid was present in the media in higher concentrations than caffeic acid. Nevertheless, curcumin was produced in higher amounts than bisdemethoxycurcumin. The curcumin yield reached 0.2 mg/L from 3 mM of tyrosine. Although the titer was low, this work by Rodrigues et al. [80] was the first report on the curcumin production from an amino acid.

The use of heat shock promoters to produce curcuminoids was also evaluated by the same research group [99]. These promoters may comprise in the future good alternatives to replace T7 promoters frequently used in the expression of heterologous pathways, such as the one of curcuminoids. The expression using T7 promoters is induced through the supplementation of the chemical inducer IPTG that is potentially toxic and expensive. Although the use of these promoters is feasible at the laboratory scale, at a large scale, their use should be avoided if possible [100]. However, heat shock promoters have the disadvantage of not being as strong as the T7 promoters. Nevertheless, this may not always be a disadvantage as it is important to fine-tune the expression of the enzymes of the heterologous pathway. For example, the use of weaker promoters for the expression of highly efficient enzymes to avoid the accumulation of several intermediary compounds can be beneficial. Bearing this in mind, several *E. coli* heat shock promoters were characterized [101], and *dnaK* promoter was further used in

the construction of curcumin biosynthetic pathway using ferulic acid as substrate. This heat shock promoter was used for DCS and CURS1 expression while 4CL was under the expression of a constitutive *lac* promoter [99]. Heat shock was applied for 5 min at 48 ºC to induce the expression. The curcumin production obtained was very low (0.4 mg/L) and it was verified using the ribosome binding site (RBS) calculator tool (https://salislab.net/ software/) that the translation initiation rates (TIR) where low when compared to the ones related to T7 promoters. Therefore, the RBS calculator tool was used to optimize the RBSs and curcuminoids production increased significantly to 6.3 mg/L. Although the production obtained was very low when compared to the ones obtained using T7 promoters, it was demonstrated that heat shock promoters may be used in specific cases to control the fine-tuning of the pathway [99].

Afterwards, Couto et al. [81] using the pathway containing DCS and CURS1 (and T7 promoters) optimized the fermentation conditions to maximize curcumin production from ferulic acid. The parameters analysed included the *E. coli* host strain, the pathway expression induction time and inducer concentration, the culture media, and the carbon source concentration. The greatest performance was obtained using BL21 strain (a strain known to efficiently convert acetate to acetyl-CoA, the precursor of malonyl-CoA) [102]. Regarding the induction parameters, an induction at an optical density at 600 nm of 0.9 with the supplementation of IPTG at a concentration of 0.1 mM was found to maximize the curcumin production. Overall, the curcumin production increased to 959.3 μM (353.4 mg/L) in 63 h. This production, as others obtained in previous studies, was achieved using a two-step fermentation process involving a first growth phase in lysogeny broth (LB) to increase the heterologous protein production and a curcumin production phase in M9 minimal media. As this two-step production process is laborious and not desirable whenever scale up is considered, other culture media were studied. Optimized terrific broth (TB) demonstrated to be a good option as culture media as it allowed to produce up to 817.7 μM (301.2 mg/L) of curcumin in 63 h. Although the production in TB was lower at 63 h, at 20 h, the production in this medium was significantly higher, which can be advantageous. Overall, the optimization of fermentation conditions in this study [81] resulted in almost five-fold improvement on curcumin production relatively to the previous report from Rodrigues et al. [80] and to a 3.1-fold increase in relation to Katsuyama's study [78].

More recently, the same research group optimized the curcumin production at genetic and fermentative level (Rodrigues et al. 2020) [82]. They started to optimize ferulic acid biosynthesis from tyrosine. Since the researchers [80] had previously shown that the conversions of tyrosine to caffeic acid and ferulic

acid to curcumin were very efficient, it was hypothesized that the combination of 4CL and CCoAOMT was the main bottleneck. In this sense, instead of using CCoAOMT (conversion of caffeoyl-CoA to feruloyl-CoA), this enzyme was replaced by COMT (conversion of caffeic acid to ferulic acid) from *A. thaliana*. First, to test COMT efficiency, an engineered *E. coli* BL21 expressing COMT was evaluated, and it was found to be capable of completely converting 1 mM of caffeic acid into ferulic acid. Next, the expression of TAL, C3H, and COMT, corresponding to the first part of the pathway (module 1), led to the synthesis of ferulic acid. These genes were individually expressed in different plasmid backbones and several plasmid/gene combinations were tested to optimize ferulic acid synthesis. The highest ferulic acid accumulation was achieved by expressing TAL in pRSFDuet-1, C3H in pCDFDuet-1, and COMT in pACYDuet-1. However, accumulation of *p*-coumaric acid was also observed as in other previously constructed pathways. This limitation is related to the low conversion rate of *p*-coumaric acid into caffeic acid because of the C3H low efficiency. Nevertheless, 172.6 mg/L of ferulic acid were synthesized from 3 mM of tyrosine. These researchers also studied the optimization of the second part of the curcumin biosynthesis pathway that corresponds to the conversion of ferulic acid into curcumin. To optimize this second module, the best plasmid backbone for 4CL expression was addressed. It was observed that the combination of pCDFDuet_DCS, pRSFDuet_CURS, and pACYDuet_4CL yielded the highest curcumin titer. The resulting strain could produce 446.7 mg/L of curcumin from 3 mM of supplemented ferulic acid (2 mM in the beginning of the fermentation and 1 mM after 15 h), a 20.9% improvement on productivity. After optimizing both pathway modules separately, the curcuminoid biosynthesis was evaluated from caffeic acid in a strain with COMT, 4CL, DCS, and CURS1 genes, and from tyrosine in a strain harbouring the complete pathway (TAL, C3H, 4CL, DCS, and CURS1) expressed in four plasmids. As expected, when caffeic was supplemented, the curcumin titer (46.6 mg/L) and yield decreased significantly when compared with that obtained when ferulic acid was directly supplemented, since in this case ferulic acid was produced in low amounts. Using tyrosine as substrate, the curcumin production was even lower (0.82 mg/L). Nevertheless, it increased significantly in relation to the pathway that contained CCoAOMT instead of COMT, demonstrating that COMT is a better option. Next, to increase the production efficiency, the high metabolic charge caused by the expression of several plasmids was distributed using a coculture strategy. Two strains, each one carrying a different module for the curcumin synthesis, were constructed. The coculture cultivation of the two strains leads to the production of 5.5 mg/L of curcumin, 6.8 times more than the one achieved with the monoculture system. The authors predicted that the metabolic burden caused by the expression of the complete

pathway reduced the titers and yields in the monoculture system. In order to reduce this metabolic burden, the number of plasmids carrying the heterologous enzymes was reduced in all pathways tested. The reduction of the number of plasmids of the *E. coli* strain harbouring the complete pathway (from TAL to CURS1) to three resulted in the production of 6.1 mg/L of curcumin from 3 mM of tyrosine, 7.5 times higher than the one achieved with four plasmids. Afterwards, the plasmid number of each module was also reduced to optimize production. By reducing the number of plasmids from three to two, it was possible to produce 563.4 mg/L of curcumin from ferulic acid (module 2) which represents a percent yield of 100%. Currently, this value represents the highest curcumin titer produced from ferulic acid by a microorganism. The same strategy was also applied to the first module of the pathway reaching an improvement of 49% (257.3 mg/L) on produced ferulic acid from tyrosine. Then, the optimized modules were then applied to a coculture system which resulted in the production of 15.9 mg/L of curcumin, representing a 6.8-fold improvement relatively to the optimized monoculture. This highest titer was obtained using a coculture ratio of 2:1, where the strain carrying the first module of the pathway was inoculated in a higher concentration. This report represents the highest amount of curcumin obtained from tyrosine in a genetically modified microorganism. During the monoculture and coculture experiments, the other curcuminoids were also produced. The proportion of curcuminoids produced was highly dependent on the coculture ratio evaluated. The highest total curcuminoids titer obtained was 41.5 mg/L and was achieved when the strain carrying the second part of the pathway was inoculated in a higher amount which was not in concordance with what was verified to achieve high concentrations of curcumin. This demonstrated that the increased expression of the first module is more important for the curcumin production as its production is more dependent on the expression of C3H and COMT while the production of, for example, bisdemethoxycurcumin is only dependent on TAL step that is highly efficient and fast. On top of that, during the experiments it was demonstrated that the strain carrying the first part of the module was in a clear disadvantage, because even when it was inoculated in higher amounts, the strain carrying the second module prevailed during the fermentation. Therefore, in the future, coculture engineering can be more explored to favour the production of one specific curcuminoid.

2.4.1.2 *De Novo* Curcuminoid Production in *E. coli*

From an economic point of view, the development of engineered microbes capable of producing natural added-value compounds such as curcuminoids from inexpensive substrates is very advantageous at

industrial level since it makes the process more profitable. Furthermore, the use of organic wastes instead of purified compounds will contribute to a circular process valuing industrial by-products and wastes that until then were worthless. The unique report addressing the use of wastes to produce curcumin was the one already mentioned by Katsuyama et al. [78], which used ferulic acid-rich rice bran pitch as substrate to produce curcumin in a genetically modified *E. coli*. However, the production of curcumin from simple sugars is still a more profitable process than the ones requiring the supplementation of expensive phenylpropanoid acids or the aromatic amino acids directly to the media. To achieve that, the metabolic fluxes of the chassis may be adjusted to improve the native biosynthesis of aromatic amino acids since it is strictly regulated.

The production of curcuminoids from sugars was first reported by Fang et al. [83]. For that purpose, a pathway composed by TAL gene from *R. glutinis* was expressed in a tyrosine overproducing *E. coli* strain (*E. coli* rpoA14) and 4CL1 from *A. thaliana* and CUS from *O. sativa* were expressed in an *E. coli* BL21 wild type strain. To develop the tyrosine-overproducing strain, the genes encoding tyrosine repressor (TyrR) and bifunctional chorismate mutase/prephenate dehydratase (PheA) were deleted to direct the pathway to tyrosine production. Also, feedback-insensitive versions of phospho-2-dehydro-3-deoxyheptonate aldolase ($AroG^{fbr}$) and chorismate mutase-prephenate dehydrogenase ($TyrA^{fbr}$) were overexpressed to eliminate tyrosine and phenylalanine-mediated repression [103]. A coculture strategy was used (ratio 10:1 -*E. coli* BL21: *E. coli* rpoA14) and optimized using both genetically engineered strains. The obtained titer of bisdemethoxycurcumin was 6.28 mg/L in a lab-scale bioreactor starting with 10 g/L of glucose and then supplementing 10 g/h of glucose until 100 g.

Kim et al. [84] described for the first time the *de novo* production of curcuminoids by a single *E. coli* strain. At first, the production of bisdemethoxycurcumin was tested by two different constructs: the first one where *O. sativa* 4CL and CUS expression were controlled by an independent T7 promoter in the same plasmid and the second one where 4CL and CUS were organized in an operon (same promoter). Both constructs were transformed in an *E. coli* BL21 wild type strain along with a plasmid carrying *S. espanaensis* TAL. The operon-type construct resulted in higher bisdemethoxycurcumin production. Next, the same pathway was transformed in a tyrosine overproducing *E. coli* strain (TyrR and PheA deletion mutant). The bisdemethoxycurcumin production increased almost 15 times in this strain relatively to the wild type strain. Afterwards, to maximize the tyrosine pool, AroG and 3-phosphoshikimate 1-carboxyvinyltransferase (AroA) were overexpressed resulting in 6.02 mg/L of bisdemethoxycurcumin which represented a 1.3-fold increment on production. In another experiment, the production of

dicinnamoylmethane was addressed. For that purpose, *A. thaliana* PAL and the 4CL/CUS operon were expressed in an *E. coli* strain with TyrA and TyrR deleted to increase the supply of phenylalanine. The production level reached 6.95 mg/L. Finally, the authors developed an engineered strain for *de novo* bisdemethoxycurcumin and dicinnamoylmethane production co-expressing both TAL and PAL with 4CL/CUS operon in a tyrosine/phenylalanine overproducing strain (ΔTyrR, AroG, TyrA). The resulting strain presented production values of 0.16 mg/L for dicinnamoylmethane, 6.02 mg/L for bisdemethoxycurcumin, and 1.11 mg/l for cinnamoyl *p*-coumaroylmethane (asymmetric curcuminoid synthesized from *p*-coumaroyl-CoA and cinnamoyl-CoA). All the curcuminoids produced were synthesized from 10 g/L of glucose.

As previously mentioned, to develop an *E. coli* strain increasingly adapted to the production of curcumin, several heterologous enzymatic steps are required. The number of reactions increases when simpler substrates are used. Moreover, the endogenous synthesis of the aromatic amino acids is strictly regulated being required to construct tyrosine/phenylalanine overproducing strains, as reported above, to ensure the *de novo* biosynthesis of curcumin in appropriate amounts. As mentioned, for large-scale applications, the use of simpler substrates is advantageous because it makes the process more profitable. The implemented overexpression systems usually rely on the use of T7 promoters to control the pathway expression. This often results in an excessive metabolic burden for the cells. Therefore, strategies to overcome that charge have been explored, namely the use of coculture systems [82, 83]. However, the biosynthetic metabolic flux may be optimal when the enzymes are expressed in a proper ratio than at maximal. Kang et al. [86] applied the multiplex automatic genome engineering (MAGE) tool to optimize the expression ratios of curcumin biosynthetic genes. MAGE was used to randomly modify the 5' untranslated region (5' -UTR) of the genes used in a *de novo* artificial curcumin biosynthetic pathway. The pathway was composed by TAL and C3H from *S. espanaensis*, COMT from *Nicotiana tabacum*, 4CL2 from *A. thaliana*, and DCS and CURS2 from *C. longa*. The pathway was divided into two modules: the first one, for *de novo* ferulic acid production and the second one, for curcumin production from ferulic acid. Each module was integrated in a specific region of *E. coli* genome. The *E. coli* strain used was previously constructed by the same research group for overproduction of tyrosine (ΔTyrR, $TyrA^{fbr}$, $AroG^{fbr}$) [104]. The engineered strain could produce the three main curcuminoids from 15 g/L of glucose, however, in very low amounts (0.01 mg/L of curcumin and 0.03 mg/L of total curcuminoids). The developed strain was the first engineered strain to successfully synthesize curcuminoids by inserting the full biosynthetic pathway into *E. coli* chromosome. Afterwards, the MAGE tool was applied

to this strain to fine-tune the expression of curcumin biosynthetic genes. In total, 25 mutant strains were obtained with an increased curcuminoid production relative to the parent strain, but only 8 of the 25 exhibited more than fourfold increment on curcumin production. The strain with lower expression levels of the enzymes 4CL and DCS resulted in a 38.2-fold improvement in the curcumin titer (3.8 mg/L) and 12.6-fold improvement in the total of curcuminoids (3.9 mg/L). Therefore, the genetic expression fine-tune of curcumin pathway genes may lead to higher titers by reducing the host metabolic charge resultant of the expression of the biosynthetic pathway. This is extremely useful for the design of complex pathways with several reactions involved such as the *de novo* biosynthesis of curcumin.

2.4.1.3 *E. coli* Chassis Optimization

To increase the curcumin productivity on a genetically modified *E. coli*, in addition to the introduction of the heterologous genes, the chassis also needs to be optimized to increase the bioavailability of all the precursors needed. Besides the mentioned construction of aromatic amino acids overproducing strains, other intrinsic modifications should be aforethought such as the increase of the endogenous biosynthesis of malonyl-CoA. Some studies speculated that the endogenous supply of the curcuminoid extender unit malonyl-CoA was limiting the curcuminoid production [70]. Malonyl-CoA is synthesized from acetyl-CoA and is involved in fatty acid production that may compete with the curcumin biosynthesis for the use of malonyl-CoA. Katsuyama et al. [78] suggested that the ACC overexpression may improve curcuminoid synthesis. However, they did not test the curcuminoids production without the ACC expression to support that argument. Other works also speculated that the low availability of this curcuminoid precursor was constraining the production [83]. Fang and coworkers [83] tested four different approaches to enhance malonyl-CoA availability in its curcuminoid producer *E. coli* BL21 expressing 4CL and CUS. The strategies included: (1) the overexpression of the *E. coli* ACC enzyme cluster to directly improve malonyl-CoA biosynthesis via carboxylation of acetyl-CoA; (2) targeted gene deletions in tricarboxylic acid (TCA) cycle to redirect the flux for the synthesis of phosphoenolpyruvate, the precursor of acetyl-CoA; (3) overexpression of malonate synthetase (MatB) and malonate carrier protein (MatC) from *Rhizobium leguminosarum* and supplementation of malonate to directly synthesize malonyl-CoA; and (4) inhibition of fatty acids biosynthesis with cerulenin to prevent malonyl-CoA deviation. However, only strategy (3) was found to drastically improve the production of bisdemethoxycurcumin. The synthesized bisdemethoxycurcumin increased 25-fold (5 mg/L) using strategy (3) and five-fold using strategy (4). These results demonstrated that the enhancement of

malonyl-CoA pool may be important to increase the synthesis of curcuminoids. Nevertheless, Rodrigues et al. [82] concluded that the bioavailability of malonyl-CoA was not limiting production as they obtained a percent yield of 100% and higher titers than Katsuyama's and Fang's research group [78, 83]. However, Rodrigues et al [82]. suggested that malonyl-CoA could limit the obtention of higher titers in the future.

Novel synthetic biology techniques have continuously been developed increasing the genetic toolkits available for researchers to perform genetic modifications in microorganisms [105, 106]. The most notable one is the clustered regularly interspaced short palindromic repeats (CRISPR) that appears as a simple, efficient, cheap, and rapid technology for genetic engineering purposes. The applications of CRISPR range from common genetic procedures, such as genome editing, to more complex processes, as controlling the genetic expression of targeted native genes (see **Chapter 3**, **Section 3.1.2**). Recently, Chu et al. [85] applied CRISPR interference (CRISPRi) in a curcuminoid *E. coli* producer expressing 4CL from *Petroselinum crispum* and *O. sativa* CUS. CRISPRi allows to silence multiple genes at the transcriptional level, which may be very advantageous to study complex pathways. The goal of applying CRISPRi in this study was to increase the intracellular malonyl-CoA by regulating some genes involved in TCA cycle and fatty acid biosynthesis thus preventing acetyl-CoA consumption (malonyl-CoA precursor) and/or malonyl-CoA deviation, respectively. The triple repression of FabF (3-oxoacyl-[acyl-carrier-protein] synthase), FabD ([acyl-carrier-protein] S-malonyltransferase) (fatty acid biosynthesis) and malate dehydrogenase (TCA cycle) using CRISPRi resulted in the highest dicinnamoylmethane production (11.6 mg/L) from cinnamic acid, increasing the production titer in 5.76 times relatively to the wild type. The authors also tested if the solo expression of the heterologous ACC cluster from *Nocardia farcinica* could also improve the curcuminoid synthesis. In fact, the dicinnamoylmethane production increased twofold relatively to the wild type, demonstrating that the expression of the heterologous ACC cluster increased the endogenous malonyl-CoA pool and consequently the production titers.

Besides the increment of malonyl-CoA supply, other chassis optimizations may include the inhibition of metabolic pathways to prevent product deviation or even the modification of chassis phenotypic characteristics to accommodate the production. Wu et al. [87] constructed a curcumin *E. coli* BW25113 producer expressing CUS from *O. sativa* and a 4CL mutant version of *A. thaliana*. This primary strain produced 5.5 mg/L of curcumin from ferulic acid. Next, to increase the supply of malonyl-CoA, the genes *poxB* (pyruvate oxidase; TCA cycle), *adhE* (aldehyde-alcohol dehydrogenase; acetyl-CoA

degradation), and *fabF* (fatty acids biosynthesis) were inactivated and acetyl-CoA synthetase (ACS) was overexpressed to direct metabolic fluxes through acetyl-CoA synthesis and thus malonyl-CoA. These genetic modifications resulted in a curcumin titer 2.8 times higher relatively to the primary strain. The authors also reported that the deletion of the native *curA* gene, encoding for curcumin reductase, seemingly responsible for curcumin reduction, resulted in a 1.7-fold improvement on the production. Moreover, it was demonstrated that the use of medium copy plasmids to express curcuminoid biosynthetic genes increased curcumin yields over high copy plasmids. Furthermore, 4CL and CUS genes were arranged in an operon, and the operon architecture was optimized. The operon containing CUS gene upstream of 4CL gene improved five times the curcumin titer. Afterwards, the authors used random mutagenesis to find a CUS with increased expression levels. The use of a mutated CUS with high expression levels improved curcumin levels 3.8 times (95.8 mg/L). In addition, as it is known that hydrophobic compounds in *E. coli*, such as curcumin, accumulate in membrane compartments and only at high concentrations pass to the media, the authors hypothesized that by increasing the hydrophobic compound content of the cell membrane, the curcumin production would also increase. To evaluate that, a monoglucosyldiacylglycerol synthase (mgs) gene from *Acholeplasma laidlawii* was overexpressed. The mgs overexpression in *E. coli* led to the formation of massive intracellular membrane vesicles, which could enhance the storage of hydrophobic compounds (Eriksson et al. 2009). Membrane-engineered cells became bigger in length and smaller in width and curcumin production increased 2.2-fold. Moreover, it was found that curcumin reduced the *E. coli* membrane fluidity. To prevent membrane rigidity caused by curcumin accumulation, unsaturated fatty acids such as oleic acid and palmitoleic acid were added to the culture media which also promoted curcumin biosynthesis. Shake flask of the final strain resulted in 1.46 mM (537.8 mg/L) of curcumin from 4 mM of ferulic acid. Nevertheless, after all these modifications, the titers obtained are in the same range of the titers obtained by Rodrigues et al. [82] (563.4 mg/L, from 3 mM of ferulic acid) that did not perform chassis modifications and used DCS and CURS1 enzyme instead of CUS. This demonstrates that DCS and CURS1 may be a better option than CUS to produce curcuminoids in *E. coli*.

More recently, Chen et al. [88] used a previously modified *E. coli* strain for caffeic acid [107] and introduced COMT and 4CL from *A. thaliana* and DCS and CURS1 from *C. longa* resulting in the *de novo* production of 613.4 μg/L of curcumin. To increase the production levels DCS and CURS were fused to form a single protein and the endogenous malonyl-CoA synthesis optimized by knocking-out the genes *fadR,* encoding for a regulatory element of β-oxidation pathway and *mcrC* to prevent malonyl-CoA

utilization in *E. coli* metabolism. Moreover, *curA* gene was deleted and *srpB* gene, a solvent resistance membrane pump from *Pseudomonas putida*, was expressed to decrease the toxic accumulation of ferulic acid inside the cells. The final strain produced 137.5 mg/L of curcumin. Despite the efforts, the authors were not able to find a strategy to promote curcumin secretion. In addition, a fed-batch process was employed reaching a production of 524.1 mg/L. However, the process was associated with the supplementation of costly supplements including IPTG, four antibiotics (required for plasmid maintenance) and methionine.

2.4.2 Metabolic Engineering of Other Organisms to Produce Curcuminoids

Until now, *E. coli* has been the main biological chassis used to produce curcuminoids. However, in the last years, other microorganisms have been explored towards the same purpose. The filamentous fungi *Aspergillus oryzae* was the first organism to be engineered to produce curcuminoids after *E. coli* [89]. In a first attempt, the *O. sativa* CUS, 4CL from *L. erythrorhizon* and PAL from the yeast *Rhodotorula rubra*, a multi-substrate PAL capable of producing *p*-coumaric acid/cinnamic acid from tyrosine/phenylalanine were expressed. However, the engineered strains were not capable of producing any curcuminoids. But when feruloyl-N-acetylcysteamine (feruloyl-NAC), a feruloyl-CoA analogue, was added to the agar plates, curcumin was produced. On the other hand, bisdemethoxycurcumin was not produced when *p*-coumaroyl-NAC was supplemented. The researchers postulated that *p*-coumaroyl-NAC might be degraded by endogenous enzymes since its consumption was observed. Therefore, the authors postulated that mutants did not produce curcumin in the initial test due to a failed functional expression of 4CL. Hereupon, they constructed a recombinant *A. oryzae* strain expressing only CUS under control of the *amyB* promoter. The *amyB* promoter is a strong, maltose-inducible promoter usually used to express recombinant genes in *A. oryzae*. The produced curcumin was found to be accumulated in the mycelium. The yield obtained was 64.1 μg/plate, representing a conversion rate from feruloyl-NAC to curcumin of 9%. To increase the production, the authors attempted to increase the endogenous supply of the curcuminoid extender molecule malonyl-CoA. For that purpose, the genes for acetyl-CoA hydrolase (ACH) (responsible to convert the acetyl-CoA into acetate), serine protein kinase (*snfA*) (capable of inhibiting ACC via phosphorylation), and palmitoyl-CoA ligase (*faaA*) (involved in malonyl-CoA metabolism) were individually disrupted in the recombinant strain. In addition, the native ACC gene was also overexpressed through the replacement of the native promoter by *tef1* promoter which is a strong and constitutive promoter. The deletion of *snfA* resulted in the highest yield, increasing the production to 151 μg/plate. The other disrupted strains also showed increments on curcumin production, while ACC

overexpression did not generate significant results. To further increase the curcumin titers, two genes involved on the regulation of ergosterol biosynthesis were deleted (sterol regulatory element-binding protein (SREBP) and SREBP cleavage-activating protein (SCAP)). The downregulation of ergosterol served to prevent the acetyl-CoA deviation to ergosterol biosynthesis. The final engineered strain increased the production of curcumin to 404.2 μg/plate. The authors confirmed that indeed the malonyl-CoA levels increased in the final strain which led to a higher curcumin production. This work also represented the first report of the production of a plant secondary metabolite in the fungi *A. oryzae*.

Some microorganisms have been reported as capable of metabolizing aromatic compounds, such as the hydroxycinnamic acids, the precursors of curcuminoids. The metabolic pathways present in these microorganisms may share common reactions to the synthesis of curcuminoids. Hereupon, instead of developing engineered microorganisms carrying a complete curcumin artificial pathway it may be employed a microbe with some of the desirable reactions already available on it. This can drastically reduce the number enzymes required to be expressed. Moreover, model microbes such as *E. coli* do not naturally have the robustness traits desired for industrial applications such as high solvent and pH toleration [108]. Therefore, Incha et al. [90] used the bacteria *P. putida* to produce the *p*-coumaric acid-derived curcuminoid, bisdemethoxycurcumin. *P. putida* has known ability to catabolize ferulic and *p*-coumaric acids. The first reaction of this catabolic pathway starts with the condensation of the phenylpropanoids with a CoA molecule, a similar reaction to the one performed by 4CL in plants, that in *P. putida* is catalyzed by feruloyl/*p*-coumaroyl-CoA synthetase (Fcs). The following reaction is carried by enoyl-CoA hydratase lyase (Ech) to form vanillin. To produce bisdemethoxycurcumin in *P. putida*, the authors first studied the optimal conditions to express a type III PKS addressing the optimal glucose concentration to maximize the synthesis of malonyl-CoA. Next, to prevent *P. putida* from consuming *p*-coumaroyl-CoA, Ech gene was knocked out. The native Fcs gene was then overexpressed using an arabinose-inducible *araBAD* promoter. This engineered strain, in the presence of *p*-coumaric acid, had a relatively high lag time suggesting that accumulation of *p*-coumaroyl-CoA was toxic to the cells. To avoid that, instead of overexpressing Fcs, the Fcs expression was only relied on its native chromosomal expression. To synthesize bisdemethoxycurcumin, CUS from *O. sativa* was expressed in a plasmid also under control of *araBAD* promoter. The engineered strain was grown during 72 h to induce CUS expression. After 72 h, the cells were harvested and incubated in a media with *p*-coumaric acid for another 72 h. Interestingly, when 10 mM of *p*-coumaric acid were added, the production levels were very low (0.1 mg/L). However, using half of the substrate concentration (5 mM), the production reached

2.15 mg/L, once again suggesting the toxicity of *p*-coumaroyl-CoA, or even *p*-coumaric acid. To extract bisdemethoxycurcumin throughout the fermentation the authors used oleyl alcohol. In the end, the authors concluded that more genetic modifications are still required to avoid the observed intermediary toxicity. Nevertheless, the natural biological characteristics of *P. putida* (high solvent toleration, broad carbon source metabolisms, endogenous phenylpropanoid activation capacity) make it an attractive host to produce curcumin mainly from organic wastes such as lignocellulosic feedstocks (rich in *p*-coumaric/ ferulic acids) and contributing to the circular economy.

Due to the reported antimicrobial activity of curcumin [109], its production in microorganisms seems to be contradictory since high concentrations of this compound could lead to cell death or affect the microbial growth, thus limiting production yields. However, some microorganisms have evolved to adapt to extreme conditions. Consequently, the use of a high-tolerant microbe as a host chassis to produce curcumin may lead to high production titers. The oleaginous yeast *Yarrowia lipolytica* has reported high tolerance to phenolic compounds [110]. Therefore, Palmer et al. [91] constructed a recombinant strain for bisdemethoxycurcumin production. For that purpose, a previously engineered *Y. lipolytica* strain overexpressing Pex10p, a peroxisome biogenesis factor, was used as background. Although Pex10p is a structural protein associated with the formation of peroxisomes, being not directly involved with acetyl-CoA biosynthesis, the engineered strain showed high capacity to synthesize acetyl-CoA relatively to the wild type. Furthermore, the native ACC was overexpressed to increase the malonyl-CoA concentration synthesized from acetyl-CoA. To produce curcuminoids, the codon optimized versions of 4CL from *N. tabacum* and *O. sativa* CUS were expressed in this recombinant strain. Flask fermentations supplemented with 2 mM of *p*-coumaric acid led to the production of 0.17 mg/L of bisdemethoxycurcumin.

Curcumin biosynthesis in *S. cerevisiae* was also achieved in a recent work by Utomo et al. [92]. The researchers studied three different paths for the synthesis of feruloyl-CoA and curcumin biosynthesis was achieved by expressing DCS and CURS. The highest curcumin titers were achieved using a pathway that converts *p*-coumaric acid to *p*-coumaroyl-CoA and *p*-coumaroyl-CoA back to caffeic acid through *p*-coumaroyl shikimate. Caffeic acid is then activated by 4CL and CCoAOMT converts the activated caffeic acid into feruloyl-CoA. The gene coding for enoyl reductase (TSC13) involved in fatty acid synthesis was also replaced by a plant version to prevent *p*-coumaroyl-CoA deviation. Curcumin production from glucose reached 1.5 mg/L.

As demonstrated, up to date, the curcumin production in microorganisms was mainly achieved in the model bacteria *E. coli*. More recently, other organisms have started to be explored. This newly explored microorganisms is expected to bring new advantages for the microbial production of curcumin. For instance, the use eukaryotic model *S. cerevisiae* might facilitate the correct expression of plant genes due to its ability to perform posttranslational modifications. However, the levels of curcumin obtained in yeast are still relatively low, indicating the necessity for further studies.

2.5 Conclusions and Future Perspectives

Curcumin has shown over the last years a great potential to be employed as a natural therapeutic agent due to its wide biological activities. The microbial production of curcumin appears as a solution to overcome limitations associated with the plant extraction of this compound. The microbial production allows obtaining curcumin in a rapid, cheaper, and more environmentally friendly way. Remarkable advances have been made regarding the heterologous production of curcumin using *E. coli* as a biological chassis. However, additional genetic modifications are still required to maximize the production yields by directing more carbon flux to the biosynthesis of curcumin. Nevertheless, curcumin production in *E. coli* already reached interesting titers. Using ferulic acid as substrate the curcumin produced reached 563.4 mg/L with a 100% conversion yield. *De novo* curcumin biosynthesis reached 524.1 mg/L in bioreactor scale fermentation. In addition, the use of coculture systems proved to be important to increase the curcumin titers in genetically modified *E. coli*. In the future, the engineering of the coculture systems must be evaluated, for instance, by using an arrangement of different organisms. The combination of the lessons learned in the different studies appears as one of the next steps to increase production yields in *E. coli*. For example, the most efficient enzymes and pathways must be introduced in efficient tyrosine/phenylalanine *E. coli* overproducing strains for *de novo* synthesis of curcumin. In addition, the strain engineering to increase the malonyl-CoA pool must also be taken into consideration. The use of other microorganisms remains scarcely explored although their use as biological chassis might bring advantages over *E. coli*. *S. cerevisiae* has already been extensively studied to produce other polyphenols (e.g., resveratrol) yielding good results, however curcumin production remains relatively underexplored. Moreover, the use of renewable feedstocks to produce curcumin is not very much explored. This can be very important to monetize the process and contribute to circular economy.

CHAPTER 3. *Saccharomyces cerevisiae* as Microbial Cell Factory

ABSTRACT: *Saccharomyces cerevisiae* is a key laboratorial and industrial microorganism and represents an excellent chassis for metabolic engineering and synthetic biology approaches. This microorganism has been extensively engineered to produce a wide variety of compounds and proteins. In addition, the knowledge on its physiology, genetics and fermentation patterns is vast, similarly to the model bacteria *Escherichia coli*. However, it presents some unique characteristics over the bacteria concerning the production of plant compounds. Being a eukaryotic organism, it is capable of post-translational modifications such as glycosylation and it possesses intracellular compartments similarly to plants. Moreover, *S. cerevisiae*, unlike *E. coli*, has a food-grade status allowing its use in human nutrition and pharmaceuticals. In recent years, many efforts have been developed to heterologously produce hydroxycinnamic acids and polyphenols using *S. cerevisiae.* This chapter will first explore the strategies and advancements of synthetic biology tools, particularly those associated with clustered regularly interspaced palindromic repeats (CRISPR), and their applications in the context of *S. cerevisiae* genetic engineering. Subsequently, a literature review will be conducted focusing on the production of polyphenolic compounds that share common biosynthetic pathways with curcumin—specifically, the phenylpropanoid pathway. This discussion aims to explore valuable insights into the metabolic engineering strategies employed to increase yields in the production of curcumin using genetically engineered yeast.

The information presented in this chapter was partially published in two publications in the Life journal:

Rainha, J., Rodrigues, J. L., & Rodrigues, L. R. (2021). CRISPR-Cas9: A powerful tool to efficiently engineer *Saccharomyces cerevisiae*. *Life*, *11*(1), 13.

Rainha, J., Gomes, D., Rodrigues, L. R., & Rodrigues, J. L. (2020). Synthetic biology approaches to engineer *Saccharomyces cerevisiae* towards the industrial production of valuable polyphenolic compounds. *Life*, *10*(5), 56.

3.1 Genetic Engineering Tools for *Saccharomyces cerevisiae*

Saccharomyces cerevisiae has long been a common model for fundamental biological studies because of its safety and ease of handling. Additionally, it was the first eukaryotic organism whose genome was fully sequenced [45]. This yeast has been extensively used to elucidate eukaryotic processes from basic metabolism to protein/gene interaction or even evolution [111]. Moreover, it is also a popular biotechnological engineering platform used to produce chemicals, fuels, and pharmaceuticals [112]. Associated with these two lines of research is the need to effectively edit the native genetic elements or introduce heterologous pathways into the yeast genome. For instance, for metabolic engineering purposes, several genetic modifications are required besides the introduction of heterologous genes to stream the metabolic fluxes toward the production of the desired product. Therefore, the development of an efficient cell factory is also associated with several native gene deletions, overexpression, or replacements.

3.1.1 Homologous Recombination

Most of the metabolic engineering approaches in *S. cerevisiae* used high copy number 2 micron (2μ) episomal plasmids. High copy plasmids can be maintained at 10–80 copies per cell [113] providing a convenient platform for the overexpression of heterologous genes. However, there are inherent problems associated with episomal plasmids, namely their instability, variations in gene expression within a population, as well as the high maintenance costs to ensure the selective pressure [114]. The genomic integration appears as an alternative to the use of episomal plasmids since it allows the stable expression of the heterologous pathways. *S. cerevisiae* is known to possess a very efficient homologous recombination (HR) machinery [115]. Simple knock-in or knock-out of genes are routinely used in *S. cerevisiae* to develop novel strains adapted to produce useful chemicals. These modifications are easily achieved by conventional gene recombination, due to the high HR capability of this yeast [116]. A modification requires a cycle of individual transformation, selection, and confirmation, thus making the process very time-consuming. Furthermore, each cycle is associated with the integration of a selective marker. However, the number of markers available is limited, which also limits the number of sequential modifications that can be performed. Although recombinase-based methods such as Cre/LoxP or Flp/FRT have been extensively used in marker recycling [117, 118], they are laborious since they require another transformation cycle to remove the marker. In addition, these methods have the drawback of

leaving a copy of a repeat sequence in the genome. These "scars" may lead to genome instability after multiple rounds of marker recovery [119].

3.1.2 CRISPR-Cas9

Double-strand breaks (DSBs) in the genome occur due to several environmental factors and can be repaired by HR or nonhomologous end-joining (NHEJ). In *S. cerevisiae* it is known that the dominant repair is performed by HR. The introduction of a DSB has been shown to increase the efficiency of homologous integration of linear DNA fragments with homologous ends [120]. These features led researchers to develop methods that use DSBs for site-directed genome editing. These methods could be used for marker-free modifications and examples include zinc finger nucleases (ZFN) and transcription-activator-like effector nucleases (TALEN). Both methods involve the design of proteins that recognize a specific DNA sequence and cause a site-specific DSB through DNA–protein interaction. The DSB is then repaired by HR with a provided DNA fragment with homologous ends. However, a new ZFN or TALEN protein must be engineered for each target modification, making these methods also very laborious [105, 106].

Evolution allowed bacteria to develop several systems to degrade foreign DNA as a defence mechanism. The most well-known are restriction enzymes, which rapidly became the "workhorses of molecular biology" [121]. More recently, another prokaryotic immune system was identified [122]. This system consists of clustered, regularly interspaced, short palindromic repeats (CRISPR) and CRISPR-associated nucleases (CRISPR-Cas), widely distributed among bacteria and archaea [123]. CRISPR-Cas has the function of recognizing and degrading invading nucleic acids. The increased knowledge of CRISPR action mechanism broke new ground regarding a possible applicability for this system to edit genetic elements of an organism.

Due to their simplicity relative to other classes, class II CRISPR-Cas systems have the most well-developed methods for genomic engineering nowadays. In class II, all the functions of the effector complex are performed by a single protein [124]. The following components are required: the RNA-guided nuclease Cas9, a CRISPR RNA (crRNA), an auxiliary trans-activating crRNA (tracrRNA), and an RNase III. The action mechanism is simple and aims at the creation of a DSB in the target DNA. A hybrid of the RNA molecules directs Cas9 to the target DNA site and the Cas9 cleaves a targeting DNA sequence containing a protospacer-adjacent motif (PAM) sequence (**Figure 3.1**). Jinek et al. [125] postulated that the requirement for RNase and tracRNA can be bypassed by fusion crRNA and tracrRNA

to form a single-guide RNA (gRNA) simplifying the process and application. The gRNAs are composed of a homologous sequence 20 nt upstream of the PAM sequence (guide sequence) and the scaffolding loop structure to attach the Cas9.

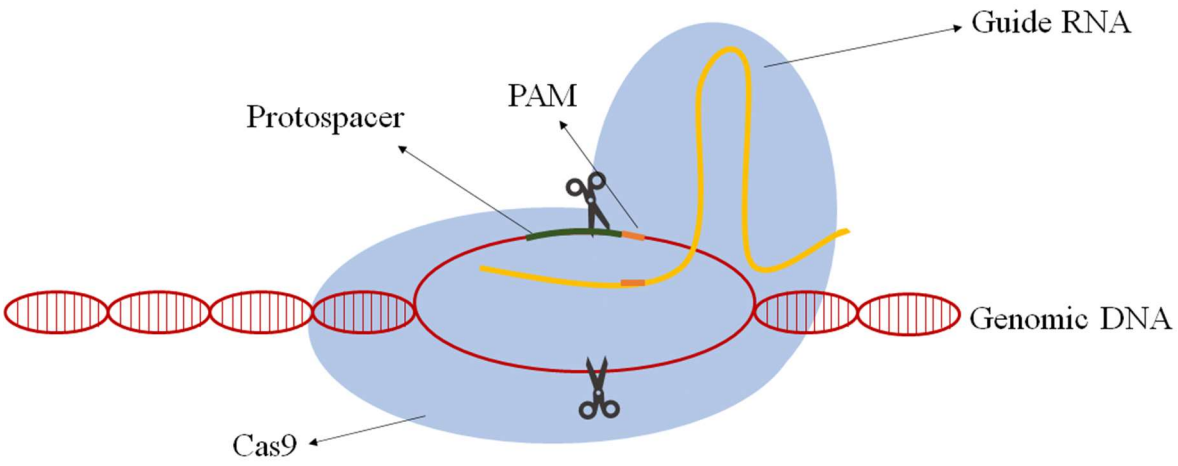


Figure 3.1: The mechanism of action of clustered, regularly interspaced, short palindromic repeats–associated Cas9 (CRISPR-Cas9). The guide RNA (gRNA) molecule directs Cas9 protein to the target DNA and Cas9 cleaves genomic DNA 3–4 bp upstream of the PAM (protospacer-adjacent motif) site.

3.1.2.1 CRISPR-Cas9 Applications in *Saccharomyces cerevisiae*

The type II CRISPR-Cas9 system was implemented in *S. cerevisiae* for genetic modification purposes by DiCarlo et al. [126]. The researchers demonstrated that co-transforming a gRNA targeting a negative selectable marker together with a 90-bp double-stranded HR donor with a frameshift mutation in the targeted reading frame and PAM replacement by a stop codon resulted in almost 100% of mutated cells. Following this, numerous new CRISPR application have emerged. The following sections describe the applications of CRISPR-Cas9 technology within the context of genetic engineering *S. cerevisiae*.

3.1.2.1.1 Gene Knock-in and Gene Knock-out

The development of the CRISPR-Cas9 system has allowed the researchers to perform high-efficiency and markerless knock-in and knock-out of genetic elements due to the combinatorial effects of high-efficiency HR apparatus of *S. cerevisiae* and CRISPR system efficacy to introduce a DSB.

Regarding the knock-out of genes, Generoso et al. [127], for instance, designed a CRISPR-Cas9 system to create a DSB in the threonine deaminase (ILV) gene. The single-stranded donor DNA used for

recombination was composed of 40 nt upstream and 40 nt downstream of the ILV open reading frame (ORF), and the knockout was 100% efficient. No marker integration was required to delete an entire ORF (**Figure 3.2a**). For the knockout of genes, besides deleting an entire ORF, other strategies can be employed such as a frameshift modification or the insertion of a STOP codon. To knockout the canavanine resistance (CAN1) gene, Bao et al. [128] caused a 8-bp deletion leading to a frameshift and resulting in CAN1 knockout by putting a STOP codon in the frame in the beginning of the gene. The 8-bp included the PAM site and the last 3-bp of the gRNA sequence to prevent the continuous recognition and cleavage by the CRISPR-Cas after recombination.

The knock-in of genes or other genomic components is also an important element in *S. cerevisiae* genetic studies. The knock-in of genetic parts is common practise for the development of yeast cell factories. Therefore, knock-in events may include the integration of heterologous genes (**Figure 3.2b**), the replacement of genes by a feedback-insensitive orthologue or the promoter replacement to adjust the expression of a specific gene.

3.1.2.1.2 Multiple Gene Deletion and Point-Mutations

Multiple gene disruptions can be used for gene characterization in complex genetic pathways [129] and to facilitate the development of an efficient chassis for heterologous production [130]. Sequential gene disruptions are traditionally achieved by the replacement of the target gene with a selectable marker through HR in a sequential manner. The markers are usually recycled by different systems, which is a very laborious process. CRISPR-Cas9 can bypass this limitation, however there are some problems associated with multiple gRNA's expression, mainly the need to use various RNA polymerase III regulatory elements to express them. Bao et al. [128] developed a CRISPR system to overcome this limitation. For that purpose, the expression of three gRNAs was carried by a single promoter and the sequences were separated by direct repeats. In a different experiment, to knock-out three genes in a single step, Generoso et al. [127] expressed the gRNAs separately, also obtaining good results.

Precise, direct point mutations (single-nucleotide changes) can also be performed using CRISPR-Cas9. Mans et al. [131] efficiently caused point mutations in specific genes using a CRISPR approach. This kind of approach can be useful for studies of the biological significance of mutations caused by artificial evolution, since not all mutations obtained in this kind of experiments contribute to a desired phenotype [132].

Combining gene disruption with the integration of a desired component may be advantageous since it makes it possible to perform various modifications in a single step. For example, Mans et al. [131]developed a CRISPR-Cas9 system to target an undesired gene and simultaneously transform the donor DNA repair with other five DNA fragments with homologous arms to *in vivo* combine the fragments and replace the undesired ORF. This kind of approach is very useful for the development of yeast cell factories as discussed below (**Figure 3.2c**).

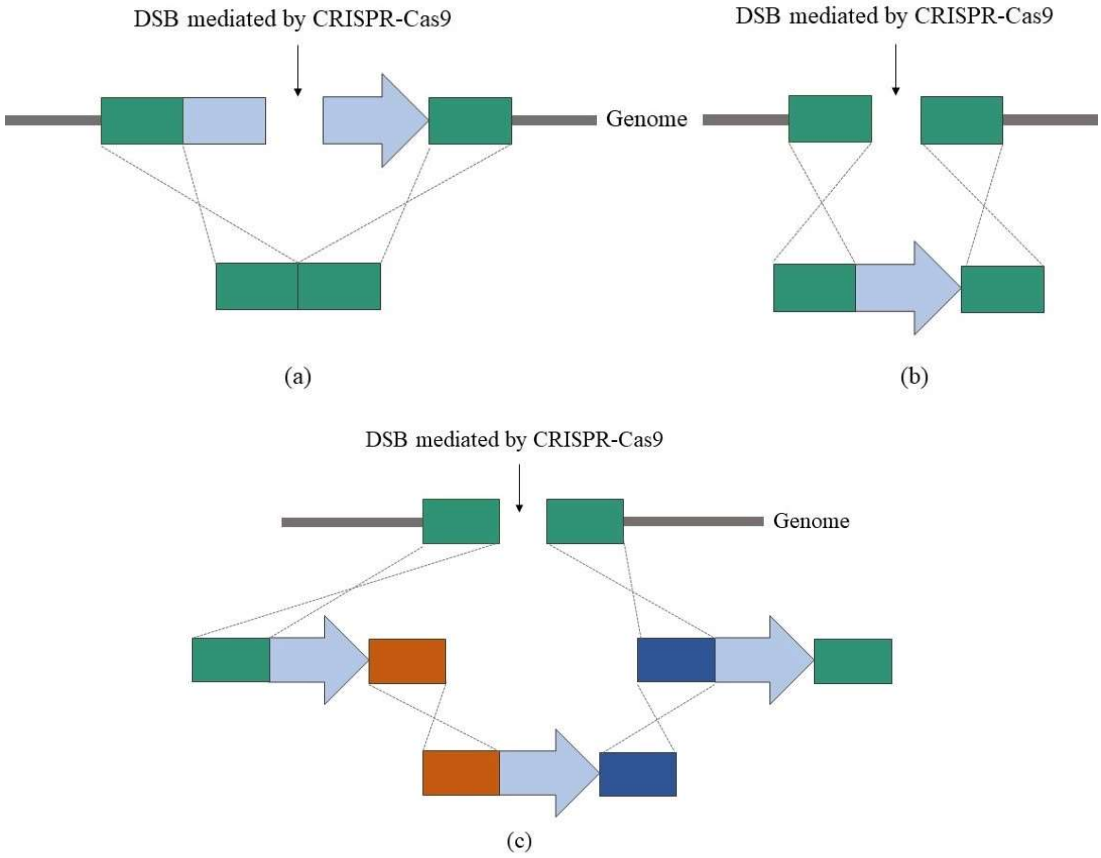


Figure 3.2: Strategies used to integrate DNA fragments using double-strand breaks (DSB) originated by clustered, regularly interspaced, short palindromic repeats–associated Cas9 (CRISPR-Cas9). The knock-out can be performed by providing a homologous repair fragment for gene integration (**a**) or knock-in (**b**). (**c**) Combination of *in vivo* recombination and fragment integration using a created DSB. The homologous repair fragment can be *in vivo* assembled using *Saccharomyces cerevisiae* machinery by providing the fragments with homologous ends. The assembled fragment is used to homology repair the DSB.

3.1.2.1.3 Cell Factory Development

The design and construction of microbial cell factories is more than ever an attractive approach to develop bioengineering processes to produce chemicals, fuels, or pharmaceutics. Furthermore, *S. cerevisiae* is an appealing model for bioengineering processes due to its rapid production cycles, ease of

maintenance, manipulation, and suitability for large-scale fermentation. The molecular "tools" available have helped the researchers to make yeast cell factories increasingly adapted to produce a desired product [112]. The development of efficient cell factories is associated with several genetic modifications, since not only the insertion of the heterologous genes is required but also the rewiring of the carbon flux toward the precursor synthesis or even other convenient modifications to improve the process. The CRISPR-Cas9 system appeared as a "Swiss army knife" [131] in the researcher's molecular toolbox because it allowed the performance of several genetic modifications in a fast and efficient way. Furthermore, the requirement of a constant selective pressure during fermentation is negated since CRISPR-Cas9 allows a markerless genetic manipulation. In addition, several design-build-test-learn cycles are always necessary, which increases the number of modifications required [106]. By using CRISPR-Cas9 systems, genetic editing has become multiplex possible, which may significantly decrease the time to perform the designed genetic modifications for a cell factory construction. The flexibility of CRISPR-Cas9 allied with the researcher's inventiveness resulted in the development of systems that facilitate and accelerate metabolic engineering processes. Researchers are not only focused on developing new CRISPR-based strategies for direct genome engineering but also on applying CRISPR-Cas9 to improve other conventional molecular biology lab practices, speeding up the strain building process. For example, Li et al. [133] developed a CRISPR system capable of sequential rounds of gene targeting with simultaneous gRNA plasmid curing mediated by CRISPR-Cas9. All this flexibility and simplicity of the CRISPR-Cas9 system made it well accepted by genetic engineers for the development of yeast cell factories. Genome integration, as previously mentioned, has several benefits over plasmids because it allows gene expression stability and lower heterogeneity and eliminates the requirement of using selective growth media after confirmation. However, the use of plasmids brings the advantage of expressing a heterologous protein/pathway in a multi-copy way. Shi et al. [134] developed a CRISPR-based method that allows a multi-integration of a heterologous fragment at the Ty retrotransposon, a set of repetitive sequences (delta (δ) sequences) in the yeast genome. The introduction of Cas9-mediated DSBs at δ sites allowed the integration of eighteen copies of a 24 kb DNA fragment carrying a xylose utilization pathway and a butanediol production pathway. The high copy number of the pathways resulted in both higher xylose consumption and butanediol production by the engineered strain comparatively to the one copy integration one (**Figure 3.3**).

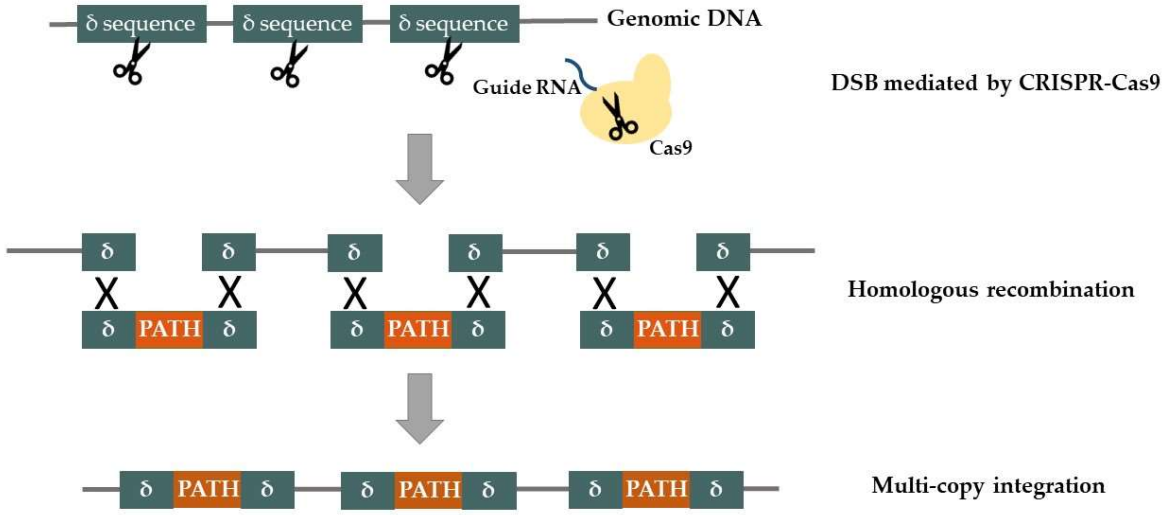


Figure 3.3: Clustered, regularly interspaced, short palindromic repeats–associated Cas9 (CRISPR-Cas9) associated with delta (δ) integration. CRISPR-Cas9 system creates a double-strand break (DSB) at the repetitive δ sequences present in the *S. cerevisiae* genome allowing the multi-copy integration of a DNA fragment containing a gene or even a pathway.

3.1.2.1.4 Innovative CRISPR Toolkits

New emergent procedures into how CRISPR-Cas9 is applied have recently been developed demonstrating the potentialities of this tool. The target specificity of CRISPR-Cas9 systems allowed researchers to develop technologies that take advantage of its precise DNA targeting namely for the delivery of other molecules. EvolvR, for instance, combines the target specificity of CRISPR-Cas9 technology with the error-prone capacity of a mutant DNA polymerase for *in vivo* targeted nucleotide diversification [135] (**Table 3.1**). The system employs the use of a nicking variant of Cas9 (nCas9) that cuts only one DNA strand avoiding native homology repair, and the DNA polymerase uses the nick as a start point to initiate mutation insertion. The results demonstrated that EvolvR was able to insert random mutations in both directions of the target sequence, and in addition, it was possible to target two genomic loci at the same time [135]. This technology could be important for instance to *in vivo* improve the enzymatic activity of heterologous enzymes.

Table 3.1: Developed toolkits for genetic engineering *S. cerevisiae* based on Clustered, regularly interspaced, short palindromic repeats–associated Cas9 (CRISPR-Cas9). dCas9: Cas9 defective in DNA cleavage; gRNA: guide RNA; nCas9: nicking Cas9.

Toolkit	Function	Toolkit nuance	Reference
yEvolvR	Random mutagenesis	nCas9	[135]
CRISPRi	Gene repression	dCas9	[136]
CRISPRa	Gene activation	dCas9 fused to an activator domain	[137]
CRISPRi/a	Grade modulation	dCas9 fused with RNA domain	[138]
CRISPR-AID	Simultaneous gene modulation and editing	Truncated gRNAs	[139]
CRISPR-ARE	Simultaneous gene modulation and editing using a single Cas9 protein	Truncated gRNAs	[140]

Targeted regulation of gene expression is important both in the context of metabolic engineering and functional genomics [141]. In yeast, the control of genetic expression is usually performed using characterized gene promoters with different strengths; however, the prediction of the expression level remains a challenge. Qi et al. [136] developed an enzymatic version of Cas9 mutated in the nuclease nucleotide sites designated as dead or defective Cas9 (dCas9). This Cas9 mutant is defective in DNA cleavage, and it can act as a simple specific DNA binding complex. Using this version of Cas9 for targeting a specific promoter, results in an efficient gene repression. The dCas9 binds to the target sequence blocking the action of RNA polymerase. This approach was named CRISPR interference (CRISPRi) [136]. In addition, the repression can be enhanced by fusing a transcriptional repressor domain to dCas9. Alternatively, Farzadfard et al. [137] fused dCas9 to an activator domain and reported an activation or repression depending on the targeting site. When the target was outside the TATA box, the promoter was activated (CRISPR activation (CRISPRa)), while targeting adjacent to the TATA box resulted in gene repression (CRISPRi). Other activator-domain-fused dCas9 proteins were also developed achieving higher regulation levels [67]. Zalatan et al. [138] used a different approach for up/downregulation of a target gene. Instead of including fusion domains in dCas9, the authors included effector protein recruitment RNA domains into the gRNA converting it to a scaffold RNA (scRNA). The RNA hairpins of scRNA can recruit a specific RNA-binding protein, an activator or a repressor, thus used for locus-specific regulation. Moreover, a grade modulation of genetic expression was reported by Deaner and Alper [142]. The range of genetic expression was related to the proximity of dCas9-based regulators to the core of the promoter. The grade modulation applicability represents a step forward to enable a fine tuning of metabolic pathways in *S. cerevisiae*. The possible applications of CRISPRi/a are massive, and they have already been used to improve a yeast cell factory to produce β-amyrin [143].

Another possible approach, besides the use of a modified CRISPR protein, to guide effector molecules without creating a DSB, is by adjusting the gRNA molecule length. Truncated gRNAs, usually of 14 nt, proved to be able to guide the binding of Cas9 to the target sequence without the introduction of a DSB [144, 145]. Hereupon, truncated gRNAs can be used for transcriptional regulation and, simultaneously, full-length gRNAs can be used for genome editing. This feature allowed researchers to develop multifunctional systems capable of one-pot CRISPRi, CRISPRa, and CRISPR editing. Lian et al. [139] reported the first trifunctional CRISPR system for simultaneous gene inactivation, activation, and editing in *S. cerevisiae* called CRISPR-AID. However, to avoid competition between gRNAs for the same Cas9 protein, three different PAM-recognizing CRISPR proteins were used. More recently, Dong et al. [140] established a trifunctional CRISPR system using a single Cas9 protein. The system was named CRISPR-ARE and employed the use of a Cas9 fused to a VP64-p65-Rta (VPR) activation domain. The authors demonstrated the applicability of CRISPR-ARE by optimizing α-santalene biosynthesis. The system used truncated gRNAs to target the genes for activation and repression, and full-length gRNAs to edit one gene by transforming together the donor repair DNA. The editing efficiency was 100% and gene activation and gene repression were confirmed using a reporter protein. Regarding the α-santalene biosynthesis, it increased 2.66-fold.

3.1.2.2 CRISPR-Cas9: Key Messages

The CRISPR-Cas9 system's discovery is with no doubt a landmark in the synthetic biology field. The simplicity and flexibility of the system enabled the researchers to develop a panoply of CRISPR applications. Consequently, it is now possible to build more and more complex designs in yeast by multiplexed CRISPR-Cas9 genome editing. Besides allowing multiple modifications, the emergence of CRISPR-Cas9 enabled the researchers to perform genetic modifications faster, cheaper, and more efficiently. The possibility to perform genetic modifications without the requirement of selective markers or the multiplex genomic edits are examples of the possibilities brought by this technology. The scientific community is taking advantage of the fantastic teamwork between CRISPR and yeast with results ranging from the introduction of large chromosomal segments to point mutations and by developing improved genome editing systems. Moreover, CRISPR applications have transgressed the conventional genome editing application through the creation of novel mutated versions of Cas9 such as nCas9 or dCas9. CRISPRi/a is a tremendously useful tool for transcriptional regulation because it allows to balance and optimize gene expression without genome editing. This tool may be tremendously useful when dealing with essential genes in *S. cerevisiae* mainly for the development of industrial strains where

the metabolic fluxes need to be meticulously balanced. The application of multifunctional systems, such as CRISPR-ARE, accelerates the design–build–test–learn processes and, consequently, the productivity of the research.

3.2 Heterologous Production of Polyphenols in *Saccharomyces cerevisiae*

Polyphenols are compounds of immense interest due to their diverse biological activities and potential industrial applications. These group of compounds share the initial pathways for biosynthesis namely the shikimate and phenylpropanoid pathways. Afterwards, some of the final reactions are catalysed by type III polyketide synthases (PKSs) and despite their structural simplicity, type III PKSs produce a wide array of compounds [146]. There are several varieties and each one catalyses the formation of a different polyphenol or a polyphenol group. Given all the advantages of *S. cerevisiae* for cell factory development a numerous initiatives have emerged to produce polyphenols and their precursors (hydroxycinnamic acids) employing genetic modified *S. cerevisiae* (**Table 3.2**).

3.2.1 Pathway Enzyme Selection and Engineering

Finding the right enzyme combination is a key step in the genetic engineering of any heterologous pathway. The enzymes for producing polyphenols in an engineered yeast should be carefully selected to ensure a metabolic balance between all the intermediary reactions and, consequently, obtain higher production yields. Moreover, the use of enzymes that catalyse more than one reaction may decrease the metabolic burden caused to the host, hence resulting in an enhanced production. As previously mentioned (**Chapter 2**, **Section 2.3.1**), phenylalanine ammonia lyase (PAL) is the first enzyme of the phenylpropanoids pathway. Some PALs also have tyrosine ammonia lyase (TAL) activity, converting tyrosine directly into *p*-coumaric acid. The use of these enzymes allows the production of *p*-coumaric acid without requiring cinnamate-4-hydroxylase (C4H) (a membrane-bound cytochrome P450-dependent enzyme). This represents an advantage since the native cytochrome P450 activity could not be enough to support P450-dependent plant enzymes. Trantas et al. [166] engineered a set of yeasts to produce flavonoids and stilbenoids using phenylalanine as the initial precursor. Depending on the final phenylpropanoid, the constructed pathways contained four to eight enzymatic steps. In addition, the researchers tested if the co-expression of a heterologous cytochrome P450 reductase (CPR) would enhance the activity of the cloned C4H. When the CPR was co-expressed, the production of *p*-coumaric

acid was enhanced by four times. This indicated that the activity of the endogenous yeast CPR was not sufficient to support the maximum substrates fluxes through C4H.

The 4-coumarate-CoA ligase (4CL) enzymes family catalyses the conversion of *p*-coumaric acid, ferulic acid and caffeic acid to the respective CoA esters. Furthermore, 4CL has been shown to occur in multiple isoforms with distinct substrate affinities [82]. In the heterologous production of flavonoids and stilbenoids in *S. cerevisiae*, 4CLs from *Arabidopsis thaliana* are the most used (**Table 3.2**). *A. thaliana* possesses four isoforms of 4CL (*At*4CL1, *At*4CL2, *At*4CL3 and *At*4CL4). From the expression patterns and phylogenetic similarity, only *At*4CL3 is suggested to play a role in flavonoid biosynthesis. *At*4CL1 and *At*4CL2 are presumed to be involved in the lignin production [73]. Li et al. [163] evaluated if the use of different A*. thaliana* 4CL isoforms (*At*4CL1 and *At*4CL2) would have an impact on the production of resveratrol by the engineered yeasts. The results confirmed that *At*4CL1 resulted in slightly higher resveratrol titers than *At*4CL2. These results confirmed that *At*4CL1 has higher activity towards *p*-coumaric acid as described by Ehlting et al. [73]. Altogether, these results demonstrated that choosing the right enzymes combination is a key step to produce heterologous compounds such as polyphenols in yeast.

The expression of heterologous genes in *S. cerevisiae* can lead to translation errors, frameshifting events, stalling or premature translational termination due to the existence of rare codons. Consequently, it can result in the expression of a non-functional enzyme. To overcome that, codon optimization must be considered to optimize the heterologous production of polyphenols. For instance, in the work developed by Wang et al. [160], the enzyme TAL from *Rhodobacter sphaeroides* did not show *in vivo* activity in *S. cerevisiae*. In contrast, the use of a codon-optimized TAL enabled the resveratrol biosynthesis in the engineered yeast.

Table 3.2: Production of hydroxycinnamic acids and polyphenols in *Saccharomyces cerevisiae*. Genes, genetic systems, chassis, chassis modifications, substrates, conditions and titers obtained.

Phenolic compound	Genes [1]	Genetic system	Chassis / Chassis modification [2]	Substrate[3]	Conditions	Titer (mg/L)	Reference
p-Coumaric acid	*Fj*TAL	One copy genome integration	*S. cerevisiae* CEN.PK102-5B / Aromatic amino acids overproducing strain	Synthetic fed-batch medium	Microtiter plates	1900	[147]
p-Coumaric acid	*Fj*TAL	One copy genome integration	*S. cerevisiae* CEN.PK102-5B / Knockout of the downregulated transporter TAT1	Glucose (10 g/L)	Fed-batch	2400	[148]
p-Coumaric acid	*Fj*TAL, xylose utilization genes	One copy genome integration	*S. cerevisiae* CMB.GS010 / Aromatic amino acids overproducing strain	Xylose (15 g/L)	Batch bioreactor	242	[149]
p-Coumaric acid	*At*PAL, *At*C4H, *Fj*TAL	One copy genome integration	*S. cerevisiae* IMX / Aromatic amino acids overproducing strain; Overexpression of CYB5 and expression of *At*CPR to enhance cytochrome P450 activity	Glucose (20 g/L)	Fed-batch bioreactor	12500	[150]
Caffeic acid	*Rt*TAL, *Pa*HpaB, *Se*HpaC	Episomal plasmid	*S. cerevisiae* BY4741/-	Tyrosine (0.5 g/L)	Shake flask	289.4	[151]
Caffeic acid	*Rc*TAL, *At*C3H, *At*CPR	One copy genome integration	*S. cerevisiae* BY4742 / Aromatic amino acids overproducing strain; Expression of *At*CPR to enhance cytochrome P450 activity	Glucose (40 g/L)	Shake flask	11.4	[152]
Caffeic acid	*Rg*TAL, *Pa*HpaB, *Se*HpaC	One copy genome integration	*S. cerevisiae* BY4741 / Aromatic amino acids overproducing strain	Glucose (20 g/L)	Shake flask	569.0	[153]
Caffeic acid	*Rc*TAL, AtC3H	Multiple copy genome integration	*S. cerevisiae* BY4742 / Aromatic amino acids overproducing strain	Glucose (20 g/L)	Shake flask	15.1	[154]
Ferulic acid	*Fj*TAL, SbPAL, *Pa*HpaB, *Se*HpaC, PtrC4H2, PtrC4H1, PtrC3H3, NtCOMT	One copy genome integration	*S. cerevisiae* CEN.PK113-11C / Aromatic amino acids overproducing strain; Expression of *At*CPR to enhance cytochrome P450 activity; Four copies integration of *Nt*COMT; Engineering NADPH, FAD and SAM supply by several genomic modifications including overexpression of heterologous and native genes and gene deletions	Glucose (20 g/L)	Shake flask	420	[155]
					Fed-Batch	3800	
Resveratrol	*Ph*4CL216, *Vv*ST1	Episomal plasmid	*S. cerevisiae* FY23 /-	*p*-Coumaric acid (10 mg/L)	Shake flask	0.0014	[156]
Resveratrol	*Nt*4CL2, *Vv*STS	One copy genome integration	*S. cerevisiae* CEN-PK113-3B /-	*p*-Coumaric acid (820 mg/L)	Shake flask	5.8	[157]
Resveratrol	*At*4CL1, *Vv*STS	Episomal plasmid	*S. cerevisiae* strain isolated from a Brazilian sugar cane plantation.	*p*-Coumaric acid (2.46 g/L)	Shake flask	391	[158]
Resveratrol	*At*4CL1, *Ah*STS	Episomal plasmid	*S. cerevisiae* W303-1A / PAD knock-out	*p*-Coumaric acid (16 mg/L)	Shake flask	3.1	[159]
Resveratrol	*At*4CL1 and *Vv*STS fusion protein	One copy genome integration	*S. cerevisiae* WAT11 / Expression of *araE* transporter	*p*-Coumaric acid (10 mg/L) every 24h	Shake flask	2.3	[160]
Resveratrol	*Rt*PAL, *At*C4H, *At*4CL1, *Ah*STS	Episomal plasmid	*S. cerevisiae* W303-1A / ACC overexpression	Tyrosine (2.17 g/L)	Batch bioreactor	5.8	[161]

Table 3.2: *Continuation*

Phenolic compound	Genes [1]	Genetic system	Chassis / Chassis modification [2]	Substrate[3]	Conditions	Titer (mg/L)	Reference
Resveratrol	*At*4CL1 and *Vi*STS synthetic scaffold	Episomal plasmid	*S. cerevisiae* WAT11 / -	*p*-Coumaric acid (20 mg/L)	Shake flask	14.4	[162]
Resveratrol	*Ha*TAL, *At*4CL1, *Vi*WST	Multiple copy genome integration	*S. cerevisiae* CEN.PK102-5B / Aromatic amino acids overproducing strain	Glucose (40 g/L)	Fed-batch bioreactor	531.4	[163]
Resveratrol	*At*PAL, *At*C4H, *At*4CL2, *Vi*WST1	Multiple copy genome integration	*S. cerevisiae* CEN.PK102-5B / Aromatic amino acids overproducing strain; Expression of *At*CPR and CYB5 to enhance cytochrome P450 activity	Glucose (88 g/L)	Fed-batch bioreactor	800	[164]
Naringenin chalcone	*Rt*PAL, *At*4CL1, *Ha*CHS	Episomal plasmids	*S. cerevisiae* AH22 / PAD knock-out	Galactose (20 g/L)	Shake flask	7	[165]
Naringenin	*Ph*PAL, *Gm*4CL2, *Gm*CHS, *Gm*CHI	One copy genome integration	*S. cerevisiae* YPH499 / Expression of *Ph*CPR to enhance cytochrome P450 activity	Phenylalanine (1.7 g/L)	Shake flask	8.9	[166]
Genistein	*Ph*PAL, *Gm*4CL2, *Gm*CHS, *Gm*CHI, *Gm*IFS					0.1	
Kaempferol	*Ph*PAL, *Gm*4CL2, *Gm*CHS, *Gm*CHI, *Gm*F3'H, *St*FLS					1.3	
Quercetin	*Ph*PAL, *Gm*C4H, *Gm*4CL2, *Gm*CHS, *Gm*CHI, *Gm*F3'H, *St*FLS					0.26	
Naringenin	*At*PAL, *At*CHI, *At*CHS, *At*4CL3, *At*TAL, *At*C4H, *At*CHS3	One copy genome integration	*S. cerevisiae* CEN.PK717.5A / Aromatic amino acids overproducing strain; Expression of *At*CPR to enhance cytochrome P450 activity	Glucose (20 g/L)	Batch bioreactor	108.9	[167]
Naringenin	*Fj*TAL, *Pc*4CL, *Ph*CHS, *Ms*CHI	One copy genome integration	*S. cerevisiae* CEN.PK102-5B / Aromatic amino acids overproducing strain; Expression of *Cr*CPR to enhance cytochrome P450 activity	Synthetic fed-batch medium	Microtiter plates	1.55	[168]
Liquiritigenin	*Fj*TAL, *Pc*4CL, *Ph*CHS, *Ms*CHI, *Am*CHR					5.31	
Kaempferol	*Fj*TAL, *Pc*4CL, *Ph*CHS, *Ms*CHI, *Am*F3H, *At*FLS					26.57	
Resokaempferol	*Fj*TAL, *Pc*4CL, *Ph*CHS, *Am*CHR, *Ms*CHI, *Am*F3H, *At*FLS					0.51	
Quercetin	*Fj*TAL, *Pc*4CL, *Ph*CHS, *Ms*CHI, *Am*F3H, *At*FLS, *Ph*FMO					20.38	
Fisetin	*Fj*TAL, *Pc*4CL, *Ph*CHS, *Am*CHR, *Ms*CHI, *Am*F3H, *At*FLS, *Ph*FMO					1.65	
Naringenin	*Fj*TAL, *At*4CL2, *Ha*CHS, *Ms*CHI	One copy genome integration	*S. cerevisiae* BY4741 / Aromatic amino acids overproducing strain; ACC overexpression; decrease of flux towards fatty acid synthesis	Sucrose (10 g/L)	Shake flask	90	[169]

Table 3.2: *Continuation*

Phenolic compound	Genes [1]	Genetic system	Chassis / Chassis modification [2]	Substrate[3]	Conditions	Titer (mg/L)	Reference
Naringenin	*At*PAL, *At*C4H, *At*4CL, *Rs*CHS, *Ps*CHI	One copy genome integration	*S. cerevisiae* IMX581 / Aromatic amino acids overproducing strain; Expression of *At*CPR to enhance cytochrome P450 activity; Overexpression of mutant ACC1; Expression of malonate assimilation genes	Glucose (30 g/L)	Fed-batch bioreactor	2000	[170]
Pinocembrin	*At*PAL, *At*C4H, *Pha*CNL *At*4CL, *Rs*CHS, *Ps*CHI, *Sb*CHI2	One copy genome integration	*S. cerevisiae* IMX581 / Aromatic amino acids overproducing strain; Expression of CPR to enhance cytochrome P450 activity; Overexpression of mutant ACC1; Expression of malonate assimilation genes; Replacement of TSC13 by *Md*ECR	Glucose (20 g/L)	Shake flask	80	[171]
Curcumin	*At*PAL, *At*4CL, *At*C4H, *Aa*CPR, *At*HCT *At*CCoAOMT *At*C3'H, *At*CSE, *Cl*DCS, *Cl*CURS	One copy genome integration and episomal plasmids	*S. cerevisiae* BY4742 / Replacement of TSC13 by *Md*ECR	Glucose (20 g/L)	Shake flask	1.5	[92]

[1] 4CL: 4-coumarate-CoA ligase; C3'H: *p*-coumaroyl shikimate-3'-hydroxylase; C3H: 4-coumarate 3-hydroxylase; C3H3: *p*-coumaroyl ester 3-hydroxylase; C4H: cinnamate-4- hydroxylase; CCoAOMT: caffeoyl-CoA O methyltransferase; COMT: caffeic acid *O* -methyltransferase; CHI: chalcone isomerase; CHS: chalcone synthase; CNL: cinnamate-CoA ligase; CPR: cytochrome P450 reductase; CSE: caffeoyl-shikimate esterase; CURS: curcumin synthase; DCS: diketide-CoA synthase; HpaB and HpaC: 4-hydroxyphenylacetate 3-hydroxylase; F3H: flavanone 3-hydroxylase; FLS: flavonol synthase; FMO: cytochrome P450 flavonoid monooxygenases; HCT: shikimate hydroxycinnamoyl transferase; IFS: isoflavone synthase; PAL: phenylalanine ammonia lyase; STS: stilbene synthase; TAL: tyrosine ammonia lyase; VST: resveratrol synthase; *Aa: Artimisia annua*; *Ah: Arachis hypogaea; Am: Astragalus mongholicus; At: Arabidopsis thaliana; Cr: Catharanthus roseus; Fj : Flavobacterium johnsoniaeu; Gm: Glycine max; Ha:Hypericum androsaemum; Ms:Mendicago sativa; Nt: Nicotiana tabacum; Pa: Pseudomonas aeruginosa; Pc: Petroselinum crispum; Ph: Populus hybrid; Phd: Petunia hybrida; Ptr: Populus trichocarpa; Ps: Paeonia suffruticosa; Rc: Rhodobacter capsulatus; Rg: Rhodotorula glutinis; Rt: Rhodosporidium toruloides; Rs: Rhododendron simsii; Sb: Scutellaria baicalensis; Se: Salmonella enterica; Sf: Sophora flavescens; St: Solanum tuberosum; Vv: Vitis vinifera.*[2] Chassis modifications in addition to pathway integration when applied. ACC: acetyl-CoA carboxylase; *araE:* arabinose-H$^+$ transporter, CPR: cytochrome P450 reductase; *Md*ECR: enoyl-CoA reductase gene from *Malus domestica*; PAD: phenylacrylic acid decarboxylase; TAT1: Tyrosine and tryptophan amino acid transporter; CIB5: cytochrome B5; TSC13: double-bond reductase involved in fatty acid synthesis. [3] Synthetic fed-batch medium contains a glucose polymer which is converted into glucose monomers by glucose releasing enzymes during the fermentation process.

3.2.2 Spatial Location of Heterologous Enzymes

Organelles are important suppliers of cofactors. In mitochondria, the pool of acetyl-CoA is higher than in cytoplasm [172]. This may be advantageous for the expression of enzymes related with polyphenol synthesis since malonyl-CoA plays a key role in the biosynthetic pathway. In higher plants, polyphenol biosynthetic enzymes are co-localized and assembled in protein complexes and the metabolic channelling effect decreases the formation of by-products. In analogy, compartmentalization or scaffolding the polyphenol enzymes in yeast may have a positive effect on the enzymatic activity and therefore on the polyphenol production. The compartmentalization of the phenylpropanoid pathway has never been achieved. However, this strategy was already used to produce terpenoids in genetically modified yeasts yielding good results [173]. For this reason, the compartmentalization of the polyphenol pathway appears as a must-try in future works.

Closely locating two active sites or channelling the intermediate compounds between the enzymes may also improve the metabolic efficiency of the heterologous enzymes. This can be accomplished by using fusion proteins or by constructing synthetic scaffolds, respectively. Zhang et al. [174] constructed a translational fusion protein of 4CL from *A. thaliana* and stilbene synthase (STS) from *Vitis vinifera* (4CL:STS). The fusion protein was constructed by replacing the stop codon of the 4CL gene by a three-amino acid linker and the STS sequence. Resveratrol biosynthesis in yeasts transformed with 4CL:STS increased 15-fold as compared with the transformants co-expressing 4CL and STS. Moreover, Wang and Yu [162] constructed synthetic scaffolds to recruit 4CL and STS to improve resveratrol production. The scaffolds interacted with the heterologous enzymes through the small peptide ligands that were expressed in the end of each heterologous gene. This strategy allowed the substrate channelling between the two enzymes. The engineered strain produced five-fold more resveratrol over the one where scaffolds were not used. In addition, the production of resveratrol was 2.7-fold improved comparing with the production obtained using fusion proteins [174], thus suggesting more effectiveness when scaffolds are used.

3.2.3 Strain Optimization

The optimization of the heterologous pathways is a key step for the development of efficient yeast cell factories to produce polyphenols. Besides that, the yeast chassis should also be genetically engineered to maximize the production yields. These genetic modifications may include the overexpression or deletion of endogenous genes to increase the polyphenol precursors supply or to prevent the

intermediate consumption. These modifications allow the production of polyphenols in higher yields from simple substrates such as glucose, which represents a big step towards an industrial application. In this section, strategies used to improve the yeast chassis for polyphenol production are described.

3.2.3.1 Amino Acids Overproducing Strains

To improve the production of the desired compounds in engineered cells it is important to perform genetic modifications to improve the amounts of precursors available. The modifications could be deletions of genes involved in the deviation of a precursor and consequently, in the production of by-products or the overexpression of genes involved in the precursor biosynthesis. The aromatic amino acids precursors of the phenylpropanoids acids are not produced in high amounts by *S. cerevisiae*, thus representing a limiting step for the polyphenol production [150]. To achieve a high polyphenol yield, the media can be supplemented with precursors such as aromatic amino acids or hydroxycinnamic acids. However, this makes the process expensive for industrial applications. Therefore, the development of strains capable of converting glucose or other simple carbon sources to polyphenols also represents an attractive engineering strategy. The aromatic amino acid biosynthesis is a branched pathway regulated at the transcriptional, translational, and allosteric levels (**Figure 3.4**). At the allosteric level, the effector molecules are the aromatic amino acids tyrosine and phenylalanine. For example, the reactions catalysed by chorismite mutase (CM) and 3-deoxy-D-arabino-heptulosonate-7-phosphate synthase (DAHPS), enzymes involved in the shikimate pathway, are feedback-inhibited by tyrosine and phenylalanine [175]. Koopman et al. [167] constructed an engineered *S. cerevisiae* strain capable of overproducing aromatic amino acids by replacing the DAHPS gene, for a feedback-insensitive version. Consequently, the replacement of this gene by an insensitive version was important to maintain the amino acids production. Moreover, the deletion of phenylpyruvate decarboxylase (PDC) that was responsible for the conversion of phenylpyruvate, the precursor of phenylalanine, into phenylacetaldehyde, was important to prevent the pathway deviation. This optimized strain produced larger amounts of naringenin comparatively to the non-optimized strain [167]. In a different study, Li et al. [163] constructed a pathway for the *de novo* biosynthesis of resveratrol from glucose, and to improve the flux towards aromatic amino acids, the researchers developed a feedback-inhibition-resistant strain overexpressing CM and DAHPS. This resulted in 4.85 mg/L resveratrol, a titer 1.8 times higher than the one obtained without the overexpressed genes [163]. More recently, a strain highly adapted to produce *p*-coumaric acid was developed by performing several modifications in yeast chassis to program the

carbon metabolism towards the aromatic amino acid biosynthesis [150]. The heterologous pathway was composed by PAL and C4H from *A. thaliana,* and the native cytochrome (CYB5) and the *A. thaliana* P450 reductase were also overexpressed to improve the cytochrome P450 activity. The chassis modifications also included the expression of a feedback insensitive DAHPS and CM. Moreover, three native shikimate pathway genes and a heterologous version of prephenate dehydrogenase (PDH) were overexpressed to increase the total shikimate pathway activity. To improve the shikimate precursor erythrose-4-phosphate (E4P) availability, a heterologous phosphoketalose-based pathway was inserted. In addition, to optimize the carbon flux from glycolysis towards the aromatic amino acid biosynthesis, promoters of key node genes were replaced. PDC was also deleted to prevent pathway deviation. The final strain produced 12.5 g/L of *p*-coumaric acid, by far the highest titer reported.

The expression of heterologous metabolic pathways impacts the cellular physiology and frequently triggers a stress response. The identification of the affected pathways and then the genetic modification of target genes can improve the titers of the desired product [176]. Rodriguez et al. [148] found after transcriptome and metabolome computational analyses significant expression changes in a set of genes in an engineered yeast strain able to produce *p*-coumaric acid. Genes involved in the transport of amino acids, polyamines and sugars were found to be downregulated. Then, the researchers knocked out these specific genes to evaluate its effect in *p*-coumaric acid production titers. The deletions improved the synthesis of the polyphenol precursor. The highest improvement (up to 50%) was obtained by the deletion of tyrosine and tryptophan amino acid transporter 1 (TAT1). The authors hypothesized that this deletion resulted in a decrease of the leakage of tyrosine from the cells, thus being more available to produce *p*-coumaric acid [148].

3.2.3.2 Extender and Cofactor Availability

To produce one polyphenol molecule, it is necessary to have at least one molecule of malonyl-CoA since this molecule acts as an extender molecule in the final reactions. However, the levels of malonyl-CoA inside the cell are low, representing a limiting step in the heterologous production of polyphenols. Malonyl-CoA is naturally synthesized by acetyl-CoA carboxylase (ACC). This enzyme catalyses the carboxylation of acetyl-CoA to malonyl-CoA in microorganisms. The malonyl-CoA is mainly used to produce fatty acids and phospholipids, leaving only a very limited amount available to produce secondary metabolites [177].

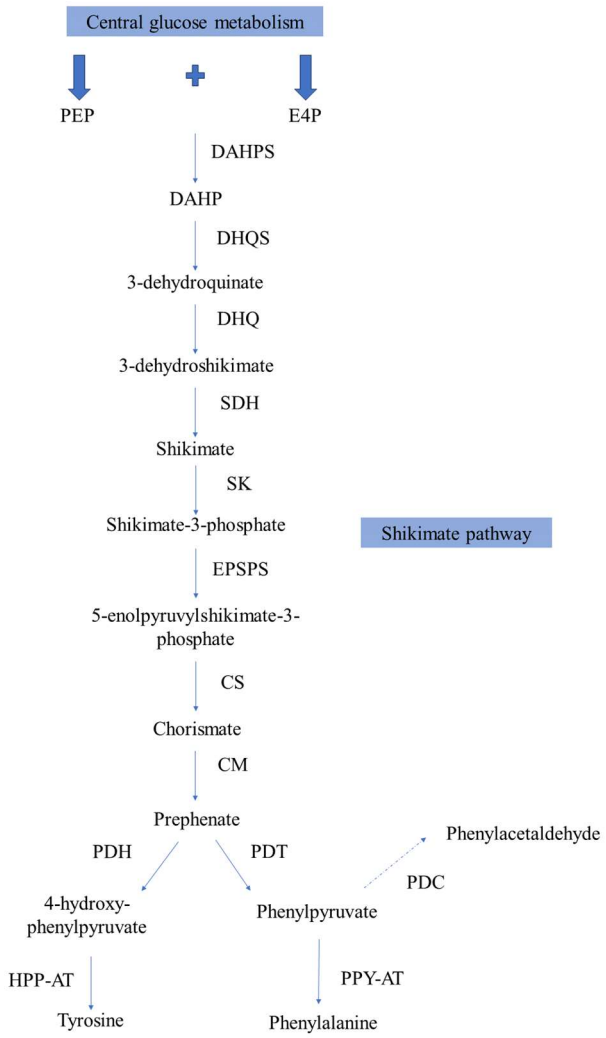


Figure 3.4: Pathways involved in the aromatic amino acids biosynthesis. CM: chorismate mutase; CS: chorismate synthase; DAHP: 3-deoxy-D-arabino-heptulosonate-7-phosphate; DAHPS: 3-deoxy-D-arabino-heptulosonate-7-phosphate synthase; DHQ: 3-dehydroquinate dehydratase; DHQS: 3-dehydroquinate synthase; E4P: D erythrose-4-phosphate; EPSPS: 5-enolpyruvylshikimate 3-phosphate synthase; HPP-AT: 4 hydroxyphenylpyruvate aminotransferase; PDC: phenylpyruvate decarboxylase; PDH: prephenate dehydrogenase; PDT: prephenate dehydratase; PEP: Phosphoenolpyruvic acid; PPY-AT: phenylpyruvate aminotransferase; SDH: shikimate dehydrogenase; SK: shikimate kinase.

Shin et al. [58] investigated the production of resveratrol from supplemented tyrosine. They introduced PAL, C4H, 4CL and STS genes into *S. cerevisiae*. In addition, the authors replaced the ACC native promoter by a stronger inducible promoter (pGAL1-galactose inducible promoter). The overexpression of the ACC gene resulted in a 1.3-fold increase in resveratrol concentration [161]. The ACC enzyme can be targeted for degradation via phosphorylation by sucrose non-fermenting protein 1 (Snf1p) in yeast decreasing the endogenous pool of malonyl-CoA inside the cell [178]. Li et al. [163], apart from the aforementioned resveratrol pathway multi-copy integration and DAHPS and CM overexpression, also used a strategy to improve the intracellular malonyl-CoA bioavailability. This strategy included the overexpression of a post-translational deregulated ACC. This version of the ACC gene was previously

described by Shi et al. [179] and it contains two-point mutations in serine residues to prevent the phosphorylation and degradation by Snf1p. The engineered strain enhanced the productivity by 31% [163]. Afterwards, the same research team [164], applied a more complex approach. They changed the heterologous pathway to use phenylalanine instead of tyrosine and overexpressed the CPR from *A. thaliana* and the native CYB5 to enhance the P450 function required by C4H. DAHPS and CM were also overexpressed and the PDC was deleted. The shikimate kinase from *E. coli* was also overexpressed to increase the metabolic flux through the shikimate pathway. Regarding the malonyl-CoA bioavailability, in addition to the mutated ACC overexpression, the acetyl-CoA synthase from *Salmonella enterica* was also overexpressed. The final strain produced 800 mg/L of resveratrol in a fed-batch fermentation. This represented by far the highest yield reported regarding the polyphenol heterologous production in *S. cerevisiae.*

The expression of heterologous enzymes in yeast might also be challenging due to ineffective cofactor supply attributable to variations in cellular environments. For instance, *S*-adenosyl methionine (SAM) acts as methyl group donor in several methylation reactions [180]. The phenylpropanoid pathway has an essential methylation step, the conversion of caffeic acid into ferulic acid catalysed by caffeic acid *O*-methyltransferase (COMT). SAM regeneration is accomplished via methyl cycle that is highly regulated [180]. Therefore, SAM engineering is a complex procedure. Chen et al. [155] studied SAM engineering strategies to improve ferulic acid biosynthesis in yeast. Since SAM is synthesized from methionine, the overexpression of genes related with SAM and methionine biosynthesis appeared as a promising strategy to improve SAM levels, however it did not improve ferulic acid biosynthesis. The researchers hypothesized that *S*-adenosylhomocysteine (SAH), the by-product of SAM methylation reactions, could inhibit COMT activity. Hereupon, the overexpression of genes related with SAH conversion improved ferulic acid biosynthesis. The authors concluded that cofactor engineering is intricate due to the complexity of the pathways involved with several feedback-regulated and limiting steps and that cofactor engineering strategies should be carefully designed.

3.2.4 Transporter Expression

The transport of small molecules into and out of the cell can be sometimes the biggest limiting factor in metabolic engineering. Transporters can maximize the productivity by improving substrate uptake or product secretion. The removal of a product with reported antimicrobial activity from the intracellular medium will increase the product biosynthesis and decrease the product toxicity for the cell and the

extraction costs. Polyphenols are characterized to often accumulate in plant vacuoles [181] and afterwards be transported to the site of action. However, the mechanism of polyphenol transportation is not yet fully understood. Wang et al. [160] [expressed the arabinose-H+ transport protein (AraE) in a resveratrol engineered yeast. The transporter greatly improved the resveratrol synthesis. This suggests that AraE may increase the resveratrol permeability through lipid membranes when the concentration inside the cell reaches the threshold. More studies on polyphenol transport are required, not only to increase their production but also to enable their extraction as soon as an industrial production process is implemented.

3.3 Final Remarks

In recent years, the demand for polyphenols by the pharmaceutical industry has increased. Consequently, the scientific community has been developing several efforts to establish a stable platform to produce these therapeutic compounds. The yeast *S. cerevisiae* has been a usual host for polyphenol production. Recent advances in the synthetic biology field allowed the creation of new and powerful genetic tools to efficiently engineer *S. cerevisiae,* such as the CRISPR-Cas9 based ones outlined in this chapter. The use of these tools and the exploration of metabolic engineering strategies is enabling genetic engineers to construct yeast strains increasingly adapted to the production of polyphenols. Nevertheless, the implementation of an industrial process to produce polyphenols using microbial cell factories still has a long way to go before becoming a reality. However, the recently high production of the precursor *p*-coumaric acid in *S. cerevisiae* [150] opened the door to producing high amounts of polyphenols soon. In addition, the production of some polyphenols, such as curcuminoids, are still very little explored in *S. cerevisiae* although the pathways are generally well characterized [70]. We believe that these pathways can be effectively expressed in yeast, possibly with higher titers, and therefore should be more explored.

CHAPTER 4. Curcumin Biosynthesis from Ferulic Acid by Engineered *Saccharomyces cerevisiae*

ABSTRACT: Curcumin is a polyphenolic compound found in *Curcuma longa*. This bioactive molecule has several reported health-benefit effects, being the anticarcinogenic activity among the most promising ones. However, curcumin extraction from natural sources is hampered by impure products obtained from harsh chemicals and limited by plant seasonality and high prices. Therefore, curcumin heterologous production emerged as an interesting alternative. *Escherichia coli* has been explored as chassis but the implementation of the pathway in *Saccharomyces cerevisiae* can have several advantages, including its generally regarded as safe status. Hence, *S. cerevisiae* was engineered for the first time to produce curcumin from its precursor ferulic acid. The enzymes 4-coumarate-CoA ligase (4CL1) from *Arabidopsis thaliana* or feruloyl-CoA synthetase (FerA) from *Pseudomonas paucimobilis* and type III polyketide synthases (PKSs) from *Oryza sativa* or *C. longa* were expressed in BY4741 strain. To avoid ferulic acid deviation, the gene FDC1 coding a ferulic acid decarboxylase was deleted. The maximum curcumin titer was obtained with FerA combined with *C. longa* PKSs (2.7 mg/L). This is the first work reporting the expression of a feruloyl-CoA synthetase and curcuminoid biosynthetic enzymes in *S. cerevisiae*, and consequently, curcumin production.

The information presented in this chapter was published in Biotechnology Journal:

Rainha, J., Rodrigues, J. L., Faria, C., & Rodrigues, L. R. (2022). Curcumin biosynthesis from ferulic acid by engineered *Saccharomyces cerevisiae*. *Biotechnology Journal*, *17*(3), 2100400.

4.1 Introduction

Curcumin, a natural polyphenolic secondary metabolite produced in the rhizome of the herb *Curcuma longa*, has received increased attention by the scientific community due to its wide pharmaceutical effects. The anticancer activity is the most documented property with very promising results. Curcumin can target several stages of carcinogenesis and, due to its low toxicity to healthy cells it is particularly appealing as a therapeutic agent (reviewed in **Chapter 2**).

For health-related research, preparations of high amounts of pure curcumin are required. However, curcumin accumulates in the plant in low quantities over long growth periods. Moreover, curcumin extraction process uses harsh chemicals [8] and produces a mix of curcuminoids which composition varies in accordance with origin and growth conditions of the plant. Consequently, *in vitro* and *in vivo* testing of curcuminoid extracts can lead to contradictory results [182]. Alternatively, chemical synthesis could be used to synthetize curcuminoids; however, this process is complex [8]. All these factors block the advances of *in vitro* and *in vivo* research. Therefore, the heterologous biosynthetic production of curcumin in microorganisms appears as an attractive alternative to overcome plant extraction limitations (**Chapter 2**). The expression of heterologous pathways in workhorse hosts displays multiple advantages, either by eliminating seasonality from the production process or by guaranteeing that the target compound is the main product of the fermentation broth and therefore greatly simplifying the downstream processes [183].

In *C. longa*, curcumin is produced from ferulic acid, a phenylpropanoid pathway derivative, in three enzymatic reactions. The first reaction is catalysed by the multiple substrate enzyme 4-coumarate-CoA ligase (4CL) responsible to convert ferulic acid to the respective CoA ester, feruloyl-CoA. Afterwards, the next reactions are catalysed by type III polyketide synthases (PKSs): diketide-CoA synthase (DCS) and the curcumin synthase (CURS) that synthesize curcumin from two molecules of feruloyl-CoA and one molecule of malonyl-CoA (**Figure 4.1**). Other curcuminoids can be produced from *p*-coumaric acid or from a combination of ferulic acid and *p*-coumaric acid. These curcuminoids are called bisdemethoxycurcumin and demethoxycurcumin, respectively [74], and are usually present in the curcumin purified extracts commercially available.

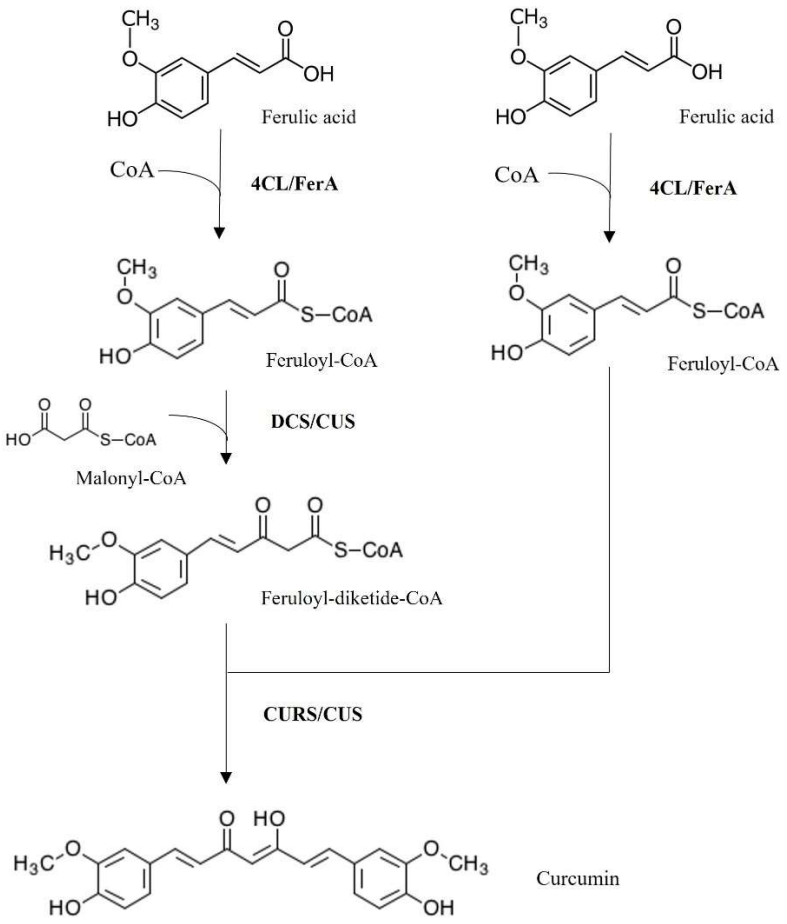


Figure 4.1: Curcumin biosynthetic pathway. The names of enzymes are abbreviated as follows: 4CL: 4-coumarate-CoA ligase; FerA: feruloyl-CoA synthetase; DCS: diketide-CoA synthase; CURS: curcuminoid synthase; CUS: curcumin synthase.

Curcumin and other curcuminoids have already been heterologously produced in some microorganisms (**Chapter 2**). Katsuyama et al. [78] were the first to report the production of curcumin in *Escherichia coli*. The curcuminoid synthase (CUS) identified in *Oryza sativa*, that is also a type III PKS and is able to perform the "one-pot" synthesis of curcumin, was found to be ideal for combinatorial biosynthesis [95] More recently, we reported the highest production titer (563.4 mg/L) and yields (up to 100% mol/mol) also using recombinant *E. coli* with several pathway and bioprocess optimizations implemented [82] Other researchers produced curcuminoids in *Aspergillus oryzae*, *Pseudomonas putida*, and *Yarrowia lipolytica* [89–91] In the present study, we evaluated the potential of the yeast *Saccharomyces cerevisiae* to be a suitable biological chassis for the heterologous production of pure curcumin. The yeast *S. cerevisiae*, besides the extensive toolbox of genetic modifications and fermentative strategies available (**Chapter 3**), possesses the generally regard as safe (GRAS) status which enables further applications in the food and pharmaceutical industries. In addition, as a eukaryotic organism, *S. cerevisiae* if often considered a preferred chassis to express eukaryotic enzymes due to its post-translational modification

machinery and higher ability for proper protein folding. Thus, *S. cerevisiae* represents an interesting organism to develop a curcumin microbial cell factory. Therefore, this work focuses for the first time on the expression of the type III PKS enzymes responsible for curcuminoids production in *S. cerevisiae*. The 4CL1 from *A. thaliana* or feruloyl-CoA synthetase (FerA) from *Pseudomonas paucimobilis* and CUS from *O. sativa* or *C. longa* DCS and CURS encoding genes were cloned in a yeast expression plasmid and the enzymes were expressed in *S. cerevisiae*. The recombinant yeast strains were tested for curcumin production by supplementing ferulic acid. This is the first report on the curcumin production in engineered *S. cerevisiae*, as well as on the use of a feruloyl-CoA synthetase for polyphenol heterologous production in this host.

4.2 Materials and Methods

4.2.1 Strains, Plasmids, and Genes

E. coli NZY5α (NZYTech, Lisbon, Portugal) competent cells were used for molecular cloning, vector propagation and storage. *E. coli* was cultured at 37°C and 200 rpm in lysogeny broth (LB) supplemented with 100 μg/L of ampicillin for selection. *S. cerevisiae* BY4741 was used as the host strain for curcumin biosynthesis. Yeast strains were cultivated at 30°C and 200 rpm in synthetic defined minimal (SD) media or in yeast extract peptone dextrose (YPD) media. SD media was composed by 6.7 g/L of yeast nitrogen base (Sigma Aldrich, Steinheim, Germany), 20 g/L of glucose, 0.38 g/L leucine, 0.10 g/L histidine, 0.10 g/L methionine and 0.10 g/L uracil (when needed) to cover for auxotrophies. YPD media was composed by 20 g/L yeast extract, 10 g/L peptone and 20 g/L of glucose and 200 μg/L of geneticin were added for selection (when required). All *S. cerevisiae* strains used in this work are listed in **Table 4.1**.

Table 4.1: *Saccharomyces cerevisiae* strains used in this work.

Strains	Genotype	Reference
S. cerevisiae BY4741	S288C isogenic yeast strain: MATa; his3Δ1; leu2Δ0; met15Δ0; ura3Δ0	[184]
S. cerevisiae B4C	*S. cerevisiae* BY4741; pSPGM-1_4CL1_CUS	This study
S. cerevisiae B4CK	*S. cerevisiae* BY4741; pSPGM-1_4CL1_CUS_KanMx	
S. cerevisiae B4DC	*S. cerevisiae* BY4741; pSPGM-1_4CL1_DCS_CURS	
S. cerevisiae Δ*fdc1*	*S. cerevisiae* BY4741; *fdc1* 105_113del	
S. cerevisiae Δ*fdc1* B4DC	*S. cerevisiae* Δ*fdc1*; pSPGM-1_4CL1_DCS_CURS	
S. cerevisiae BADC	*S. cerevisiae* BY4741; pSPGM-1_FerA_DCS_CURS	
S. cerevisiae Δ*fdc1* BADC	*S. cerevisiae* Δ*fdc1*; pSPGM-1_FerA_DCS_CURS	

The vector used for curcumin pathway construction was pSP-GM1 (Addgene plasmid #64739) [185]. The 4CL1 from *A. thaliana*, CUS from *O. sativa*, and DCS and CURS (more specifically CURS1) from *C. longa* encoding genes were codon-optimized and cloned into pNZY29 by NZYTech Portugal. *P. paucimobilis* FerA encoding gene was codon-optimized, synthetized as gBlock by Integrated DNA Technologies (IDT, Iowa, USA) and cloned into pJET1.2 (Thermo Fisher Scientific, Massachusetts, USA). For the knock-out of *fdc1* (encoding ferulic acid decarboxylase) (NCBI ID: 852152) using the CRISPR-Cas9 tool, pCRCT (Addgene plasmid #60621) was used [128]. All the plasmids and primers used are listed in **Table 4.2**. The double strand DNA fragment (gBlock) containing the protospacer and the repair fragment with an 8-bp deletion was synthetized by IDT. The sequences of the codon optimized genes and gBlocks are listed in **Appendix 1**.

Table 4.2: Plasmids used in this work.

Plasmids	Features	Source
pUC57_4CL	AmpR, ori; codon-optimized 4CL1	NZYTech, Portugal
pUC57_CUS	AmpR, ori; codon-optimized CUS	NZYTech, Portugal
pUC57_DCS	AmpR, ori; codon-optimized DCS	NZYTech, Portugal
pUC57_CURS	AmpR, ori; codon-optimized CURS	NZYTech, Portugal
pJET_FerA	AmpR, ori; codon-optimized FerA	IDT, USA
pSP-GM-1	AmpR, URA3, ori, 2µ ori	Addgene #64739
pSP-GM-1_4CL1	pSP-GM-1; P_{TEF1} -> 4CL1 -> T_{ADH1}	This study
pSP-GM-1_4CL1_CUS	pSP-GM-1_4CL1; P_{PGK1} -> CUS -> T_{CYC1}	This study
pSP-GM-1_4CL1_CUS_KanMX	pSP-GM-1_4CL1_CUS; URA3:1-189>KanMx>189-801	This study
pSP-GM-1_DCS	pSP-GM-1; P_{TEF1} -> DCS -> T_{ADH1}	This study
pSP-GM-1_DCS_TDH3	pSP-GM-1_DCS, pTDH3	This study
pSP-GM-1_DCS_TDH3_CURS	pSP-GM-1_DCS_TDH3; P_{TDH3}-> CURS -> T_{synt27}	This study
pSP-GM-1_4CL_DCS _CURS	pSP-GM-1_DCS_pTDH3_CURS; P_{PGK1} -> 4CL1 -> T_{CYC1}	This study
pSP-GM-1_FerA_DCS _CURS	pSP-GM-1_DCS_pTDH3_CURS; P_{PGK1} -> FerA -> T_{CYC1}	This study
pCRCT	AmpR, URA3, lacZ, ori, 2µ ori, iCas9, tracRNA	Addgene #60621
pCRCT_gBlock	pCRCT; P_{SNR52} -> gBlock -> T_{SUP4}	This study

4.2.2 Plasmids and Strain Construction

All the primers used are listed in **Table 4.3**. For CUS pathway construction, codon-optimized 4CL and CUS genes were PCR-amplified using Phusion High-Fidelity DNA polymerase (Thermo Fisher Scientific) with primers 4CL_FW and 4CL_RV, and CUS_FW and CUS_RV, respectively. The 4CL1 gene fragment was digested using *Sac*I and *Not*I and cloned, using T4 DNA ligase (Thermo Fisher Scientific), into

empty pSP-GM1 digested with the same enzymes forming pSP-GM1_4CL. Next, codon-optimized CUS gene was digested with *BamH*I and *Hind*III and cloned into digested pSP-GM1_4CL to form pSP-GM1_4CL_CUS. To insert KanMX into pSP-GM1_4CL_CUS in the middle of*ura3*, the plasmid was digested with *EcoR*V and KanMX was PCR-amplified from a Euroscarf strain available at our lab using KanMX primer pair. The amplified fragment was assembled into digested pSP-GM1_4CL_CUS using NEBuilder HiFi DNA Assembly kit (NEB, Massachusetts, USA) originating pSP-GM1_4CL_CUS_KanMX. To build DCS and CURS pathways, codon optimized DCS and CURS genes and TDH3 promoter (pTDH3) were amplified using the corresponding primers. DCS gene fragment and pSP-GM1 were digested with *Sac*I and *Not*I, ligated and cloned to originate pSP-GM1_DCS. Next, pTDH3 was cloned into pSP-GM1_DCS using *Asc*I and *Avr*II. The TDH3_RV primer allowed to also insert a *Sph*I restriction site right after TDH3 sequence. Next, CURS gene fragment was inserted into pSP-GM1_DCS_TDH3 between *Sph*I and *Avr*II restriction sites. Note that, CURS gene reverse primer possessed the sequence of the synthetic terminator 27. Afterwards, codon optimized 4CL gene was amplified using 4CL_assembly_FW and 4CL_assembly_RV and pSP-GM1_DCS_TDH3_CURS digested with *BamH*I and *Hind*III. The resulting 4CL gene fragment possessed 25-bp homology ends to digested pSP-GM1_DCS_TDH3_CURS. The two fragments were co-transformed into *S. cerevisiae* BY4741 using lithium acetate method [186]and *in vivo* assembled [187] to form pSP-GM1_DCS_CURS_4CL. FerA gene was amplified using FerA_FW and FerA_RV primers and *in vivo* assembled into digested pSP-GM1_DCS_TDH3_CURS to form pSP-GM1_FerA_DCS_CURS. The *in vivo* assembled plasmids were extracted from yeast following the protocol described elsewhere [188], however using lyticase (Sigma Aldrich) and NucleoSpin Plasmid Miniprep Kit (Macherey-Nagel, Düren, Germany) instead. Extracted plasmid was transformed into *E. coli* for storage, propagation, and sequencing. To construct CRISPR-Cas9 plasmid to delete FDC1 gene, the DNA fragment containing a guide sequence targeting this gene and the repair fragment (synthetized as gBlock) was cloned into pCRCT using Golden Gate Assembly as reported by Bao and co-workers [128]. Colony PCR and sequencing were performed to confirm correct cloning of DNA parts with the respective primer pairs (tADH1_FW/pTEF_RV; pPGK1_FW/tCYC1; KanColFW/RV and PCRCT_FW/RV). All the constructions were confirmed by colony-PCR (Supreme NZYTaq II DNA polymerase, NZYTech), digestion and sequencing (Eurofins, Ebersberg, Germany). Plasmids carrying the curcumin biosynthetic pathway were transformed into *S. cerevisiae* using lithium acetate method [186]. Mutants were selected in SD-URA (SD media without uracil) or YPD +G418 (YPD with geneticin). For *fdc1* gene knock-out strain construction (*S. cerevisiae* BY4741 Δ*fdc1*),

pCRCT_gBlock was transformed into BY4741 using the same method. Next, to confirm the deletion, the area upstream and downstream the *fdc1* gene was amplified by colony-PCR, using FDC_FW and FDC_REV primers. The CRISPR-Cas9 plasmid was cured by counterselection using 1 g/L of 5-fluoroorotic acid and the curcumin biosynthetic pathway plasmid inserted into *S. cerevisiae* BY4741 Δ*fdc1*.

Table 4.3: Primer pairs used to PCR-amplify DNA parts and for colony PCR (forward and reverse primers – FW and RV). Underlined sequence indicates the restriction site. Bold sequence indicates the synthetic terminator 27.

Primer Name	**Sequence 5'-3'**
4CL1_FW	AAAAAGAGCTCTCATAAACCATTTGCCAATTTAGCT (SacI)
4CL1_RV	AATTTGCGGCCGCAAAAAAATGGCACCACAAGAGCAA (NotI)
CUS_FW	AACGCGGATCCAAAAAAATGGCCCCTACTACGACAA (BamHI)
CUS_RV	AACCCAAGCTTTTAATTGACATGAGATGTTGCGTG (HindIII)
KanMx_FW	TTGTTTACTAAAAACACATGTGGATGACATGGAGGCCCAGAATA
KanMx_RV	CCTCCATGGAAAAATCAGTCAAGATCAGTATAGCGACCAGCATTC
DCS_FW	TTTTCGAGCTCTCAATTAAGCCTGCATGAA (SacI)
DCS_RV	AAAAAAGCGGCCGCAAAAAAATGGAAGCTAACGGTTATAG (NotI)
CURS_FW	ACATGCATGCATGTAAAAAAATGGCCAATCTACATGCG (SphI)
CURS_RV	TTTTTCCTAGG**TTTGAAAGATGATACTCTTTATTTCTAGACAGTTATATATATATATATATATATATATACCAC CCA**TTACAAGGGCATGGACCTTA (AvrII)
4CL_assembly_FW	TTACAACAAATATAAAACAAGGATCAAAAAAATGGCACCACAAG
4CL_assembly_RV	TCTTAGCTAGCCGCGGTACCAAGCTTCATAAACCATTTGCCAATTTA
FerA_assembly_FW	CTTTTTACAACAAATATAAAACAAGAAAAAAATGACGGTCGAGGCGG
FerA_assembly_RV	CGGATCTTAGCTAGCCGCGGTACCATCAATCTACCAACATAAGAGCATCA
pTEF_RV	CGTACCACTTCAAAACACC
tADH1_FW	GTGTCAACAACGTATCTAC
pPGK1_FW	GTGATCTCCAGAGCAAAGT
tCYC1_RV	CTTCGAGCGTCCCAAAACCTT
KanCol_FW	CTGAGAGTGCACCATACCACAG
KanCol_RV	ACAATACCTGGGCCCACCA
PCRCT_FW	CTTGGGCTAGCGGTAAAG
PCRCT_RV	AACGACACCCTAGAGGAA
FDC_FW	ATGAGGAAGCTAAATCCAG
FDC_RV	TCACATTTTACTACTGGAACC

4.2.3 Curcumin Production and Extraction

Biological transformants of each strain were inoculated in 7 mL of SD -URA media or YPD + G418 and grown during 24 h. Afterwards, these cultures were used to inoculate 50 mL of SD -URA or YPD +G418

in 250 mL shake flasks (initial optical density at 600 nm (OD_{600nm}) of 0.1). At 24 h of growth, 16 mg/L (0.08 mM) or 194 mg/L (1 mM) of ferulic acid was added to the media. Media samples were taken at 24, 48 and 72 h for ferulic acid quantification. After 72 h upon inoculation, yeast cells were pelleted (9000 rpm, 10 min) and washed with distilled water. To extract curcumin, 1 mL of methanol was added to the pellet, and the mix was vigorously vortexed for 2 min and left to rest for 2 h. Next, the tubes were centrifuged again (9000 rpm, 10 min) and the supernatant was collected for quantification. The procedure was repeated until no yellow colour was visible in the cell pellet.

4.2.4 Curcumin Quantification

HPLC was used to quantify curcumin and ferulic acid. The chromatographic system was composed by Shimadzu Nexera-X2 (Shimadzu Corporation, Kyoto, Japan) (CBM-20A system controller, LC-30AD pump unit, DGU-20A 5R degasser unit, SPD-M20A detector unit, SIL-30AC autosampler unit, CTO-20AC column oven) system and a Kinetex 2.6 μm Polar C18 100 Å LC column (150 × 4.6 mm) (Phenomenex, California, USA). Mobile phase A was composed of water with 0.1% (v/v) of trifluoracetic acid and the mobile phase B was composed of acetonitrile. The oven temperature was 25°C. For ferulic acid quantification, the following gradient was used at a flow rate of 1 mL/min: 10%–40% mobile phase B for 16 min, 40%–70% for 1 min, 70%–10% for 4 min, and 10% mobile phase B for an additional 4 min. For curcumin quantification, a gradient of 40%–43% mobile phase B for 15 min, 43%–70% for 3 min, 70%–40% for 4 min, and 40% mobile phase B for an additional 5 min was used. Curcumin was detected at 425 nm with a retention time of 18.6 min while ferulic acid was detected at 310 nm at 9.6 min.

4.3 Results and Discussion

4.3.1 Curcumin Production using 4CL and CUS Enzymes

In this study we focused on the part of the pathway specific for curcuminoids biosynthesis, that includes the steps catalysed by PKS enzymes and 4CL. The PKS enzymes responsible for curcuminoids production have never been expressed in *S. cerevisiae*. In addition, the step that converts ferulic acid to feruloyl-CoA is poorly explored as the enzyme normally used, 4CL, is usually applied in *S. cerevisiae* heterologous pathways only to convert coumaric acid to coumaroyl-CoA. Moreover, we wanted to study curcumin production without the interference of other enzymes activity. Therefore, the biosynthesis of curcumin by engineered *S. cerevisiae* was first attempted by introducing two enzymes responsible for

the conversion of phenylpropanoid ferulic acid into curcumin, namely the 4CL1 from *A. thaliana* and CUS from *O. sativa*. The genes were placed under control of two strong constitutive promoters with similar strengths pTEF1 and pPKG1, respectively [189]. The constructed recombinant plasmid pSP-GM1_4CL_CUS was introduced into *S. cerevisiae* BY4741 yielding the strain B4C (**Table 4.1**). Curcumin production was evaluated in several transformants using SD-URA minimal media by supplementing 16 mg/L (0.08 mM) of ferulic acid at 24 h upon inoculation. Since curcumin is a yellow pigment, it was expected that its presence would cause a change in the colour of the culture media as observed in the works using *E. coli* as microbial chassis [139]. This colour change was indeed observed, and it was used as a straightforward visual control for curcumin production (**Figure 4.2A**). After 72 h of fermentation, curcumin was extracted from cells with methanol (**Figure 4.2B**). The HPLC analysis confirmed the presence of curcumin in the extracts (**Figure 4.2C**) and the quantification revealed that the strain B4C produced a maximum curcumin titer of 88.8 μg/L (**Table 4.4**). The assays were performed with different transformation colonies and a high variability of curcumin titers is observed between cultures (ranging from 23.0–88.8 μg/L). This phenomenon has been reported before and derives from the *S. cerevisiae* ability to adjust the copy number of episomal plasmids (2 μ origin) in the cell, leading to the formation of heterogenous populations with different levels of expression and productivities [114].

Table 4.4: Curcumin production by the different *Saccharomyces cerevisiae* strains harbouring the curcumin biosynthetic pathway. Ferulic acid (16 mg/L) was added to the culture medium at 24 h of fermentation. Colonies 1 to 5 were picked from the transformation plate. Connected lines represent cultures that exhibit statistically significant different curcumin production values (* student t-test, $p<0.05$). SD: synthetic defined media; YPD: yeast extract peptone dextrose media; 4CL: 4-coumarate-CoA ligase; FerA: feruloyl-CoA synthetase; DCS: diketide-CoA synthase; CURS: curcuminoid synthase; CUS: curcumin synthase

		Curcumin colony titer (μg/L)					
Name	**Medium**	**1**	**2**	**3**	**4**	**5**	**Average (±Standard deviation)**
B4C (↑4CL↑CUS)	SD	78.2	88.8	73.9	87.3	23.0	70.2 (±22.1) *
B4CK (↑4CL↑CUS↑KanMX)	YPD	79.8	120.0	103.1	119.4	86.3	101.7 (±15.1)**
B4DC (↑4CL↑DCS↑CURS)	SD	609.1	1067.0	704.3	356.1	173.6	582.5 (±279.5) *;**;***
ΔB4DC (Δ*fdc1*↑4CL↑DCS↑CURS)	SD	852.3	808.2	1365.8	1171.8	969.0	1033.4 (±190.3)***;****
BADC (↑FerA↑DCS↑CURS)	SD	1127.3	1413.3	1014.0	1321.3	1248.8	1224.9 (±128.7)
ΔBADC (Δ*fdc1*↑FerA↑DCS↑CURS)	SD	2728.1	1789.1	2036.2	1585.5	1275.9	1883.0 (±548.5)****

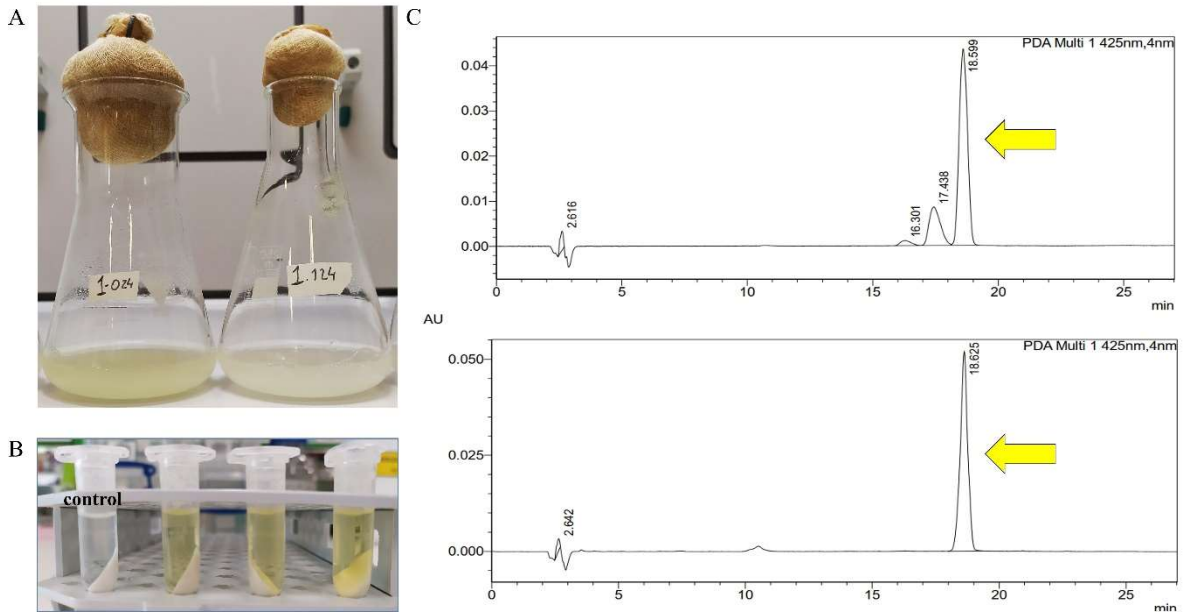


Figure 4.2: Curcumin production in *Saccharomyces cerevisiae* after 72 h of growth. (**A**) Strain B4C (with 4-coumarate-CoA ligase (4CL) and curcumin synthase (CUS) genes) in shake flasks containing SD-URA with glucose. The precursor ferulic acid was added 24 h upon inoculation at a concentration of: 16 mg L−1 (0.08 mM) (Left flask); and 194 mg L−1 (1 mM) (Right flask). The yellow colour in the right flask indicates the presence of curcumin; (**B**) Curcumin was extracted with methanol from *S. cerevisiae* B4C cells. After extraction the solution turned yellow; (**C**) HPLC analysis of curcumin produced by the recombinant strain B4C. Upper chromatogram represents the curcumin standard. Note: The other peaks visualized in the standard correspond to other curcuminoids also present in the mixture (demethoxycurcumin and bisdemethoxycurcumin). Lower chromatogram represents one extract that contains curcumin produced by the recombinant S. cerevisiae B4C

The ferulic acid concentration supplemented was selected according to the literature and preliminary experiments. Ferulic acid is a plant phenolic compound involved in plant physiological processes and defence mechanisms [190]. The toxicity of ferulic acid in yeast fermentation has been reported and its threshold was defined as 1.8 mM [191]. Therefore, initial fermentations were carried with 1 mM of ferulic acid and although no inhibitory effect on cellular growth was observed, no curcumin production was detected either. The phenolic compounds toxicity mechanism in yeast is not well understood. Despite cellular growth was not inhibited at 1 mM concentration (**Table 4.5**), the yeast metabolism was probably affected at this concentration since ferulic acid is known to affect lipid metabolism, pentose phosphate pathway, ergosterol biosynthesis and to induce reactive oxygen species formation [192]. Therefore, supplementation of high concentrations of phenolic compounds may not be a good approach at this stage of pathway development. For instance, Shin et al. [159] that used *p*-coumaric acid, a ferulic acid analogue, to produce resveratrol in yeast reported the highest yields using 16 mg/L (0.08 mM) of substrate. Hereupon, we defined this concentration to produce curcumin from ferulic acid. However, although the ferulic acid concentration added was low, significant amounts remained at the end of the fermentation. The concentration of ferulic acid during fermentation with strain B4C dropped from the initial 16 mg/L to 5.8 ± 0.63 mg/L at 48 h, and to 4.5 ± 1.04 mg/L at 72 h. This decrease in ferulic

acid concentration was not reflected in curcumin production suggesting that the supplemented ferulic acid was probably being deviated by endogenous metabolic pathways. It is known that *S. cerevisiae* can convert ferulic acid (or other hydroxycinnamic acids) to 2-methoxy-4-vinylphenol using FDC1 as a detoxification mechanism [193]. Therefore, it is possible that this enzyme may have deviated some of the ferulic acid added to the culture medium to other pathways.

Table 4.5: Cell densities of the different *Saccharomyces cerevisiae* strains during the fermentations. The values represent the media of different transformants with the respective standard deviation. SD: Synthetic Defined media; YPD: Yeast Peptone Dextrose media; FA: Ferulic Acid; DCW: Dry Cell Weight.

Strain	Media	[FA] mg/L	$DCW_{24\,h}$ (g/L)	$DCW_{48\,h}$ (g/L)	$DCW_{72\,h}$ (g/L)
S. cerevisiae BY4741 with empty vector	SD	0	0.91 (± 0.09)	1.17 (± 0.04)	1.26 (± 0.04)
	SD	16	0.96 (± 0.06)	1.14 (± 0.05)	1.32 (± 0.02)
	SD	194	0.91 (± 0.10)	1.14 (± 0.09)	1.31 (± 0.06)
S. cerevisiae Δ*fdc1*	SD	0	0.90 (± 0.13)	1.19 (± 0.07)	1.23 (± 0.07)
	SD	16	0.89 (± 0.07)	1.10 (± 0.03)	1.24 (± 0.01)
S. cerevisiae B4C	SD	16	0.91 (± 0.04)	1.20 (± 0.06)	1.29 (± 0.07)
S. cerevisiae B4CK	YPD	16	1.91 (± 0.08)	3.21 (± 0.39)	3.79 (± 0.53)
S. cerevisiae B4DC	SD	16	0.96 (± 0.04)	1.05 (± 0.04)	1.33 (± 0.03)
S. cerevisiae Δ*fdc1* B4DC	SD	16	0.86 (± 0.11)	1.07 (± 0.08)	1.33 (± 0.04)
S. cerevisiae BADC	SD	16	0.78 (± 0.05)	1.03 (± 0.10)	1.34 (± 0.04)
S. cerevisiae Δ*fdc1* BADC	SD	16	0.90 (± 0.12)	1.02 (± 0.06)	1.28 (± 0.05)

4.3.2 Curcumin Production using Rich Culture Medium

In Liu et al. [194] work, the use of rich media instead of synthetic minimal media to produce resveratrol using genetic modified yeast improved the production yields. Hence, to evaluate if fermentation in rich media would result in higher curcumin production, the KanMX selection marker (G418 resistance) was inserted into pSP-GM1_4CL_CUS disrupting URA3, creating the pSP-GM1_4CL_CUS_KanMX. The constructed plasmid was transformed into *S. cerevisiae* BY4741, originating the strain B4CK. The production of curcumin by B4CK was tested using YPD + G418 media and ferulic acid (16 mg/L) was supplemented at 24 h upon inoculation as described before. The maximum titer of curcumin increased almost 1.4-fold, with the best producer reaching 120.0 μg/L of curcumin (**Table 4.4**). However, it was not possible to conclude about the significance of these results due to the high variability found among the tested colonies. In addition, as expected, higher biomass concentrations were achieved using rich medium. Consequently, besides the overall amount of extracted curcumin increased, the produced curcumin per cell was not improved using rich media.

4.3.3 Curcumin Production using Type III PKS from *C. longa*

After evaluating the pathway containing CUS enzyme, a pathway harbouring DCS and CURS from *C. longa* was also tested to evaluate if the curcumin production could be further increased. For that purpose, codon optimized DCS and CURS were inserted in pSP-GM1 together with 4CL1 to form pSP-GM1_4CL_DCS_CURS. The plasmid was introduced into BY4741 and transformants were labelled as strain B4DC. The curcumin productivity was evaluated in SD media using the same conditions as described before. B4DC transformants showed a higher capacity to produce curcumin from supplemented ferulic acid (**Figure 4.3**). BDCP colony 2 was the best producer reaching 1067.0 µg/L (13.3 mol% yield) of curcumin (**Table 4.4**), 12 times more than the best producer using CUS enzyme. Overall, the production of curcumin using the DCS/CURS system was much higher than when CUS was used. The two-enzyme system proved to be more suitable for the development of a curcumin cell factory.

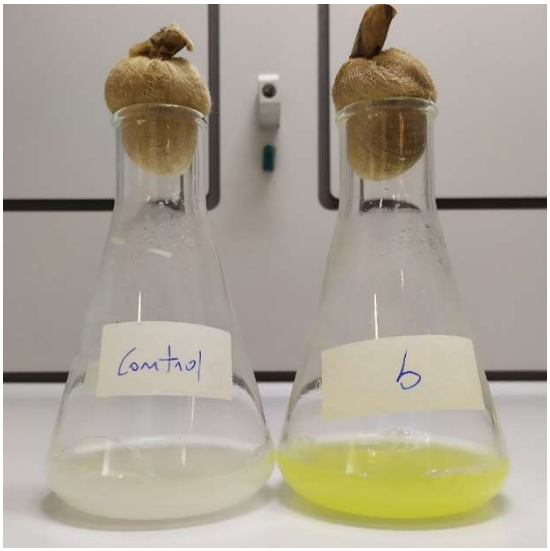


Figure 4.3: *Saccharomyces cerevisiae* strain B4DC fermentation flasks. Left flask: No ferulic acid was added to the culture media; Right flask: 16 mg/L of ferulic acid were added to the media at 24 h of fermentation; the yellow colour formation in the culture media indicate the presence of curcumin.

4.3.4 Suppressing FDC Activity in *S. cerevisiae*

Since it was found that the ferulic acid consumed was not being solely used to produce curcumin, we decided to investigate if the knock-out of *fdc1* gene, that encodes FDC1, could further improve the curcumin productivity. We developed a mutant *S. cerevisiae* BY4741 defective in FDC1 activity (*S. cerevisiae* Δ*fdc1*) using the CRISPR-Cas9 technology. Cas9 was directed to target an upstream zone of *fdc1* and the repair fragment was designed to insert an 8- bp deletion on *fdc1*. This deletion caused a

frameshift mutation putting an early stop codon in frame and resulting in no enzyme translation. It was verified that *S. cerevisiae* BY4741 Δ*fdc1* was not able to degrade ferulic acid (*data not shown*), thus indicating that FDC1 was responsible for its previous consumption in the culture medium. After confirming that the ferulic acid was not being consumed, the plasmid carrying the curcumin biosynthetic pathway (pSP-GM1_4CL_DCS_CURS) was transformed into this strain and the curcumin biosynthesis was evaluated (**Table 4.4**). The best producer, the *S. cerevisiae* strain B4DC Δ*fdc1* colony 3, produced 1.3 more curcumin than the B4DC higher value. Overall, the deletion of *fdc1* seems to have improved curcumin production although there is a high variability among colonies as previously observed. The influence of this gene deletion can be more significant in the future when higher concentrations and yields of curcumin are obtained.

4.3.5 Curcumin Production using Feruloyl-CoA Synthetase (FerA)

FerA is an enzyme identified in the bacteria *P. paucimobilis* that can convert ferulic acid into feruloyl-CoA, such as the 4CL from plants [195]. FerA has never been used to develop a curcumin microbial cell factory. Feruloyl-CoA synthetases have never been expressed in *S. cerevisiae*. Hereupon, we tested if the use of FerA instead of 4CL could further improve the curcumin titers. For that purpose, we constructed the plasmid pSP-GM1_FerA_DCS_CURS and we inserted it in BY4741 to obtain the recombinant *S. cerevisiae* strain BADC. The curcumin production was evaluated using the conditions previously established. Strain BADC top producer reached 1.4 mg/L of curcumin (1.3-fold improvement comparing to the *S. cerevisiae* B4DC best producer) (**Table 4.4**). In general, curcumin production seems to have been improved when replacing 4CL by FerA. One reason for this higher efficiency may be related to the energy requirements of each enzyme, as FerA is an ADP-forming enzyme [195], catalysing the reaction in a single step, while 4CL is an AMP forming enzyme [196], catalysing the conversion of ferulic acid to feruloyl-CoA in two steps. The use of FerA represents a step forward in the heterologous production of curcuminoids in different hosts since the conversion of ferulic acid to feruloyl-CoA has been previously identified as the limiting step in the production of curcumin [78]. Moreover, pSP-GM1_FerA_DCS_CURS was transformed in *S. cerevisiae* Δ*fdc1*, as it was demonstrated that this deletion can be beneficial for the curcumin production. Using *S. cerevisiae* Δ*fdc1* BADC the curcumin titers (**Table 4.4**) reached 2728.1 μg/L (yielding 34.1% mol per mol and 2.1 mg/g DCW) representing a 1.9-fold improvement comparatively with *S. cerevisiae* BADC best producer. This value represents the highest one achieved in an engineered yeast.

4.4 Conclusions

The recent increasing demand for curcumin inspired research on the development of microbial cell factories for its heterologous production. In this work, we demonstrated that the GRAS yeast *S. cerevisiae* has potential to be used as platform to produce curcumin. Curcuminoid biosynthetic enzymes were successfully expressed in *S. cerevisiae* and the recombinant yeast was able to produce pure curcumin from supplemented ferulic acid using 4CL1 from *A. thaliana* or FerA from *P. paucimobilis* combined with the type III PKS from *O. sativa* (CUS), or from *C. longa* (CURS and DCS). As far as we know, this work represents the first report on the production of curcumin in yeast. In the future, to increase pathway stability and reduce the heterogenicity between transformants, genome integration of curcumin biosynthetic pathway must be performed. In addition, more strain improvements are still required to increase production yields, namely the increase of the bioavailability of the malonyl-CoA precursor for curcumin synthesis. In *S. cerevisiae*, malonyl-CoA concentration is maintained at low levels due to the intrinsic tight regulation of the fatty acid biosynthesis [197] The remaining malonyl-CoA may not be sufficient to produce high production yields in our strain. The precursor tolerance also needs to be improved to produce high amounts of curcumin in the future. Possible targets were already identified [198] The integration of genes from phenylpropanoid pathway for *de novo* curcumin biosynthesis using a tyrosine overproducing strain is also an appealing strategy to reduce the toxic effects of ferulic acid supplementation to the cells and decrease the production costs foreseeing an industrial application. We believe that this work represents a good basis for the development of a *S. cerevisiae* cell factory to produce high purity preparations of curcumin.

CHAPTER 5. *De novo* Curcumin Production in *Saccharomyces cerevisiae*

ABSTRACT: Curcumin, a natural polyphenol derived from turmeric, has gathered immense interest due to its diverse pharmacological properties. Traditional extraction methods from *Curcuma longa* plants present limitations in meeting the growing demand for this bioactive compound, giving significance to its production by genetically modified microorganisms. Here, we have developed an engineered *Saccharomyces cerevisiae* to produce curcumin from glucose. A pathway composed by 4-hydroxyphenylacetate 3-hydroxylase complex from *Pseudomonas aeruginosa* and *Salmonella enterica*, caffeic acid *O*-methyltransferase from *Arabidopsis thaliana*, feruloyl-CoA synthetase from *Pseudomonas paucimobilis*, diketide-CoA synthase and curcumin synthase from *C. longa*, was introduced in a *p*-coumaric acid overproducing *S. cerevisiae* strain. This strain produced 240.1 ± 15.1 μg/L of curcumin. Following optimization of phenylpropanoids conversion, a strain capable of producing 4.2 ± 0.6 mg/L was obtained. This study reports the successful *de novo* production of curcumin in *S. cerevisiae* for the first time.

The information presented in this chapter was published in ACS Synthetic Biology:

Rainha, J., Rodrigues, J. L., Rodrigues, L. R. (2024). *De novo* Curcumin Production in *Saccharomyces cerevisiae*, *ACS Synthetic Biology*.

5.1 Introduction

Curcumin, a natural yellow-orange phenolic compound found in turmeric (*Curcuma longa*), has recently gained recognition due to its potential as cancer-fighting drug [31]. However, curcumin versatility extends beyond its potential as a cancer-fighting agent. Pre-clinical trials have unveiled a spectrum of additional biological and therapeutic activities, due to its anti-inflammatory and antioxidant activities [8, 70]. These findings open opportunities to explore the curcumin potential for a wide range of health-related issues, making it an exciting candidate for further research and development in the field of natural medicine. Numerous dietary supplements containing curcumin are derived from raw turmeric rhizomes, which may contain impurities and do not provide a pure representation of curcumin [199]. Several conditions can affect the curcumin content of turmeric rhizomes that ranges from 2 to 5% of curcumin by weight [19]. Curcumin extraction is usually accomplished using organic solvents and high temperatures such as in Soxhlet extraction [77]. Turmeric extracts usually contain a mixture of three curcuminoids with curcumin being the most representative (±77%), followed by demethoxycurcumin (±17%) and bisdemethoxycurcumin (±3%) [12]. Pure curcumin can be obtained from a curcuminoid extract using purification techniques like chromatography procedures [76]. In summary, the process of extracting and purifying curcumin from plants is quite laborious. Moreover, for large scale production, curcumin plant extraction is limited by plant seasonality and by the large costs and sustainability problems associated with plant crops. On the other hand, curcumin can be chemically synthesized using acetylacetone and boron trioxide in a very complex and harsh process [200]. A promising biotechnological solution for high-level production of curcumin involves fermentation using genetically engineered microorganisms. Microorganisms have fast production cycles and can grow in inexpensive substrates surpassing limitations of traditional curcumin production methods. The microbial production of curcuminoids has been achieved in *Escherichia coli*, and in other less conventional hosts such as *Pseudomonas putida*, *Aspergillus oryza*, *Yarrowia lipolytica* (**Chapter 2**, **Section 2.4**). However, most of these works involve the supplementation of costly curcumin precursors, which is a limitation for potential industrial applications. The *de novo* synthesis of curcumin in microbes offers an attractive and cost-effective solution for scalability. However, curcumin has mostly been synthesized from simple carbon sources in genetic modified *E. coli* [86, 88]. *E. coli* is not a GRAS (generally regarded as safe) organism, and the expression of the heterologous genes usually relies on the use of plasmids, that require constant selective antibiotic pressure for maintaining, and the supplementation of expensive inductors, which is also not desirable. The yeast *S. cerevisiae* is a role model microorganism for genetic

engineering purposes due to its safety status and clear metabolic pathways. The extensive molecular tools available, such as the clustered regularly interspaced palindromic repeats (CRISPR)-Cas9 based ones, allow the genomic integration of multiple heterologous genes without requiring antibiotic markers (**Chapter 3, Section 3.1.2)**. Furthermore, significant research has been dedicated to the biosynthesis of plant polyphenols in this yeast (**Chapter 3, Section 3.2**).

Curcumin biosynthesis, in *C. longa*, is accomplished by reactions catalysed by the type III polyketide synthases (PKSs), diketide-CoA synthase (DCS) and curcumin synthase (CURS). Three isoforms of CURS were identified in *C. longa*, each one with a different substrate affinity explaining the diversity of curcuminoids found in turmeric [75]. The phenylpropanoids *p*-coumaric and/or ferulic acid are the precursors of curcuminoids. In the case of curcumin, two molecules of ferulic acid are required while for demethoxycurcumin, for instance a ferulic acid and a *p*-coumaric acid molecule are used. First, phenylpropanoids are activated by condensation with a coenzyme A (CoA) molecule, a reaction carried by 4-coumarate-CoA ligase (4CL). After that, DCS adds a malonyl group to the activated phenylpropanoid through reaction with an extender molecule, the malonyl-CoA. Afterwards, CURS catalyses the curcuminoid synthesis by condensation of the extended activated phenylpropanoid with another activated phenylpropanoid molecule [71]. The phenylpropanoids are synthesized from the aromatic amino acids, phenylalanine and tyrosine, via the phenylpropanoid pathway which involves the reactions catalysed by tyrosine ammonia lyase (TAL), phenylalanine ammonia lyase (PAL), trans-cinnamate 4-monooxygenase (C4H), 4-coumarate 3-hydroxylase (C3H) and caffeic acid *O*-methyltransferase (COMT) and having cinnamic acid, *p*-coumaric acid, caffeic acid and ferulic acid as intermediates [72].

In this study, our goal was to accomplish curcumin *de novo* biosynthesis, eliminating the need for precursor supplementation. In addition, our previous approach involved the use of a plasmid for gene expression (**Chapter 4**), which is not conducive to large-scale applications. To address this, we herein integrated the curcumin biosynthesis genes into the yeast genome using a CRISPR-Cas9 approach. In summary, we explored metabolic engineering strategies with the aim of developing an efficient cell factory for curcumin production.

5.2 Materials and Methods

5.2.1 Genes, Plasmids and Strains

The native yeast genes coding for acetyl-CoA carboxylase (ACC1), fatty-acyl coenzyme A oxidase (FOX1) and methylenetetrahydrofolate reductase (MET13) were PCR-amplified from *S. cerevisiae* genomic DNA. The genes for 4-hydroxyphenylacetate 3-monooxygenase reductase component (HpaC) from *Salmonella enterica* (*Se*HpaC) and the native version of 4-hydroxyphenylacetate 3-monooxygenase oxygenase component (HpaB) from *Pseudomonas aeruginosa* (*Pa*HpaB) were amplified by colony-PCR from strains available in our lab. Genes DCS and CURS from *C. longa* (*Cl*DCS and *Cl*CURS), and feruloyl-CoA synthetase (FerA) from *Pseudomonas paucimobilis* (*Pp*FerA) were previously codon-optimized for *S. cerevisiae* (**Chapter 4**). COMT from Arabidopsis thaliana (*At*COMT) and the optimized version of *Pa*HpaB (*Pa*HpaB (opt)) were also codon-optimized for *S. cerevisiae* and PCR-amplified from synthetic fragments (TWIST Bioscience, USA). All gene sequences are present in the **Appendix 1**. Genes were cloned using restriction ligation or by Gibson assembly and confirmed via colony PCR, digestion, and sequencing.

The plasmids pSP-GM1 (Addgene #64739) [185] and pBEVY_GL (Addgene #51225) [201] were used for the construction of the integration cassettes, placing the genes under control of the respective promoters. The plasmid pSP-GM1 was also used for the overexpression of *S. cerevisiae* native genes. Guide RNA (gRNA) plasmids were kindly provided by Liu et al. [150] targeting genomic loci where heterologous genes could be efficiently and stably expressed.

E. coli NZY5α (NZYTech, Portugal) was used for plasmid cloning, storage, and propagation. *S. cerevisiae* IMX581 [131] and QL158 [150] (both with Cas9 integrated) were used as host strains for the integration of curcumin biosynthetic pathways. *S. cerevisiae* strains, primers sequences and plasmids used in this work are listed in **Table 5.1, 5.2, 5.3** respectively.

Table 5.1: *Saccharomyces cerevisiae* strains used in this study.

Strains	Genotype	Reference
IMX581	MATa ura3-52 can1D::cas9-natNT2 TRP1 LEU2 HIS3	Euroscarf: Y40593 [131]
QL158	IMX581, pdc5Δ, aro10Δ, XII-2::(p_{GPM1}-*At*PAL2-t_{FBA1})+(p_{TDH3}-*At*C4H-t_{CYC1})+(p_{HXT7}-*At*ATR2-t_{YX212})+(p_{PGK1}-CYB5-t_{ADH1}), X-3::(p_{TPI1}-*Ec*aroL-t_{YX212})+(t_{ADH1}-ARO7 G141S-p_{TEF1})+(p_{PGK1}-ARO4 K229L-CYC1t), X-4::(t_{CYC1}-ARO1-p_{TPI1})+(p_{TDH3}-ARO2-t_{ADH1})+(t_{TDH2}-ARO3-p_{TEF1}), XI-3::(p_{TEF1}-*Fj*TAL-t_{TDH2})+(t_{FBA1}-*Mt*PDH1-p_{TDH3})	[150]
JI1	IMX581, XII-4::(p_{TEF1}-*Cl*DCS-t_{ADH1}; p_{TDH3}-*Cl*CURS-t_{synt27}; p_{PGK1}-*Pp*FerA-t_{CYC1}), pQLC10	This study
JI2	JI1, XII-1::(p_{TEF1}-*At*COMT-t_{ADH1}), pQLC032	
JI3	JI2, XI-5::(p_{TEF1}-*Se*HpaC-t_{ADH1}; p_{PGK1}-*Pa*HpaB-t_{CYC1}), pQLC09	
JG0	IMX581, XII-4::(p_{GAL1}-*Cl*DCS-t_{ADH1}; p_{GAL10}-*Cl*CURS-t_{ADH2}), pQLC10	
JG1	JG0, XII-3::(p_{GAL10}-*Pp*FerA-T_{ADH2}), pQLC133	
JQ01	QL158, XII-4::(p_{TEF1}-*Cl*DCS-t_{ADH1}; p_{TDH3}-*Cl*CURS-t_{synt27}; p_{PGK1}-*Pp*FerA-t_{CYC1}), pQLC10	
JQ02	JQ01, XII-1::(p_{TEF1}-*At*COMT-t_{ADH1}), pQLC032	
JQ1	JQ02, XI-5::(p_{TEF1}-*Se*HpaC-t_{ADH1};p_{PGK1}-*Pa*HpaB-t_{CYC1}), pQLC09	
JQCA1	QL158, XI-5::(p_{TEF1}-*Se*HpaC-t_{ADH1};p_{PGK1}-*Pa*HpaB-t_{CYC1}), pQLC09	
JQCA2	QL158, XI-5::(p_{TEF1}- coC3H-t_{ADH1};p_{PGK1}-coCPR1-t_{CYC1}), pQLC09	
JQCA3	QL158, XI-5::(p_{TEF1}-*Se*HpaC-t_{ADH1};p_{PGK1}-*Pa*HpaB(opt)-t_{CYC1}), pQLC09	
JQ2	JQ02, XI-5::(p_{TEF1}-*Se*HpaC-t_{ADH1};p_{PGK1}-*Pa*HpaB(opt)-t_{CYC1}), pQLC09	
JQ3	JQ2, XII-3::(p_{TEF1}-*Se*HpaC-t_{ADH1}; p_{PGK1}-*Pa*HpaB-t_{CYC1}), pQLC133	
JQ4	JQ3, XI-2::(p_{TEF1}-*At*COMT-t_{ADH1}), pQLC130	

5.2.2 Strain Construction

For strain construction, genomic integration was mediated by CRISPR-Cas9 technology (Mans et al., 2015). Integration cassettes harbouring the (promoter-gene-terminator)$_n$ were amplified from the corresponding constructed plasmid with a forward primer containing 25-bp homology to the upstream homology arm and a reverse primer with 25-bp homology to the downstream homology arm of the specific integration site. For instance, for the construction of JQ01 a cassette harbouring pTDH3-ClCURS1-tsynt27-tADH1-ClDCS-pPGK1-pTEF-PpFerA-tCYC was amplified from pSP-GM1_FerA_DCS_CURS using XII-4_pTDH3_FW and XII-4_tCYC_RV primers. Parallelly, the specific upstream and downstream homologous regions were amplified from *S. cerevisiae* genomic DNA, for this case using XII-4_US_FW/RV and XII-4_DS_FW/RV. The sequences of homology regions are provided in the **Appendix 2**. Next, the three fragments (100 ng/kb) were co-transformed in QL158 together with 1000 ng of the specific gRNA plasmid (pQLC010, in this case) using lithium acetate method [202] for *in vivo* assembly and simultaneous gap repair. The resulting strains were selected in yeast nitrogen base (YNB) minimal media (20 g/L glucose, 6.7 g/L of YNB and 0.10 g/L uracil) agar plates (15 g/L) and

the pathway integration confirmed via PCR of extracted genomic DNA. After confirmation, gRNAs plasmids were cured by plating with 1 g/L of 5-fluoroorotic acid (5-FOA).

Table 5.2: Primers used in this work. For gene amplification primers, the bold sequence represents the restriction enzyme sequence used to clone the gene, and the underlined sequence represents the homology sequence for cloning via assembly cloning. For cassette amplification primers, the underlined sequence represents the 25-bp homology sequence for the corresponding homology arms.

Primer name	**Sequence 5'-3'**
Gene amplification	
HpaB_FW	GC**GGATCC**AAAAAAATGAAACCAGAAGACTTTAGA (BamHI)
HpaB_RV	AACCC**AAGCTT**TTACTGACGTATTCTGTCCA (HindIII)
HpaC_FW	AAAAA**GAGCTC**TTAAACAGGCGCTTCCATC (SacI)
HpaC_RV	A**GCGGCCGC**AAAAAAATGCAAGTAGATGAACAACG (NotI)
HpaBopt_FW	CGTAATACGACTCACTATAGGGCCCAAAAAAATGAAACCAGAAGACTTTAGA
HpaBopt_RV	CAACTTCTGTTCCATGTCGACGCCCTTACTGACGTATTCTGTCCA
COMT_FW	TTTTC**GAGCTC**CTATAGTTTCTTCAACAATTCTATTAA (SacI)
COMT_RV	AAAA**GCGGCCGC**AAAAAAATGGGAAGTACCGCTGAA (NotI)
DCS_GAL_FW	AAAA**TCTAGA**TCAATTAAGCCTGCATGAA (XbaI)
DCS_GAL_RV	AAAA**GGATCC**AAAAAAATGGAAGCTAACGG (BamHI)
CURS_GAL_FW	AAAA**GGTACC**AAAAAAATGGCCAATCTACAT (KpnI)
CURS_GAL_RV	AAAA**GAATTC**TTACAAGGGCATGGACCTTA (EcoRI)
FerA_GAL_FW	AAAA**GGTACC**AAAAAAATGGCCAATCTACAT (KpnI)
FerA_GAL_RV	AAAA**GAATTC**TCAATCTACCAACATAAGAG (EcoRI)
ACC_FW	AAA**GAGCTC**TTATTTCAAAGTCTTCAACAATTT (SacI)
ACC_RV	T**GCGGCCGC**AAAAAAATGAGCGAAGAAAGCTTATT (NotI)
FOX_FW	CGTAATACGACTCACTATAGGGCCCAAAAAAATGACGAGACGTACTACTATTAA
FOX_RV	CAACTTCTGTTCCATGTCGACGCCCTCACTTGTTTATTTTCGATAAAAT
MET13_FW	CGTAATACGACTCACTATAGGGCCCAAAAAAATGAAGATCACAGAAAAATTA
MET13_RV	CAACTTCTGTTCCATGTCGACGCCCTTATAGGCTTAGTAGGATGG
Colony PCR	
pPGK1_FW	GTGATCTCCAGAGCAAAGT
tCYC_RV	CTTCGAGCGTCCCAAAAC
tAHD1_FW	GTCACTTTAAAATTTGTATAC
pTEF_RV	CGTACCACTTCAAAACACC
pGAL_FW	CAACCATAGGATGATAATGCGAT
pGAL_RV	TTTACATTTCCACAACATATAAGTAAG
tADH2_RV	TTATTCGTGAAACTTCGAACAC
Homology arms amplification	
XII-4_US_FW	GTATCCGGCTGTTCCTTCATA
XII-4_US_RV	TGCCATAGTATGTGTGATGGAA

Table 5.2: *Continuation*

Primer name	**Sequence 5'-3'**
XII-4_DS_FW	ATTCCCCATTAGAGTCAAATAAA
XII-4_DS_RV	TTTCTGCCGTACCTGGAT
XI-5_US_FW	GCGGAGAAGTCGTTGATAG
XI-5_US_RV	TGGTGCACGGAGTTTATGG
XI-5_DS_FW	GCCCACAACCCAAGTTAA
XI-5_DS_RV	GATCATAGATCCGGCACTT
XI-2_US_FW	TAACTCTTCGTATGAGGATTTTC
XI-2_US_RV	TTCTATGGCACATTTTTCTGT
XI-2_DS_FW	CCACAAGTAAAGCTCGTTGA
XI-2_DS_RV	ATGGTTGAAAAGGTTACAGAG
XII-1_US_FW	GTTGAGCTCTGTCCTTCATG
XII-1_US_RV	GAAAGAACCGAACCGATGC
XII-1_DS_FW	GTTCAGTTTAGTGCTCTGT
XII-1_DS_RV	TGATGACTGTTTCTCAATCTTT
XII-3_US_FW	TGTGCCCCTTAAAATTCATATAC
XII-3_US_RV	GAATGAGCAGGTACCCCTTAT
XII-3_DS_FW	GCATAGAGCTAATTAGGTTTGAG
XII-3_DS_RV	GAACTTACAAGCTGATTTTGGTTC
Cassette amplification	
XII-4_pTDH3_FW	TTTTTCCATCACACATACTATGGCACTATTTTCGAGGACCTTGTCACC
XII-4_tCYC1_RV	CTTTTATTTGACTCTAATGGGGAATCTTCGAGCGTCCCAAAACC
XI-5_tADH1_FW	AATGTGCCATAAACTCCGTGCACCAGAGCGACCTCATGCTATACC
XI-5_tCYC1_RV	CTTATGATTAACTTGGGTTGTGGGCCTTCGAGCGTCCCAAAACC
XI-2_tADH1_FW	CTCAACAGAAAAATGTGCCATAGAAGAGCGACCTCATGCTATACCTG
XI-2_pTEF1_RV	ACTGGTCAACGAGCTTTACTTGTGGGCACACACCATAGCTTCAAAAT
XII-1_tADH1_FW	ATTTTGGCATCGGTTCGGTTCTTTC GAGCGACCTCATGCTATACCTG
XII-1_pTEF1_RV	ACTCAGACAGAGCACTAAACTGAACGCACACACCATAGCTTCAAAAT
XII-3_tADH1_FW	TATAATAAGGGGTACCTGCTCATTCGAGCGACCTCATGCTATACCTG
XII-3_tCYC1_RV	AACTCAAACCTAATTAGCTCTATGCCTTCGAGCGTCCCAAAACC
XII-4_tADH1_FW	TTTTTCCATCACACATACTATGGCA CCGGTAGAGGTGTGGTCA
XII-4_tADH2 _RV	CTTTTATTTGACTCTAATGGGGAATATGAGAAATATCGAGGGAGAC
XII-1_pGAL_FW	ATTTTGGCATCGGTTCGGTTCTTTCTTTCAAAAATTCTTACTTTTTTTTT
XII-1_tADH2_RV	ACTCAGACAGAGCACTAAACTGAACATGAGAAATATCGAGGGAGA

Table 5.3: Plasmids used in this work.

Plasmids	Features	Reference
pSP-GM1	AmpR, URA3, ori, 2μ ori	Addgene plasmid: #64739 [185]
pBEVY-GL	AmpR, LEU, ori, 2μ ori	Addgene plasmid: #51225 [201]
pSP-GM1_FerA_DCS_CURS	pSPGM1; p_{TEF1}-*Cl*DCS-t_{ADH1}; p_{TDH3}-*Cl*CURS1-t_{synt27}; p_{PGK1}-*Pp*FerA-t_{CYC1}	Chapter 4
pSP-GM1_HpaC	pSPGM1; p_{TEF1}-*Se*HpaC-t_{ADH1}	This study
pSP-GM1_HpaB_HpaC	pSPGM1_*Se*HpaC; p_{PGK1}-*Pa*HpaB-t_{CYC1}	
pSP-GM1_HpaBopt_HpaC	pSPGM1_*Se*HpaC; p_{PGK1}-*Pa*HpaBopt-t_{CYC1}	
pSP-GM1_COMT	pSPGM1; p_{TEF1}-*At*COMT-t_{ADH1};	
pBEVY-GL_DCS	pBEVY-GL; p_{GAL10}-*Cl*DCS-t_{ADH1}	
pBEVY-GL_DCS_CURS	pBEVY-GL_DCS; p_{GAL1}-*Cl*CURS1-t_{ADH2}	
pBEVY-GL_FerA	pBEVY-GL; p_{GAL1}-*Pp*FerA-t_{ADH2}	
pSP-GM1_FOX	pSP-GM1; p_{PGK1}-FOX1-t_{CYC1}	
pSP-GM1_ACC	pSP-GM1; p_{TEF1}-ACC1-t_{ADH1}	
pSP-GM1_FOX1_ACC	pSP-GM1_ACC; p_{PGK1}-FOX1-t_{CYC1}	
pSP-GM1_MET13	pSPGM1; p_{PGK1}-MET13-t_{CYC1}	
pLC-C3	AmpR, HIS3, ori, 2μ ori, p_{PGK1}-coC3H-t_{CYC1}, p_{TEF1}-coCPR1-t_{ADH1}	[154]
gRNA plasmids		
pQLC09	2μ ori, AmpR, KIURA3, gRNA-XI-5.Y	[150]
pQLC10	2μ ori, AmpR, KIURA3, gRNA-XII-4.Y	
pQLC133	2μ ori, AmpR, URA3, gRNA-XII-3.Y	
pQLC130	2μ ori, AmpR URA3 gRNA-XI-2.Y	
pQLC032	2μ ori, AmpR URA3, gRNA-XII-1.Y	

5.2.3 Strain Cultivation and Curcumin Extraction

E. coli was cultivated at 37 °C, 200 rpm in lysogeny broth (LB) - Lennox containing 100 μ g/mL of ampicillin. S. cerevisiae was cultivated in a yeast extract peptone dextrose (YPD) medium containing 20 g/L peptone, 10 g/L yeast extract, 20 g/L glucose or YNB minimal media containing the same concentration of glucose. For shake-flask fermentation, a 5 mL pre-culture was grown overnight at 30 °C, 200 rpm and used to inoculate 250 mL flasks containing 50 mL of media (YPD or YNB) with an initial optical density at 600 nm (OD_{600nm}) of 0.1. For galactose induction, 2% galactose was supplemented at 12 h. When necessary, ferulic acid, caffeic acid, or *p*-coumaric acid were supplemented at 24 h at a final concentration of 30 mg/L. Shake-flask fermentations were maintained

for 72 h. Samples were centrifuged and the supernatant was used to quantify phenylpropanoids, sugars and ethanol. Curcumin was extracted from cell pellets at the final timepoint, unless otherwise specified, using methanol as previously described (**Chapter 4, Section 4.2.3**).

5.2.4 Metabolites Analysis

For quantification of curcuminoids, *p*-coumaric acid, caffeic acid and ferulic acid, UHPLC was performed as previously reported (**Chapter 4, Section 4.2.4**). The method used for ferulic acid quantification was employed for the other phenylpropanoids. Caffeic acid, *p*-coumaric acid and ferulic acid were detected at 310 nm with retention times of 6.0 min, 8.0 min and 8.7 min, respectively. Curcuminoids were detected at 425 nm with detection times of 11.8 min for bisdemethoxycurcumin, 12.7 min for demethoxycurcumin and 13.5 min for curcumin. HPLC was used to quantify glucose, galactose, and ethanol. The chromatographic system was composed by Shimadzu LC-2060C equipped with Biorad Aminex HPX-87H (300 x 7.8 mm, 9 µm particle size) column. The oven temperature was set to 60 °C. Mobile phase was composed by 5 mM of sulphuric acid at flowrate of 0.6 mL/min for 25 min. Glucose was detected at 8.8 min, galactose at 9.5 min and ethanol at 21.8 min.

5.2.5 Bioinformatic Analysis

The yeast7.6cobra model (available at https://sourceforge.net/projects/yeast/files/) was used as the initial chassis for our study. Subsequently, we incorporated the heterologous genes, reactions, and metabolites involved in curcumin biosynthesis, resulting in the creation of the yeast7.6_curcumin model (Available online at: https://shorturl.at/epxA0). To validate the yeast7.6_curcumin model, we conducted various simulations, employing the following algorithms: parsimonious Flux Balance Analysis (pFBAs) [203], Minimization of metabolic adjustment (MOMA) [204] and regulatory on/off minimization (ROOM) [205]. These simulations were carried out with a fixed glucose uptake rate of 10 mmol/g_{DW}/h. For optimization, we utilized the gene over/under expression optimization problem (GOUProblem) module from MEWpy [206]. The optimization process aimed to enhance the production of curcumin. Three distinct objective functions were employed for solution evaluation: biomass-product coupled yield (BPCY); weighted yield (WYIELD); and modification type. The optimization algorithm was executed with a maximum of 500 generations and each generation consisted of 1000 individuals. To assess the robustness of optimization results, flux variability analysis (FVA) was employed [207].

Basic local alignment search tool (BLAST) analysis was conducted using protein-protein BLAST (blastp) algorithm available in NCBI BLAST tool (https://blast.ncbi.nlm.nih.gov). The *E. coli* CurA protein

sequence (NCBI Reference Sequence: NP_415966.6) was compared with the reference proteome of *S. cerevisiae* S288C found in the non-redundant protein sequences (nr) database. The algorithm parameters were set to default values, with the exception for word size, which was specifically set to 3.

5.3 Results and Discussion

5.3.1 Curcumin Biosynthesis from Supplemented Substrates

In the previous study (**Chapter 4**) we compared the efficiency of different pathways to synthesize curcumin in *S. cerevisiae* from supplemented ferulic acid. A pathway composed of *Pp*FerA and type III PKS *Cl*DCS and *Cl*CURS1 (**Figure 5.1**), achieved the highest curcumin titer relatively to other enzyme combinations. This previous work relied on the use of plasmids to express the heterologous genes in *S. cerevisiae* BY4741. However, the use of plasmids is less desirable for metabolic engineering purposes due to their instability and constant selective pressure for maintenance. Hereupon, the same pathway was integrated using CRISPR-Cas9 into *S. cerevisiae* IMX581, a strain with integrated Cas9 [131].

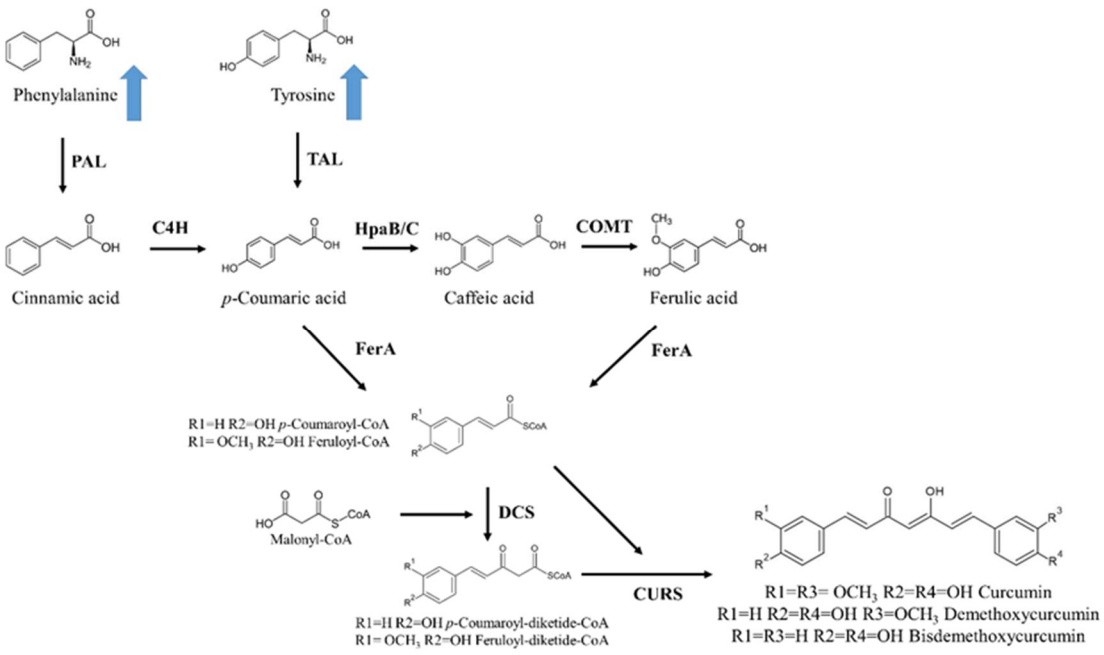


Figure 5.1: Schematic representation of the artificial biosynthetic pathway constructed for de novo curcumin biosynthesis in *Saccharomyces cerevisiae*. Blue arrows indicate that the strain is overproducing aromatic amino acids. Enzymes names: PAL: Phenylalanine ammonia lyase; TAL: Tyrosine ammonia lyase; C4H: Trans-cinnamate 4-monooxygenase; HpaB/C: 4-hydroxyphenylacetate 3-monooxygenase oxygenase and reductase components; COMT: Caffeic acid *O*-methyl transferase; FerA: feruloyl-CoA synthetase; DCS: Diketide-CoA synthase, CURS1: Curcumin synthase 1

This new strain (JI1 strain) produced 762.0 ± 59.2 µg/L of curcumin in YNB minimal medium when supplemented with 30 mg/L of ferulic acid (**Table 5.4**). The higher curcumin production obtained previously using plasmids (2.7 mg/L, **Chapter 4**) is likely attributed to the high copy number of

plasmids inside the cell resulting in a high genetic expression of curcumin biosynthetic genes and, consequently, a higher curcumin yield. Next, we introduced COMT enzyme allowing the curcumin biosynthesis from caffeic acid (JI2 strain). During the development of this study, only *A. thaliana* COMT (*At*COMT) has been expressed in yeast to construct a biosynthetic pathway for synthesizing vanillin [208]. Consequently, we choose the same enzyme for the construction of the curcumin artificial biosynthetic pathway. Meanwhile, other COMT enzymes were expressed in yeast including the ones from *Nicotiana tabacum* and *Rehmannia glutinosa* [155, 209]. Supplementation of 30 mg/L caffeic acid to JI2 strain resulted in the production of 497.6 ± 35.7µg/L of curcumin. The absence of any other curcuminoids indicates that *Pp*FerA, *Cl*DCS, and *Cl*CURS1 enzymes cannot utilize caffeic acid to produce alternative curcuminoid compounds. Subsequently, to synthesize curcumin from *p*-coumaric acid, *Pa*HpaB and *Se*HpaC which have previously demonstrated high proficiency in caffeic acid synthesis in yeast [210], were selected to construct the JI3 strain. The supplementation of 30 mg/L *p*-coumaric acid resulted in 88.4 ± 26.0 µg/L of curcumin, a significantly lower yield comparing to the yields obtained with the previous strains. When a second coumaric acid pulse at 48 h was fed, the curcumin titer increased to 128 ± 36.7 µg/L. In addition, demethoxycurcumin, a curcuminoid formed by conjugation of *p*-coumaric acid and ferulic acid derivatives, was also synthesized (14.9 ± 1.6 µg/L) revealing the capacity of the enzymes *Pp*FerA, *Cl*DCS and *Cl*CURS to use *p*-coumaric acid to synthesize other curcuminoids, although with significantly lower efficiency (**Table 5.4**). In conclusion, we successfully validated, for the first time, the biosynthesis of curcumin in an engineered yeast through the supplementation of the phenylpropanoids caffeic acid and *p*-coumaric acid.

Table 5.4: Curcumin production by different *Saccharomyces cerevisiae* strains after 72 h. Cur: curcumin, DMC: demethoxycurcumin, *Pp*FerA: feruloyl-CoA synthetase from *Pseudomonas paucimobillis*; *Cl*DCS: diketide-CoA synthase from *Curcuma longa*, *Cl*CURS1: curcumin synthase 1 from *C. longa*, *At*COMT: caffeic acid *O*-methyl transferase from *Arabidopsis thaliana*; *Pa*HpaB: 4-hydroxyphenylacetate 3-monooxygenase oxygenase subunit B from *Pseudomonas aeruginosa*, *Se*HpaC: 4-hydroxyphenylacetate 3-monooxygenase reductase subunit C from *Salmonella enterica*. The presented average values ± standard deviations were derived from three independent biological replicates.

Strain	**Substrate (concentration)**	**[Curcuminoid] (µg/L)**
JI1: IMX581; ↑*Pp*FerA; ↑*Cl*DCS; ↑*Cl*CURS1	Ferulic acid (30 mg/L)	[Cur] = 762.0 ± 59.2
JI2: JI1; ↑*At*COMT	Caffeic acid (30 mg/L)	[Cur] = 497.6 ± 35.7
JI3: JI2; ↑*Pa*HpaB; ↑*Se*HpaC	*p*-Coumaric acid (30 mg/L)	[Cur] = 88.4 ± 26.0
	p-Coumaric acid (30 + 30 mg/L)	[Cur] = 128.0 ± 36.7
		[DMC] = 14.9 ± 1.6

In parallel, to examine an alternative promoter control for curcumin biosynthesis in *S. cerevisiae*, the genes *Pp*FerA, *Cl*DCS and *Cl*CURS1 were placed under control of galactose inducible promoters (GAL 1,10) and were integrated into the IMX581 genome, resulting in the strain JG1. The induction of curcumin biosynthesis in JG1 strain was initiated by adding 20 g/L galactose and 30 mg/L of ferulic acid at 12 h. However, contrarily to what was observed with JI strains using constitutive promoters, as JG1 fermentation progressed, the intensity of the yellowish colour, indicative of curcumin presence, gradually decreased between 48 h and 72 h, prompting us to monitor curcumin production over time. Indeed, curcumin was firstly detected at 24 h and peaked at 48 h, reaching 1705.4 ± 63.6 µg/L, after which it began declining, reaching a concentration of 484.8 ± 68.1 µg/L at 72 h (**Figure 5.2**). Galactose inducible promoters are activated by glucose depletion in the presence of galactose. Complete galactose depletion was observed at 48 h, which means that the expression of genes from curcumin biosynthetic pathway was inactivated from this point. Nevertheless, the inactivation of the expression itself does not justify the curcumin degradation. Hereupon, we hypothesize that the curcumin degradation might be caused by autooxidation [211] or by any yeast endogenous enzyme. Regarding the second hypothesis, while *E. coli* features the *curA* gene encoding curcumin reductase (CurA), there is no reported gene responsible for curcumin degradation identified in *S. cerevisiae*. Upon subjecting CurA sequence (NCBI Reference Sequence: NP_415966.6) to a protein BLAST against the *S. cerevisiae* S288C proteome, the outcome revealed a low match with an uncharacterized protein (E-value = $9e^{-22}$, Identity = 25%, Positives = 43% and cover =97%) with the systematic name YML131W and with possible oxidoreductase activity. The alignment is presented in the **Appendix 3**. These findings suggest a possible role of YML131W linked to curcumin degradation in *S. cerevisiae*. However, further studies are required to clearly evaluate the function of YML131W. Nevertheless, the utilization of the GAL system led to higher curcumin production at its peak compared to the constitutive control strain (JI1). Further investigation using this system, particularly through the deletion of gal80 repressor to eliminate the dependency on galactose induction [212], is necessary to comprehensively assess its potential for enhancing curcumin production. Hereupon, we decided to further investigate curcumin biosynthesis by expressing genes under control of constitutive promoters since no curcumin degradation was observed, thus suggesting that in these strains the rate of curcumin degradation is slower than the rate of its production.

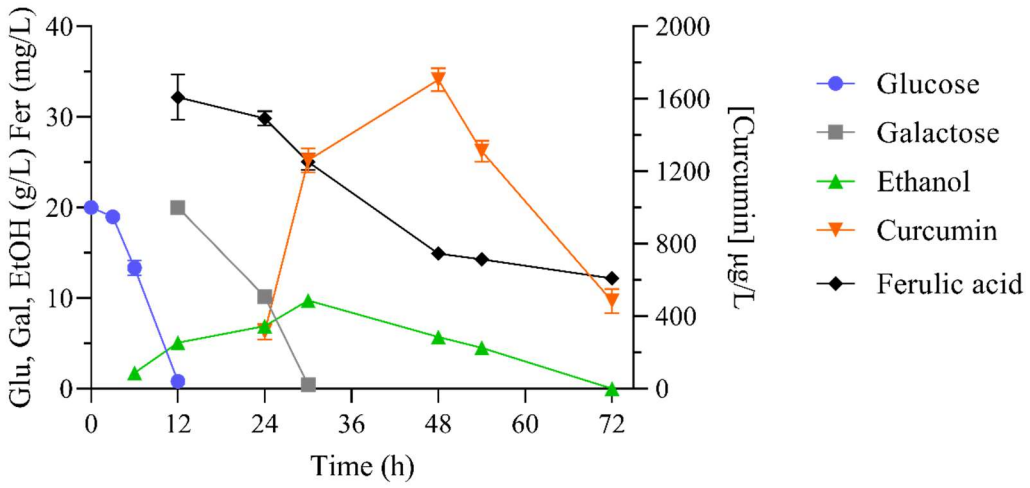


Figure 5.2: Metabolic profile and curcumin production of strain JG1 cultivated in YPD media with 20 g/L glucose. At 12h, 2% galactose and 30 mg/L ferulic acid were added to the media. Glu: Glucose, Gal: Galactose, EtOH: Ethanol, Fer: Ferulic acid. The presented average values ± standard deviations were derived from three independent biological replicates.

5.3.2 *De novo* Curcumin Biosynthesis

After the verification of curcumin biosynthesis resulting from the supplementation of phenylpropanoids, we evaluated if *S. cerevisiae* was capable of produce curcumin from glucose. To accomplished this, an engineered *p*-coumaric acid overproducing strain (QL158) was strategically employed [150]. This strain was genetically engineered for *de novo* production of high amounts of p-coumaric acid through the optimization of the metabolic flux towards the biosynthesis of the aromatic amino acids, tyrosine, and phenylalanine, and by the introduction of TAL from *Flavobacterium johnsoniae* and PAL and C4H from *A. thaliana*. In our preliminary assays, QL158 strain produced 310.6 ± 18.4 mg/L of p-coumaric acid (rich media - YPD) and 213.2 ± 18.4 mg/L (minimal media - YNB). Hereupon, we introduced the previously studied genes (*Pa*HpaB, *Se*HpaC, *At*COMT, *Pp*FerA, *Cl*DCS and *Cl*CURS1) in the QL158 strain, thus creating the JQ1 strain (**Figure 5.1**). The *de novo* curcumin production was evaluated in minimal YNB and in rich YPD media. In minimal media, curcumin production reached 108.5 ± 7.0 µg/L, while in rich media the production reached 240.1 ± 15.1 µg/L (**Figure 5.3a**). Moreover, demethoxycurcumin was also detected in extracts reaching 13.5 ± 0.4 µg/L in minimal media and 22.0 ± 0.3 µg/L in rich media (**Figure 5.3b**). No degradation of curcuminoids was observed over time. Relatively to the synthesis of phenylpropanoids (**Table 5.5**), at 24 h, *p*-coumaric acid significantly accumulated reaching 141.5 ± 38.8 mg/L and 257.0 ± 14.2 mg/L, in minimal and rich media, respectively. At the end of fermentation, p-coumaric concentrations attained 125.0 ± 27.4 mg/L (minimal media) and 146.7 ± 17.1 mg/L (rich media). Caffeic acid concentrations were significantly

lower than p-coumaric acid ones, however a slight increase during fermentation course was observed, accumulating at 8.1 ± 1.8 and 11.5 ± 1.4 mg/L, in minimal and rich media, respectively. The last phenylpropanoid, ferulic acid, was not detected in minimal media and in rich media it was only detected after 48 h in very low concentrations. Overall, *de novo* curcumin biosynthesis was achieved in both minimal and rich media. The highest curcumin levels were obtained in rich media possibly due to the highest cell concentration as previously stated in **Chapter 4**. The substantial accumulation of *p*-coumaric acid suggests that its hydroxylation into caffeic acid was inefficient, as previously observed, potentially hindering the biosynthesis of curcumin. From this point forward, all fermentations were conducted using YPD rich media, as it is a cheaper culture media and it allowed to produce the highest curcumin titers.

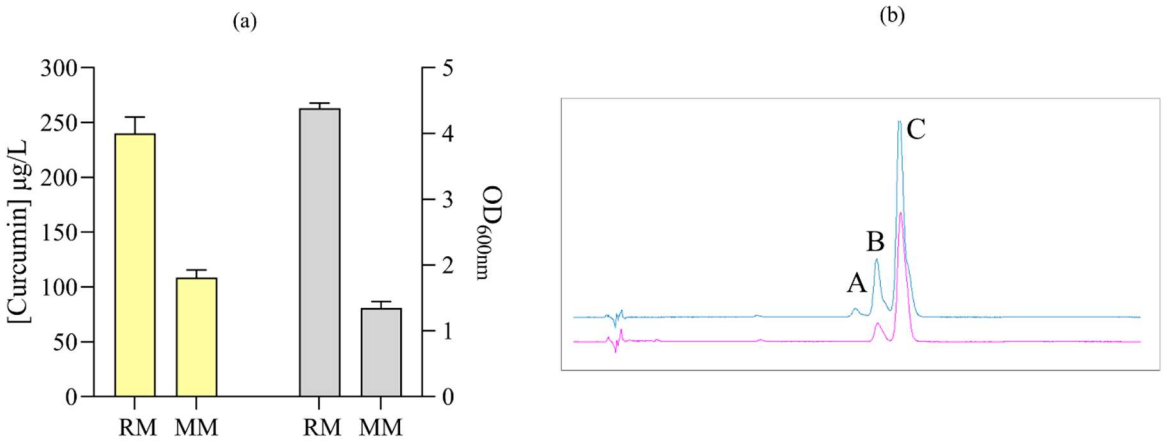


Figure 5.3: **(a)** Curcumin production (yellow bars) and optical density at 600 nm (OD_{600nm}) (grey bars) obtained after 72 h fermentation by JQ1 strain in rich (RM) and minimal (MM) media. The presented average values ± standard deviations were derived from three independent biological replicates. (**b**) HPLC analysis of the curcuminoid standard (blue spectrum) and curcuminoid extract from JQ1 (purple spectrum). Identification of peaks stand for A: bisdemethoxycurcumin, B: demethoxycurcumin, C: curcumin.

Table 5.5: Phenylpropanoids produced during fermentation by engineered *Saccharomyces cerevisiae* strains for *de novo* curcumin production. The presented average values ± standard deviations were derived from three independent biological replicates.

			[Phenylpropanoid] (mg/L)		
Strain	**Media**	**Time point**	***p*-Coumaric acid**	**Caffeic acid**	**Ferulic acid**
JQ1	Rich media	24 h	257.0 ± 14.2	6.3 ± 0.31	-
		48 h	218.0 ± 19.1	9.9 ± 1.1	1.9 ± 0.2
		72 h	146.7 ± 17.1	11.5 ± 1.4	1.7 ± 0.2
JQ1	Minimal media	24 h	141.5 ± 38.8	5.7 ± 1.9	-
		48 h	150.8 ± 48.0	6.5 ± 2.3	-
		72 h	125.0 ± 27.4	8.1 ± 1.8	-
JQ2	Rich media	24 h	377.5 ± 20.1	27.9 ± 1.6	15.1 ± 0.18
		48 h	455.8 ± 32.9	80.2 ± 11.0	20.1 ± 1.0
		72 h	452.9 ± 10.3	84.7 ± 6.3	22.0 ± 2.7
JQ3	Rich media	24 h	169.4 ± 3.0	62.5 ± 0.9	23.4 ± 0.3
		48 h	57.5 ± 3.1	101.8 ± 6.7	20.1 ± 0.7
		72 h	93.4 ± 7.4	147.9 ± 4.4	32.7 ± 5.9
JQ3	Rich media + 100 mg/L methionine	24 h	151.9 ± 4.1	68.5 ± 5.6	26.4 ± 2.9
		48 h	168.9 ± 17.9	206.7 ± 18.5	50.7 ± 8.7
		72 h	121.5 ± 38.6	432.7 ± 51.9	75.0 ± 6.2
JQ3 + pSP-GM1	Minimal media	24 h	32.8 ± 1.2	41.3 ± 7.3	18.0 ± 2.3
		48 h	56.4 ± 3.9	69.7 ± 6.2	20.8 ± 1.6
		72 h	56.3 ± 3.4	62.0 ± 13.4	18.9 ± 0.67
JQ3 + pSP-GM1_MET13	Minimal media	24 h	29.5 ± 7.3	31.3 ± 12.1	16.4 ± 2.4
		48 h	46.9 ± 13.7	43.6 ± 18.6	18.8 ± 3.4
		72 h	43.6 ± 10.0	47.2 ± 21.9	16.0 ± 1.3
JQ4	Rich media	24 h	117.5 ± 5.4	48.8 ± 2.3	37.1 ± 1.4
		48 h	86.3 ± 5.7	89.4 ± 7.7	28.4 ± 1.4
		72 h	136.9 ± 20.8	98.7 ± 10.1	33.2 ± 3.1
JQ4	Rich media + 100 mg/L methionine	24 h	144.2 ± 27.5	59.2 ± 5.3	36.2 ± 5.2
		48 h	231.3 ± 35.1	140.1 ± 0.13	66.0 ± 3.8
		72 h	180.3 ± 10.1	190.9 ± 18.4	92.2 ± 4.3

5.3.3 Enhancing *p*-Coumaric Acid Conversion to Caffeic Acid

Since the conversion of *p*-coumaric acid into caffeic acid was not efficient in strain JQ1 and in strain JI3 the curcumin biosynthesis dropped significantly when p-coumaric acid was used as substrate, we explored the possibility of enhancing this reaction by using a different enzyme. For that purpose, the caffeic acid biosynthesis was compared in QL158 expressing native versions of *Pa*HpaB and *Se*HpaC

(JQCA1) (as in JQ1 when the complete pathway was integrated), with QL158 expressing C3H and cytochrome P450 reductase (CPR1) (JQCA2) from *A. thaliana* [213]. However, while JQCA1 strain produced 25.3 ± 0.26 mg/L caffeic acid, no caffeic acid was detected in JQCA2, regardless of being observed a high accumulation of *p*-coumaric acid. This lack of production may be attributed to the incorrect expression of C3H in *S. cerevisiae*, which is a plant-specific cytochrome P450 dependent enzyme, despite the codon-optimization [213]. As the attempt to synthesize caffeic acid through C3H and CPR proved unsuccessful, we opted to revert to our initial approach. Consequently, we decided to assess the impact of codon optimization on the *Pa*HpaB gene as stated by Zhou et al.[153]. In fact, the replacement of *Pa*HpaB with its codon-optimized version (JQCA3), significantly increased the production of caffeic acid to 89.7 ± 15.1 mg/L, nearly tripling the titer (**Figure 5.4**). Moreover, Chen et al. achieved comparable levels of caffeic acid by expressing the same enzymes in a *p*-coumaric acid overproducing strain [155]

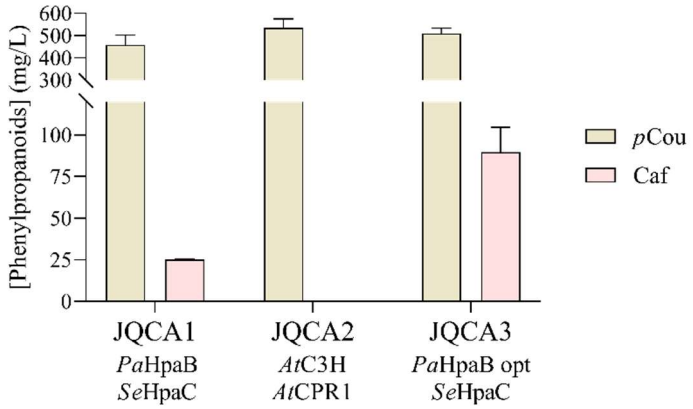


Figure 5.4: Caffeic acid and *p*-coumaric production by strains JQCA1, JQCA2 and JQCA3 cultivated in rich media with 20 g/L glucose after 72 h of fermentation. The presented average values ± standard deviations were derived from three independent biological replicates. *p*Cou: *p*-Coumaric acid, Caf: Caffeic acid.

Afterall, to accomplish *de novo* biosynthesis of curcumin, we replaced *Pa*HpaB by its codon optimized version in JQ1 creating JQ2. Fermentation of JQ2 in YPD rich medium resulted in the synthesis of 861.9 ± 113.4 µg/L of curcumin from 20 g/L glucose. Additionally, 44.3 ± 4.3 µg/L of demethoxycurcumin were obtained. The replacement of *Pa*HpaB with its codon optimized version led to a threefold increase in curcumin production. Evaluating JQ2 strain metabolic profile, glucose depletion was observed at 12 h, simultaneous with the ethanol peak of 4.2 ± 0.08 g/L, and complete exhaustion of ethanol was achieved at 48 h (**Figure 5.5a**). Notably, the manifestation of curcumin production became visible around the 36 h, evident through the development of a yellowish colour in the culture medium. The detection of curcumin coincided with the phase of ethanol consumption, indicating that its production

may occur during this phase such as the production of other polyphenols in *S. cerevisiae* [163]. Throughout the fermentation, the accumulation of *p*-coumaric acid was observed during the exponential growth phase, attaining a concentration of 377 ± 20.1 mg/L at 24 h. However, the concentrations of both caffeic acid and ferulic acid remained relatively low, registering 27.9 ± 1.6 mg/L and 15.1 ± 0.18 mg/L, respectively. During the stationary growth phase and ethanol consuming phase, there was an increment in the levels of caffeic acid, culminating in a maximal concentration of 85.3 ± 11.9 mg/L at 54 h. By the end of the fermentation, a high accumulation of *p*-coumaric acid was evident, reaching a substantial concentration of 452 ± 10.3 mg/L (**Figure 5.5b**).

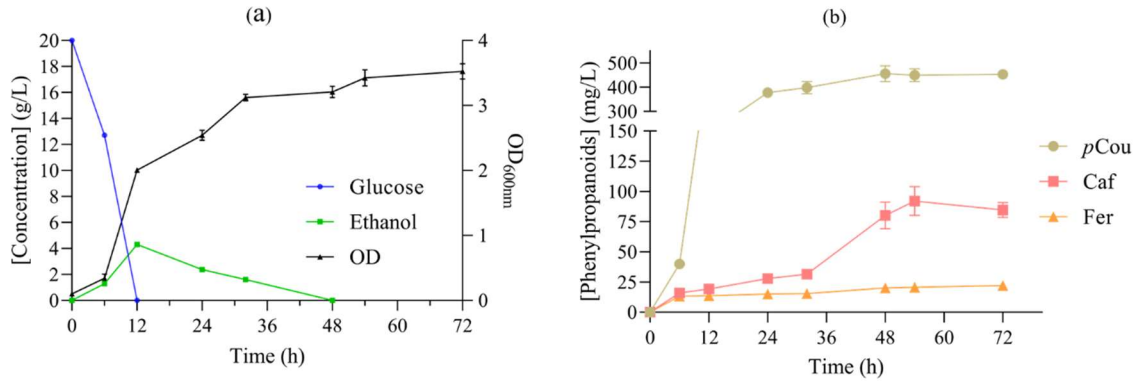


Figure 5.5: (**a**) Metabolic profile and optical density at 600 nm (OD_{600nm}) of the strain JQ2 in rich media with 20 g/L glucose and (**b**) production of phenylpropanoids during fermentation. The presented average values ± standard deviations were derived from three independent biological replicates. *p*Cou: *p*-Coumaric acid, Caf: Caffeic acid and Fer: Ferulic acid.

In response to the persistent substantial accumulation of *p*-coumaric acid by JQ2 and to increase the fluxes through curcumin biosynthetic pathway, an additional copy of *Pa*HpaB codon-optimized and *Se*HpaC genes was introduced in JQ2. This culminated in the development of a derivative strain denoted as JQ3. The supplementary genetic copy instigated the synthesis of curcumin, yielding a titer of 1.4 ± 0.17 mg/L (1408.6 µg/L), thus representing an enhancement of 77% compared to the previous strain JQ2. Demethoxycurcumin levels also increased reaching 133.8 ± 4.9 µg/L. Furthermore, colonies of JQ3 growth on solid media during plasmid curing exhibited a yellow colour, a characteristic not observed in the preceding strains (**Figure 5.6**).

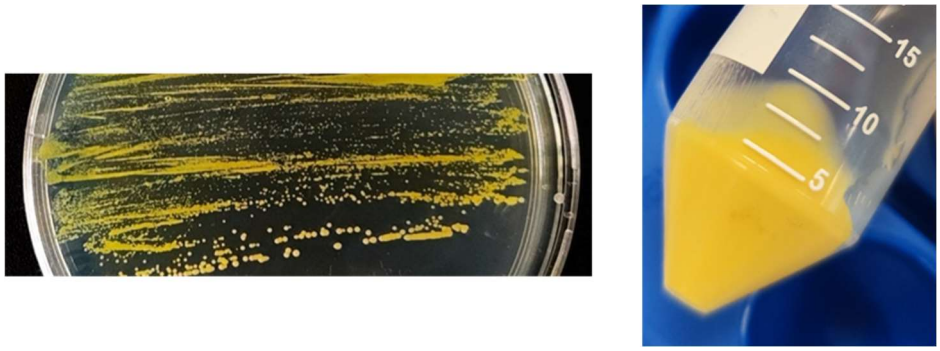


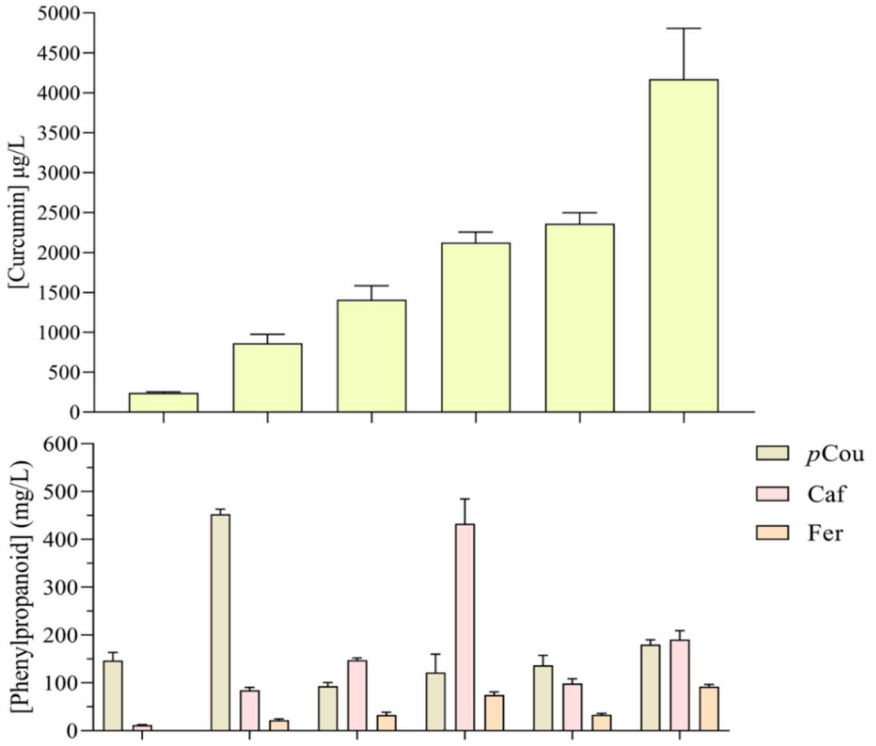
Figure 5.6: Strain JQ3 growth in solid minimal media (on the left) and biomass pellet after fermentation in rich media (on the right), exhibiting yellow biomass due to curcumin production.

Remarkably, the augmented HpaB/C genetic charge resulted in a considerable reduction in the accumulation of *p*-coumaric acid to 93.4 ± 7.4 mg/L (**Figure 5.7**), indicative of an increased conversion to caffeic acid due to a higher hydroxylation activity. Accumulation of caffeic acid reached 147.9 ± 4.4 mg/L, 1.7 times higher than JQ2. As observed for JQ2, at 24 h, during exponential growth, *p*-coumaric acid was the main phenylpropanoid. After this phase, there was a subsequent increase in caffeic acid concentrations, doubling from the 24 h time point and the end of fermentation (**Table 5.5**). Additionally, the accumulation of ferulic acid at 72 h increased 1.5 times to 32.7 ± 5.9 mg/L, relatively to JQ2 (**Figure 5.7**). Concluding, the extra copy of HpaB/C improved the fluxes through the curcumin biosynthetic pathway increasing the biosynthesis of caffeic and ferulic acid and consequently curcumin titers.

5.3.4 Methylation of Caffeic Acid to Ferulic Acid

The conversion of caffeic acid to ferulic acid involves a crucial methylation step, wherein a methyl group is transferred to the ferulic acid molecule. In yeast, the methyl group donor for methylation reactions is linked to the S-adenosylmethionine (SAM) cycle. SAM serves as the primary methyl group donor in various cellular methylation reactions. As the conversion of caffeic acid to ferulic acid requires a methyl group transfer, the availability of SAM becomes critical in determining the efficiency of this reaction. To enhance the SAM pool and thereby boost the conversion of caffeic acid to ferulic acid, the supplementation of methionine, the precursor of SAM, emerged as a strategy. In fact, the supplementation of 100 mg/L of methionine to JQ3 increased curcumin yield to 2.2 ± 0.13 mg/L (2125.7 µg/L), representing a 1.6 improvement in production (**Figure 5.7**). In addition, ferulic acid accumulation increased to 75.0 ± 6.2 mg/L (2.3-fold higher than without methionine supplementation) revealing that methionine elevated the methylation efficiency of *At*COMT. Interestingly, caffeic acid levels reached 432.7 ± 51.9 mg/L, almost 3 times more than without methionine supplementation (**Figure**

5.7). This might be attributed to an increased flow through the *At*COMT reaction, which alleviated the bottleneck in the previous step, leading to elevated levels of caffeic acid. Therefore, caffeic acid and ferulic acid final concentrations significantly increased (**Figure 5.7**). Moreover, when methionine was fed, significantly less demethoxycurcumin was produced, with only trace amounts detected. This could mean that when ferulic acid availability surpasses a certain threshold, *p*-coumaric acid may not be utilized for curcuminoid synthesis.



Strain name	JQ1	JQ2	JQ3	JQ3	JQ4	JQ4
Methionine fed (100 mg/L)	-	-	-	+	-	+
*Se*HpaC, *At*COMT, *Pp*FerA, *Cl*DCS, *Cl*CURS	+	+	+	+	+	+
*Pa*HpaB	+	-	-	-	-	-
*Pa*HpaB (opt)	-	+	+	+	+	+
HpaB/C (x2)	-	-	+	+	+	+
COMT (x2)	-	-	-	-	+	+

Figure 5.7: *De novo* curcumin production and phenylpropanoid accumulation in JQ1, JQ2, JQ3, JQ4 *Saccharomyces cerevisiae* strains in rich media with 20 g/L of glucose after 72 h of fermentation. SeHpaC: 4-hydroxyphenylacetate 3-monooxygenase reductase component from *Salmonella enterica*; *At*COMT: Caffeic acid *O*-methyl transferase from Arabidopsis thaliana; *Pp*FerA: feruloyl-CoA synthetase from *Pseudomonas paucimobilis*; ClDCS: diketide-CoA synthase, ClCURS1: curcumin synthase 1 from Curcuma longa; *Pa*HpaB: 4-hydroxyphenylacetate 3-monooxygenase oxygenase component; *Pa*HpaB (opt): *Pa*HpaB codon-optimized; pCou: *p*-coumaric acid; Caf: Caffeic acid; Fer: Ferulic acid. The presented average values ± standard deviations were derived from three independent biological replicates.

5.3.5 Precursor Supply Enhancement

The availability of the extender molecule malonyl-CoA is essential for curcumin biosynthesis. To assess whether the availability of malonyl-CoA was restricting curcumin production, we overexpressed the native genes of cytosolic acetyl-CoA carboxylase (ACC1) and fatty-acyl coenzyme A oxidase (FOX1) within the JQ3 strain using a plasmid system. ACC1 is responsible for the direct conversion of acetyl-CoA to malonyl-CoA (Fernandez-Moya and Da Silva, 2017) and FOX1 is a key enzyme in fatty acid β-oxidation. FOX1 may increase malonyl-CoA by increasing levels of precursor acetyl-CoA, a strategy already employed to promote carminic acid biosynthesis, that requires seven malonyl-CoA molecules, in yeast (Zhang et al., 2023). Plasmids harbouring ACC1 and FOX1 alone or together were transformed into JQ3 strain, and the curcumin biosynthesis was evaluated in minimal media (YNB), required for plasmid maintenance, and compared with JQ3 harbouring the empty plasmid (pSP-GM1). However, either overexpression of ACC1 or FOX1 or both together did not increase curcumin production relative to the control (**Figure 5.8**). Overexpressing native ACC1 gene was found to enhance the levels of malonyl-CoA dependent molecules in yeast (Fernandez-Moya and Da Silva, 2017; Shin et al., 2012). Nevertheless, studies have highlighted the use of a feedback-resistant ACC1 mutant version to further augment the malonyl-CoA pool (Li et al., 2016). The phosphorylation of ACC1 by Snf1 reduces its activity, and Snf1 is activated in response to glucose depletion (Shi et al., 2014). Since curcumin synthesis occurs during the ethanol phase, exploring the use of mutated ACC1 as a potential strategy for improvement curcumin yields is worth considering in the future. In addition, despite the efforts to enhance malonyl-CoA availability through overexpressing ACC1 and FOX1 genes, the lack of significant increase in curcumin production could also suggests that, at this stage, malonyl-CoA availability might not be the limiting factor for curcumin biosynthesis.

Furthermore, following the examination of optimization results obtained through bioinformatic analysis using GOUProblem module from MEWpy, it was observed that the overexpression of the MET13 gene was consistently present in all solutions obtained (**Appendix 4**) and a FVA analysis for *met13* overexpression revealed high robustness with a predicted curcumin yield of [0.463-0.886] mmol/gDCW/h. MET13 is involved in methionine biosynthesis pathway (catalyses the reduction of 5,10-methylenetetrahydrofolate to 5-methyltetrahydrofolate) making it a good study candidate since it could increase SAM levels and methylation capacity and, consequently, ferulic acid biosynthesis [214]. To evaluate that, MET13 gene was overexpressed in JQ3 using a plasmid system. Curcumin productivity was compared between JQ3 overexpressing MET13 and JQ3 harbouring the empty plasmid (pSP-GM1)

in minimal media (YNB) required for plasmid maintenance. However, overexpression of MET13 in JQ3 did not improve curcumin yield or ferulic accumulation (**Figure 5.8**, **Table 5.5**). The metabolism of SAM is recognized as highly complex [215]. In their work on developing an engineered strain for *de novo* biosynthesis of ferulic acid, Chen et al. [155] attempted various strategies to enhance SAM supply. Despite several efforts, none of the tested strategies resulted in an improvement in ferulic acid yield. Instead, conversion of caffeic acid to ferulic acid was increased by enhancing the degradation of *S*-adenosyl-*L*-homocysteine (SAH), the by-product of methylation reactions and inhibitor of methyltransferases activity. In the future, we could adopt a comparable approach in our strain to eliminate the need of methionine supplementation to elevate curcumin levels.

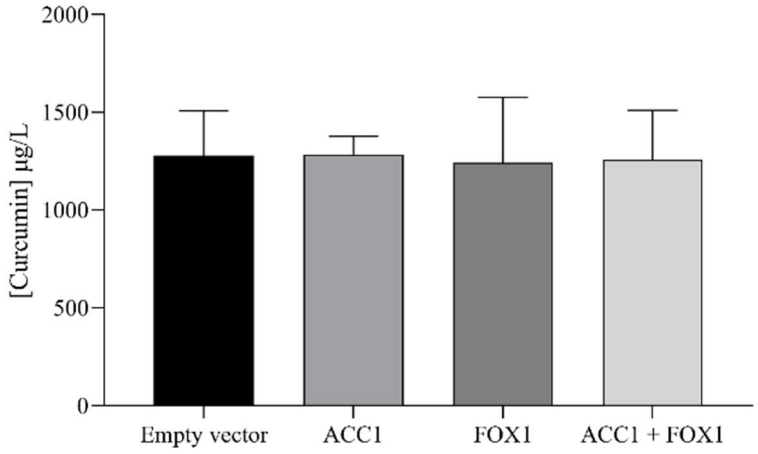


Figure 5.8: Curcumin produced by strain JQ3 expressing plasmids harbouring different genes. ACC1: Acetyl-CoA carboxylase; FOX1: Fatty-acyl coenzyme A oxidase; MET13: methylenetetrahydrofolate reductase. The presented average values ± standard deviations were derived from three independent biological replicates.

5.3.6 Increasing Flux through Ferulic Acid Biosynthesis

Since in JQ3 caffeic acid was the highest accumulated phenylpropanoid, we tested the same strategy as previously by introducing an extra copy of *At*COMT to increase caffeic acid conversion to ferulic acid. The resulting strain was labelled as JQ4. As previously, the extra copy *At*COMT elevated curcumin levels to 2.4 mg/L ± 0.1 mg/L (2360.7 µg/L), 1.7 times more than in JQ3 (**Figure 5.7**). Again, only traces of demethoxycurcumin were detected. Furthermore, less caffeic acid was accumulated relatively to JQ3, reaching 98.7 ± 10.1 mg/L, hence revealing a higher capacity for ferulic acid biosynthesis. Nevertheless, ferulic acid accumulation levels were similar in JQ3 and JQ4, indicating that the extra ferulic acid produced was utilized for the synthesis of curcumin (**Figure 5.7**). Methionine supplementation to JQ4 elevated the levels of curcumin 1.8 times to 4.2 ± 0.6 mg/L (4171.3 µg/L). Moreover, a higher accumulation of all phenylpropanoids was detected (**Figure 5.7**). Notably, ferulic

acid accumulation reached 92.2 ± 4.3 mg/L (2.8 times more than without methionine supplementation) (**Figure 5.7**). Overall, besides increased expression of *At*COMT, the supplementation of methionine still increased the levels of ferulic acid. This suggests that SAM availability still might have been a limiting factor for ferulic acid synthesis. Chen et al., [155] demonstrated that the augmentation of COMT activity could be obtained by integrating more copies of the gene. Specifically, the integration of four copies led to increased ferulic acid yields in their study. Here, it was demonstrated that enhancing the expression levels of phenylpropanoid pathway genes improves the fluxes through curcumin biosynthesis. Nevertheless, a significant accumulation of phenylpropanoid precursors was observed. Chen et al., [155] also showed that enhancing the supply of cofactors essential for the phenylpropanoid pathway – namely NADH, $FADH_2$, and SAM- resulted in substantial increase in ferulic acid biosynthesis. In the future, a more deliberate and systematic approach should be explored to effectively direct the flux towards curcumin synthesis either by defining the optimal expression levels for each pathway gene (fine tuning) or by using a different promoter system. Moreover, strategies to enhance the bioavailability of auxiliary molecules, such as malonyl-CoA, SAM, and redox cofactors must be considered. Overall, we developed a *S. cerevisiae* strain capable of producing curcumin without requiring the supplementation of phenylpropanoids precursors. Our final strain (JQ4) produced 2.4 ± 0.1 mg/L of curcumin from 20 g/L of glucose. Methionine supplementation to JQ4 elevated curcumin yield to 4.2 mg/L. Prior to our study, *de novo* curcumin biosynthesis had only been achieved in genetically modified *E. coli* [88].

5.4 Conclusions

In the past recent years, curcumin has emerged as a promising natural therapeutic agent because of its diverse biological effects. Using microbes to produce curcumin offers a solution to the challenges linked with curcumin plant extraction. Microbial production might enable a rapid, cost-effective, and eco-friendly way to produce curcumin mainly when simple substrates are used. In our earlier research, we assessed curcumin production from supplemented ferulic acid, identifying the most efficient enzymes for the process. Nonetheless, the dependency on plasmids for curcumin synthesis poses limitations. Therefore, to overcome such limitations, herein we integrated the curcumin genes into the yeast genome and further confirmed the synthesis of curcumin from ferulic acid. Next, we introduced the genes responsible for the curcumin biosynthesis from the upstream intermediates, namely *p*-coumaric and caffeic acids. After successfully confirming the curcumin biosynthesis, this same pathway was

integrated in a *p*-coumaric acid overproducing strain. To overcome accumulation of intermediate phenylpropanoids, the expression of HpaB/C and *At*COMT was increased by expressing an extra copy of each gene. Also, the expression of curcumin biosynthetic genes under control of galactose inducible promoters revealed the possible existence of an endogenous yeast gene capable of degrading curcumin (YML131W). In the future, the deletion of this gene could provide important insights on its role in curcumin degradation. In conclusion, we report for the first time the *de novo* biosynthesis of curcumin in *S. cerevisiae* achieving up to 4.2 mg/L. By integrating genes from different organisms into the *S. cerevisiae* genome we constructed an artificial pathway for *de novo* curcumin biosynthesis from glucose. Indeed, the *de novo* production of curcumin holds potential for significant further improvement by additional genetic modifications, such as the fine tuning of curcumin pathway genes and the enhancement precursor supply. Additionally, the titer of curcumin can be substantially increased by scaling up the fermentation process. Finally, we believe that our work represents a solid basis for development of an extremely efficient cell factory for microbial curcumin production.

CHAPTER 6. Optimization of the Operational Conditions to Produce Curcumin by Engineered Yeast

ABSTRACT: In the last years, researchers have been exploring innovative approaches to optimize the production of curcumin through genetic engineering of microorganisms, aiming to enhance yields, reduce production costs, and ultimately meet the growing global demand for this bioactive compound. Previously, we successfully engineered a *Saccharomyces cerevisiae* strain capable of synthesizing curcumin from fermentable carbon sources at the lab scale flask fermentation (**Chapter 5**). In this chapter, the production of curcumin by engineered yeast was explored in lab-scale bioreactor aiming to increase production yields. A glucose fed-batch strategy comproved that curcumin is only synthesized after glucose depletion and during ethanol consumption. Hereupon, a feeding strategy involving the addition of ethanol was explored to prolong the ethanol consumption phase, thereby potentially extending the period during which curcumin synthesis occurs. The ethanol fed strategy yielded 3.8 mg/L of curcumin, however curcumin degradation was also observed possibly due to autoxidation. Furthermore, the production of curcumin by engineered yeast was assessed using agro-industrial residues from the rice industry, rice bran and rice husk. Different methods were used to obtain extracts from rice bran and husk products. Among these, a hydrothermal pre-treatment followed by enzymatic digestion proved particularly effective in obtaining rice bran extracts with enhanced suitability for curcumin production. Curcumin production from rice bran extracts reached 3.0 mg/L.

The information presented in this chapter is in preparation for publishing in a peer reviewed journal:

Rainha, J., Braga, A., Rodrigues, J. L., Rodrigues, L. R.. Enhanced curcumin production in engineered yeast through operational optimization. *In preparation*.

6.1 Introduction

Curcumin, a polyphenol produced by *Curcuma longa,* presents interesting therapeutic properties (**reviewed in Chapter 2**). In the last years, several efforts have been made to develop genetically engineered microorganisms capable of producing curcumin to answer to increasing demands for this compound. The development of microbial cell factories for curcumin production (**Table 2.2**) may overcome the limitations associated to natural curcumin production methods. Besides constructing an efficient cell factory to produce a non-native compound, that involves the optimization of the heterologous pathway and of the endogenous reactions, another important factor for consideration is the bioprocess engineering. Any heterologous compound produced by engineered *Saccharomyces cerevisiae* or any microorganism competes for precursors and ATP with biomass formation and maintenance processes [216]. In yeast, alcoholic fermentation leads to 2 mol of ATP per mol of glucose while respiration yields 8-fold more ATP [217]. *S. cerevisiae* is a Crabtree positive organism meaning that even at fully aerobic conditions it prefers fermentative metabolism at high carbon concentrations [217]. Respiration only occurs at low specific growth-rates and low sugar concentrations. Hereupon, an efficient process engineering will enhance the formation of heterologous products that require ATP [216]. The use of bioreactors for strain cultivation offers advantages over shake-flask fermentation, including the real time monitoring and automated control of key parameters such as temperature, pH, oxygen levels, and agitation speed. Additionally, it simulates the scalability of industrial settings. Moreover, the implementation of fed-batch operation mode in bioreactors allows the formation of high-cell densities which could greatly improve the product yields [218]. In genetically modified yeast, fed-batch cultivation techniques have been shown to be essential for greatly increasing the production of polyphenols, such as naringenin and resveratrol [164, 170].

In recent years, the global drive towards sustainable and circular economic practices has prompted researchers to explore methods for the valorisation of organic wastes, such as lignocellulosic biomass. The rice industry, a major player in the global food sector, generates two main by-products during the processing of white rice for human consumption: rice husk and rice bran. Unfortunately, a considerable portion of these by-products is discarded due to their inedibility and low-cost as feedstock. Rice husk, for instance, is composed of approximately 50% carbohydrates (28% cellulose, 26% of hemicellulose and 24% of lignin) [219]. Hereupon, rice residues hold potential as a source of fermentable sugars such as monosaccharides (e.g. glucose) through hydrolysis processes [220]. Moreover, due to the lignin content,

phenolic compounds such as *p*-coumaric and ferulic acids, that are intermediates in the curcumin biosynthetic pathway, can be extracted from these rice residues [221].

In this chapter, the optimization at an operational level of the curcumin production by a genetically engineered *S. cerevisiae* will be explored. The use of bioreactors and the implementation of a fed-batch operation mode will be assessed. In addition, the potential of using industrial rice by-products as a culture medium for curcumin production will be evaluated.

6.2 Materials and Methods

6.2.1 Strains, Media and Cultivation

The genetically engineered *S. cerevisiae* strains harbouring a pathway for *de novo* curcumin biosynthesis used in this work are listed in **Table 6.1**. Yeast Peptone Dextrose media (YPD) was composed by 10 g/L peptone, 20 g/L yeast extract and 20 g/L of glucose. For flask fermentation experiments, a 5 mL pre-culture was grown overnight at 30 °C, 200 rpm and used to inoculate 250 mL flasks containing 50 mL of YPD media or rice residues extracts with an initial optical density at 600 nm (OD_{600nm}) of 0.1. Flask fermentations were performed for 72 h, at 30 °C with shaking at 200 rpm. For the experimental design experiments, glucose concentration and initial OD_{600nm} were adjusted accordingly (**Section 6.2.2**). For ethanol pulse experiments, 1 g/L of ethanol was supplemented to the flasks at 24 h and 48 h.

Table 6.1: Strains used in this work.

Strain name	Genotype	Reference
S. cerevisiae JQ2	MATa, ura3-52, can1Δ::cas9-natNT2, TRP1, LEU2, HIS3, pdc5Δ, aro10Δ, XII-2::(p_{GPM1}-*At*PAL2-t_{FBA1})+(p_{TDH3}-*At*C4H-t_{CYC1})+(p_{HXT7}-*At*ATR2-t_{YX212})+(p_{PGK1}-CYB5-t_{ADH1}), X-3::(p_{TPI1}-*Ec*aroL-t_{YX212})+(t_{ADH1}-ARO7 G141S-p_{TEF1})+(p_{PGK1}-ARO4 K229L-CYC1t), X-4::(t_{CYC1}-ARO1-p_{TPI1})+(p_{TDH3}-ARO2-t_{ADH1})+(t_{TDH2}-ARO3-p_{TEF1}), XI-3::(p_{TEF1}-*Fj*TAL-t_{TDH2})+(t_{FBA1}-*Mt*PDH1-p_{TDH3}), XII-4::(p_{TEF1}-*Cl*DCS-t_{ADH1}; p_{TDH3}-*Cl*CURS-t_{sym27}; p_{PGK1}-*Pp*FerA-t_{CYC1}), XII-1::(p_{TEF1}-*At*COMT-t_{ADH1}), (p_{TEF1}-*Se*HpaC-t_{ADH1};p_{PGK1}-*Pa*HpaB(opt)-t_{CYC1}),	**Chapter 5**
S. cerevisiae JQ3	JQ2, XII-3::(p_{TEF1}-*Se*HpaC-t_{ADH1}; p_{PGK1}-*Pa*HpaB-t_{CYC1})	
S. cerevisiae JQ4	JQ3, XI-2::(p_{TEF1}-*At*COMT-t_{ADH1})	

6.2.2 Experimental Design

StatGraphics software was employed to formulate the experimental design experiments using the Box-Behnken design, a three-level factorial experience. The variables evaluated included initial glucose concentrations (20, 40, 60 g/L), initial ethanol concentrations (0, 2.5, 5%), initial pH levels (4, 5, 6), and initial inoculation OD_{600nm} (0.1, 0.2, 0.3).

6.2.3 Bioreactors Experiments

6.2.3.1 Inoculum Preparation

The inoculum for bioreactors was prepared as follows: yeast strains from -80 °C frozen glycerol stocks were used to inoculate a pre-culture of 7 mL of YPD in 50 mL tubes. Cultures were incubated overnight at 30 °C with shaking at 200 rpm. The pre-culture was used to inoculate 150 mL of YPD in 500 mL shake flasks at an initial OD_{600nm} of 0.1 and incubated for 12 h in the same conditions. After growth, the OD_{600nm} was measured and the appropriate volume of inoculum for an initial OD_{600nm} of 0.1 in the bioreactor was centrifuged at 5000 rpm for 10 min. The supernatant was removed, and the cells used to inoculate the bioreactors.

6.2.3.2 Bioreactor Settings and Operation

Batch and fed-batch fermentations were performed in 2-L bioreactors (DASGIP® Parallel Bioreactor System, Eppendorf) containing 500 mL of YPD media, with pH adjusted to 5.5. Reactors were autoclaved at 121 °C for 20 min containing 450 mL of YPD media without glucose. For an initial glucose concentration of 20 g/L, 25 mL of sterile 400 g/L of glucose solution was added to bioreactors after autoclaving. A volume of 25 mL of previously sterilized YPD without glucose was used to dissolve the cells for inoculation. Fermentations were carried out at constant oxygen feeding of 0.5 vvm (15 L/h), at temperature of 30 °C and initial agitation of 350 rpm. The dissolved oxygen percentage (%DO) was maintained above 30% by adjusting stirring speed up to 1000 rpm, unless otherwise specified. A 2 M NaOH solution was used for the pH control experiment by automatic feeding. All the bioreactor experiments were performed in duplicate. Samples (5 mL) were taken at regular intervals to measure OD_{600nm} and subsequently centrifuged (10000 rpm, 2 min). Supernatants were stored at -20 °C until Ultra-Performance-Liquid-Chromatography (HPLC) analysis for quantification of phenylpropanoids, glucose and ethanol. For curcumin extraction, the cell pellets were mixed with 1 mL of methanol,

vortexed for 1 min and centrifuged. The supernatant was collected and stored at -20 °C for HPLC curcumin quantification.

6.2.3.3 Fed-batch Experiments

For the glucose fed-batch experiment, a solution containing 250 g/L of glucose and 15 g/L of yeast extract was used. The solution was fed at flowrate of 5 mL/h after glucose depletion. Glucose concentrations were monitored over time using dinitrosalicylic acid (DNS) method [222], and the feed was stopped when glucose concentrations started to increase.

For ethanol fed-batch experiment, a solution containing 43 g/L of ethanol and 15 g/L of yeast extract was used. The concentration of the ethanol solution was calculated based on the ethanol consumption rate from the previous batch fermentation to ensure that the feeding rate matched the consumption rate. The feed started at 27 h and was maintained throughout the entire process.

For ethanol-pulse experiments, 625 µL of pure ethanol (corresponding to a concentration of 1 g/L) was manually supplemented at 24 h and 48 h of fermentation.

6.2.4 Rice By-Products Characterization

The raw materials, rice husk and rice bran, were supplied by the rice processing company NOVARROZ – PRODUTOS ALIMENTARES, S.A., Portugal. The chemical characterization of rice husk and bran was performed as described by Teixeira-Guedes et al. [223] for the analysis of ash, crude protein, crude lipid, water extractives, ethanol extractives, carbohydrates, uronic acid, glucose, xylose, arabinose, and acid insoluble residues content.

6.2.5 Rice By-Products Hydrolysis

To obtain fermentable sugars through acidic hydrolysis, a solution containing 1.5% sulfuric acid (H_2SO_4) was mixed with rice husk or rice bran residues at a solid-to-solvent ratio of 1:10. Hydrolysis was performed at 121 °C for 20 min. Following hydrolysis, the aqueous phase was collected by centrifugation (10000 rpm, 10 min), and the pH was adjusted to 5.5 using calcium carbonate ($CaCO_3$). Subsequently, the solution was filtered through 0.46 µm membranes and sterilized by autoclaving at 110 °C for 30 min. The obtained extracts were then characterized by HPLC.

Non-isothermal hydrothermal treatments were performed at a temperature of 180 °C in the pressurized Parr 4523 reactor (Parr Instrument Company). The solid-to-solvent ratio employed was 1:6.66 Kg/Kg.

Following the hydrothermal treatment, an enzymatic saccharification was conducted using the enzyme cocktail Cellic CTec2 (Sigma) at a concentration of 15 enzyme units per gram of biomass (FPU/g), at a pH of 5 and a temperature of 50 °C, over a period of 72 h. After that, the obtained extracts were characterized by HPLC. Next, the extracts were diluted with sterile double-distilled water (ddH_2O) to achieve an initial glucose concentration of 20 g/L, and the pH was adjusted to 5.5. Subsequently, the solution was filtered through 0.46 μm membranes and sterilized by autoclaving at 110 °C for 30 min. When required, prior to filtration, 10 g/L of yeast extract were added to the solution.

6.2.6 Carbon/Nitrogen Ratio

Total organic carbon (TOC), total nitrogen (TN), concentration in rice by-products extracts obtained through non-isothermal hydrothermal treatments were determined spectrophotometrically using the cuvette test kits LCK 387 and LCK 338 (Hach-Lange GmbH), respectively.

6.2.7 Analytical Methods

Optical densities (ODs) were measured on a Multiskan SkyHigh Microplate Spectrophotometer (Thermo Scientific). The HPLC quantification of glucose, ethanol, xylose, arabinose, furfural and hidroximetilfurfural (HMF) was performed using chromatographic system composed by Shimadzu LC-2060C equipped with Biorad Aminex HPX-87H (300 x 7.8 mm, 9 μm particle size) column. The oven temperature was set to 60 °C. Furfural and HMF were detected by absorbance at 254 nm. Glucose, ethanol, xylose, and arabinose were quantified by refractive index detection. The mobile phase was composed by 5 mM of H_2SO_4 at flowrate of 0.6 mL/min for 60 min. The UHPLC quantification of curcumin, *p*-coumaric acid, caffeic acid and ferulic acid was performed as before (**Chapter 4, Section 4.2.4**). Glucose quantification using the DNS method involved mixing equal volumes of the sample and DNS reagent (3,5-dinitrosalicylic acid, sodium potassium tartrate, and sodium hydroxide)[222]. The mixture was boiled and subsequently cooled by the addition of ddH_2O. The OD_{540nm} was then measured to determine the glucose concentration.

6.3 Results and Discussion

6.3.1 Optimization Culture Conditions using Experimental Design

To improve curcumin titres synthesized by engineered *S. cerevisiae*, an experimental design was employed to study four variables: initial glucose concentration, ethanol concentration, pH and Inoculum

concentration (measured as OD_{600nm}). The curcumin production was evaluated using the JQ2 strain (**Chapter 5**). The set of experiments and the respective response is presented in **Table 6.2**.

Table 6.2: Set of experiments conducted based on the experimental design framework and respective responses.

Run n.	Glucose (g/L)	Ethanol (%)	Media pH	Initial OD_{600nm}	[Curcumin] (µg/L)
1	40	0	6	0.2	658.7
2	40	2.5	5	0.2	47.4
3	40	5	4	0.2	33.9
4	40	0	4	0.2	854.2
5	40	2.5	6	0.3	33.2
6	60	2.5	4	0.2	31.7
7	20	2.5	5	0.3	680.9
8	60	2.5	6	0.2	32.2
9	40	5	5	0.1	33.1
10	40	2.5	4	0.3	118.3
11	40	0	5	0.1	303.9
12	60	2.5	5	0.3	32.3
13	20	2.5	6	0.2	629.2
14	20	2.5	4	0.2	717.2
15	40	0	5	0.3	569.0
16	60	2.5	5	0.1	31.8
17	40	5	6	0.2	32.4
18	60	0	5	0.2	135.5
19	40	5	5	0.3	38.0
20	20	0	5	0.2	821.7
21	60	5	5	0.2	32.7
22	20	2.5	5	0.1	551.8
23	20	5	5	0.2	31.2
24	40	2.5	5	0.2	51.2
25	40	2.5	4	0.1	51.4
26	40	2.5	5	0.2	32.3
27	40	2.5	6	0.1	39.4

After analysing the experimental design results, the p-values for the variables pH and initial OD_{600nm} were found to be very high (p-value = 0.4907, p-value= 0.4079, respectively), suggesting that these variables may not have a substantial impact on the curcumin production under the tested conditions. Regarding the variables initial glucose and ethanol, the low p-values suggest that they influence the response. However, the optimal points were found to be 20 g/L for glucose and 0% for ethanol. This implies that increasing initial glucose concentration and initial ethanol feeding did not improve curcumin production. Nevertheless, we evaluated curcumin production using the optimal conditions retrieved by StatGraphics (20 g/L glucose, no ethanol, pH 4.5 and initial OD_{600nm} = 0.3) against the non-optimized conditions (20 g/L glucose, no ethanol, pH not controlled and initial OD_{600nm} = 0.1; Curcumin production: 704.9 µg/L (**Chapter 5**)). The optimized conditions did not lead to an improvement in curcumin production, yielding a value of 694.9 ± 58.3 µg/L. This outcome underscores the lack of success in the experimental design experiment herein conducted. Higher concentrations of glucose and ethanol

negatively impact curcumin production. In the experiments conducted using 60 g/L of glucose, the curcumin produced was substantially lower relatively with experiments using lower glucose concentrations. Regarding tests with 40 g/L of glucose, curcumin production significantly decreased in the presence of ethanol, while it was higher in its absence. In experiments with 20 g/L of glucose, the presence of 2.5% ethanol appears to have no impact on production. Contrarily, in the presence of 5% ethanol, curcumin production decreases considerably.

6.3.2 Curcumin Production in Bioreactors using Genetic Modified Yeast

To enhance curcumin production titers obtained previously by flask fermentation, a bioreactor was used to evaluate curcumin production by the strain JQ2. Given that, from the experimental design results, initial pH did not significantly impact the curcumin production, an initial pH of 5.5 was adopted. This pH value is frequently used in bioreactor approaches involving *S. cerevisiae*. Using a 2-L lab-scale stirring bioreactor two experiments were performed: (a) one where pH was not automatically regulated, and (b) another where the pH was maintained at 5.5 through the automatic addition of 2 M NaOH. Dissolved oxygen levels were regulated by adjusting the stirring control to ensure they remained above 30%.

In both experiments, the consumption of glucose and ethanol, as well as the obtained $OD600_{nm}$, demonstrated similar profiles, indicating that pH control did not impact cellular growth (**Figure 6.1a** and **c**). Glucose was mainly consumed in the first 12 h, at which ethanol reached its peak. In the test with no pH control, the pH dropped from the initial 5.5 to 4.5 during the first 24 h and maintained approximately this value until the end of the process.

Concerning curcumin production, it was slightly higher in the experiment with no pH control (**Figure 6.1b** and **d**). Curcumin production was detected at 30 h in both experiments peaking at 72 h (724.6 ± 73.7 for no pH control and 555.3 ± 25.3 for controlled pH). Between the 72 h and 96 h curcumin levels decreased, indicating its possible degradation. Additionally, the production and accumulation of curcumin intermediates exhibited a similar profile (**Figure 6.1b** and **d**). *p*-Coumaric and caffeic acids levels increased during the exponential growth phase reaching values on the order of magnitude of 300 mg/L and 60 mg/L, respectively in both tests. Ferulic acid concentrations were relatively low (~13 mg/L) and constant during the whole process. In summary, pH control did not increase synthesis of curcumin and curcumin precursors.

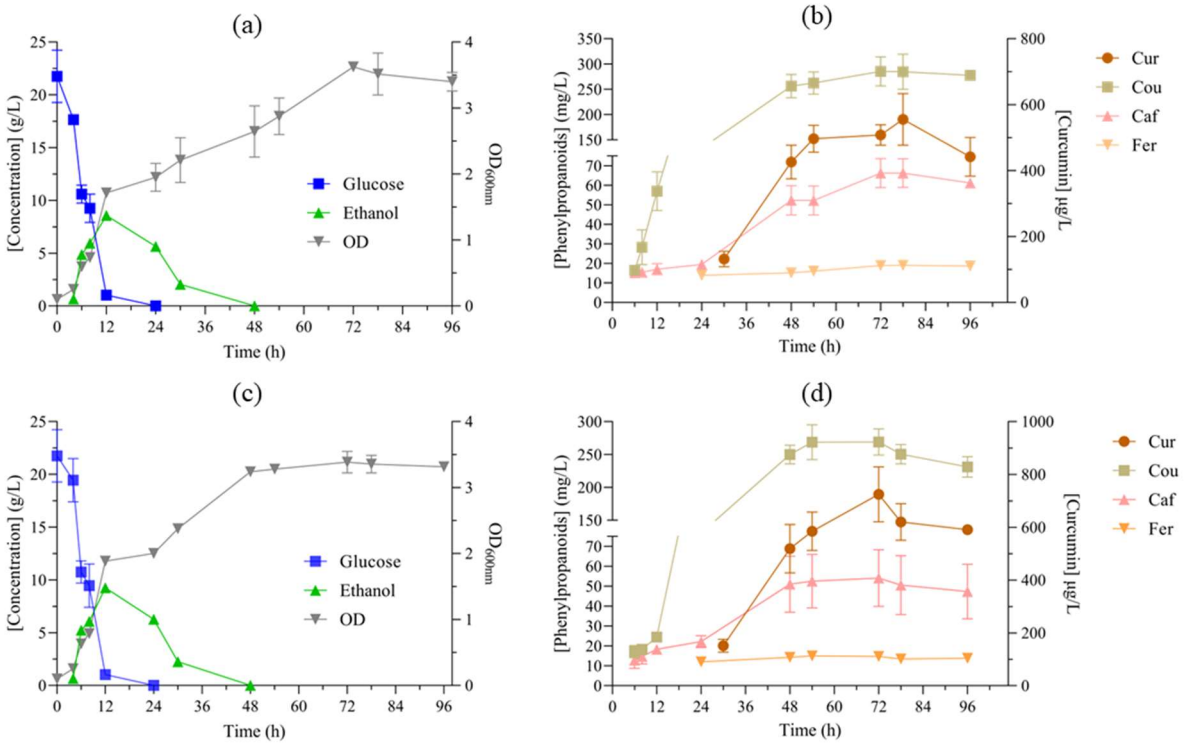


Figure 6.1: (**a,c**) Metabolic profile and optical densities at 600 nm (OD_{600nm}) of JQ2 strain in rich media with 20 g/L glucose and (**b,d**) production of phenylpropanoids and curcumin during fermentation in batch 2-L bioreactor with pH control (**a,b**) by automatic fed of 2 M of NaOH and (**c,d**) with no pH control. The presented average values ± standard deviations were derived from two independent biological replicates. Cur: Curcumin; Cou: *p*-Coumaric acid; Caf: Caffeic acid; and Fer: Ferulic acid.

In the pursuit of enhancing curcumin production using genetically engineered yeast, a fed-batch approach was explored. The gradual addition of glucose and a nitrogen source during fermentation aimed to increase conditions for yeast growth and curcumin synthesis due to the formation of high cell densities. The reactor was set as previously for the no pH control assay, and the feeding started at 12 h, since it was the point where glucose depleted which was coincident with the point that oxygen reached lowest levels. A constant flowrate of 5 mL/h was used to feed a solution of 250 g/L of glucose and 15 g/L of yeast extract. Glucose, ethanol and OD_{600nm} profiles, as well as curcumin and intermediates productions are shown in **Figure 6.1**. The fed-batch operation mode allowed the obtainment of 2-fold higher cellular densities compared to batch assays.

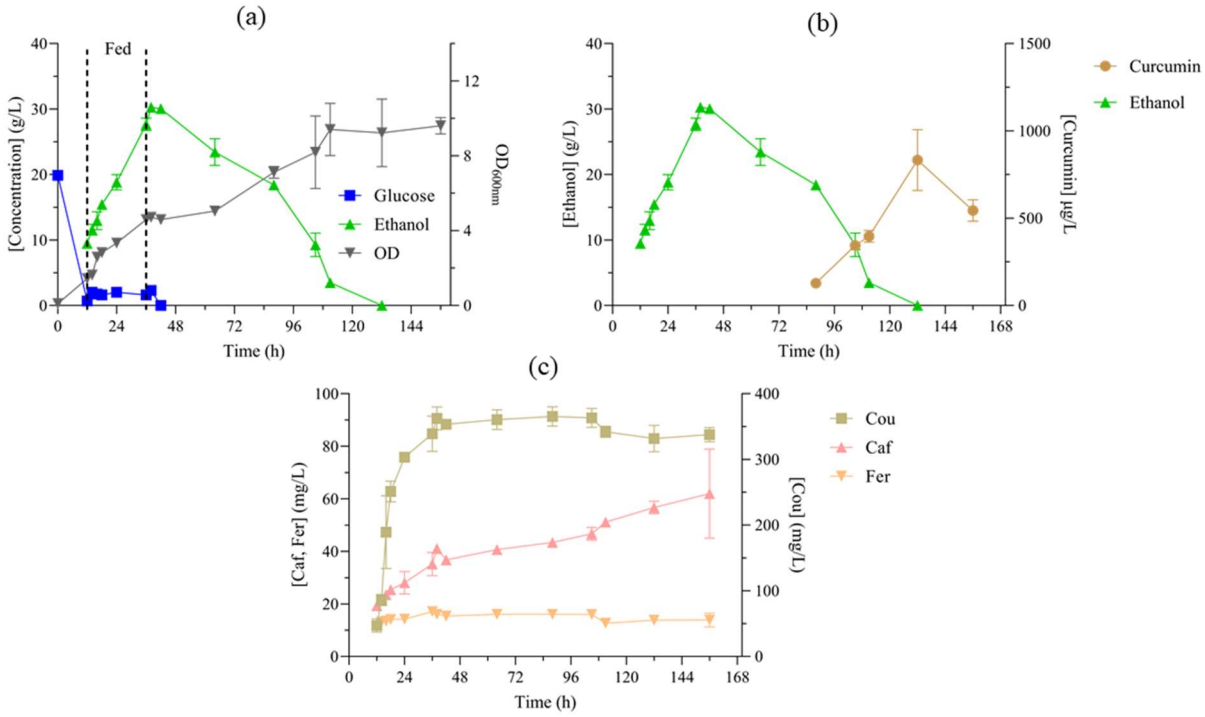


Figure 6.2: (**a**) Metabolic profile and optical density at 600 nm (OD_{600nm}) of JQ2 strain in rich media with 20 g/L glucose, (**b**) production of curcumin (**c**) and production of phenylpropanoids during fermentation in fed-batch bioreactor (feed: 250 g/L of glucose, 10 g/L yeast extract at a flowrate of 5 mL/h). The presented average values ± standard deviations were derived from two independent biological replicates. Cou: *p*-Coumaric acid; Caf: Caffeic acid; and Fer: Ferulic acid.

The feeding stopped at 36 h, as at this point glucose began to accumulate. From this timepoint, the ethanol stopped to accumulate, peaking at 30 g/L and began to be consumed, thus indicating the shift from the glucose to the ethanol metabolism. Curcumin was not detected until 84 h, peaking at 132 h, coinciding with the time of ethanol depletion. As speculated, curcumin biosynthesis occurred during the ethanol consumption phase (**Figure 6.2b**). However, the levels of curcumin produced, although slightly higher (832.7 ± 123.0 µg/L vs 724.6 ± 73.7 µg/L), were not significantly different from the batch assays. In addition, intermediates accumulation presented the same levels and profiles as previously (**Figure 6.2c**). Overall, it was not possible to implement a glucose fed-batch bioreactor process capable of significantly increasing curcumin production titers by engineered *S. cerevisiae*.

6.3.3 Bioreactor Fermentation of Strain JQ4

Afterwards, the production of curcumin in bioreactors using *S. cerevisiae* JQ4 strain was evaluated. This strain, compared to the JQ2 strain, was genetically modified for a more efficient conversion of curcumin intermediates (**Figure 6.3**). Strain JQ4 presented similar consumption profiles of glucose and ethanol to strain JQ2. However, higher OD_{600nm} were obtained (**Figure 6.3a**). Curcumin production reached its maximum at 60 h of fermentation, degrading quickly after. Previously, in flask fermentation, curcumin

production reached 2360.7 ± 111.5 µg/L (**Chapter 5**), while in bioreactor curcumin production reached 3004.3 ± 307.3 µg/L at its peak representing, a statistically significant (t-test: p-value = 0.0385) 1.3 increase in production (**Figure 6.3b**). As anticipated based on the results obtained in flasks (**Chapter 5**), JQ4 yielded a 4.2-fold increase in curcumin titers compared to JQ2 strain.

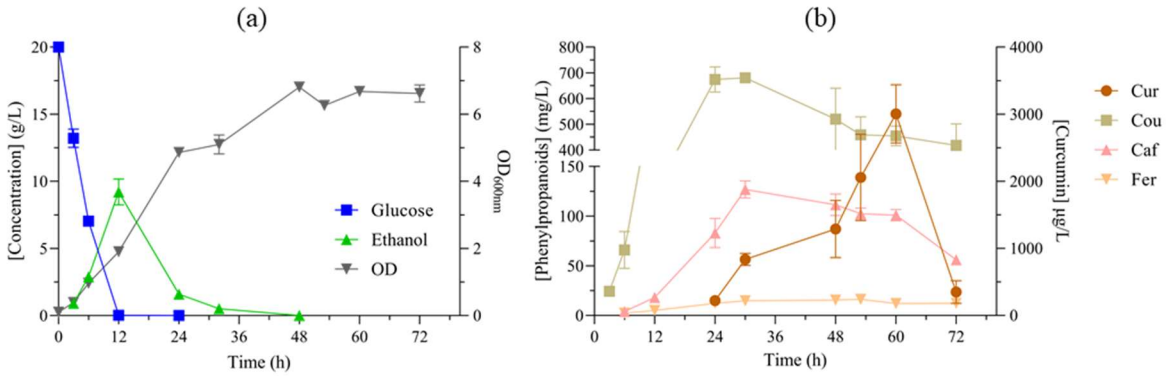


Figure 6.3: (**a**) Metabolic profile and optical density at 600 nm (OD_{600nm}) of the strain JQ4 in rich media with 20 g/L glucose and (**b**) production of phenylpropanoids and curcumin during fermentation in batch 2-L bioreactor. The presented average values ± standard deviations were derived from two independent biological replicates. Cur: Curcumin; Cou: *p*-Coumaric acid; Caf: Caffeic acid; and Fer: Ferulic acid.

Regarding the formation of intermediates, *p*-coumaric acid concentrations were substantial higher, comparing with JQ4 flask fermentations (**Chapter 5**). The concentrations of *p*-coumaric acid achieved in the bioreactor were more than five times greater than those observed in flask experiments. On the other hand, concentrations of downstream intermediates, caffeic acid and ferulic acid, did not increased in the same order of magnitude, inclusively ferulic acid concentrations were lower than the ones obtained in flasks. We hypothesize that the high accumulation of *p*-coumaric acid, the first intermediate, and the relatively low accumulation of the downstream intermediates could be attributed to the insufficient availability of enzyme redox co-factors (NADH and $FADH_2$) in bioreactor fermentation required for the reactions of synthesis of caffeic acid which could also impact ferulic acid and curcumin production. [155]. This may be attributed to specific conditions in bioreactor environment that result in a higher demand for redox co-factors compared to flask cultures. Additionally, differences in mass and/or oxygen transfer, among other factors, may contribute to the observed variation in intermediate accumulation between reactor and flask cultures.

Moreover, to investigate if the reactor settings were impacting the curcumin production, specifically the dissolved oxygen, the use of fixed stirring speed instead of a programmed stirring speed was tested. The stirring speeds were set to 400 rpm and 800 rpm. However, curcumin production was lower at the

maximal point than the obtained with programmed stirring speed, reaching 2156 ± 108.7 µg/L (for 400 rpm) and 2630.4 ± 108.7 µg/L (for 800 rpm). This result indicates that the fixation of the stirring speed may not be beneficial for maximizing curcumin production, thus suggesting the importance of dynamic control to achieve higher yields.

6.3.4 Enhancement of Curcumin Production using Ethanol Fed

Since curcumin synthesis occurred only during the ethanol consumption phase (**Figure 6.2b** and **6.3**), the potential impact of ethanol pulse addiction on the amount of curcumin produced during flask fermentation was investigated. Two pulses of 1 g/L of ethanol were administered to JQ3 strain (**Chapter 5**) during flask fermentation at 24 h and 48 h. The feeding of ethanol led to a 1.5 times improvement in curcumin titers, with no significant differences observed in the synthesis of intermediates (**Table 6.3**). We previously observed that adding ethanol at the beginning of fermentation did not improve curcumin yields. Conversely, the supplementation of ethanol after glucose depletion, during the ethanol consumption phase, enhanced curcumin production probably by extending the period during which curcumin synthesis occurs.

Table 6.3: Phenylpropanoids and curcumin production by JQ3 strain in YPD media without and with ethanol (EtOH) supplementation (1 g/L of EtOH added at 24 h and 48 h) in 250 mL flasks. The presented average values ± standard deviations were derived from three independent biological replicates. Cur: Curcumin; Cou: *p*-Coumaric acid; Caf: Caffeic acid; and Fer: Ferulic acid.

	Time (h)	Cou (mg/L)	Caf (mg/L)	Fer (mg/L)	Cur (µg/L)
JQ3	24 h	169.4 ± 3.0	62.5 ± 0.89	23.4 ± 0.28	1408.6 ± 172.8
	48 h	57.5 ± 3.1	101.8 ± 6.7	20.1 ± 0.67	
	72 h	93.4 ± 7.4	147.9 ± 4.4	32.7 ± 5.9	
JQ3 + EtOH	24 h	148.1 ± 19.1	64.56 ± 1.7	24.9 ± 0.80	2103.5 ± 168.5
	48 h	69.1 ± 2.2	137.28 ± 14.9	21.9 ± 0.56	
	72 h	77.3 ± 3.1	162.68 ± 8.7	24.3 ± 0.27	

Hereupon, it was explored if an ethanol fed-batch approach would improve curcumin biosynthesis by strain JQ4 in a bioreactor. Two experiments were performed: (a) in the first one, ethanol pulses of 1 g/L were added to the bioreactor at 24 h and 48 h of fermentation similarly to the flask experiment and, (b) in the second one, a 4 mL/h flowrate was used to feed a solution containing 15 g/L yeast extract and 43 g/L of ethanol. To ensure that the ethanol supplementation aligned with the consumption rate, the concentration of ethanol in the feed solution was calculated using the ethanol consumption rate from the previous JQ4 batch assay (**Figure 6.3**).

The ethanol pulse and ethanol fed-batch experiments yielded higher cell densities than the batch experiment, as anticipated (**Figure 6.4a** and **c**). Compared to the batch experiment, a slightly higher amount of curcumin was produced at the 36 h peak (3797.9 µg/L ± 120.7 for the ethanol pulse experiment and 3520.9 ± 112.1 µg/L for ethanol fed-batch) (**Figure 6.4b** and **d**). Moreover, the highest value of curcumin was obtained earlier, around the 36 h, while in batch culture curcumin concentrations only peaked at 60 h. As noted in the batch culture, curcumin degradation was evident. In the ethanol pulse experiment, curcumin levels peaked at 36 h and remained relatively stable until 60 h, after which a rapid decline was observed, suggesting that during this period, the rate of curcumin synthesis matched the rate of degradation. In the fed-batch experiment, curcumin also peaked at 36 h, however, a decline in concentration was observed thereafter, indicating that the degradation rate exceeded its production rate after this point. Similar intermediate concentrations, metabolic profiles and optical densities were observed in both experiments. Regarding the ethanol fed-batch, no ethanol was detected after the feeding started indicating that ethanol feeding did not exceed the ethanol consumption.

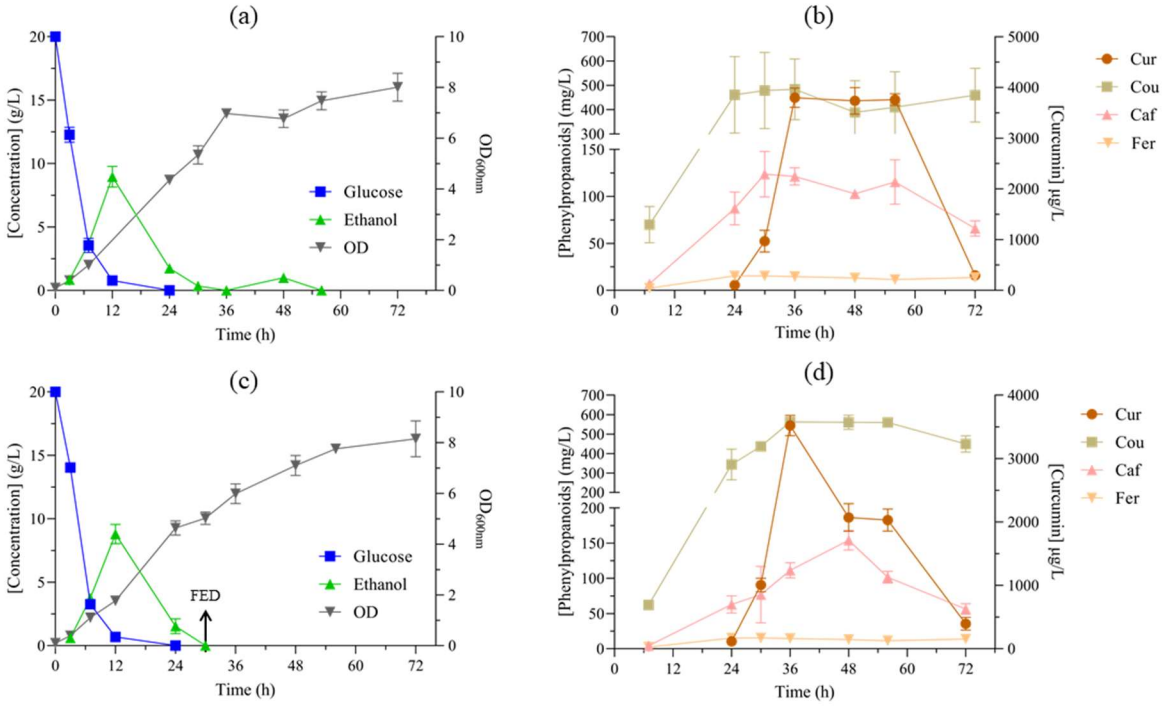


Figure 6.4: (**a,c**) Metabolic profiles and optical densities at 600 nm (OD_{600nm}) of JQ4 strain in rich media with 20 g/L glucose and (**b,d**) production of phenylpropanoids and curcumin during fermentation in 2-L bioreactor experiment with an ethanol pulse of 1 g/L (at 24 h and 48 h) (**a,b**) and in fed-batch experiment (**c,d**) by automatic fed of 4.3 g/L ethanol and 10 g/L of yeast extract at a flowrate of 4 mL/h - feed was initiated at 27 h of fermentation. The presented average values ± standard deviations were derived from two independent biological replicates. Cur: Curcumin; Cou: *p*-Coumaric acid; Caf: Caffeic acid; and Fer: Ferulic acid.

Scaling up a bioprocess from a small flask to a larger bioreactor presents a complex challenge. The transition involves more than simply increasing the volume since various factors must be carefully considered to ensure a successful and efficient upscaling. Herein, an attempt was made to develop a bioreactor-based bioprocess to increase curcumin yields produced by genetically modified *S. cerevisiae*. However, the results obtained were not found to considerably improve curcumin titers relatively compared to flask fermentation as reported for the synthesis of other phenylpropanoids [164, 170]. Overall, batch fermentations produced higher levels of curcumin relatively to the levels obtained in flasks using JQ4 strain. The feeding of glucose allowed to understand that the presence of glucose impairs the synthesis of curcumin since it was only produced during the ethanol consumption phase. The feed of ethanol proved to improve 1.5 times the curcumin titers in flask fermentations. In bioreactor fermentations, the feeding of ethanol improved 1.3 times the curcumin titers compared to the batch fermentations with no feeding. In our experiments, mainly the ones using JQ4 strain, a high accumulation of the first intermediate, *p*-coumaric acid, was detected. We hypothesized that the high accumulation of *p*-coumaric acid is related to the low availability of redox cofactors NADH and $FADH_2$ required for the hydroxylation into caffeic acid [155]. In addition, curcumin degradation was observed in the bioreactor experiments. This was only observed in previous assays using inducible promoters (see **Chapter 5 Section 5.3.1**). Curcumin degradation in bioreactor may occur by the spontaneous non enzymatic reaction with oxygen – autooxidation [211]. In other words, an excessive amount of dissolved oxygen may lead to curcumin degradation as it has been observed in resveratrol production bioreactor experiments [224]. In all the experiments performed, there was an increase in the %OD concentration from 30% to saturation during the shift from the exponential phase to the stationary phase coinciding with curcumin degradation phase (**Figure 6.5**) and supporting the autooxidation hypothesis.

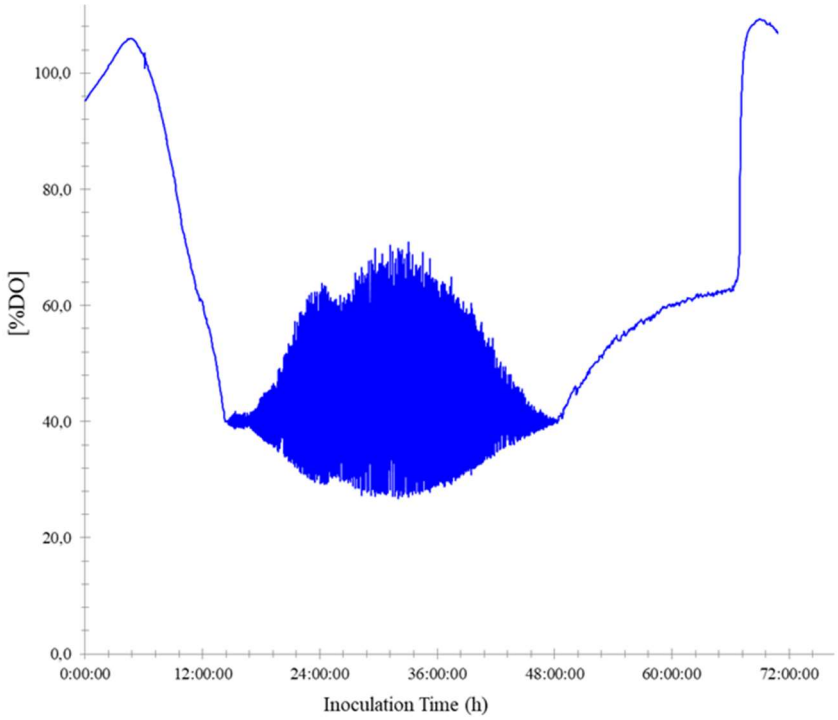


Figure 6.5: Dissolved oxygen levels (%DO) during a batch bioreactor experiment with JQ4 strain growing in YPD media with 20 g/L of glucose with an oxygen flowrate of 15 L/h.

6.3.5 Curcumin Production Using Residues

6.3.5.1 Characterization of Raw Materials

Aiming at contributing to a circular economy through the valorisation of waste products to produce high-value compounds, the potential application of rice industry by-products as culture media ingredients for curcumin biosynthesis using genetically engineered *S. cerevisiae* was explored. Two by-products were selected for evaluation: the rice husk and rice bran. Both residues were chemically characterized to reveal their composition and provide a comprehensive understanding of their potential applications in our study (**Table 6.4**).

Table 6.4: Chemical characterization of rice husk and rice bran raw materials.

%	Husk	Bran
Ash	17.4	9.9
Crude Protein	10.9	15.3
Crude Lipid	3.9	20.2
Water extractives	19.2	26.6
Ethanol extractives	3.9	16.4
Carbohydrates	52.8	49.7
Uronic acids	3.1	5.0
Glucose units	36.1	26.9
Xylose units	8.7	7.2
Arabinose units	3.2	6.4
Acid insoluble residues	24.7	10.7

A high carbohydrate content (approximately 50%) and glucose units (36.1 %) were found in both residues, which is in accordance with the literature [219]. When compared to rice husk, rice bran showed a significantly higher protein content, suggesting a higher potential as nitrogen source. The biggest difference was found in the lipid content, where rice husk displayed a more moderate 3.9 % and rice bran registered a substantial 20.2 %. In summary, both residues exhibited potential as culture media since they could both provide nitrogen and glucose to support cellular growth.

6.3.5.2 Acidic Hydrolysis of Residues

An acidic hydrolysis was carried out on both residues to obtain extracts rich in fermentable sugars. The obtained extracts were examined for the presence of glucose and fermentation inhibitors. Additionally, it was assessed if the extracts contained any curcumin intermediates. The characterization of the extracts is presented in **Table 6.5**.

Table 6.5: Chemical characterization of rice husk and rice bran extracts obtained after acidic hydrolysis. HMF: Hydroxymethylfurfural.

Compound	Husk	Bran
Glucose (g/L)	15.5	12.4
Xylose (g/L)	9.1	8.3
Arabinose (g/L)	3.0	4.0
Ethanol (g/L)	-	-
Acetic acid (g/L)	0.87	0.76
Glycerol (g/L)	0.86	0.99
Furfural (g/L)	0.052	0.029
HMF (g/L)	0.25	0.738
p-Coumaric acid (mg/L)	64.9	36.3
Caffeic acid (mg/L)	23.3	19.4
Ferulic acid (mg/L)	50.3	77.5

In both residues, the extracts contained the monosaccharides glucose, xylose, arabinose. In addition, the presence of inhibitors, furfural and hydroxymethylfurfural (HMF), was detected. The acidic hydrolysis resulted in the obtention of curcumin intermediates. As a preliminary assay, we evaluated the curcumin production by JQ3 strain using rice husk and rice bran extracts. To mimic YPD conditions, 20 g/L of peptone, 10 g/L yeast extract, and glucose to a final concentration of 20 g/L were added. At the end of fermentation, curcumin production reached 254.8 ± 24.5 µg/L using rice bran and 139.2 ± 11.0 µg/L from rice husk. Comparing to the results obtained using YPD media, curcumin production was substantially lower, however both extracts contained considerable concentrations of inhibitors, specifically HMF, with inhibitory effects documented for 1 g/L [225]. HMF is reported to inhibit crucial reactions of primary metabolism and reduce the availability of catabolic redox charge (NADH) and ATP, both essential for curcumin biosynthesis [226]. Hereupon, the use of these extracts was considered not suitable for curcumin production.

6.3.5.3 Hydrothermal Treatment in Pressurised Bioreactor

An alternative method assessed for obtaining extracts consisted in using water in a pressurized reactor, followed by enzymatic digestion. The resulting extracts contained higher glucose concentrations, fewer xylose, and considerably less inhibitors than the extracts obtained by acidic hydrolysis. Curcumin intermediates were also detected (**Table 6.6**).

Table 6.6: Chemical characterization of rice husk and rice bran extracts obtained after hydrolysis in pressurized reactor followed by enzymatic digestion. HMF: Hydroxymethylfurfural.

Compound	Husk	Bran
Glucose (g/L)	45.9	49.8
Xylose (g/L)	4.3	6.1
Arabinose (g/L)	1.7	2.7
Ethanol (g/L)	-	-
Acetic acid (g/L)	1.2	0.57
Glycerol (g/L)	0.65	0.27
Furfural (g/L)	-	-
HMF (g/L)	0.040	0.021
p-Coumaric acid (mg/L)	53.2	20.9
Caffeic acid (mg/L)	17.3	26.9
Ferulic acid (mg/L)	17.7	20.2

Next, curcumin production in JQ4 strain was evaluated using these extracts after glucose concentration being adjusted to 20 g/L. The produced curcumin and curcumin intermediates accumulation are presented in **Table 6.7**. The curcumin synthesis was 3.6-fold higher using rice bran extracts than the ones with rice husk. Moreover, the synthesis of intermediates was also superior using rice bran extracts. Comparing to the results achieved with extracts obtained via acid hydrolysis, as anticipated, the curcumin production increased by 2.1-fold in rice husk and 4.2-fold in rice bran revealing greater suitability of this method for extract preparation.

Table 6.7: Curcumin production and intermediates accumulation after fermentation of JQ4 strain using extracts obtained by hydrolysis in pressurised reactor followed by enzymatic digestion without/with supplementation of 10 g/L of yeast extract. RH: rice husk; RB: rice bran; YE: yeast extract. The presented average values ± standard deviations were derived from three independent biological replicates.

	[Curcumin] (µg/L)	*p*-Coumaric acid (mg/L)	Caffeic acid (mg/L)	Ferulic acid (mg/L)
RH	296.3 ± 35.3	128.7 ± 25.3	23.3 ± 5.9	13.2 ± 1.9
RB	1066.5 ± 91.3	184.5 ± 15.1	43.5 ± 4.6	33.5 ± 2.5
RH + YE	388.4 ± 54.1	152.34 ± 10.7	20.1 ± 1.1	15.9 ± 0.9
RB + YE	3015.7 ± 101.7	157.0 ± 12.8	93.8 ± 2.1	33.1 ± 1.1

Maintaining an optimal C/N ratio in a culture media is essential for achieving desirable microbial growth, metabolism, and product formation [227]. Hereupon, the C/N ratio was calculated and compared to YPD media. Rice husk and rice bran showed similar C/N ratios, 44.1 and 47.7

respectively. However, YPD media presented a C/N ratio of 5.7 evidencing that extracts contain a nitrogen deficit. To increase nitrogen levels, 10 g/L of yeast extract were added to the extracts, in a new experiment, and curcumin production evaluated (**Table 6.7**). The addition of yeast extract slightly increased the curcumin production in rice husk and increased 2.8-fold the produced curcumin using rice bran extracts. Moreover, for the case of rice bran extracts, the synthesis of the curcumin intermediate, caffeic acid, increased more than 2-fold revealing a better flux through phenylpropanoid path after adjusting the C/N ratio of rice bran residues.

The biosynthesis of curcumin was successfully achieved by incorporating extracts from both rice by-products as the culture media substrate using genetically modified *S. cerevisiae*. Notably, the utilization of rice bran extracts facilitated the generation of a significantly higher curcumin yield compared to extracts derived from rice husk. Furthermore, employing a pressurized hydrothermal pre-treatment, followed by enzymatic hydrolysis, resulted in the obtainment of extracts with elevated glucose concentrations and reduced inhibitor content relatively to the acidic hydrolysis. Strain JQ4 produced 2.4 ± 0.1 mg/L of curcumin in YPD media and 4.2 ± 0.6 mg/L after supplementing YPD with 100 mg/L of methionine (**Chapter 5**). Using rice bran extracts supplemented with 10 g/L of yeast extract JQ4 yielded a production of 3.0 mg/L ± 0.1 mg/L curcumin, notably surpassing that obtained with YPD without methionine supplementation. This result may indicate that the curcumin intermediates present in the extracts were assimilated by yeast and used for curcumin biosynthesis.

Curcumin has been successfully produced in the past by genetically modified *E. coli*, utilizing rice bran pitch as a source of ferulic acid [78]. In this study, we present, for the first time, the use of an agro-industrial waste as a culture media capable of supporting the growth of genetically modified yeast and leading to the biosynthesis of curcumin. Furthermore, the detection of curcumin intermediates in the extracts has the potential to enhance production titers by assimilation of intermediates for curcumin synthesis. However, the C/N ratio of rice by-products extracts was relatively high indicating a nitrogen deficiency. This can be easily overcome by the supplementation of cheap ingredients such as yeast extract as proved, or even by the addition of nitrogen rich residues such as corn steep liquor [228].

6.4 Conclusions

Numerous efforts have been made to genetically engineer microorganisms for the synthesis of the bioactive compound curcumin. However, existing approaches mostly rely on laboratory-scale flask fermentations. The transition of any biological process to industrial-scale production poses inherent

challenges. In this study, we attempted to enhance curcumin production levels by a genetically engineered *S. cerevisiae*, utilizing a 2-L lab-scale bioreactor. The upscaling yielded statistically significant improvements in curcumin yield relative to that achieved in flask fermentations for strain JQ4. Furthermore, a glucose fed-batch process unveiled that curcumin biosynthesis exclusively occurs during the ethanol consumption phase. Additionally, the ethanol supplementation enhanced curcumin yields in flask fermentations and in bioreactor experiments. However, curcumin degradation was observed in the bioreactor environment, likely due to its reaction with oxygen. In summary, curcumin production by genetically engineered yeast in bioreactors still require further research to achieve industrially desired levels.

Furthermore, aiming at contributing to a circular economy, the utilization of rice by-products as substrate to produce curcumin was investigated. The utilization of a pressurized reactor followed by enzymatic saccharification proved to be the most effective method for obtaining extracts rich in fermentable sugars and lower inhibitors concentrations. However, the C/N ratio of the extracts was found to be high. The supplementation of a nitrogen source led to an improvement in curcumin yields. Furthermore, curcumin production using rice bran residues surpassed that obtained using YPD media. In conclusion, the utilization of rice by-products, holds promise for curcumin synthesis and advancing towards a more sustainable circular economy bioprocess.

CHAPTER 7. Conclusions and Perspectives

ABSTRACT: This thesis focused on the biosynthesis of curcumin by engineered *Saccharomyces cerevisiae*. However, while promising, the production levels achieved herein could be further enhanced through genetic and operational optimizations. In this chapter the main conclusions of this thesis are drawn and some recommendations for further research are presented.

The work presented in this thesis describes the efforts to engineer *Saccharomyces cerevisiae* to produce curcumin. At the beginning of this project there were no to scarce reports addressing the biosynthesis in yeast of curcumin and its intermediates, respectively. Our knowledge was primarily derived from studies using *Escherichia coli* as host for curcumin production and the use of yeast for synthesis of other polyphenols. Indeed, curcumin biosynthesis was successfully achieved in *S. cerevisiae*. However, the titers obtained in this study are still significantly lower compared to those reported for *E. coli*. Nevertheless, our work reports the highest titers obtained in *S. cerevisiae* to date. Based on the results and findings herein presented, we have expanded our comprehension of curcumin biosynthesis in *S. cerevisiae* and highly contributed to the curcumin heterologous production state-of-art. Following, a summary of the main conclusions drawn from this thesis is provided.

The initial experimental investigation conducted in this thesis focused on the biosynthesis of curcumin from ferulic acid. Our objective was to validate engineered *S. cerevisiae* capability to synthesize curcumin. Moreover, different enzymes combinations were tested to find the most efficient pathway for curcumin biosynthesis. Regarding the activation of ferulic acid, highest curcumin titers were obtained using feruloyl-CoA synthetase (FerA) from *Pseudomonas paucimobilis* over 4-coumarate-CoA ligase (4CL1) from *Arabidopsis thaliana* which has been predominantly used in *E. coli* studies. In addition, our report addresses for the first time the expression FerA in *S. cerevisiae*. Regarding the reactions catalysed by type III polyketide synthases (PKS), some *E. coli* reports addressed the advantages of using one-pot curcuminoid synthase (CUS) from *Oryza sativa*. In our study, it was found that type III PKS from *Curcuma longa,* diketide-CoA synthase (DCS) and curcumin synthase CURS, allowed to obtain higher curcumin titers in yeast which represents a good advancement. Moreover, the deletion of *fdc* gene, coding for a ferulic acid decarboxylase (FDC) in yeast, further improved curcumin production, leading to the production of 2.7 mg/L from 30 mg/L of ferulic acid.

As our ultimate goal was to construct a yeast microbial cell factory capable of producing curcumin from simpler substrates, our subsequent experimental work aimed at the development of a strain able of *de novo* biosynthesis of curcumin. Due to the high variability of the results previously obtained using a plasmid system to express the heterologous genes, a CRISPR-Cas9 based strategy was employed to genome integrate heterologous genes. First, the synthesis of curcumin was sequentially confirmed from supplemented phenylpropanoids confirming the activities of the selected enzymes to complete the pathway: 4-hydroxyphenylacetate 3-monooxygenase complex (HpaB/C) from *Pseudomonas aeruginosa* and *Salmonella enterica* for the hydroxylation of *p*-coumaric acid into caffeic acid; and caffeic acid-*O*-

methyltransferase (COMT) from *A. thaliana* for caffeic acid methylation to ferulic acid. By integration of the designed pathway in a well-established *p*-coumaric overproducing yeast strain, *de novo* biosynthesis of curcumin was achieved. Codon optimization of HpaB and the genome integration of a second copy of HpaB/C and COMT genes improved fluxes through phenylpropanoid pathway and consequently curcumin titers. The supplementation of methionine improved curcumin by elevating S-adenosyl methionine (SAM) levels, required for caffeic acid methylation. However, the overexpression of *met13*, selected after *in silico* analysis and involved in SAM regeneration did not improve the curcumin titers probably due to the complexity of SAM regeneration. Additionally, overexpression of genes involved in malonyl-CoA synthesis, acetyl-CoA carboxylase (ACC) and fatty-acyl coenzyme A oxidase (FOX1), did not result in improved titers, indicating that malonyl-CoA is not limiting curcumin production at these levels. The use of galactose inducible promoters suggest that curcumin is degraded either by autooxidation or by some endogenous yeast enzyme. BLAST analysis of *curA* sequence, which codes for *E. coli* curcumin reductase, revealed a match with an uncharacterized protein (YML131W), suggesting the presence of a potential enzyme capable of degrading curcumin in yeast. At the end, a curcumin titer of 4.2 mg/L was achieved, representing the highest titer reported so far in yeast.

Our subsequent studies aimed to optimize operational parameters for curcumin biosynthesis using the engineered yeasts. Although an experimental design intended to optimize culture conditions did not achieve the intended results. The implementation of a lab-scale bioreactor fermentation significantly improved the curcumin titers relatively to flask fermentation of the final strain (JQ4), from 2.4 mg/L to 3.0 mg/L. In a fed-batch operation with glucose feed it was found that curcumin is only produced after glucose depletion. However, it was also found that, in bioreactor environment curcumin degrades after ethanol depletion probably by autooxidation due to the presence of elevated levels of dissolved oxygen in this phase. Moreover, since ethanol feed produced good results at flask scale fermentations, a fed-batch procedure by ethanol feeding at bioreactor scale was studied. Higher curcumin titers were obtained relatively to the batch operation mode reaching 3.8 mg/L. A relatively high concentration of the first phenylpropanoid intermediate, *p*-coumaric acid, was observed in bioreactor experiments relatively to the flask. Hereupon, we reason that in bioreactor environment the low availability of redox cofactors NADH and $FADH_2$ is blocking the pathway.

In pursuit of a sustainable process for curcumin production, we explored the use of rice industry by-products as a culture media for curcumin biosynthesis. The use of hydrothermal treatments in a pressurized bioreactor yielded extracts abundant in fermentable sugars while maintaining low

concentrations of inhibitors. Notably, the synthesis of curcumin was more pronounced using rice bran extracts (1.1 mg/L) compared to rice husk residues (0.3 mg/L). Furthermore, both extracts presented an elevated C/N ratio relatively to a culture media, indicating a nitrogen deficit. Hereupon, the supplementation of a nitrogen source improved curcumin yields to 3.0 mg/L using rice bran. In fact, curcumin production using rice bran residue was higher than obtained with a laboratorial culture media (2.4 mg/L) underscoring the promising potential of rice extracts for curcumin biosynthesis.

Overall, the proposed objectives for this thesis were accomplished which included the development of *S. cerevisiae* strain capable of *de novo* biosynthesis of curcumin, the scale-up of the process and the employment of by-products as culture media for curcumin production. However, further studies are still required to improve the curcumin production both at genetic and operational levels.

Based on the above summarised results and findings, we propose the following strategies to further improve curcumin production in engineered *S. cerevisiae*:

1. **Genetic optimization: Push-Pull-Block strategy**

Herein, we successfully developed a yeast strain capable of *de novo* curcumin biosynthesis. However, several genetic optimizations may still be performed to improve the production yields. We suggest implementing the conceptual framework of the push-pull-block strategies to enhance curcumin production as outlined below.

Push: This refers to increase the flux of precursor metabolites. The accumulation of phenylpropanoid precursors in our strains reveals its inefficient conversion to curcumin. To improve fluxes through curcumin biosynthesis, the availability of cofactors and auxiliary molecules must be optimized. Curcumin biosynthetic pathway requires the involvement of redox cofactors, NADH and $FADH_2$, for *p*-coumaric acid hydroxylation; SAM cofactor for caffeic acid methylation; and an extender molecule malonyl-CoA to curcumin formation. Regarding the redox cofactors, $FADH_2$ bioavailability appears to be the limiting one because in *S. cerevisiae* the total NADH level is 20 times higher than $FADH_2$ [155]. Moreover, $FADH_2$ concentrations are higher inside mitochondria than in cytosol [229]. $FADH_2$ synthesis may be engineered using different strategies which may include the strengthening of its native biosynthesis, the expression of a bacterial $FADH_2$ biosynthetic pathway or by manipulating its exportation from mitochondria. On the other hand, SAM regeneration is strictly regulated and complex to engineer. It was found that reducing the accumulation of SAH (SAM reactions by-product and COMT inhibitor) improves SAM levels and, consequently, the synthesis of ferulic acid in yeast. Regarding malonyl-CoA

availability, strategies may include the overexpression of the feedback-resistant version of ACC1, as well as the optimization of precursor acetyl-CoA supply, a strategy that is very well documented.

Pull: Increasing the efficiency of the curcumin pathway. Increasing the copy number of the pathway genes allowed to increase the fluxes thought curcumin biosynthesis. However, this strategy was relatively unexplored. As future work, we propose the copy number fine tuning of curcumin pathway genes which could significantly enhance the pathway performance. Additionally, the use of scaffolds or fusion proteins may improve yields by facilitating a more effective substrate channelling, as demonstrated in the synthesis of other polyphenols [160]. The use of galactose inducible promoters to control the expression of curcumin pathway genes may also improve production yields as demonstrated. However, it requires the supplementation of galactose to induce expression. This can be bypassed by *gal80* deletion in the strain. The implementation of this strategy will ensure that genes are only expressed upon glucose depletion, aligning with the curcumin production phase. This may relieve any metabolic burden during glucose consumption phase. We suggest a rational approach to identify pathway genes that will benefit from this type of control. Furthermore, the identification of limiting steps in the pathway could be overcome by engineering enzymes through random mutagenesis to enhance their performance, for example, by employing tools such as EvolvR.

Block: Eliminating competing pathways or side reactions that could degrade curcumin or intermediates. In our study, we highlight the potential presence of a gene, YML131W, which may be involved in curcumin degradation. Deleting this gene will provide insight into whether enzymatic curcumin degradation is indeed taking place in yeast. Furthermore, enzymes known to degrade curcumin precursors, *p*-coumaric and ferulic acid, have been reported, phenylacrylic acid decarboxylase (PAD) and FDC respectively. The deletion of *fdc1* did not significantly improve curcumin levels in our experiments. However, it is conceivable that, in the future, particularly with the use of a high-performance strain, this deletion may yield more significant results. Additionally, TSC13 is a gene essential for the elongation of long chain fatty acids and studies have indicated its capability to reduce *p*-coumaroyl-CoA into phloretic acid. TSC13 may also act in the reduction of feruloyl-CoA. The replacement of *tsc13* with a plant enoyl-CoA reductase can maintain the elongation function with no activity toward *p*-coumaroyl-CoA. Therefore, a similar strategy must be evaluated in our strain.

2. Genetic Optimisations driven by *in Silico* Analysis and Simulations

Besides the rational genetic optimizations mentioned above, the use of *in silico* analysis and simulations could potentially identify genetic targets that may not be intuitively apparent. In our study, we used a genome-scale model to identify genes that could be targeted to improve curcumin production. However, enzyme-constrained models (ECMs) offer more comprehensive insights into enzyme-level regulation and kinetics within metabolic pathways. The design of an ECM for the curcumin overproducing strain will facilitate the elucidation of regulatory mechanisms and metabolic fluxes within curcumin biosynthetic pathway, enabling a precise identification of genetic targets that may improve production yields.

3. Bioprocess Optimization

The bioprocess optimization involves refining the bioreactor-scale fermentation to enhance productivity. The optimizations must include adjustments to culture conditions such as the stirring, air flowrate, and media composition. Since curcumin accumulated mainly during the ethanol phase, further investigation into the fed-batch strategy involving ethanol feed is warranted. However, yeast grows faster during the glucose phase. Therefore, besides the study of ethanol feed strategy, we propose investigating a mixed feed strategy incorporating both glucose and ethanol as demonstrated previously for amorphadiene production [230].

During our experiments curcumin degradation was observed in bioreactors, possibly due to autooxidation. To avoid curcumin degradation in bioreactor environment we propose the implementation of a continuous *in situ* product recovery strategy using a solid adsorbent. Besides avoiding curcumin degradation, this may improve productivity since curcumin possesses antimicrobial properties. Favourably, curcumin has low water solubility which is advantageous for developing a selective recovery. The recovery methods may consist in an internal recovery, using resin adsorbent beads dispersed within the bioreactor vessel, or an external recovery, where the beads are in a separate column unit and the media continuously recirculated through it. These approaches have been successfully implemented, for example, in the production of taxadiene in engineered yeast [231] .

4. Explore Alternative Industrial By-Products

While we have achieved successful curcumin production from rice industry by-products extracts, we observed an increase in production titers after supplementation with a nitrogen source. In future studies, it would be beneficial to assess the utilization of nitrogen-rich residues (e.g.: corn steep liquor,

brewer's spent grain, or even yeast extracts derived from prior fermentations) in combination with rice residues for curcumin production.

CHAPTER 8. References

1. Pham, J. V., Yilma, M. A., Feliz, A., Majid, M. T., Maffetone, N., Walker, J. R., ... Yoon, Y. J. (2019). A review of the microbial production of bioactive natural products and biologics. *Frontiers in Microbiology*, *10*, 449147. https://doi.org/10.3389/FMICB.2019.01404/BIBTEX

2. Baeshen, N. A., Baeshen, M. N., Sheikh, A., Bora, R. S., Ahmed, M. M., Ramadan, H. A. I., ... Redwan, E. M. (2014). Cell factories for insulin production. *Microbial Cell Factories*, *13*(1). https://doi.org/10.1186/S12934-014-0141-0

3. Zhao, L., Zhu, Y., Jia, H., Han, Y., Zheng, X., Wang, M., & Feng, W. (2022). From plant to yeast—Advances in biosynthesis of artemisinin. *Molecules,* *27*(20), 6888. https://doi.org/10.3390/MOLECULES27206888

4. Schwechheimer, S. K., Park, E. Y., Revuelta, J. L., Becker, J., & Wittmann, C. (2016). Biotechnology of riboflavin. *Applied Microbiology and Biotechnology*, *100*(5), 2107–2119. https://doi.org/10.1007/S00253-015-7256-Z

5. Hanlon, P., & Sewalt, V. (2021). GEMs: genetically engineered microorganisms and the regulatory oversight of their uses in modern food production. *Critical Reviews in Food Science and Nutrition*, *61*(6), 959–970. https://doi.org/10.1080/10408398.2020.1749026

6. Majidian, P., Tabatabaei, M., Zeinolabedini, M., Naghshbandi, M. P., & Chisti, Y. (2018). Metabolic engineering of microorganisms for biofuel production. *Renewable and Sustainable Energy Reviews*, *82*, 3863–3885. https://doi.org/10.1016/J.RSER.2017.10.085

7. Perrone, D., Ardito, F., Giannatempo, G., Dioguardi, M., Troiano, G., Lo Russo, L., ... Lo Muzio, L. (2015). Biological and therapeutic activities, and anticancer properties of curcumin. *Experimental and Therapeutic Medicine*, *10*(5), 1615–1623. https://doi.org/10.3892/etm.2015.2749

8. Priyadarsini, K. I. (2014). The chemistry of curcumin: from extraction to therapeutic agent. *Molecules, 19*(12), 20091–20112. https://doi.org/10.3390/MOLECULES191220091

9. Schuller, D., & Casal, M. (2005). The use of genetically modified *Saccharomyces cerevisiae* strains in the wine industry. *Applied Microbiology and Biotechnology*, *68*(3), 292–304. https://doi.org/10.1007/S00253-005-1994-2/FIGURES/1

10. Niranjan, A., & Prakash, D. (2008). Chemical constituents and biological activities of turmeric (*Curcuma longa* L.) -A review. *Journal of Food Science and Technology*, *45*(2), 109–116.

11. Hewlings, S. J., & Kalman, D. S. (2017). Curcumin: A review of its effects on human health. *Foods*, *6*(10), 92. https://doi.org/10.3390/FOODS6100092

12. Amalraj, A., Pius, A., Gopi, S., & Gopi, S. (2016). Biological activities of curcuminoids, other biomolecules from turmeric and their derivatives - A review. *Journal of Traditional and Complementary Medicine*, *7*(2), 205–233. https://doi.org/10.1016/J.JTCME.2016.05.005

13. Gupta, S. C., Patchva, S., Koh, W., & Aggarwal, B. B. (2012). Discovery of curcumin, a component of the golden spice, and its miraculous biological activities. *Clinical and Experimental Pharmacology & Physiology*, *39*(3), 283. https://doi.org/10.1111/J.1440-1681.2011.05648.X

14. Goel, A., & Aggarwal, B. B. (2010). Curcumin, the golden spice from Indian saffron, is a chemosensitizer and radiosensitizer for tumors and chemoprotector and radioprotector for normal organs. *Nutrition and Cancer*, *62*(7), 919–930. https://doi.org/10.1080/01635581.2010.509835

15. Fortune Business Insights - Curcumin Market Size, Share [2032]. (2024). Retrieved from: https://www.fortunebusinessinsights.com/industry-reports/curcumin-market-101453

16. Kanai, M., Otsuka, Y., Otsuka, K., Sato, M., Nishimura, T., Mori, Y., … Shibata, H. (2013). A phase I study investigating the safety and pharmacokinetics of highly bioavailable curcumin (Theracurmin) in cancer patients. *Cancer Chemotherapy and Pharmacology*, *71*(6), 1521–1530. https://doi.org/10.1007/S00280-013-2151-8

17. Belcaro, G., Cesarone, M. R., Dugall, M., Pellegrini, L., Ledda, A., Grossi, M. G., … Appendino, G. (2010). Efficacy and safety of Meriva®, a curcumin-phosphatidylcholine complex, during extended administration in osteoarthritis patients. *Alternative Medicine Review*, *15*(4), 337–344.

18. Ranjan, A. P., Mukerjee, A., Helson, L., & Vishwanatha, J. K. (2012). Scale up, optimization and stability analysis of Curcumin C3 complex-loaded nanoparticles for cancer therapy. *Journal of Nanobiotechnology*, *10*(1), 1–18. https://doi.org/10.1186/1477-3155-10-38/FIGURES/13

19. Poudel, A., Pandey, J., & Lee, H. K. (2019). Geographical discrimination in curcuminoids content of turmeric assessed by rapid UPLC-DAD validated analytical method. *Molecules*, *24*(9). https://doi.org/10.3390/MOLECULES24091805

20. Zielińska, A., Alves, H., Marques, V., Durazzo, A., Lucarini, M., Alves, T. F., … Souto, E. B. (2020). Properties, extraction methods, and delivery systems for curcumin as a natural source of beneficial health effects. *Medicina*, *56*(7), 1–19. https://doi.org/10.3390/MEDICINA56070336

21. Nagavekar, N., & Singhal, R. S. (2019). Supercritical fluid extraction of *Curcuma longa* and *Curcuma amada* oleoresin: Optimization of extraction conditions, extract profiling, and comparison of bioactivities. *Industrial Crops and Products*, *134*, 134–145. https://doi.org/10.1016/J.INDCROP.2019.03.061

22. Aydin, F., Yilmaz, E., & Soylak, M. (2018). Vortex assisted deep eutectic solvent (DES)-emulsification liquid-liquid microextraction of trace curcumin in food and herbal tea samples. *Food Chemistry*, *243*, 442–447. https://doi.org/10.1016/J.FOODCHEM.2017.09.154

23. Mandal, V., Mohan, Y., & Hemalatha, S. (2008). Microwave assisted extraction of curcumin by sample-solvent dual heating mechanism using Taguchi L9 orthogonal design. *Journal of Pharmaceutical and Biomedical Analysis*, *46*(2), 322–327. https://doi.org/10.1016/J.JPBA.2007.10.020

24. Menghwar, P., Yilmaz, E., & Soylak, M. (2018). Development of an ultrasonic-assisted restricted access supramolecular solvent-based liquid phase microextraction (UA-RAS-LPME) method for separation-preconcentration and UV-VIS spectrophotometric detection of curcumin, *Separation Science and Technology,* *53*(16), 2612–2621. https://doi.org/10.1080/01496395.2018.1462389

25. Sahne, F., Mohammadi, M., Najafpour, G. D., & Moghadamnia, A. A. (2017). Enzyme-assisted ionic liquid extraction of bioactive compound from turmeric (*Curcuma longa*): Isolation, purification and analysis of curcumin. *Industrial Crops and Products*, *95*, 686–694. https://doi.org/10.1016/J.INDCROP.2016.11.037

26. Gupta, A. P., Gupta, M. M., & Kumar, S. (2006). Simultaneous determination of curcuminoids in curcuma samples using high performance thin layer chromatography, *Journal of Liquid Chromatography & Related Technologies*, *22*(10), 1561–1569. https://doi.org/10.1081/JLC-100101751

27. Revathy, S., Elumalai, S., Benny, M., & Antony, B. (2011). Isolation, purification and identification of curcuminoids from turmeric (*Curcuma longa* L .) by column chromatography, *Journal of Experimental Sciences, 2*(7), 21–25.

28. Pabon, H. J. J. (1964). A synthesis of curcumin and related compounds. *Recueil des Travaux Chimiques des Pays-Bas*, *83*(4), 379–386. https://doi.org/10.1002/RECL.19640830407

29. Venkata Rao, E., & Sudheer, P. (2011). Revisiting curcumin chemistry part I: A new strategy for the synthesis of curcuminoids. *Indian Journal of Pharmaceutical Sciences*, *73*(3), 262. https://doi.org/10.4103/0250-474X.93508

30. Yixuan, L., Qaria, M. A., Sivasamy, S., Jianzhong, S., & Daochen, Z. (2021). Curcumin production and bioavailability: A comprehensive review of curcumin extraction, synthesis, biotransformation and delivery systems. *Industrial Crops and Products*, *172*, 114050. https://doi.org/10.1016/J.INDCROP.2021.114050

31. Tomeh, M. A., Hadianamrei, R., & Zhao, X. (2019). A review of curcumin and its derivatives as anticancer agents. *International Journal of Molecular Sciences*, *20*(5), 1033. https://doi.org/10.3390/ijms20051033

32. Rodrigues, F. C., Kumar, N. A., & Thakur, G. (2021). The potency of heterocyclic curcumin analogues: An evidence-based review. *Pharmacological Research*, *166*, 105489. https://doi.org/10.1016/J.PHRS.2021.105489

33. Kunnumakkara, A. B., Bordoloi, D., Padmavathi, G., Monisha, J., Roy, N. K., Prasad, S., & Aggarwal, B. B. (2017). Curcumin, the golden nutraceutical: multitargeting for multiple chronic diseases. *British Journal of Pharmacology*, *174*(11), 1325–1348. https://doi.org/10.1111/BPH.13621

34. Marín, Y. E., Wall, B. A., Wang, S., Namkoong, J., Martino, J. J., Suh, J., ... Ryu, J. H. (2007). Curcumin downregulates the constitutive activity of NF-kB and induces apoptosis in novel mouse

melanoma cells. *Melanoma Research*, *17*(5), 274–283. https://doi.org/10.1097/CMR.0B013E3282ED3D0E

35. Marquardt, J. U., Gomez-Quiroz, L., Arreguin Camacho, L. O., Pinna, F., Lee, Y. H., Kitade, M., ... Thorgeirsson, S. S. (2015). Curcumin effectively inhibits oncogenic NF-kB signaling and restrains stemness features in liver cancer. *Journal of Hepatology*, *63*(3), 661. https://doi.org/10.1016/J.JHEP.2015.04.018

36. Shanmugam, M. K., Rane, G., Kanchi, M. M., Arfuso, F., Chinnathambi, A., Zayed, M. E., ... Sethi, G. (2015). The multifaceted role of curcumin in cancer prevention and treatment. *Molecules*, *20*(2), 2728–2769. https://doi.org/10.3390/MOLECULES20022728

37. Singh, S., & Aggarwal, B. B. (1995). Activation of transcription factor NF-kB is suppressed by curcumin (diferuloylmethane) [corrected]. *The Journal of Biological Chemistry*, *270*(42), 24995–25000. https://doi.org/10.1074/JBC.270.42.24995

38. Hahn, Y. Il, Kim, S. J., Choi, B. Y., Cho, K. C., Bandu, R., Kim, K. P., ... Surh, Y. J. (2018). Curcumin interacts directly with the Cysteine 259 residue of STAT3 and induces apoptosis in H-Ras transformed human mammary epithelial cells. *Scientific Reports*, *8*(1). https://doi.org/10.1038/S41598-018-23840-2

39. Yen, H. Y., Tsao, C. W., Lin, Y. W., Kuo, C. C., Tsao, C. H., & Liu, C. Y. (2019). Regulation of carcinogenesis and modulation through Wnt/β-catenin signaling by curcumin in an ovarian cancer cell line. *Scientific Reports 2019 9:1*, *9*(1), 1–14. https://doi.org/10.1038/s41598-019-53509-3

40. Patiño-Morales, C. C., Soto-Reyes, E., Arechaga-Ocampo, E., Ortiz-Sánchez, E., Antonio-Véjar, V., Pedraza-Chaverri, J., & García-Carrancá, A. (2020). Curcumin stabilizes p53 by interaction with NAD(P)H:quinone oxidoreductase 1 in tumor-derived cell lines. *Redox Biology*, *28*, 101320. https://doi.org/10.1016/J.REDOX.2019.101320

41. Talib, W. H., Al-Hadid, S. A., Ali, M. B. W., Al-Yasari, I. H., & Ali, M. R. A. (2018). Role of curcumin in regulating p53 in breast cancer: an overview of the mechanism of action. *Breast Cancer: Targets and Therapy*, *10*, 207. https://doi.org/10.2147/BCTT.S167812

42. Amin, A. R. M. R., Haque, A., Rahman, M. A., Chen, Z. G., Khuri, F. R., & Shin, D. M. (2015). Curcumin induces apoptosis of upper aerodigestive tract cancer cells by targeting multiple pathways. *PloS One*, *10*(4). https://doi.org/10.1371/JOURNAL.PONE.0124218

43. Hassan, F. U., Rehman, M. S. U., Khan, M. S., Ali, M. A., Javed, A., Nawaz, A., & Yang, C. (2019). Curcumin as an alternative epigenetic modulator: Mechanism of action and potential effects. *Frontiers in Genetics*, *10*, 514. https://doi.org/10.3389/FGENE.2019.00514/BIBTEX

44. Lin, X., Bai, D., Wei, Z., Zhang, Y., Huang, Y., Deng, H., & Huang, X. (2019). Curcumin attenuates oxidative stress in RAW264.7 cells by increasing the activity of antioxidant enzymes and activating the Nrf2-Keap1 pathway. *PloS One*, *14*(5), e0216711. https://doi.org/10.1371/JOURNAL.PONE.0216711

45. Guo, Y. L., Li, X. Z., & Kuang, C. T. (2011). Antioxidant pathways and chemical mechanism of curcumin. *Advanced Materials Research*, *236*, 2311–2314. https://doi.org/10.4028/WWW.SCIENTIFIC.NET/AMR.236-238.2311

46. Amor, S., Peferoen, L. A. N., Vogel, D. Y. S., Breur, M., van der Valk, P., Baker, D., & Van Noort, J. M. (2014). Inflammation in neurodegenerative diseases – an update. *Immunology*, *142*(2), 151–166. https://doi.org/10.1111/IMM.12233

47. Chapple, I. L. C. (1997). Reactive oxygen species and antioxidants in inflammatory diseases. *Journal of Clinical Periodontology*, *24*(5), 287–296. https://doi.org/10.1111/J.1600-051X.1997.TB00760.X

48. Biswas, S. K. (2016). Does the interdependence between oxidative stress and inflammation explain the antioxidant paradox? *Oxidative Medicine and Cellular Longevity*, *2016*. https://doi.org/10.1155/2016/5698931

49. Parameswaran, N., & Patial, S. (2010). Tumor necrosis Factor-α signaling in macrophages. *Critical Reviews in Eukaryotic Gene Expression*, *20*(2), 87. https://doi.org/10.1615/CritRevEukarGeneExpr.v20.i2.10

50. Aggarwal, B. B., Gupta, S. C., & Sung, B. (2013). Curcumin: an orally bioavailable blocker of TNF and other pro-inflammatory biomarkers. *British Journal of Pharmacology*, *169*(8), 1672. https://doi.org/10.1111/BPH.12131

51. Paulino, N., Paulino, A. S., Diniz, S. N., De Mendonça, S., Gonçalves, I. D., Faião Flores, F., ... Quincoces Suarez, J. A. (2016). Evaluation of the anti-inflammatory action of curcumin analog (DM1): Effect on iNOS and COX-2 gene expression and autophagy pathways. *Bioorganic & Medicinal Chemistry*, *24*(8), 1927–1935. https://doi.org/10.1016/J.BMC.2016.03.024

52. Zorofchian Moghadamtousi, S., Abdul Kadir, H., Hassandarvish, P., Tajik, H., Abubakar, S., & Zandi, K. (2014). A review on antibacterial, antiviral, and antifungal activity of curcumin. *BioMed Research International*, *2014*. https://doi.org/10.1155/2014/186864

53. Kaur, S., Modi, N. H., Panda, D., & Roy, N. (2010). Probing the binding site of curcumin in *Escherichia coli* and *Bacillus subtilis* FtsZ–a structural insight to unveil antibacterial activity of curcumin. *European Journal of Medicinal Chemistry*, *45*(9), 4209–4214. https://doi.org/10.1016/J.EJMECH.2010.06.015

54. Mun, S. H., Joung, D. K., Kim, Y. S., Kang, O. H., Kim, S. B., Seo, Y. S., ... Kwon, D. Y. (2013). Synergistic antibacterial effect of curcumin against methicillin-resistant *Staphylococcus aureus*. *Phytomedicine : International Journal of Phytotherapy and Phytopharmacology*, *20*(8–9), 714–718. https://doi.org/10.1016/J.PHYMED.2013.02.006

55. Alihosseini, F., Azarmi, S., Ghaffari, S., Haghighat, S., & Sorkhabadi, S. M. R. (2016). Synergic antibacterial effect of curcumin with ampicillin; free drug solutions in comparison with SLN dispersions. *Advanced Pharmaceutical Bulletin*, *6*(3), 461. https://doi.org/10.15171/APB.2016.060

56. Sharma, M., Manoharlal, R., Puri, N., & Prasad, R. (2010). Antifungal curcumin induces reactive oxygen species and triggers an early apoptosis but prevents hyphae development by targeting the global repressor TUP1 in *Candida albicans*. *Bioscience Reports*, *30*(6), 391–404. https://doi.org/10.1042/BSR20090151

57. Phuna, Z. X., Yu, J. K. E., Tee, J. Y., Chuah, S. Q., Tan, N. W. H., Vijayabalan, S., ... Madhavan, P. (2020). In vitro evaluation of nanoemulsions of curcumin, piperine, and tualang honey as antifungal agents for *Candida* species. *Journal of Applied Biotechnology Reports*, *7*(3), 189–197. https://doi.org/10.30491/JABR.2020.109997

58. Gupta, M., Chandra, A., & Aggarwal, G. (2018). Curcumin: potential therapeutic moiety for fungal infections. *Current Traditional Medicine*, *4*(4), 249–262. https://doi.org/10.2174/2215083805666181120124245

59. Mathew, D., & Hsu, W. L. (2018). Antiviral potential of curcumin. *Journal of Functional Foods*, *40*, 692–699. https://doi.org/10.1016/J.JFF.2017.12.017

60. Jennings, M. R., & Parks, R. J. (2020). Curcumin as an antiviral agent. *Viruses*, *12*(11). https://doi.org/10.3390/V12111242

61. Marín-Palma, D., Tabares-Guevara, J. H., Zapata-Cardona, M. I., Flórez-álvarez, L., Yepes, L. M., Rugeles, M. T., … Taborda, N. A. (2021). Curcumin inhibits *in vitro* SARS-CoV-2 infection in vero E6 cells through multiple antiviral mechanisms. *Molecules*, *26*(22). https://doi.org/10.3390/MOLECULES26226900

62. Phipps, K. R., Quesnot, N., Privat, K., Baldwin, N. J., Ahlborn, E., & Fança-Berthon, P. (2020). Toxicological safety evaluation of a novel highly bioavailable turmeric extract formulation. *Journal of Applied Toxicology*, *40*(2), 285–299. https://doi.org/10.1002/JAT.3903

63. Kocaadam, B., & Şanlier, N. (2017). Curcumin, an active component of turmeric (*Curcuma longa*), and its effects on health. *Critical Reviews in Food Science and Nutrition*, *57*(13), 2889–2895. https://doi.org/10.1080/10408398.2015.1077195

64. Lao, C. D., Ruffin IV, M. T., Normolle, D., Heath, D. D., Murray, S. I., Bailey, J. M., … Brenner, D. E. (2006). Dose escalation of a curcuminoid formulation. *BMC Complementary and Alternative Medicine*, *6*(1), 10. https://doi.org/10.1186/1472-6882-6-10

65. Siviero, A., Gallo, E., Maggini, V., Gori, L., Mugelli, A., Firenzuoli, F., & Vannacci, A. (2015). Curcumin, a golden spice with a low bioavailability. *Journal of Herbal Medicine*, *5*(2), 57–70. https://doi.org/10.1016/J.HERMED.2015.03.001

66. Yang, K.-Y., Lin, L.-C., Tseng, T.-Y., Wang, S.-C., & Tsai, T.-H. (2007). Oral bioavailability of curcumin in rat and the herbal analysis from *Curcuma longa* by LC-MS/MS. *Journal of Chromatography*, *853*(1–2), 183–9. https://doi.org/10.1016/j.jchromb.2007.03.010

67. Vareed, S. K., Kakarala, M., Ruffin, M. T., Crowell, J. A., Normolle, D. P., Djuric, Z., & Brenner, D. E. (2008). Pharmacokinetics of curcumin conjugate metabolites in healthy human subjects.

Cancer epidemiology, Biomarkers & Prevention, *17*(6), 1411–1417. https://doi.org/10.1158/1055-9965.EPI-07-2693

68. Ferrari, E., Lazzari, S., Marverti, G., Pignedoli, F., Spagnolo, F., & Saladini, M. (2009). Synthesis, cytotoxic and combined cDDP activity of new stable curcumin derivatives. *Bioorganic & Medicinal Chemistry*, *17*(8), 3043–3052. https://doi.org/10.1016/J.BMC.2009.03.016

69. Cao, Y. K., Li, H. J., Song, Z. F., Li, Y., & Huai, Q. Y. (2014). Synthesis and biological evaluation of novel curcuminoid derivatives. *Molecules,* *19*(10), 16349–16372. https://doi.org/10.3390/MOLECULES191016349

70. Rodrigues, J. L., Prather, K. L. J., Kluskens, L. D., & Rodrigues, L. R. (2015). Heterologous production of curcuminoids. *Microbiology and Molecular Biology Reviews*, *79*(1), 39–60. https://doi.org/10.1128/MMBR.00031-14

71. Katsuyama, Y., Kita, T., Funa, N., & Horinouchi, S. (2009). Curcuminoid biosynthesis by two type III polyketide synthases in the herb *Curcuma longa*. *Journal of Biological Chemistry*, *284*(17), 11160–11170. https://doi.org/10.1074/jbc.M900070200

72. Ramirez-Ahumada, M. del C., Timmermann, B. N., & Gang, D. R. (2006). Biosynthesis of curcuminoids and gingerols in turmeric (*Curcuma longa*) and ginger (*Zingiber officinale*): identification of curcuminoid synthase and hydroxycinnamoyl-CoA thioesterases. *Phytochemistry*, *67*(18), 2017–29. https://doi.org/10.1016/j.phytochem.2006.06.028

73. Ehlting, È., Bu, D., Wang, Q., & Kombrink, E. (1999). Three 4-coumarate : coenzyme A ligases in *Arabidopsis thaliana* represent two evolutionarily divergent classes in angiosperms. The Plant Journal, *19*(1), 9-20. *19*. https://doi.org/10.1046/j.1365-313X.1999.00491.x

74. Katsuyama, Y., Kita, T., & Horinouchi, S. (2009). Identification and characterization of multiple curcumin synthases from the herb *Curcuma longa*. *FEBS Letters*, *583*(17), 2799–2803. https://doi.org/10.1016/j.febslet.2009.07.029

75. Santhoshkumar, R., & Yusuf, A. (2020). *In silico* structural modeling and analysis of physicochemical properties of curcumin synthase (CURS1, CURS2, and CURS3) proteins of *Curcuma longa*. *Journal of Genetic Engineering and Biotechnology*, *18*(1), 1–9. https://doi.org/10.1186/S43141-020-00041-X/FIGURES/6

76. Inoue, K., Nomura, C., Ito, S., Nagatsu, A., Hino, T., & Oka, H. (2008). Purification of curcumin, demethoxycurcumin, and bisdemethoxycurcumin by high-speed countercurrent chromatography. *Journal of Agricultural and Food Chemistry*, *56*(20), 9328–9336. https://doi.org/10.1021/jf801815n

77. Kulkarni, S. J., Maske, K. N., Budre, M. P., & Mahajan, R. P. (2012). Extraction and purification of curcuminoids from Turmeric (*Curcuma longa* L.). *International Journal of Pharmacology and Pharmaceutical Technology*, *1*(2), 2277–3436.

78. Katsuyama, Y., Matsuzawa, M., Funa, N., & Horinouchi, S. (2008). Production of curcuminoids by *Escherichia coli* carrying an artificial biosynthesis pathway. *Microbiology*, *154*(9), 2620–2628. https://doi.org/10.1099/mic.0.2008/018721-0

79. Wang, S., Zhang, S., Zhou, T., Zeng, J., & Zhan, J. (2013). Design and application of an *in vivo* reporter assay for phenylalanine ammonia-lyase. *Applied Microbiology and Biotechnology*, *97*(17), 7877–7885. https://doi.org/10.1007/S00253-013-5122-4

80. Rodrigues, J. L., Araújo, R. G., Prather, K. L. J., Kluskens, L. D., & Rodrigues, L. R. (2015). Production of curcuminoids from tyrosine by a metabolically engineered *Escherichia coli* using caffeic acid as an intermediate. *Biotechnology Journal*, *10*(4), 599–609. https://doi.org/10.1002/biot.201400637

81. Couto, M. R., Rodrigues, J. L., & Rodrigues, L. R. (2017). Optimization of fermentation conditions for the production of curcumin by engineered *Escherichia coli*. *Journal of The Royal Society Interface*, *14*(133), 20170470. https://doi.org/10.1098/rsif.2017.0470

82. Rodrigues, J. L., Gomes, D., & Rodrigues, L. R. (2020). A combinatorial approach to optimize the production of curcuminoids from tyrosine in *Escherichia coli*. *Frontiers in Bioengineering and Biotechnology*, *8*(2), 1–15. https://doi.org/10.3389/fbioe.2020.00059

83. Fang, Z., Jones, J. A., Zhou, J., & Koffas, M. A. (2018). Engineering *Escherichia coli* co-cultures for production of curcuminoids from glucose. *Biotechnology Journal*, *13*(5). https://doi.org/10.1002/BIOT.201700576

84. Kim, E. J., Cha, M. N., Kim, B.-G., & Ahn, J.-H. (2017). Production of curcuminoids in engineered *Escherichia coli*. *Journal of Microbiology and Biotechnology*, *27*(5), 975–982. https://doi.org/10.4014/jmb.1701.01030

85. Chu, L. L., Pandey, R. P., Dhakal, D., & Sohng, J. K. (2020). Increased production of dicinnamoylmethane via improving cellular malonyl-CoA level by using a CRISPRi in *Escherichia coli*. *Applied Biochemistry and Biotechnology*, *190*(1), 325–340. https://doi.org/10.1007/S12010-019-03206-8

86. Kang, S.-Y., Heo, K. T., & Hong, Y.-S. (2018). Optimization of artificial curcumin biosynthesis in *E. coli* by randomized 5′-UTR sequences to control the multienzyme pathway. *ACS Synthetic Biology*, *7*(9), 2054–2062. https://doi.org/10.1021/ACSSYNBIO.8B00198

87. Wu, J., Chen, W., Zhang, Y., Zhang, X., Jin, J.-M., & Tang, S.-Y. (2020). Metabolic engineering for improved curcumin biosynthesis in *Escherichia coli*. *Journal of Agricultural and Food Chemistry*, *68*(39), 10772–10779. https://doi.org/10.1021/ACS.JAFC.0C04276

88. Chen, J., Wang, W., Wang, L., Wang, H., Hu, M. L., Zhou, J., ... Zeng, W. (2024). Efficient *de novo* biosynthesis of curcumin in *Escherichia coli* by optimizing pathway modules and increasing the malonyl-CoA supply. *Journal of Agricultural and Food Chemistry*, *72*(1), 566–576. https://doi.org/10.1021/ACS.JAFC.3C07379

89. Kan, E., Katsuyama, Y., Maruyama, J. I., Tamano, K., Koyama, Y., & Ohnishi, Y. (2019). Production of the plant polyketide curcumin in *Aspergillus oryzae*: Strengthening malonyl-CoA supply for yield improvement. *Bioscience, Biotechnology and Biochemistry*, *83*(7), 1372–1381. https://doi.org/10.1080/09168451.2019.1606699

90. Incha, M. R., Thompson, M. G., Blake-Hedges, J. M., Liu, Y., Pearson, A. N., Schmidt, M., ... Keasling, J. D. (2019). Leveraging host metabolism for bisdemethoxycurcumin production in *Pseudomonas putida*. *Metabolic Engineering Communications, 10, e00119.*. https://doi.org/10.1101/753889

91. Palmer, C. M., Miller, K. K., Nguyen, A., & Alper, H. S. (2020). Engineering 4-coumaroyl-CoA derived polyketide production in *Yarrowia lipolytica* through a β-oxidation mediated strategy. *Metabolic Engineering*, *57*, 174–181. https://doi.org/10.1016/J.YMBEN.2019.11.006

92. Utomo, J. C., Barrell, H. B., Kumar, R., Smith, J., Brant, M. S., De la Hoz Siegler, H., & Ro, D. K. (2024). Reconstructing curcumin biosynthesis in yeast reveals the implication of caffeoyl-shikimate esterase in phenylpropanoid metabolic flux. *Metabolic Engineering*, *82*, 286–296. https://doi.org/10.1016/J.YMBEN.2024.02.011

93. Gomes, D., Rainha, J., Rodrigues, L. R., & Rodrigues, J. L. (2021). Yeast synthetic biology approaches for the production of valuable polyphenolic compounds. In *Synthetic Biology of Yeasts: Tools and Applications*.

94. Katsuyama, Y., Funa, N., & Horinouchi, S. (2007). Precursor-directed biosynthesis of stilbene methyl ethers in *Escherichia coli*. *Biotechnology Journal*, *2*(10), 1286–1293. https://doi.org/10.1002/BIOT.200700098

95. Katsuyama, Y., Matsuzawa, M., Funa, N., & Horinouchi, S. (2007). *In vitro* synthesis of curcuminoids by type III polyketide synthase from *Oryza sativa*. *Journal of Biological Chemistry*, *282*(52), 37702–37709. https://doi.org/10.1074/jbc.M707569200

96. Morita, H., Wanibuchi, K., Kato, R., Sugio, S., & Abe, I. (2010). Expression, purification and crystallization of a plant type III polyketide synthase that produces diarylheptanoids. *Acta Crystallographica Section F: Structural Biology and Crystallization Communications, 66*(8), 948-950. https://doi.org/10.1107/S1744309110023572

97. Miyazono, K. ichi, Um, J., Imai, F. L., Katsuyama, Y., Ohnishi, Y., Horinouchi, S., & Tanokura, M. (2011). Crystal structure of curcuminoid synthase CUS from *Oryza sativa*. *Proteins: Structure, Function and Bioinformatics*, *79*(2), 669–673. https://doi.org/10.1002/prot.22888

98. Katsuyama, Y., Hirose, Y., Funa, N., Ohnishi, Y., & Horinouchi, S. (2010). Precursor-directed biosynthesis of curcumin analogs in *Escherichia coli*. *Bioscience, Biotechnology and Biochemistry*, *74*(3), 641–645. https://doi.org/10.1271/bbb.90866

99. Rodrigues, J. L., Couto, M. R., Araújo, R. G., Prather, K. L. J., Kluskens, L., & Rodrigues, L. R. (2017). Hydroxycinnamic acids and curcumin production in engineered *Escherichia coli* using heat shock promoters. *Biochemical Engineering Journal*, *125*, 41–49. https://doi.org/10.1016/J.BEJ.2017.05.015

100. Rodrigues, J. L., & Rodrigues, L. R. (2018). Potential Applications of the Escherichia coli Heat Shock Response in Synthetic Biology. *Trends in biotechnology*, *36*(2), 186–198. https://doi.org/10.1016/J.TIBTECH.2017.10.014

101. Rodrigues, J. L., Sousa, M., Prather, K. L. J., Kluskens, L. D., & Rodrigues, L. R. (2014). Selection of *Escherichia coli* heat shock promoters toward their application as stress probes. *Journal of Biotechnology*, *188*, 61–71. https://doi.org/10.1016/J.JBIOTEC.2014.08.005

102. Castaño-Cerezo, S., Bernal, V., Röhrig, T., Termeer, S., & Cánovas, M. (2015). Regulation of acetate metabolism in *Escherichia coli* BL21 by protein Nε-lysine acetylation. *Applied Microbiology and Biotechnology*, *99*(8), 3533–3545. https://doi.org/10.1007/S00253-014-6280-8/FIGURES/6

103. Santos, C. N. S., Xiao, W., & Stephanopoulos, G. (2012). Rational, combinatorial, and genomic approaches for engineering L-tyrosine production in *Escherichia coli*. *Proceedings of the National Academy of Sciences*, *109*(34), 13538–13543. https://doi.org/10.1073/PNAS.1206346109/-/DCSUPPLEMENTAL

104. Kang, S. Y., Choi, O., Lee, J. K., Ahn, J. O., Ahn, J. S., Hwang, B. Y., & Hong, Y. S. (2015). Artificial *de novo* biosynthesis of hydroxystyrene derivatives in a tyrosine overproducing *Escherichia coli* strain. *Microbial Cell Factories*, *14*(1), 1–11. https://doi.org/10.1186/S12934-015-0268-7/TABLES/1

105. Rodrigues, J. L., Ferreira, D., & Rodrigues, L. R. (n.d.). Synthetic biology strategies towards the development of new bioinspired technologies for medical applications. In *Bioinspired materials for medical applications*.

106. Rodrigues, J. L., & Rodrigues, L. R. (2017). Synthetic Biology: Perspectives in Industrial Biotechnology. In *Foundations of Biotechnology and Bioengineering, Volume 1 - Current Developments in Biotechnology & Bioengineering*.

107. Wang, L., Li, N., Yu, S., & Zhou, J. (2023). Enhancing caffeic acid production in *Escherichia coli* by engineering the biosynthesis pathway and transporter. *Bioresource Technology*, *368*, 128320. https://doi.org/10.1016/J.BIORTECH.2022.128320

108. Mukhopadhyay, A. (2015). Tolerance engineering in bacteria for the production of advanced biofuels and chemicals. *Trends in Microbiology*, *23*(8), 498–508. https://doi.org/10.1016/J.TIM.2015.04.008

109. Tyagi, P., Singh, M., Kumari, H., Kumari, A., & Mukhopadhyay, K. (2015). Bactericidal activity of curcumin I is associated with damaging of bacterial membrane. *PloS One*, *10*(3), e0121313. https://doi.org/10.1371/JOURNAL.PONE.0121313

110. Konzock, O., Zaghen, S., & Norbeck, J. (2021). Tolerance of *Yarrowia lipolytica* to inhibitors commonly found in lignocellulosic hydrolysates. *BMC Microbiology*, *21*(1), 1–10. https://doi.org/10.1186/S12866-021-02126-0/TABLES/1

111. Botstein, D., & Fink, G. R. (2011). Yeast: An experimental organism for 21st century biology. *Genetics*, *189*(3), 695–704. https://doi.org/10.1534/genetics.111.130765

112. Nielsen, J., Larsson, C., van Maris, A., & Pronk, J. (2013). Metabolic engineering of yeast for production of fuels and chemicals. *Current Opinion in Biotechnology*. https://doi.org/10.1016/j.copbio.2013.03.023

113. Gnügge, R., & Rudolf, F. (2017). *Saccharomyces cerevisiae* shuttle vectors. *Yeast*, *34*(5), 205–221. https://doi.org/10.1002/yea.3228

114. Karim, A., Curran, K. A., & Alper, H. S. (2013). Characterization of plasmid burden and copy number in *Saccharomyces cerevisiae* for optimization of metabolic engineering applications. FEMS Yeast Research, *13*(1), 107-116.

115. Bernardi, B., & Wendland, J. (2020). Homologous recombination: A GRAS yeast genome editing tool. *Fermentation*, *6*(2), 57. https://doi.org/10.3390/fermentation6020057

116. Da Silva, N. A., & Srikrishnan, S. (2012). Introduction and expression of genes for metabolic engineering applications in *Saccharomyces cerevisiae*. *FEMS Yeast Research*, *12*(2), 197–214. https://doi.org/10.1111/j.1567-1364.2011.00769.x

117. Park, Y.-N., Masison, D., Eisenberg, E., & Greene, L. E. (2011). Application of the FLP/FRT system for conditional gene deletion in yeast *Saccharomyces cerevisiae*. *Yeast*, *28*(9), 673–681. https://doi.org/10.1002/yea.1895

118. Yamanishi, M., & Matsuyama, T. (2012). A modified Cre-lox genetic switch to dynamically control metabolic flow in *Saccharomyces cerevisiae*. *ACS Synthetic Biology*, *1*(5), 172–180. https://doi.org/10.1021/sb200017p

119. Solis-Escalante, D., Kuijpers, N. G. A., van der Linden, F. H., Pronk, J. T., Daran, J.-M., & Daran-Lapujade, P. (2014). Efficient simultaneous excision of multiple selectable marker cassettes using I-SceI-induced double-strand DNA breaks in *Saccharomyces cerevisiae*. *FEMS Yeast Research*, *14*(5), 741–754. https://doi.org/10.1111/1567-1364.12162

120. Kuijpers, N. G. A., Chroumpi, S., Vos, T., Solis-Escalante, D., Bosman, L., Pronk, J. T., ... Daran-Lapujade, P. (2013). One-step assembly and targeted integration of multigene constructs assisted by the I-SceI meganuclease in *Saccharomyces cerevisiae*. *FEMS Yeast Research*, *13*(8), 769–781. https://doi.org/10.1111/1567-1364.12087

121. Roberts, R. J. (2005). How restriction enzymes became the workhorses of molecular biology. *Proceedings of the National Academy of Sciences*. *102*(17), 5905-5908 https://doi.org/10.1073/pnas.0500923102

122. Barrangou, R., Fremaux, C., Deveau, H., Richards, M., Boyaval, P., Moineau, S., ... Horvath, P. (2007). CRISPR provides acquired resistance against viruses in prokaryotes. *Science*, *315*(5819), 1709–1712. https://doi.org/10.1126/science.1138140

123. Luo, M. L., Leenay, R. T., & Beisel, C. L. (2016). Current and future prospects for CRISPR-based tools in bacteria. *Biotechnology and Bioengineering*, *113*(5), 930–943. https://doi.org/10.1002/bit.25851

124. Makarova, K. S., Haft, D. H., Barrangou, R., Brouns, S. J. J., Charpentier, E., Horvath, P., ... Koonin, E. V. (2011). Evolution and classification of the CRISPR-Cas systems. *Nature Reviews Microbiology*, *9*(6), 467–477. https://doi.org/10.1038/nrmicro2577

125. Jinek, M., Chylinski, K., Fonfara, I., Hauer, M., Doudna, J. A., & Charpentier, E. (2012). A programmable dual-RNA-guided DNA endonuclease in adaptive bacterial immunity. *Science*, *337*(6096), 816–821. https://doi.org/10.1126/science.1225829

126. DiCarlo, J., Norville, J. E., Mali, P., Rios, X., Aach, J., & Church, G. M. (2013). Genome engineering in Saccharomyces cerevisiae using CRISPR-Cas systems. *Nucleic Acids Research*, *41*(7), 4336-4343. https://doi.org/10.1093/nar/gkt135

127. Generoso, W. C., Gottardi, M., Oreb, M., & Boles, E. (2016). Simplified CRISPR-Cas genome editing for *Saccharomyces cerevisiae*. *Journal of Microbiological Methods*, *127*, 203-205. https://doi.org/10.1016/j.mimet.2016.06.020

128. Bao, Z., Xiao, H., Liang, J., Zhang, L., Xiong, X., Sun, N., ... Zhao, H. (2015). Homology-Integrated CRISPR–Cas (HI-CRISPR) system for one-step multigene disruption in *Saccharomyces cerevisiae*. *ACS Synthetic Biology*, *4*(5), 585–594. https://doi.org/10.1021/sb500255k

129. Yu, B. J., & Kim, S. C. (2007). Minimization of the *Escherichia coli* genome using the Tn5-targeted Cre/loxP excision system. *Methods in Molecular Biology*, *416*, 261–277. https://doi.org/10.1007/978-1-59745-321-9_17

130. Komatsu, M., Uchiyama, T., Omura, S., Cane, D. E., & Ikeda, H. (2010). Genome-minimized *Streptomyces* host for the heterologous expression of secondary metabolism. *Proceedings of the National Academy of Sciences*, *107*(6), 2646–2651. https://doi.org/10.1073/pnas.0914833107

131. Mans, R., van Rossum, H. M., Wijsman, M., Backx, A., Kuijpers, N. G. A., van den Broek, M., ... Daran, J. M. G. (2015). CRISPR/Cas9: A molecular Swiss army knife for simultaneous introduction of multiple genetic modifications in *Saccharomyces cerevisiae*. *FEMS Yeast Research*, *15*(2), 1–15. https://doi.org/10.1093/femsyr/fov004

132. González-Ramos, D., Gorter De Vries, A. R., Grijseels, S. S., Van Berkum, M. C., Swinnen, S., Van Den Broek, M., ... Van Maris, A. J. A. (2016). A new laboratory evolution approach to select for constitutive acetic acid tolerance in *Saccharomyces cerevisiae* and identification of causal mutations. *Biotechnology for Biofuels*, *9*(1), 1–18. https://doi.org/10.1186/s13068-016-0583-1

133. Hai, Z., Hao, L., Bin, M., Xinyi, M., Min, T., Feng, L., ... Zhi, D. (2020). Immediate , multiplexed and sequential genome engineering facilitated by CRISPR/Cas9 in *Saccharomyces cerevisiae*. *Journal of Industrial Microbiology & Biotechnology*, *47*(1), 83–96. https://doi.org/10.1007/s10295-019-02251-w

134. Shi, S., Liang, Y., Zhang, M. M., Ang, E. L., & Zhao, H. (2016). A highly efficient single-step, markerless strategy for multi-copy chromosomal integration of large biochemical pathways in *Saccharomyces cerevisiae*. *Metabolic Engineering*, *33*, 19-27. https://doi.org/10.1016/j.ymben.2015.10.011

135. Tou, C. J., Schaffer, D. V, & Dueber, J. E. (2020). Targeted diversification in the *S. cerevisiae* genome with CRISPR-guided DNA polymerase I. *ACS Synthetic Biology*, *9*(7), 1911-1916 https://doi.org/10.1021/acssynbio.0c00149

136. Qi, L. S., Larson, M. H., Gilbert, L. A., Doudna, J. A., Weissman, J. S., Arkin, A. P., & Lim, W. A. (2013). Repurposing CRISPR as an RNA-guided platform for sequence-specific control of gene expression. *Cell*, *152*(5), 1173–1183. https://doi.org/10.1016/j.cell.2013.02.022

137. Farzadfard, F., Perli, S. D., & Lu, T. K. (2013). Tunable and multifunctional eukaryotic transcription factors based on CRISPR/Cas. *ACS Synthetic Biology*, *2*(10), 604–613. https://doi.org/10.1021/sb400081r

138. Zalatan, J. G., Lee, M. E., Almeida, R., Gilbert, L. A., Whitehead, E. H., La Russa, M., ... Lim, W. A. (2015). Engineering complex synthetic transcriptional programs with CRISPR RNA scaffolds. *Cell*, *160*(1–2), 339–350. https://doi.org/10.1016/j.cell.2014.11.052

139. Lian, J., Hamedirad, M., Hu, S., & Zhao, H. (2017). Combinatorial metabolic engineering using an orthogonal tri-functional CRISPR system. *Nature Communications*, *8*(1), 1–9. https://doi.org/10.1038/s41467-017-01695-x

140. Dong, C., Jiang, L., Xu, S., Huang, L., Cai, J., Lian, J., & Xu, Z. (2020). A Single Cas9-VPR nuclease for simultaneous gene activation, repression, and editing in *Saccharomyces cerevisiae*. *ACS Synthetic Biology*, *9*(9), 2252-2257 https://doi.org/10.1021/acssynbio.0c00218

141. Stovicek, V., Holkenbrink, C., & Borodina, I. (2017). CRISPR/Cas system for yeast genome engineering: advances and applications. *FEMS Yeast Research*, *17*(5), fox030. https://doi.org/10.1093/femsyr/fox030

142. Deaner, M., & Alper, H. S. (2017). Systematic testing of enzyme perturbation sensitivities via graded dCas9 modulation in *Saccharomyces cerevisiae*. *Metabolic Engineering*, *40*, 14-22. https://doi.org/10.1016/j.ymben.2017.01.012

143. Yu, Y., Chang, P., Yu, H., Ren, H., Hong, D., Li, Z., ... Li, C. (2018). Productive amyrin synthases for efficient α -amyrin synthesis in engineered *Saccharomyces cerevisiae*. *ACS synthetic biology*, *7*(10), 2391–2402. https://doi.org/10.1021/acssynbio.8b00176

144. Kiani, S., Chavez, A., Tuttle, M., Hall, R. N., Chari, R., Ter-ovanesyan, D., ... Church, G. (2015). Cas9 gRNA engineering for genome editing, activation and repression. *Nature Methods*, *12*(11), 1051-1054. https://doi.org/10.1038/nmeth.3580

145. Dahlman, J. E., Abudayyeh, O. O., Joung, J., Gootenberg, J. S., Zhang, F., & Konermann, S. (2015). Orthogonal gene knockout and active Cas9 nuclease. *Nature Biotechnology*, *33*(11), 1159-1161.. https://doi.org/10.1038/nbt.3390

146. Yu, D., Xu, F., Zeng, J., & Zhan, J. (2012). Type III polyketide synthases in natural product biosynthesis. *IUBMB Life*, *64*(4), 285–295. https://doi.org/10.1002/iub.1005

147. Rodriguez, A., Kildegaard, K. R., Li, M., Borodina, I., & Nielsen, J. (2015). Establishment of a yeast platform strain for production of *p*-coumaric acid through metabolic engineering of aromatic amino acid biosynthesis. *Metabolic Engineering*, *31*, 181-188. https://doi.org/10.1016/j.ymben.2015.08.003

148. Rodriguez, A., Chen, Y., Khoomrung, S., Özdemir, E., Borodina, I., & Nielsen, J. (2017). Comparison of the metabolic response to over-production of *p*-coumaric acid in two yeast strains. *Metabolic Engineering*, *44*, 265-272. https://doi.org/10.1016/j.ymben.2017.10.013

149. Borja, G. M., Rodriguez, A., Campbell, K., Borodina, I., Chen, Y., & Nielsen, J. (2019). Metabolic engineering and transcriptomic analysis of *Saccharomyces cerevisiae* producing *p*-coumaric acid from xylose. *Microbial Cell Factories*, *18*(1). https://doi.org/10.1186/s12934-019-1244-4

150. Liu, Q., Yu, T., Li, X., Chen, Y., Campbell, K., Nielsen, J., & Chen, Y. (2019). Rewiring carbon metabolism in yeast for high level production of aromatic chemicals. *Nature Communications*, *10*(1), 1–13. https://doi.org/10.1038/s41467-019-12961-5

151. Liu, L., Liu, H., Zhang, W., Yao, M., Li, B., Liu, D., & Yuan, Y. (2019). Engineering the biosynthesis of caffeic acid in *Saccharomyces cerevisiae* with heterologous enzyme combinations. *Engineering*, *5*(2), 287-295. https://doi.org/10.1016/j.eng.2018.11.029

152. Li, Y., Li, Y., Mao, J., Liu, Q., Song, X., Wu, Y., Cai, M., ... & Qiao, M. (2020). De novo biosynthesis of caffeic acid from glucose by engineered Saccharomyces cerevisiae. *ACS Synthetic Biology*, *9*(4), 756-765. https://doi.org/10.1021/acssynbio.9b00431

153. Zhou, P., Yue, C., Shen, B., Du, Y., Xu, N., & Ye, L. (2021). Metabolic engineering of *Saccharomyces cerevisiae* for enhanced production of caffeic acid. *Applied Microbiology and Biotechnology 2021*, 1–11. https://doi.org/10.1007/S00253-021-11445-1

154. Qi, H., Yu, L., Li, Y., Cai, M., He, J., Liu, J., ... Qiao, M. (2022). Developing multi-copy chromosomal integration strategies for heterologous biosynthesis of caffeic acid in *Saccharomyces cerevisiae*. *Frontiers in Microbiology*, *13*, 851706. https://doi.org/10.3389/FMICB.2022.851706/BIBTEX

155. Chen, R., Gao, J., Yu, W., Chen, X., Zhai, X., Chen, Y., ... Zhou, Y. J. (2022). Engineering cofactor supply and recycling to drive phenolic acid biosynthesis in yeast. *Nature Chemical Biology*, *18*(5), 520–529. https://doi.org/10.1038/s41589-022-01014-6

156. Becker, J. V. W., Armstrong, G. O., van der Merwe, M. J., Lambrechts, M. G., Vivier, M. A., & Pretorius, I. S. (2003). Metabolic engineering of *Saccharomyces cerevisiae* for the synthesis of the wine-related antioxidant resveratrol. *FEMS Yeast Research*, *4*(1), 79–85. https://doi.org/10.1016/S1567-1356(03)00157-0

157. Beekwilder, J., Wolswinkel, R., Jonker, H., Hall, R., De Rie Vos, C. H., & Bovy, A. (2006). Production of resveratrol in recombinant microorganisms. *Applied and Environmental Microbiology*, *72*(8), 5670–5672. https://doi.org/10.1128/AEM.00609-06

158. Sydor, T., Schaffer, S., & Boles, E. (2010). Considerable increase in resveratrol production by recombinant industrial yeast strains with use of rich medium. *Applied and Environmental Microbiology*, *76*(10), 3361–3363. https://doi.org/10.1128/AEM.02796-09

159. Shin, S. Y., Han, N. S., Park, Y. C., Kim, M. D., & Seo, J. H. (2011). Production of resveratrol from p-coumaric acid in recombinant *Saccharomyces cerevisiae* expressing 4-coumarate:coenzyme A ligase and stilbene synthase genes. *Enzyme and Microbial Technology*, *48*(1), 48–53. https://doi.org/10.1016/j.enzmictec.2010.09.004

160. Wang, Y., Halls, C., Zhang, J., Matsuno, M., Zhang, Y., & Yu, O. (2011). Stepwise increase of resveratrol biosynthesis in yeast *Saccharomyces cerevisiae* by metabolic engineering. *Metabolic Engineering*, *13*(5), 455–463. https://doi.org/10.1016/j.ymben.2011.04.005

161. Shin, S.-Y., Jung, S.-M., Kim, M.-D., Han, N. S., & Seo, J.-H. (2012). Production of resveratrol from tyrosine in metabolically engineered *Saccharomyces cerevisiae*. *Enzyme and Microbial Technology*, *51*(4), 211–216. https://doi.org/10.1016/j.enzmictec.2012.06.005

162. Wang, Y., & Yu, O. (2012). Synthetic scaffolds increased resveratrol biosynthesis in engineered yeast cells. *Journal of Biotechnology*, *157*(1), 258–260. https://doi.org/10.1016/j.jbiotec.2011.11.003

163. Li, M., Kildegaard, K. R., Chen, Y., Rodriguez, A., Borodina, I., & Nielsen, J. (2015). *De novo* production of resveratrol from glucose or ethanol by engineered *Saccharomyces cerevisiae*. *Metabolic Engineering*, *32*, 1–11. https://doi.org/10.1016/j.ymben.2015.08.007

164. Li, M., Schneider, K., Kristensen, M., Borodina, I., & Nielsen, J. (2016). Engineering yeast for high-level production of stilbenoid antioxidants. *Scientific Reports*, *6*(1), 1–8. https://doi.org/10.1038/srep36827

165. Jiang, H., Wood, K. V., & Morgan, J. A. (2005). Metabolic engineering of the phenylpropanoid pathway in *Saccharomyces cerevisiae*. *Applied and Environmental Microbiology*, *71*(6), 2962–2969. https://doi.org/10.1128/AEM.71.6.2962-2969.2005

166. Trantas, E., Panopoulos, N., & Ververidis, F. (2009). Metabolic engineering of the complete pathway leading to heterologous biosynthesis of various flavonoids and stilbenoids in *Saccharomyces cerevisiae*. *Metabolic Engineering*, *11*(6), 355–366. https://doi.org/10.1016/j.ymben.2009.07.004

167. Koopman, F., Beekwilder, J., Crimi, B., van Houwelingen, A., Hall, R. D., Bosch, D., ... Daran, J. M. (2012). *De novo* production of the flavonoid naringenin in engineered *Saccharomyces cerevisiae*. *Microbial Cell Factories*, *11*(1), 1–15. https://doi.org/10.1186/1475-2859-11-155

168. Rodriguez, A., Strucko, T., Stahlhut, S. G., Kristensen, M., Svenssen, D. K., Forster, J., ... Borodina, I. (2017). Metabolic engineering of yeast for fermentative production of flavonoids. *Bioresource Technology*, *245*, 1645–1654. https://doi.org/10.1016/j.biortech.2017.06.043

169. Lyu, X., Ng, K. R., Lee, J. L., Mark, R., & Chen, W. N. (2017). Enhancement of naringenin biosynthesis from tyrosine by metabolic engineering of *Saccharomyces cerevisiae*. *Journal of Agricultural and Food Chemistry*, *65*(31), 6638–6646. https://doi.org/10.1021/acs.jafc.7b02507

170. Mao, J., Mohedano, M. T., Fu, J., Li, X., Liu, Q., Nielsen, J., ... Chen, Y. (2023). Fine-tuning of *p*-coumaric acid synthesis to increase (2S)-naringenin production in yeast. *Metabolic Engineering*, *79*, 192–202. https://doi.org/10.1016/J.YMBEN.2023.08.003

171. Tous Mohedano, M., Mao, J., & Chen, Y. (2023). Optimization of pinocembrin biosynthesis in *Saccharomyces cerevisiae*. *ACS Synthetic Biology*, *12*(1), 144–152. https://doi.org/10.1021/ACSSYNBIO.2C00425/SUPPL_FILE/SB2C00425_SI_001.PDF

172. Lv, X., Wang, F., Zhou, P., Ye, L., Xie, W., Xu, H., & Yu, H. (2016). Dual regulation of cytoplasmic and mitochondrial acetyl-CoA utilization for improved isoprene production in *Saccharomyces cerevisiae*. *Nature Communications*, *7*(1), 1–12. https://doi.org/10.1038/ncomms12851

173. Farhi, M., Marhevka, E., Masci, T., Marcos, E., Eyal, Y., Ovadis, M., ... Vainstein, A. (2011). Harnessing yeast subcellular compartments for the production of plant terpenoids. *Metabolic Engineering*, *13*(5), 474–481. https://doi.org/10.1016/j.ymben.2011.05.001

174. Zhang, Y., Li, S. Z., Li, J., Pan, X., Cahoon, R. E., Jaworski, J. G., ... Yu, O. (2006). Using unnatural protein fusions to engineer resveratrol biosynthesis in yeast and mammalian cells. *Journal of the American Chemical Society*, *128*(40), 13030–13031. https://doi.org/10.1021/ja0622094

175. Gorman, S. D., & Boehr, D. D. (2019). Energy and enzyme activity landscapes of yeast chorismate mutase at cellular concentrations of allosteric effectors. *Biochemistry*, *58*(39), 4058–4069.. https://doi.org/10.1021/acs.biochem.9b00721

176. Nielsen, J., Nielsen, J., & Keasling, J. D. (2016). Engineering cellular metabolism. *Cell*, *164*(6), 1185-1197. https://doi.org/10.1016/j.cell.2016.02.004

177. Chen, X., Yang, X., Shen, Y., Hou, J., & Bao, X. (2017). Increasing malonyl-CoA derived product through controlling the transcription regulators of phospholipid synthesis in *Saccharomyces cerevisiae*. *ACS Synthetic Biology*, *6*(5), 905–912. https://doi.org/10.1021/acssynbio.6b00346

178. Chen, X., Yang, X., Shen, Y., Hou, J., & Bao, X. (2018). Screening phosphorylation site mutations in yeast acetyl-CoA carboxylase using malonyl-CoA sensor to improve malonyl-CoA-derived product. *Frontiers in Microbiology*, *9*(1), 1–8. https://doi.org/10.3389/fmicb.2018.00047

179. Shi, S., Chen, Y., Siewers, V., & Nielsen, J. (2014). Improving production of malonyl Coenzyme A-Derived metabolites by abolishing snf1-dependent regulation of Acc1. *mBio*, *5*(3), e01130-14-e01130-14. https://doi.org/10.1128/mBio.01130-14

180. Thomas, D., & Surdin-Kerjan, Y. (1997). Metabolism of sulfur amino acids in *Saccharomyces cerevisiae*. *Microbiology and Molecular Biology Reviews*, *61*(4), 503. https://doi.org/10.1128/MMBR.61.4.503-532.1997

181. Dixon, R. A., & Paiva, N. L. (1995). Stress-induced phenylpropanoid metabolism. *The Plant Cell*, *7*(7), 1085–1097. https://doi.org/10.1105/tpc.7.7.1085

182. Nelson, K. M., Dahlin, J. L., Bisson, J., Graham, J., Pauli, G. F., & Walters, M. A. (2017). The essential medicinal chemistry of curcumin. *Journal of Medicinal Chemistry*, *60*(5), 1620–1637. https://doi.org/10.1021/acs.jmedchem.6b00975

183. Park, S. Y., Yang, D., Ha, S. H., & Lee, S. Y. (2019). Metabolic engineering of microorganisms for the production of natural compounds. *Advanced Biosystems*, *3*(7), 1900122. https://doi.org/10.1002/ADBI.201900122

184. Winston, F., Dollard, C., & Ricupero-Hovasse, S. L. (1995). Construction of a set of convenient *Saccharomyces cerevisiae* strains that are isogenic to S288C. *Yeast*, *11*(1), 53–55. https://doi.org/10.1002/YEA.320110107

185. Chen, Y., Partow, S., Scalcinati, G., Siewers, V., & Nielsen, J. (2012). Enhancing the copy number of episomal plasmids in *Saccharomyces cerevisiae* for improved protein production. *FEMS Yeast Research*, *12*(5), 598–607. https://doi.org/10.1111/j.1567-1364.2012.00809.x

186. Agatep, R., Kirkpatrick, R. D., Parchaliuk, D. L., Woods, R. A., & Gietz, R. D. (1998). Transformation of *Saccharomyces cerevisiae* by the lithium acetate/single-stranded carrier DNA/polyethylene glycol protocol. *Technical Tips Online*, *3*(1), 133–137. https://doi.org/10.1016/s1366-2120(08)70121-1

187. Shao, Z., Zhao, H., & Zhao, H. (2009). DNA assembler, an *in vivo* genetic method for rapid construction of biochemical pathways. *Nucleic Acids Research*, *37*(2), 1–10. https://doi.org/10.1093/nar/gkn991

188. Singh, M. V., & Weil, P. A. (2002). A method for plasmid purification directly from yeast. *Analytical Biochemistry*, *307*(1), 13–17. https://doi.org/10.1016/S0003-2697(02)00018-0

189. Partow, S., Siewers, V., Bjørn, S., Nielsen, J., & Maury, J. (2010). Characterization of different promoters for designing a new expression vector in *Saccharomyces cerevisiae*. *Yeast*, *27*(11), 955–64. https://doi.org/10.1002/yea.1806

190. Marchiosi, R., dos Santos, W. D., Constantin, R. P., de Lima, R. B., Soares, A. R., Finger-Teixeira, A., ... Ferrarese-Filho, O. (2020). Biosynthesis and metabolic actions of simple phenolic acids in plants. *Phytochemistry Reviews*, *19*, 865-906. https://doi.org/10.1007/s11101-020-09689-2

191. Adeboye, P. T., Bettiga, M., & Olsson, L. (2014). The chemical nature of phenolic compounds determines their toxicity and induces distinct physiological responses in *Saccharomyces cerevisiae* in lignocellulose hydrolysates. *AMB Express*, *4*(1), 1–10. https://doi.org/10.1186/s13568-014-0046-7

192. Fletcher, E., Gao, K., Mercurio, K., Ali, M., & Baetz, K. (2019). Yeast chemogenomic screen identifies distinct metabolic pathways required to tolerate exposure to phenolic fermentation inhibitors ferulic acid, 4-hydroxybenzoic acid and coniferyl aldehyde. *Metabolic Engineering*, *52*, 98–109. https://doi.org/10.1016/j.ymben.2018.11.010

193. Nagy, E. Z. A., Nagy, C. L., Filip, A., Nagy, K., Gál, E., Tőtős, R., ... Bencze, L. C. (2019). Exploring the substrate scope of ferulic acid decarboxylase (FDC1) from *Saccharomyces cerevisiae*. *Scientific Reports*, *9*(1), 1–10. https://doi.org/10.1038/s41598-018-36977-x

194. Liu, D., Li, B., Liu, H., Guo, X., & Yuan, Y. (2017). Profiling influences of gene overexpression on heterologous resveratrol production in *Saccharomyces cerevisiae*. *Frontiers of Chemical Science and Engineering*, *11*(1), 117–125. https://doi.org/10.1007/s11705-016-1601-3

195. Masai, E., Harada, K., Peng, X., Kitayama, H., Katayama, Y., & Fukuda, M. (2002). Cloning and characterization of the ferulic acid catabolic genes of *Sphingomonas paucimobilis* SYK-6. *Applied*

and Environmental Microbiology, *68*(9), 4416–4424. https://doi.org/10.1128/AEM.68.9.4416-4424.2002

196. Shockey, J. M., Fulda, M. S., & Browse, J. (2003). *Arabidopsis* contains a large superfamily of acyl-activating enzymes. Phylogenetic and biochemical analysis reveals a new class of acyl-Coenzyme A synthetases. *Plant Physiology*, *132*(2), 1065–1076. https://doi.org/10.1104/PP.103.020552

197. Chen, X., Yang, X., Shen, Y., Hou, J., & Bao, X. (2017). Increasing Malonyl-CoA Derived Product through Controlling the Transcription Regulators of Phospholipid Synthesis in *Saccharomyces cerevisiae*. *ACS Synthetic Biology*, *6*(5), 905–912. https://doi.org/10.1021/acssynbio.6b00346

198. Pereira, R., Mohamed, E. T., Radi, M. S., Herrgård, M. J., Feist, A. M., Nielsen, J., & Chen, Y. (2020). Elucidating aromatic acid tolerance at low pH in *Saccharomyces cerevisiae* using adaptive laboratory evolution. *Proceedings of the National Academy of Sciences*, *117*(45), 27954–27961. https://doi.org/10.1073/pnas.2013044117

199. Kim, S. B., Bisson, J., Friesen, J. B., Bucchini, L., Gafner, S., Lankin, D. C., ... McAlpine, J. B. (2021). The untargeted capability of NMR recognizes nefarious adulteration in natural products. *Journal of Natural Products*, *84*(3), 846. https://doi.org/10.1021/ACS.JNATPROD.0C01196

200. Khudhayer Oglah, M., & Fakri Mustafa, Y. (2020). Curcumin analogs: synthesis and biological activities. *Medicinal Chemistry Research*, *29*(3), 479–486. https://doi.org/10.1007/s00044-019-02497-0

201. Iii, C. A. M., Martinat, M. A., & Hyman, L. E. (1998). Assessment of aryl hydrocarbon receptor complex interactions using pBEVY plasmids: expression vectors with bi-directional promoters for use in *Saccharomyces cerevisiae*. *Nucleic Acids Research*, *26*(15). https://doi.org/10.1093/nar/26.15.3577

202. Gietz, R. D., & Schiestl, R. H. (2007). High-efficiency yeast transformation using the LiAc/SS carrier DNA/PEG method. *Nature Protocols*, *2*(1), 31–34. https://doi.org/10.1038/nprot.2007.13

203. Labhsetwar, P., Melo, M. C., Cole, J. A., & Luthey-Schulten, Z. (2017). Population FBA predicts metabolic phenotypes in yeast. *PLoS Computational Biology*, *13*(9), e1005728.. https://doi.org/10.1371/journal.pcbi.1005728

204. Andrade, R., Doostmohammadi, M., Santos, J. L., Sagot, M. F., Mira, N. P., & Vinga, S. (2020). MOMO-multi-objective metabolic mixed integer optimization: application to yeast strain engineering. *BMC Bioinformatics*, *21*, 1-13. https://doi.org/10.1186/s12859-020-3377-1

205. Kleessen, S., & Nikoloski, Z. (2012). Dynamic regulatory on/off minimization for biological systems under internal temporal perturbations. *BMC Systems Biology*, *6*. https://doi.org/10.1186/1752-0509-6-16

206. Pereira, V., Cruz, F., & Rocha, M. (2021). MEWpy: a computational strain optimization workbench in Python. *Bioinformatics*, 37(16), 2494-2496.. https://doi.org/10.1093/bioinformatics/btab013

207. Kenefake, D., Armingol, E., Lewis, N. E., & Pistikopoulos, E. N. (2022). An improved algorithm for flux variability analysis. *BMC Bioinformatics*, *23*(1), 1–14. https://doi.org/10.1186/S12859-022-05089-9/TABLES/3

208. Qiu, D., Wang, M., Zhou, C., Zhao, J., & Zhang, G. (2022). *De novo* biosynthesis of vanillin in engineered *Saccharomyces cerevisiae*. *Chemical Engineering Science*, *263*, 118049. https://doi.org/10.1016/J.CES.2022.118049

209. Yang, Y. H., Song, H. W., Lai, J. Y., Li, R. F., Wang, Z. C., Jia, H. C., & Yang, Y. (2023). A *Rehmannia glutinosa* caffeic acid O-methyltransferase functional identification: Reconstitution of the ferulic acid biosynthetic pathway in *Saccharomyces cerevisiae* using *Rehmannia glutinosa* enzymes. *Biotechnology Journal*, *18*(11), 2300064. https://doi.org/10.1002/BIOT.202300064

210. Liu, L., Liu, H., Zhang, W., Yao, M., Li, B., Liu, D., & Yuan, Y. (2019). Engineering the biosynthesis of caffeic acid in *Saccharomyces cerevisiae* with heterologous enzyme combinations. *Engineering*, *5*(2), 287–295. https://doi.org/10.1016/J.ENG.2018.11.029

211. Schneider, C., Gordon, O. N., Edwards, R. L., & Luis, P. B. (2015). Degradation of curcumin: from mechanism to biological implications. *Journal of Agricultural and Food Chemistry*, *63*(35), 7606-7614. https://doi.org/10.1021/acs.jafc.5b00244

212. Ai, L., Guo, W., Chen, W., Teng, Y., & Bai, L. (2019). The gal80 deletion by CRISPR-Cas9 in engineered *Saccharomyces cerevisiae* produces artemisinic acid without galactose induction. *Current Microbiology*, *76*(11), 1313–1319. https://doi.org/10.1007/S00284-019-01752-2

213. Li, Y., Mao, J., Liu, Q., Song, X., Wu, Y., Cai, M., … Qiao, M. (2020). *De novo* biosynthesis of caffeic acid from glucose by engineered *Saccharomyces cerevisiae*. *ACS Synthetic Biology*, *9*(4), 756–765. https://doi.org/10.1021/ACSSYNBIO.9B00431

214. Raymond, R. K., Kastanos, E. K., & Appling, D. R. (1999). *Saccharomyces cerevisiae* expresses two genes encoding isozymes of methylenetetrahydrofolate reductase. *Archives of Biochemistry and Biophysics*, *372*(2), 300–308. https://doi.org/10.1006/abbi.1999.1498

215. Chan, S. Y., & Appling, D. R. (2002). Regulation of S-Adenosylmethionine levels in *Saccharomyces cerevisiae*. *Journal of Biological Chemestry*, *277*, 4056–4061. https://doi.org/10.1074/jbc.M308696200

216. Vos, T., de la Torre Cortés, P., van Gulik, W. M., Pronk, J. T., & Daran-Lapujade, P. (2015). Growth-rate dependency of *de novo* resveratrol production in chemostat cultures of an engineered *Saccharomyces cerevisiae* strain. *Microbial Cell Factories*, *14*(1), 133. https://doi.org/10.1186/S12934-015-0321-6

217. Pfeiffer, T., & Morley, A. (2014). An evolutionary perspective on the crabtree effect. *Frontiers in Molecular Biosciences*, *1*(10), 108877. https://doi.org/10.3389/FMOLB.2014.00017/BIBTEX

218. van Hoek, P., de Hulster, E., van Dijken, J. P., & Pronk, J. T. (2000). Fermentative capacity in high-cell-density fed-batch cultures of baker's yeast. *Biotechnology and Bioengineering*, *68*(5), 517–523. https://doi.org/10.1002/(sici)1097-0290(20000605)68:5<517::aid-bit5>3.3.co;2-f

219. Gao, Y., Guo, X., Liu, Y., Fang, Z., Zhang, M., Zhang, R., … Liu, R. H. (2018). A full utilization of rice husk to evaluate phytochemical bioactivities and prepare cellulose nanocrystals. *Scientific Reports*, *8*(1), 10482. https://doi.org/10.1038/S41598-018-27635-3

220. Abaide, E. R., Ugalde, G., Di Luccio, M., Moreira, R. de F. P. M., Tres, M. V., Zabot, G. L., & Mazutti, M. A. (2019). Obtaining fermentable sugars and bioproducts from rice husks by subcritical water hydrolysis in a semi-continuous mode. *Bioresource Technology*, *272*, 510–520. https://doi.org/10.1016/J.BIORTECH.2018.10.075

221. Xavier, L., Rocha, M., Pisani, J., & Zecchi, B. (2024). Aqueous two-phase systems based on cholinium ionic liquids for the recovery of ferulic and *p*-coumaric acids from rice husk hydrolysate. *Applied Food Research*, *4*(1), 100381. https://doi.org/10.1016/J.AFRES.2023.100381

222. Wood, I. P., Elliston, A., Ryden, P., Bancroft, I., Roberts, I. N., & Waldron, K. W. (2012). Rapid quantification of reducing sugars in biomass hydrolysates: Improving the speed and precision of the dinitrosalicylic acid assay. Biomass and Bioenergy, 44, 117-121. https://doi.org/10.1016/j.biombioe.2012.05.003

223 Teixeira-Guedes, C., Gomes-Dias, J. S., Cunha, S. A., Pintado, M. E., Pereira, R. N., Teixeira, J. A., & Rocha, C. M. R. (2023). Enzymatic approach for the extraction of bioactive fractions from red, green and brown seaweeds. *Food and Bioproducts Processing*, *138*, 25–39. https://doi.org/10.1016/J.FBP.2022.12.005

223. Wood, I. P., Elliston, A., Ryden, P., Bancroft, I., Roberts, I. N., & Waldron, K. W. (2012). Rapid quantification of reducing sugars in biomass hydrolysates: Improving the speed and precision of the dinitrosalicylic acid assay. *Biomass and Bioenergy*, *44*, 117-121. https://doi.org/10.1016/j.biombioe.2012.05.003

224. Braga, A., Silva, M., Oliveira, J., Silva, A. R., Ferreira, P., Ottens, M., ... Faria, N. (2018). An adsorptive bioprocess for production and recovery of resveratrol with *Corynebacterium glutamicum*. *Journal of Chemical Technology & Biotechnology*, *93*(6), 1661–1668. https://doi.org/10.1002/JCTB.5538

225. Almeida, J. R., Modig, T., Petersson, A., Hähn-Hägerdal, B., Lidén, G., & Gorwa-Grauslund, M. F. (2007). Increased tolerance and conversion of inhibitors in lignocellulosic hydrolysates by *Saccharomyces cerevisiae*. *Journal of Chemical Technology & Biotechnology: International Research in Process, Environmental & Clean Technology*, *82*(4), 340-349. https://doi.org/10.1002/jctb.1676

226. Ask, M., Bettiga, M., Mapelli, V., & Olsson, L. (2013). The influence of HMF and furfural on redox-balance and energy-state of xylose-utilizing *Saccharomyces cerevisiae*. *Biotechnology for Biofuels*, *6*(1), 1–13. https://doi.org/10.1186/1754-6834-6-22/TABLES/4

227. Larsson, C., Von Stockar, U., Marison, I., & Gustafsson, L. (1993). Growth and metabolism of *Saccharomyces cerevisiae* in chemostat cultures under carbon-, nitrogen-, or carbon- and

nitrogen-limiting conditions. *Journal of Bacteriology*, *175*(15), 4809. https://doi.org/10.1128/JB.175.15.4809-4816.1993

228. Tan, J. P., Jahim, J. M., Wu, T. Y., Harun, S., & Mumtaz, T. (2016). Use of corn steep liquor as an economical nitrogen source for biosuccinic acid production by *Actinobacillus succinogenes*. *IOP Conference Series: Earth and Environmental Science*, *36*(1), 012058. https://doi.org/10.1088/1755-1315/36/1/012058

229. Bafunno, V., Giancaspero, T. A., Brizio, C., Bufano, D., Passarella, S., Boles, E., & Barile, M. (2004). Riboflavin uptake and FAD synthesis in Saccharomyces cerevisiae mitochondria: involvement of the Flx1p carrier in FAD export. *Journal of Biological Chemistry*, *279*(1), 95-102. https://doi.org/10.1074/jbc.M308230200

230. Westfall, P. J., Pitera, D. J., Lenihan, J. R., Eng, D., Woolard, F. X., Regentin, R., ... Paddon, C. J. (2012). Production of amorphadiene in yeast, and its conversion to dihydroartemisinic acid, precursor to the antimalarial agent artemisinin. *Proceedings of the National Academy of Sciences*, *109*(3), E111. https://doi.org/10.1073/pnas.1110740109

231. Galindo-Rodriguez, G. R., Santoyo-Garcia, J. H., Rios-Solis, L., & Dimartino, S. (2024). *In situ* recovery of taxadiene using solid adsorption in cultivations with *Saccharomyces cerevisiae*. *Preparative Biochemistry & Biotechnology*, *54*(1), 86–94. https://doi.org/10.1080/10826068.2023.2207204

Appendix

Appendix 1: DNA sequences of gBlock and codon optimized genes.

Gene (Origin)	**Sequence (5'-3')**
gBlock for *fdc1* deletion	CTTTGGTCTCACCAAAACGATGAAGATGACTTAATCGAAATTACCGAAGAGATTGATCCAAATCTCGACAATTATGAGGAAGGCC TATGAATCCCACTTACCAGCCCCGTTATTTAAAATTGATCCAAATCTCGAAGTGTTTTAGAGAGAGACCTTTC
CUS (*Oryza sativa*)	ATGGCCCCTACTACGACAATGGGATCTGCATTGTATCCGTTAGGTGAGATGAGAAGGTCGCAACGAGCCGATGGATTAGCTGCT GTTTTAGCAATAGGAACAGCCAATCCACCAAATTGTGTAACACAGGAAGAAATACCAGATTTTTATTTTCGAGTTACTAATTCCGA TCATTTAACAGCTTTGAAAGATAAGTTTAAACGCATTTGCCAGGAAATGGGTGTTCAAAGGAGATATTTGCATCATACTGAAGAAA TGCTCTCGGCACACCCTGAATTTGTTGATAGAGACGCCCCAAGTTTGGACGCTAGGTTAGACATAGCCGCTGACGCTGTACCT GAATTGGCTGCTGAAGCAGCTAAGAAAGCTATTGCCGAATGGGGTAGACCAGCCGCTGACATCACACATCTTGTCGTGACTACA AACTCTGGCGCTCACGTCCCTGGTGTGGACTTTAGATTAGTTCCACTCCTTGGGTTAAGGCCCTCTGTCCGAAGAACCATGCTC CACCTGAACGGTTGTTTTGCAGGTTGCGCTGCACTACGTCTTGCTAAGGACTTAGCTGAAAACAGCCGTGGAGCACGTGTCCT GGTAGTGGCTGCCGAATTGACGCTGATGTATTTCACAGGTCCGGATGAAGGATGCTTTCGAACCCTTTTAGTTCAAGGTCTTTTT GGGGACGGGGCAGCAGCAGTCATTGTTGGAGCTGATGCCGATGATGTCGAACGGCCATTATTTGAAATCGTTTCAGCGGCCCA AACCATAATACCCGAGTCTGATCACGCACTTAACATGAGATTCACCGAAAGGAGACTGGATGGTGTTTTAGGTAGACAAGTCCC CGGACTAATTGGTGACAACGTTGAAAGATGCCTTCTTGACATGTTTGGTCCCCTGCTAGGTGGAGATGGAGGAGGGGGTTGGA ATGATTTGTTTTGGGCAGTACATCCAGGGTCGAGCACAATCATGGATCAAGTGGATGCAGCCTTAGGTTTGGAACCTGGCAAATT GGCTGCCTCACGTCGCGTCCTGTCAGATTACGGAAACATGTCTGGTGCAACTGTTATTTTTGCGCTGGACGAACTAAGACGACA GAGAAAAGAAGCTGCTGCGGCTGGTGAGTGGCCAGAATTAGGTGTTATGATGGCTTTCGGTCCAGGTATGACAGTGGATGCCAT GTTGCTTCACGCAACATCTCATGTCAATTAA
DCS (*Curcuma longa*)	ATGGAAGCTAACGGTTATAGAATCACTCACTCTGCCGATGGTCCAGCTACGATTTTAGCTATCGGCACTGCTAACCCTACTAATG TTGTTGATCAAAATGCTTATCCAGATTTCTATTTTAGAGTCACCAATTCAGAATACTTACAGGAGTTAAAGGCTAAGTTTAGAAGAA TCTGTGAGAAGGCCGCCATAAGAAAGCGGCATTTGTACTTGACCGAGGAAATTCTTAGAGAAAATCCAAGTTTGCTGGCTCCAA TGGCGCCCAGCTTCGATGCAAGACAAGCAATTGTGGTGGAAGCGGTCCCCAAACTCGCTAAGGAAGCTGCCGAGAAGGCCAT TAAGGAGTGGGGTAGACCTAAAAGCGACATCACGCATCTCGTTTTCTGCTCGGCATCTGGTATCGATATGCCAGGTTCCGATCT GCAGTTATTAAAATTGTTGGGTCTTCCACCATCAGTCAATCGTGTCATGTTATATAACGTTGGTTGTCACGCTGGTGGTACAGCCT TGAGGGTTGCCAAAGATTTGGCGGAAAATAATAGAGGCGCCCGTGTTCTGGCAGTTTGTAGCGAAGTTACTGTCCTTAGTTATAG AGGTCCACACCCAGCACACATAGAATCACTTTTCGTCCAAGCCCTTTTCGGAGATGGAGCTGCCGCCTTGGTCGTCGGCTCC GACCCCGTAGACGGAGTAGAAAGACCCATATTTGAAATCGCTTCCGCTTCACAAGTCATGTTACCCGAATCTGCTGAAGCCGTA GGAGGGCACTTGAGGGAAATTGGCTTGACCTTCCATTTAAAATCTCAGTTACCATCCATTATTGCGTCCAATATCGAACAATCCT TGACTACAGCCTGCTCCCCATTGGGGCTGTCAGATTGGAATCAATTGTTCTGGGCCGTGCACCCTGGAGGCAGGGCCATACTT GATCAAGTGGAAGCAAGATTGGGCCTTGAAAAAGATCGTCTTGCCGCGACACGGCACGTACTGTCAGAATACGGTAACATGCAA TCAGCCACAGTGTTGTTCATTTTGGATGAAATGAGAAACAGGAGTGCCGCTGAGGGACACGCGACTACCGGCGAGGGATTGGA TTGGGGAGTGCTGTTGGGTTTTGGGCCAGGTTTGAGTATAGAAACTGTAGTCTTACATTCATGCAGGCTTAATTGA
CURS (*Curcuma longa*)	ATGGCCAATCTACATGCGCTTAGAAGGGAACAAAGAGCTCAGGGTCCAGCAACAATTATGGCTATCGGTACTGCTACTCCACCT AACTTATACGAACAGTCGACATTCCCGGACTTTTATTTTCGTGTTACAAACTCAGATGATAAGCAAGAACTCAAAAAAAAGTTTAG AAGAATGTGCGAAAAGACAATGGTGAAGAAGCGTTACCTGCATCTAACAGAGGAAATATTAAAGGAGCGTCCTAAATTATGTTCT TACAAAGAAGCCAGTTTCGACGATAGACAAGATATTGTGGTTGAAGAAATTCCACGTTTGGCTAAGGAAGCTGCTGAAAAGGCA ATTAAAGAATGGGGTCGGCCAAAATCTGAAATTACACATCTTGTCTTCTGTTCAATAAGTGGTATTGACATGCCAGGTGCGGACTA CAGGTTAGCCACTTTGCTGGGCTTACCTCTTACAGTTAATCGTCTTATGATTTATAGTCAGGCCTGTCACATGGGTGCTGCTATGT TGCGAATAGCAAAAGATTTGGCTGAGAACAACAGAGGCGCCCGCGTATTGGTTGTGGCGTGCGAAATCACAGTTCTGTCTTTCA GAGGTCCAAACGAGGGAGATTTTGAAGCATTAGCTGGACAAGCGGGCTTTGGCGACGGGGCCGGCGCGGTCGTTGTAGGTGC CGACCCGCTCGAAGGTATAGAAAAACCAATCTACGAAATCGCTGCTGCAATGCAGGAAACAGTGGCAGAATCACAGGGTGCAG TGGGGGGCCATTTGAGGGCTTTTGGATGGACCTTTTATTTCCTTAACCAGTTACCAGCAATTATTGCTGACAATTTGGGTAGAAG CCTTGAACGAGCACTTGCCCCACTCGGTGTCCGCGAATGGAATGACGTTTTTTGGGTGGCCCATCCTGGTAACTGGGCAATTA TTGATGCTATCGAAGCAAAGTTGCAATTAAGTCCCGATAAATTGAGTACCGCAAGACATGTTTTCACTGAATACGGTAACATGCA GAGTGCAACCGTTTACTTTGTAATGGATGAATTACGAAAAAGATCTGCCGTGGAGGGTAGATCAACAACTGGAGATGGTCTGCAA TGGGGTGTTCTGTTGGGGTTTGGCCCAGGATTGTCAATTGAAACCGTGGTTCTAAGGTCCATGCCCTTGTAA

Appendix 1*: Continuation*

FerA (*Pseudomonas paucimobilis*)	ATGACGGTCGAGGCGGGAGTTAGGCCGCAGGCCGGAGCCAGGGATATAAATAGGTTACTTAGACCCAGGTCCATAGCCATAGT TGGGGCAAGTGAAACGCCTGGTTCTTTGGGGGCTTCAGTCCTAGCGAACTTAGTAAGGAATGAATTTCCGGGTGACATCCATCT GGTCAACCCTAAAAGAGAAACCATAAGTGGTAGGCCTGCAGTTCCTTCCGTCGATGCACTTCCGGAAGGTGTGGATTGTGCTAT ACTAGCGATACCAAGAGTTGCCGTTCTAGACACTATGCGTCAACTTGCAGCTAGAAAGGCTGGGGCCGCCATCATTTTTGCTGC AGGGTTTGCTGAGGGTGGTGAGCAGGGAATGGCGGATCAACAAGAGATAGGGAGAATCGCCCATGAGGCCGGGATAGTGGTA GAGGGTCCGAACTGCTTGGGATCTGTTAACTATTTAGACAGGATCCCGCTGACATTCATCGACACCGATATCAAAGCACCCTCT CCAGGCGGAGTTGGTATAGTTAGCCAGTCCGGGGCTATGGCTGCGGTACTAGCGGTGATGCTAGAGAGTAGGACGTTGGATTTA ACGTACAGTGTCTCCACTGGTAATGAGGCAGGTTCCGGAGTGGAAGACTATGTCGAGTTCATGATCGCAGATGAGAAAACCAGA ATCATCGCAATGATAGTGGAGCAGTTCAGGGACCCGGCTCGTTTCTTGGCGCTAATGGACAAGGCTAATGCAGCCGGCAAGTT AGTCGTACTGTTGCATCCGGGAAAGTCTTCTGCTGCCAGAGAAAGCGCGGCGACCCATACGGGGGCAATGGCTGGCGATTATA AGCTGATGAGGGCGAAAGTAGAAAGAGCCGGCGTAGTTGTCGCTGAAACCTTAGAAGAACTAGGAGATATAACGGAAATCGCA GCTAGGTGCCCCGCTCTACCCAGCGGTGGCACAGCCGTCCTGGGGGAATCAGGTGCACTAAAGGCACTAACGTTAGACCTGG CCGAGGAACTAGAGTTGGCATTACCCACGTTGGATGACGGGAATGCGCCGGCTCTTAGAGCAGCACTGCCTGAGTTCGTCCC GGTAAGTAACCCACTAGATTTGACAGCGCAAGGATTAGTGGACCCAGATATGTACTACCGTACACTAGCCGCGCTATTCGAGGA TGACCGTGTGGGGACGATATTCGCGGGGATCATCCAAACGAATCCGGCGACCATAGGTATCAAACTACCACCGTTTCTAAAAGC AGTTCGTGAGCTGAAGGCGACCAAACCAGTCATATTTGGGGGAGTCGATGAAGGAGCGGATGTACCCGCAGATTGGATAGAGC AACTTAGAGCGGAAGGTATACCCTACTTTCCGACTACGGAACGTGCCTTGCGTGCCATTCGTCGTCTGAGTGCGGCCGGTGCG AGGGACGCCTCCAGGACGGATGCAGCTCCCGCTTCAGTCCCCGCCTTGGCTTCTGAGAAGGGGGTTGTTCCAGAGTACAAAG CAAAGGCACTGCTTGCGCCCTTGGGAATATCATTCCCAAAAGGACAGTTTGCGGCAACCGTTGAAGACGCCATCGCCGCTGC GGAAGCCATAGGGGGGCCGGTGGTAATGAAGGCACAAGCGGCCGCTCTATCTCATAAGAGTGATGCCGGGGGAGTTGCGTTG AACCTGGTGGGTGCTGAGGCCATCCGTGCTGCATGGGATAAAATGTTCGCCGATGTGAAGAGGTATGATGCCTCCATCATACTA GACGGGGTGCTTATCGAGGCTATGGGTGCGAGAGGCTTGGAGCTAATAGTAGGAGCCAAGAACGACCCACAGTGGGGTCCTGT AATCTTAGCCGGATTTGGTGGGGTGACAGCCGAAATATTGCAGGACGTGAGATTACTAAGCCCCGACATGACTAAGGAGGCCAT CGTAGCTGAACTTGGAAAACTGAAGCAAGCGGCATTGCTGCACGGTTATAGAGGTTCCCCAGCACTAGACGTGGGCGCCGTTG CTGAACTAATAGGACAAGTGGGAAGATTGCTAAGAGGGGAGCCCAGGATACAGGAACTGGATCTTAACCCGGTGGTCGTATACC CAGAAGGCCAGGGGGCAATCGCACTTGATGCTCTTATGTTGGTAGATTGA
HpaB (*Pseudomonas aeruginosa*)	ATGAAACCAGAAGACTTTAGAGCTTCAGCTACCCGTCCCTTTACTGGTGAAGAATATTTAGCATCTTTAAGGGATGATAGAGAAA TTTATATTTATGGAGATCGTGTGAAAGATGTAACTTCTCATCCGGCATTTCGTAATGCCGCTGCGTCGATGGCTAGGCTTTATGAT GCTTTACATGACCCACAATCTAAAGAGAAATTATGTTGGGAAACGGACACTGGAAATGGTGGTTACACTCATAAATTCTTCAGATA TGCAAGATCTGCGGATGAGTTAAGACAACAAAGAGATGCAATAGCGGAATGGAGTAGATTAACTTATGGTTGGATGGGTAGAACT CCTGATTATAAAGCAGCGTTTGGATCTGCTTTAGGTGCAAATCCCGGATTTTATGGCAGATTTGAAGATAATGCCAAGACTTGGTA CAAGAGAATACAAGAGGCTTGTTTATATCTTAATCACGCGATTGTAAATCCACCTATTGATCGTGATAAACCTGTTGATCAAGTGA AGGATGTCTTTATATCAGTTGATGAAGAGGTGGATGGTGGAATTGTAGTTTCTGGTGCAAAAGTCGTGGCTACAAACTCGGCTTT AACGCATTATAATTTCGTTGGTCAAGGAAGTGCCCAGTTGTTAGGTGATAATACGGATTTTGCATTAATGTTTATTGCTCCAATGAA TACTCCTGGTATGAAATTAATTTGTAGACCGTCTTATGAGCTTGTAGCCGGCATTGCAGGTAGTCCCTTTGATTATCCTTTGAGTT CCAGATTTGACGAGAACGATGCTATTTTAGTGATGGATAAGGTCTTTATACCTTGGGAAAATGTTTTAATTTACCGTGATTTTGAAA GGTGTAAACAATGGTTTCCTCAAGGCGGTTTTGGGCGTTTATTTCCTATGCAAGGGTGTACTAGGCTTGCAGTTAAATTAGATTTT ATTACGGGTGCACTGTATAAAGCATTACAGTGTACTGGAAGTTTAGAATTTCGTGGGGTTCAAGCCCAAGTGGGTGAGGTTGTTG CTTGGAGAAATTTGTTTTGGAGCTTAACTGATGCAATGTATGGTAATGCATCCGAGTGGCATGGTGGAGCTTTTCTTCCATCAGC TGAAGCATTGCAAGCATATCGTGTTTTGGCCCCACAAGCATATCCAGAAATAAAGAAAACAATTGAACAAGTTGTAGCTTCGGGT TTGATTTATTTACCGAGCGGTGTAAGGGATCTTCATAACCCCCAGTTGGATAAATACTTGTCAACATACTGTAGAGGATCTGGTGG TATGGGACATAGAGAAAGAATTAAGATATTAAAATTGTTATGGGATGCTATAGGTTCGGAATTTGGTGGTCGTCACGAACTATATGA AATAAACTATGCGGGATCACAAGATGAAATCAGAATGCAAGCATTAAGACAAGCTATTGGATCTGGTGCTATGAAAGGAATGTTG GGGATGGTAGAACAATGTATGGGTGATTATGATGAAAATGGATGGACTGTTCCTCATCTTCATAATCCTGATGATATTAATGTTTTG GACAGAATACGTCAGTAA

Appendix 1: *Continuation*

COMT (*Arabidopsis thaliana*)	ATGGGAAGTACCGCTGAAACTCAGCTAACGCCAGTTCAAGTAACAGATGATGAGGCCGCTTTATTTGCTATGCAGCTGGCTTCA GCATCAGTCTTGCCTATGGCATTGAAGTCTGCTCTTGAACTGGATTTATTAGAAATAATGGCAAAGAACGGCTCCCCAATGTCCC CAACAGAAATTGCATCAAAGTTACCAACGAAGAACCCAGAGGCACCCGTCATGTTAGATAGAATTTTGAGATTATTGACTTCATAT TCTGTGCTTACATGTTCAAATAGAAAGTTGTCAGGAGACGGTGTGGAGAGGATCTATGGTTTGGGCCCAGTGTGTAAATACTTAA CTAAGAATGAGGACGGCGTCTCGATAGCAGCGTTGTGCTTGATGAATCAGGATAAAGTATTAATGGAGTCCTGGTATCACCTAAA AGACGCTATCTTAGACGGCGGTATCCCGTTTAATAAAGCCTACGGTATGTCTGCTTTTGAATATCATGGAACGGACCCCAGGTTT AATAAAGTGTTCAATAACGGTATGAGCAATCACTCAACTATAACGATGAAGAAGATCTTGGAAACTTACAAAGGGTTCGAGGGCT TAACCAGCTTAGTCGACGTAGGCGGCGGTATAGGCGCGACGCTGAAGATGATCGTATCTAAATATCCAAACTTAAAGGGTATTAA TTTCGACTTGCCTCACGTTATTGAGGACGCACCATCACACCCCGGAATAGAACACGTGGGTGGTGACATGTTCGTCTCAGTACC AAAGGGCGACGCTATCTTTATGAAATGGATTTGCCACGATTGGTCTGATGAGCACTGTGTTAAGTTTCTAAAGAATTGTTATGAAT CTTTGCCCGAAGACGGTAAGGTTATTCTTGCTGAATGCATTCTGCCCGAAACTCCCGATTCCTCTTTAAGCACTAAGCAGGTGG TGCACGTGGACTGTATCATGCTAGCCCATAACCCAGGCGGAAAGGAGAGGACGGAAAAGGAATTCGAAGCCTTGGCTAAGGCT TCTGGTTTTAAAGGTATTAAGGTGGTTTGTGATGCATTCGGAGTCAATTTAATAGAATTGTTGAAGAAACTATAG

Appendix 2: DNA sequences of homology regions for genome integration.

Integration spot	**Sequence (5'-3')**
XI-5	**Upstream**:GCGGAGAAGTCGTTGATAGCATTTCCGAAGGCTTTTCCACATTGACTGCAGTATCTAAAAGAGCTCCAGCAGCG GTCTTAGTAGTTCCTGTGCTTGCCGCTTTGCAGTATACAGGGACATTGGGAACTACGGAGGAAAAATCGGAATGCTCTGAGCT CTTCTCAAAACCAGACGAACTCGTCTTATTTCTCAGTAAATTACCCAACATATAAACTCTCCCTCTTCACCTTCTCTACAAGGC CACACACAAGACAGTTTTAACAGGCAAATGGTACTGGAGGCTCTCACCAATGGGGTTTAAGACGCTCCAAACACACGCTCTC CTTTTTTTCTTTATATATCGGTAGCAACGAAAGCTAGTCGCAGAACGTTACACACTAAAGCAGATCAATCAATCAATCCTGAGAA CCTGCTTCGTTCAAACCATCCACTAGAAGAAACACGCACGTGTACCCAAAAATAGAGACAAACAAACAGACAAAAATAACAAT GATTCCTACCGACTAAAGTAAAACAACACTCACGTAATAAAAAATCCTAGATACAACTCACTTGTATTCCTCTCTTCTTTGACCA TCACTAAAGCTTCTCTCTTACTATATTCCTCAAATAAAAAAAAGTTGCAATGATTACTTACCAATGTGCCATAAACTCCGTGCAC CA **Downstream**:TTGTAAAACAGGTATTGGCTGCTTCATAGTACACCCAATTGCCCACAACCCAAGTTAATCATAAGCTCTTGTT GTCGATGAATTGCTCAAAATGTGGCCATTCTTTCAATTTTGCACCTCTAAAACTGCTCCGTGGGTTGTGACAACAACCTTAAGG GTAATGGACTTTTTTAGAAAGACAAATGAGATGATTTCACCTACTGGTATATCATTTATTTATACACGACCGTTTTGACATTTCAG AGTTGCACGTTGGTATATCCTAATATTCTCACAAGCATCACAGTGAAGAAACGCAAGAAAATGGAAAAAATTCCCAGGTGGTTG TTGTTTTCTCTTATATCGTCGGTGCTGTGCATACTTGGGGCCCTGTGTGTGCCGTTGTTATCGGTTGCCTTCGATAGCAAGCGC AATAGCCAATCTAAGTTGGTCAACTATGGTCTTTCTCTAAGTGCCGGATCTATGATC
XII-4	**Upstream**:GTATCCGGCTGTTCCTTCATAGCCCTTTCAATGAACGTTGCAGCCCTTTGAAGATTGGCCATTTTGTCAGGACTC GAGCCTGACAGTTGGACCAACGCAACTTTAATTTTTTGTGAAAGAATCTTCGAAGCACTCATACTGGCGATCTTCACGCCCTC CTGCTATTACAAAAGCTGTGTTTTTACAAGAATCAAATTAAGTTAGCAAGATATCATACAACATTATTGATAATTTCAATATCGTGT TCGTACCTGATGACGTATCTGTGCATTGATAAGGCCCGCATGGTTTCAGAAAGCAGAGCGGAACGATTCCAAATTAGTGGCCT TGTGCTTTGCATGTCAATTGTGTTACCTTCAGCTCGTGGATTTGTTTTATCAATACACAGTCTACAGTCAAGAATTTTTTTTTATC AAATTTTGCGTTCGAGCGTATAAAATAGCCGCTGTAGCTACTTAAGTTCCTGTTCAGCGATAGTTTTTTTCCATCACACATACTA TGGCA **Downstream**:ATTCCCCATTAGAGTCAAATAAAAGGATGCCTCACGGAGGTATGTTACCCGCGCTATTTCACATGGCTCATTG AATTAGAGGTGGAATTTGGTGTACCCTCCCCTCCTCATCTGATGAAGTAGTGATCCGACAATTCTTAAAAGTTGTAGACATTACT CTTACCACCAACTAAGTTGTATTTATATTGCTACCCTTATCCTTTTATATCTAACTAGCGCTTATAAGGTTGGGGCAATACTAAAA CTGTGATCTTATTCAGCTCATTAAATACGTGGCAGTACGTACCCTATTAGAAACAATAGGAAACAACAGAGTCGGAAGAAGCCA AATGCCAGATTTGAAGTCCAAGACCTTGTCAAGCCAATCTTTGGGAGCGGCTATTCCTCCAGAAATTGTGTACCAAATACTTAC ATACCAGTTTAGGGATTTGTTAAGAAATGACCATCCAGGTACGGCAGAAA
XII-3	**Upstream**:TGTGCCCCTTAAAATTCATATACACTTTATGTTTAATTCGACAGGTATAACAGAAAGAAACAAGGAAAACAATGCAA TTAATCATTAACTGCACCAACTTTTATATGAATATATTGTGCTACATGTCTTAATTAGTCCTCTGTGAATGAGCATCACAAAGAATC ACGAGGAAAAGATTGATTACTTAATATTGATAGGAATCAGCCGCGGAAATGGAAATCTTGGTAATATAATTTTAATGCGGCACGC TGAAAATTGATGGCGGCCTGCTAGGAGCCCTATTGATTCCGCGGAAATAGGCGGATTATTACAAACGTTGAGCATTCAGCAGG TGCGCTGTGCCTTTTCACTTTCAGCTAAGATGTTTGCAAGCAAGAATTAACAGATAAGCCGCTTCGCTAGTAACGCAACTCATT GTGTTTTTAATGGAAGCTAAGGATGGTTGAAATTATGGGTACCCTGAGATAAGATTATTAACTATGATGTAAGTATTAATCATTATA ATAAGGGGTACCTGCTCATTC **Downstream**:GCATAGAGCTAATTAGGTTTGAGTTAAGGAAAAAAATCTATCATAAGTGTCTTGAGGTATTTACTATAATGTATA CGGGAAATATTAGGTGTGATAGGCTCTAGGAACGAATATTAATATTGGGGGGGGGAAACTGGAATGAAATTAAACAAAAGCAAA AAAATCTAAAAGAAGAAAAAAAGGAGAGAGAGAGAGAGAGAGAGAGAGAGAGAGAGAGAGAGAGAGAGAGAGAGAGAGAGA GAGAGATGAGGGTTATTGATAATATAATATAATAATAAAAGAGAAGATAGTAGAAAAGGAAGAAAGAAAAAAAAAAATTAAGATGT ACTTTAATAAAAAGAGGGAAATTCTAAAAAGTGCGACTGGAATTAGAAGAATGCAGGTATTTTGTTTTCTCTCCTATGACGGAGA AGGTAACAAAATCATAAAGGTAAAATAACAAATTAATTATGATCAAAGAGAAATGCCCTTTGTAAACCGTGGTTTGTAAATGCGTT GGTAACTGCAGCAGATGTTAAGAAACAAAGATGGAAAAGAACCAAAATCAGCTTGTAAGTTC

Appendix 2: *Continuation*

XI-2	**Upstream**:TAACTCTTCGTATGAGGATTTTCGATGGAGCAGGATGAGGAGAAATAGTACCACATGTATATATCCATTACAAAAAG GTTTATATACAATTACAATAGACCCTTGTTGGGGTTTCTGAAAAAAGAAGTAGTCGATGCCATCGGCAATAATACGGAATTACGA GAAACACAATCCCGATCCTTTTTTGGGTAATTACTTCACCGATTCTACCGATTTATCATGCCAAAAAAAATTCACCGTGGGTTCT AGAAGTGCCCTTTGAGGATTGTAGCCACTCTAACCCACACGGCCTCCTTACTAGCTGACTAAGGTGACAAAACCGCAAGGAC TGGAAAGTCGCCACTCATCTGAAAATTCTCAAGTTTTTCACTACTGAGTTTATGCTTTCGAATTTTTTTGTTCGGTAATAGCACG GCGGTTCGATTCAATTCCGCCGCTCCGAGCGATGCTCCGCAAAACTCAGTAATAAGCTTTCTGATGGTTCACCCCTTTTTTAG CACGCGGGGTGTAACTCAACAGAAAAATGTGCCATAGAA **Downstream**:CCACAAGTAAAGCTCGTTGACCAGTTGATCAGTTGAGGGGGGTACACACGACTAGCGCTTTCAGATATTAAA AAGTTTAGATGTAGGTTTTAGCGGTAACAGTTATATAAATCGTGTTTCTTCTCTTGATGAAACAAAAAAATGCTAGAAAAACTTTG TCGTTTCTTACTTTTGGTGCGCTTTGCAGTTTTCGTGGCTAGACTTAGAATCATTTCTCCTCAGATTTCTTGATTAAAGTTTGGT GCGAAGCCCTACTCTAACATTGGTGTTCTTCTTTTCATTCACGCAAGTTAAGTCCAGGAAGGTGAGCAAATGCTCATCCTTCTG TTCATGCGTGACGGCTGAATTATCCTTATCTGGCGTACCCGTGCAGCCGTTTCCGTGCCTCGGTTCCTCCGAGATATCCTTAG GGACCGCCAGGGACCATGATTGCGTCAACTGTTGTCACCGCTCCAGAGGATCCTCTGTAACCTTTTCAACCAT
XII-1	**Upstream**:GTTGAGCTCTGTCCTTCATGGACTTTTTGGACCACTTCTTCTTGGACTTCTTACCACCAGCAAGAGCGGCAGCG GCTTTGGCAGCTTTAGACAATTGTTGCTTTGGAGGCATGTTATATTATGTTCTGAGACGTAAGAAAGGGTGAAAATTGATGTTAG TGTCAAAAATTATATTACAAAATACGCAGAGATATTCTAGTTCCTTTGATGAATGAATCTTTCAGAAAAAAAAGTCAAAGCAAAAG CAAAATGGCCTGCAGACTAAACTGTATGGTGGTCTTGGAATGATAAAGATCTGTTTAATAGATTTAGTAGATACAATAGCACATCT CATTACCCAGTTATGATTGACGTCATTCTGAGTTACAATGATCTTAGCGACCTGTGCTCATTATTTGCTCCACTAATTCTAATTTT CCTCGCCTTTCATATTTCGTATCTTTATTCTATATCCTAAAATTTTTTTGGCAAATCCCAGATTTGGCTTTGATTTTGGCATCGGTT CGGTTCTTTC **Downstream**:GTTCAGTTTAGTGCTCTGTCTGAGTGACTGTAATAATAAATTTTACAAGCCACTTCTCATGACATATATTGGTAA GTAACTTCATCAATACTAATTAGTCTTTGCCGGTTACCCATCTGGCCCCTGACTTGCGATGCTTAGGAAGTTCCATACTCGCGG CTCTTCCCAACAGTAGCACATCCGTGAAACTTCTGGCGCTATTCATTATGCAGTACCAGGACAAGAAGTTAAAAAAAAAGCTCT GTTACAAGTTCAATGGTGGTGCAAGGATTGAAGTTATTATCCAGGAGGCACGGATGCAAAAGATAGAAGACAAATTAATTTCCTT AAAATTCAAAATGCTCATTATTGTCACGCTGTATGAGCATTTGGTGAAGATTTCACTGGGAAATGTTGCAATAATTTGATAATCGT TCGTATTGGATGAAACTGTAACATCATCTGTTTATTAAGTATCCGTGTTATTAGTATATCATCACATACGGTGTAAGAAGATAACATA AAGATTGAGAAACAGTCATCA

Appendix 3: *Escherichia coli* CurA protein BLAST result against the *Saccharomyces cerevisiae* S288C proteome.

```
Query: CURA_ECOLI NADPH-dependent curcumin reductase |Query_26909 Length: 345


>uncharacterized protein YML131W [Saccharomyces cerevisiae S288C]
Sequence ID: NP_013575.1 Length: 365
>RecName: Full=Uncharacterized membrane protein YML131W [Saccharomyces cerevisiae S288C]
Sequence ID: Q03102.1 Length: 365
Range 1: 5 to 365

Score:98.2 bits(243), Expect:9e-22, Query Cover: 97%
Method:,
Identities:93/371(25%), Positives:161/371(43%), Gaps:44/371(11%)

Query  9    RRWVLASRP--------HGAPVPENFRLEEDDVATPG--EGQVLLRTVYLSLDPYMRGRM  58
            ++WVL + P        H       F L E ++++    +G++LL T YLS DP  +  +
Sbjct  5    KQWVLKNLPTPGEPFNFHFHDPACTFELIEKELSSEQLKDGELLLETTYLSNDPAQKFWI  64

Query  59   SD-EPSYSPPVDIGGVMVGGTVSRVVESNHPDYQSGDWVLGYSGWQDYDISSGDDLVKLG  117
            S  + +Y+  V  G ++    + +V+ S +  +  GD+V   +GW  + I S +++  L
Sbjct  65   SSMDKNYAKGVQPGEIIPARGIGKVLASRNKAFSPGDYVSAVTGWTTHAIISQENVQGLR  124

Query  118  DHPQNPS----WSLGVLGMPGFTAYMGLLDIGQPKEGEtlvvaaatgpvgatvg------  167
               +N      W L VLG    TAY       Q +E E            A
Sbjct  125  KLDKNKVGKLWWYLSVLGGTSLTAYFIFFTYAQLQEREEDYGKVYLISGAAGAVGTVCIQ  184

Query  168  -QIGKLKGCRVVGVAGGAEKCRHATEVLGFDVCLDHHADDFAEQLAKAC--PKGIDIYYE  224
              +   K  +V+ +AGG EK           V +D+    F ++L +A      +D + +
Sbjct  185  LALNVFKASKVIAIAGGPEKVAFVESFGDNVVGVDYKDPSFKQKLIEAAGGENTVDYFID  244

Query  225  NVGGKVFDAVLPLLNTSARIPVCGLVSSYNATELPPGPDRLPLL-MATVLKKRIRLQGFI  283
            NVG  V +A + LL   A +  CG +S+YN       P +      + +L KR+ ++G +
Sbjct  245  NVGSNVLEAGVLLLKQRAMLIACGAISAYN------DPSKFVFKGYSFILTKRLVVKGVL  298

Query  284  IAQDYGHRIHEFQR---EMGQWVKEDKIHYREEIT------DGLENAPQTFIGLLKGKNF  334
            +  +    I +F +   ++G  VK  KI   +  T      D  +N P  + GL  G N
Sbjct  299  VTDN----IDDFPKALDKLGSLVKHGKIDLLKSATLEDGTGDKFKNVPLIWKGLFSGVNK  354

Query  335  GKVVIRVAGDD  345
            GK++ +V  ++
Sbjct  355  GKLITKVNNEE  365
```

Appendix 4: Results obtained using the Gene Over/Under Expression Optimization Problem (GOUProblem) module from MEWpy applied to yeast7.6_curcumin model. Modification: Proposed genetic modifications (systematic gene name: expression value). Retrieved value: 0: gene deletion; >0 and <1: gene underexpression; >1: gene overexpression. BCPY: Biomass-Product Coupled Yield; WYIELD: Weighted Yield; Curcumin: Predicted curcumin production ($mmolgDW^{-1}h^{-1}$); Biomass: Predicted biomass flux (h^{-1}).

Modification	**BPCY**	**WYIELD**	**Curcumin ($mmolgDW^{-1}h^{-1}$)**	**Biomass (h^{-1})**
{YLR081W': 0, 'YJR009C': 0, 'YGL125W': 32, 'YDR158W': 32, 'YKL141W': 0.03125, 'YKR097W': 0, 'YOR025W': 0, 'YNR019W': 4}	0.0460048646998551	0.2931442940245049	0.9883779483158758	0.48925217327719045
{'YNR019W':0,'YLR081W':0,'YGL125W':32,'YJR019C':0.03125,'YDR158W':32,'YKL141W':0.03125,'YOR025W':0,'YBR265W':0.5}	0.0460048646998549	0.2961493684861279	0.9881828750301173	0.4892521732771897
{'YDR158W':16,'YGL125W':32,'YLR153C':32,'YKL141W':0.03125,'YLR092W':32,'YER023W':2,'YOL058W':8,'YLR044C':32}	0.0460048646998548	0.2961493684862624	0.9881272760921519	0.4892521732771906
{'YAR015W':8,'YGL125W':32,'YLR153C':32,'YER023W':2,'YDR158W':16,'YKL141W':0,'YLR044C':32}	0.0458160180930839	0.3648746452759633	0.9880370425272376	0.4892521732771906
{'YAR015W':8,'YKL141W':0.0625,'YGL125W':32,'YLR153C':32,'YER023W':2,'YDR158W':16,'YLR044C':32}	0.0458160180930838	0.3750828990609425	0.9875285355761497	0.4892521732771905
{'YDR158W':16,'YLR153C':32,'YGL125W':32,'YHR002W':32,'YLR092W':32,'YOL058W':8,'YKL141W':0,'YLR044C':32}	0.0458160180930839	0.4259919065941702	0.9875285355761497	0.4892521732771906
{'YAL038W':2,'YOL058W':32,'YGL125W':32,'YKR097W':0,'YMR208W':0.5,'YKL085W':0.0625,'YKL141W':0.125,'YDR158W':16}	0.0455537928774542	0.4417438557189154	0.9870488445219777	0.4892521732771897
{'YAL038W':2,'YOL058W':32,'YGL125W':32,'YKR097W':0,'YMR208W':0.5,'YKL085W':0.0625,'YKL141W':0.125,'YDR158W':16}	0.0455537907112319	0.4417439259467 26	0.9870212070772777	0.4892521732771897
{'YNR019W':0,'YAL038W':2,'YOL058W':32,'YGL125W':32,'YER060WA':0,'YKR097W':0,'YDR158W':16,'YKL141W':0}	0.0453491727868 79	0.3082898740390256	0.9866611152084942	0.4734698451069585
{'YNR019W':0,'YAL038W':2,'YKL141W':0.0625,'YOL058W':32,'YGL125W':32,'YER060W:0,'YKR097W':0,'YDR158W':16}	0.0453491726932362	0.3082898740390997	0.9856396018219695	0.4734698451069585
{'YDR158W':16,'YGL125W':32,'YLR153C':32,'YKL085W':0.125,'YLR092W':32,'YOL058W':8,'YKL141W':0,'YLR044C':32}	0.0444368305378714	0.5691942194571775	0.9853729080380711	0.4734698451069578
{'YOL058W':8,'YGL125W':32,'YLR153C':32,'YER060WA':0,'YLR092W':32,'YDR158W':16,'YKL141W':0,'YLR044C':32}	0.0444368305378714	0.5104066860123639	0.9843812622125305	0.4734698451069571 7
{'YLR153C':32,'YGL125W':32,'YHR002W':32,'YKL141W':0.03125,'YLR092W':32,'YKL085W':0.0625,'YDR158W':16,'YLR044C':32}	0.0444368305378714	0.5103689594680021	0.9843116908036 57	0.4734698451069571 7
{'YAL038W':2,'YOL058W':32,'YGL125W':32,'YLR153C':32,'YHR002W':32,'YER060WA':0,'YKL141W':0.03125,'YKR097W':0}	0.0439477183802953	0.5819088484403193	0.9830084239775313	0.4734698451069579 4
{'YLR153C':32,'YGL125W':32,'YHR002W':32,'YKL141W':0.03125,'YLR092W':32,'YDR158W':16,'YLR044C':32}	0.0439477161680527	0.5819089035388963	0.9828402856655735	0.4734698451069579 4

Appendix 4: *Continuation*

{'YGL125W':32,'YLR153C':32,'YLR231C':0,'YLR092W':32,'YKL085W':0.0625,'YDR158W':16,'YKL141W':0,'YLR044C':32}	0.04349541742697 18	0.89390366297487 23	0.98171642338626 04	0.462748294766796
{'YAL038W':2,'YOL058W':32,'YGL125W':32,'YHR002W':32,'YER060WA':0,'YER023W':4,'YKR097W':0,'YKL141W':0}	0.04349541726639 81	0.89390366355147 01	0.98099644069549 41	0.462748294766796
{'YHL003C':0.03125,'YAL038W':2,'YOL058W':32,'YGL125W':32,'YLR153C':32,'YER060WA':0,'YKR097W':0,'YKL141W':0}	0.04346121402822 14	0.89488181955486 07	0.98036643797295 99	0.462161473066233 9
{'YAL038W':2,'YOL058W':32,'YGL125W':32,'YHR002W':32,'YER060WA':0,'YKR097W':0,'YER023W':2,'YKL141W':0}	0.04346052699005 82	0.89488584652527 85	0.97915333434026 12	0.462153561679100 93
{'YAL038W':2,'YGL125W':32,'YLR153C':32,'YKL141W':0.03125,'YLR044C':32,'YER023W':2,'YDR158W':16,'YGR124W':8}	0.04267482942939 06	0.89718454506814 62	0.97761368651508 73	0.453225947786379 65
{'YNR019W':0,'YJR009C':0,'YGL125W':32,'YLR153C':32,'YER023W':2,'YDR158W':16,'YKL141W':0,'YLR044C':32}	0.04245478643849 65	0.89742229993987 87	0.97676092469211 94	0.450729397727151 5
{'YOL058W':32,'YGL125W':32,'YLR153C':32,'YKL152C':2,'YDL142C':0.0625,'YIL125W':0,'YDR158W':16,'YKL141W':0}	0.04241351348717 72	0.89791288324152 09	0.97622536325594 66	0.450260825355467 3
{'YAL038W':2,'YOL058W':32,'YGL125W':32,'YER060W':0,'YKR097W':0,'YOR025W':0,'YIL125W':0,'YKL141W':0}	0.04208232174619 22	0.91336035956248 36	0.97589239730121 52	0.446465240884459 05
{'YLR081W':0,'YGL125W':32,'YER060WA':0,'YKL152C':2,'YIL125W':0,'YKL085W':0.0625,'YJR077C':2,'YKL141W':0}	0.04206653936261 45	0.91356832873549 32	0.97435733275298 51	0.446286516584453 56
{'YAL038W':2,'YGL125W':32,'YLR153C':32,'YER060WA':0,'YKR097W':0,'YDR158W':16,'YKL141W':0,'YGR124W':8}	0.04194669577168 52	0.61810265529264 1	0.97343161261700 31	0.502857645619813 6
{'YAL038W':2,'YGL125W':32,'YLR153C':32,'YKL141W':0.5,'YKR097W':0,'YDR158W':16}	0.04194669577168 4	0.61810265529210 61	0.97211447726050 45	0.502857645619802 1
{'YAL038W':2,'YGL125W':32,'YER060W:0,'YKR097W':0,'YER023W':2,'YDR158W':16,'YKL141W':0,'YGR124W':8	0.04194669577168 44	0.61810265529043 27	0.97211447726050 45	0.502857645619802 1
{'YAL038W':2,'YGL125W':32,'YER060W':0,'YKR097W':0,'YOR025W':0,'YER023W':2,'YDR158W':16,'YKL141W':0}	0.04190959654397 09	0.61813098622488 47	0.97034016260627 46	0.502378892266506 2
{'YAL038W':2,'YGL125W':32,'YER060W:0,'YKR097W':0,'YOR025W':0,'YER023W':2,'YDR158W':16,'YKL141W':0}	0.04150719107809 49	0.62666913301734 64	0.96890132978289 73	0.497191348936330 1
{'YAL038W':2,'YGL125W':32,'YLR153C':32,'YGR124W':16,'YER060WA':0,'YKR097W':0,'YKL085W':0.0625,'YKL141W':0}	0.04150719042072 59	0.62666913469700 42	0.96751956534313 01	0.497191340467216 4
{'YAL038W':2,'YGL125W':32,'YLR153C':32,'YER060WA':0,'YKR097W':0,'YKL085W':0.0625,'YGR124W':8,'YKL141W':0}	0.04149984129101 7	0.91460030045928 46	0.96697649827256 14	0.439883067122393 83
{'YAL038W':2,'YGL125W':32,'YLR153C':32,'YER060W-A':0,'YKR097W':0,'YKL085W':0.0625,'YKL141W':0}	0.04048253779631 97	0.91743568638989 04	0.96531517652799 81	0.428440864385954 3
{'YGL125W':32,'YLR153C':32,'YLR231C':0,'YKL152C':2,'YLR092W':32,'YLR028C':0.0625,'YDR158W':16,'YKL141W':0}	0.03976668876220 71	0.91950075099640 36	0.96481556377461 67	0.420343143043418 85

Appendix 4: *Continuation*

{'YMR217W':32,'YCR005C':32,'YGL125W':32,'YLR153C':32,'YKL152C':2,'YDL142C':0.0625,'YDR158W':16,'YKL141W':0}	0.0397166477485237	0.9260419745781764	0.9644948215733802	0.4200603266141677
{'YAL038W':2,'YGL125W':32,'YLR153C':32,'YKL141W':0.5,'YKR097W':0,'YDR158W':0.5}	0.0395726957760081	0.9263297381225128	0.9625801515732186	0.41844108357037944
{'YMR217W':32,'YAL038W':2,'YCR005C':32,'YGL125W':32,'YER060WA':0,'YKR097W':0,'YOR025W':0,'YKL141W':0.125}	0.0395661608162134	0.9263440326796164	0.9619536104995846	0.41837006597684244
{'YJR009C':0,'YGL125W':32,'YLR153C':32,'YLR231C':0,'YKL152C':2,'YOL058W':8,'YKL141W':0,'YER023W':8}	0.0389233242983237	0.9286269576443388	0.9613965643753114	0.41115959295170934
{'YAL038W':2,'YGL125W':32,'YKL141W':0.5,'YKR097W':0,'YER023W':2,'YDR158W':0.5}	0.0384620617928992	0.7226459540868049	0.9606212579560665	0.4581418581129086
{'YAL038W':2,'YGL125W':32,'YKL141W':0.03125,'YKR097W':0,'YOR025W':0,'YIL125W':0,'YDR158W':2,'YPL097W':0.0625}	0.0382917780507323	0.9299478492157792	0.96042405445895	0.4040906988127531 7
{'YNR019W':0,'YAL038W':2,'YGL125W':32,'YER060W-A':0,'YKR097W':0,'YOR025W':0,'YIL125W':0,'YKL141W':0}	0.0380213691271476	0.9304369102033122	0.9589189848168119	0.4010682503979370 3
{'YAL038W':2,'YGL125W':32,'YLR231C':0.125,'YKL141W':0.5,'YKR097W':0,'YOR025W':0,'YEL027W':0.5}	0.0368871934546291	0.9317741503520652	0.9575510351011006	0.3884208960236248 4
{'YDR297W':0.125,'YGL125W':32,'YLR153C':32,'YLR044C':2,'YKL085W':0.125,'YKL152C':2,'YLR092W':32,'YKL141W':0}	0.0357322595970499	0.9359782825286084	0.9574371267908249	0.3755277774879639
{'YGL125W':32,'YLR153C':32,'YLR231C':0,'YKL152C':2,'YDR297W':16,'YLR092W':32,'YKL141W':0,'YLR044C':32}	0.0368776691753256	0.9317934869443001	0.9574371267908249	0.3883148093026937
{'YCR005C':32,'YGL125W':32,'YLR153C':32,'YKL152C':2,'YDR297W':16,'YLR092W':32,'YKL141W':0.25}	0.03565571887444	0.9361257663253388	0.9573327690016286	0.3746790979524868 3
{'YCR005C':32,'YGL125W':32,'YLR153C':32,'YLR044C':2,'YKL152C':2,'YDR297W':16,'YLR092W':32,'YKL141W':0.25}	0.0350464986376708	0.9373647677098504	0.9554966161119793	0.3679321998036735 3
{'YAL038W':2,'YGL125W':32,'YER060WA':0,'YKL152C':2,'YOL058W':16,'YBR265W':0.5,'YKL141W':0,'YGR124W':8}	0.0347640358217108	0.9394962362016004	0.9554823374679963	0.3648086953699995
{'YGL125W':32,'YLR153C':32,'YKL152C':2,'YLR231C':0,'YIL125W':0,'YOL058W':8,'YKL141W':0}	0.0329877043991351	0.9409508402154616	0.9528951714010075	0.3452311995925587 7
{'YJR009C':0,'YGL125W':32,'YLR153C':32,'YLR044C':2,'YBR265W':0.5,'YKL152C':2,'YKL141W':0.03125,'YOL058W':8}	0.0329778683035886	0.9409596932636766	0.9524824002900976	0.3451231508299188
{'YLR081W':0,'YGL125W':32,'YLR153C':32,'YKL152C':2,'YKL141W':0.25,'YIL125W':0,'YKL085W':0.0625,'YBR265W':0.5}	0.0317054889523426	0.9411672431004758	0.9515907976997321	0.3312286908250044 5
{'YGL125W':32,'YLR153C':32,'YLR044C':2,'YLR231C':0,'YKR097W':0,'YKL152C':2,'YDR158W':2,'YKL141W':0}	0.0316389270937166	0.9432358546717466	0.9514786446991185	0.3304389988901093
{'YGL125W':32,'YLR153C':32,'YER060W:0,'YKL152C':2,'YKR097W':0,'YIL125W':0,'YKL141W':0,'YLR044C':32}	0.0316389270937152	0.9432358546716747	0.9497888384448018	0.3304389988901098

Appendix 4: *Continuation*

{'YNR019W':0,'YGL125W':32,'YLR153C':32,'YKL152C':2,'YOR025W':0,'YKL141W':0.25,'YIL125W':0}	0.03156015415104	0.9433868001704	0.9497748190846	0.32957703664814
{'YLR081W':0,'YGL125W':32,'YKL152C':2,'YLR231C':0,'YOR025W':0,'YIL125W':0,'YOL058W':8,'YKL141W':0}	0.03061260759089 4	0.94739710462573 8	0.94810347120406 55	0.319225544285592 85
{'YLR081W':0,'YJR009C':0,'YGL125W':32,'YLR044C':2,'YBR265W':0.5,'YKL152C':2,'YKL141W':0.03125,'YOL05 8W':8}	0.02956104279254 31	0.94322793194111 17	0.94770405464604 8	0.307836443701877
{'YLR081W':0,'YGL125W':32,'YER060WA':0,'YKL152C':2,'YKL085W':0.0625,'YBR265W':0.5,'YKL141W':0,'YGR1 24W':8}	0.02942376666442 5	0.94350888889644 22	0.94676990028558 46	0.306344173576136 5
{'YLR081W':0,'YJR009C':0,'YGL125W':32,'YKL152C':2,'YKL141W':0.03125,'YKL085W':0.0625,'YDR158W':2,'YB R265W':0.5}	0.02888344998760 54	0.94467606735145 1	0.94581703627531 24	0.300477306990856 06
{'YNR019W':0,'YLR081W':0,'YGL125W':32,'YLR153C':32,'YER060W- A':0,'YOR025W':0,'YIL125W':0,'YKL141W':0}	0.02849467832461 67	0.94553049878444 72	0.94580765130032 73	0.296262050658860 9
{'YGL125W':32,'YER060W-A':0,'YKL152C':2,'YOR025W':0,'YKL085W':0.0625,'YKL141W':0}	0.02806272659511 76	0.95024989758220 48	0.94559366833209 07	0.291520915027880 9
{'YNR019W':0,'YLR081W':0,'YGL125W':32,'YER060W-A':0,'YKL152C':2,'YIL125W':0,'YKL141W':0}	0.02671544493905 15	0.94874113452602 84	0.94555629414096 52	0.277032303600248 2
{'YGL125W':32,'YLR044C':2,'YMR202W':2,'YNR019W':2,'YKL141W':0.03125,'YKL152C':2,'YDR268W':0.125,'YB R265W':0.5}	0.02649517696725 34	0.95054389540489 5	0.94448618026554 92	0.274605196515597 9
{'YBR023C':0.03125,'YJR009C':0,'YGL125W':32,'YLR231C':0.125,'YKL141W':0.5,'YLR044C':2,'YKL152C':2,'YE L027W':0.5}	0.02614395084102 7	0.95423559943977 92	0.94297409317392 87	0.270824547606163 7
{'YGL125W':32,'YLR153C':32,'YLR231C':0,'YIL125W':0,'YKL085W':0.0625,'YOL058W':8,'YKL141W':0,'YLR044C ':32}	0.02497331358812 98	0.95641570900652 04	0.94212787732751 73	0.258253062592443 35
{'YGL125W':32,'YLR153C':32,'YHR002W':32,'YKL141W':0.03125,'YOR025W':0,'YKL085W':0.0625,'YLR044C':3 2}	0.02459002203832 94	0.95484938751880 34	0.94210425891127 16	0.254143587975960 37
{'YJR009C':0.03125,'YNR019W':0,'YGL125W':32,'YLR153C':32,'YLR044C':32,'YBR265W':0.5,'YKL141W':0,'YGR 124W':8}	0.02361256973781 1	0.95675347672924 88	0.94160267242342 8	0.243687557406398 14
{'YGL125W':32,'YER060W-A':0,'YLR231C':0,'YKR097W':0,'YOR025W':0,'YIL125W':0,'YDR158W':2,'YKL141W':0}	0.02259114314040 85	0.95873492800100 72	0.94154075058450 99	0.232799681330898 12
{'YNR019W':0,'YLR081W':0,'YJR009C':0,'YGL125W':32,'YER060W-A':0,'YOR025W':0,'YDR158W':2,'YKL141W':0}	0.02132128749440 36	0.95987772122472 44	0.94121083149418 29	0.219373161056743 82
{'YNR019W':0,'YLR081W':0,'YJR009C':0,'YGL125W':32,'YOR025W':0,'YIL125W':0,'YKL085W':0.0625,'YKL141W' :0}	0.02132128739432 55	0.95987772136359 36	0.94003104731825 98	0.219373161056743 82
{'YNR019W':0,'YLR081W':0,'YJR009C':0,'YGL125W':32,'YER060W-A':0,'YOR025W':0,'YIL125W':0,'YKL141W':0}	0.02037995040280 63	0.96176758196108 68	0.94003000182845 02	0.209406189006053 5
{'YNR019W':0,'YBR038W':0,'YLR081W':0,'YGL125W':32,'YKR097W':0,'YOR025W':0,'YIL125W':0,'YKL141W':0}	0.01861863080091 67	0.96585664414579 12	0.93995245334072 09	0.190785041187572 45

Appendix 4: *Continuation*

{'YNR019W':0,'YLR081W':0,'YJR009C':0,'YGL125W':32,'YER060W-A':0,'YOR025W':0,'YIL125W':0}	0.0197211649137888	0.963695880811701	0.9399524533407209	0.20240111798083746
{'YJR009C':0,'YGL125W':32,'YLR153C':32,'YLR231C':0,'YKL085W':0.0625,'YKL141W':0,'YLR044C':32}	0.0179888848031715	0.9663214865229386	0.9385356004632688	0.18421275673123974
{'YGL125W':32,'YLR153C':32,'YMR202W':2,'YKL141W':0.03125,'YLR231C':0,'YIL125W':0,'YKL085W':0.0625,'YLR044C':32}	0.0183741553333112	0.9692441279480576	0.9385356004632688	0.18826543502237217
{'YLR153C':4,'YOL058W':4,'YGL125W':32,'YMR202W':2,'YNR019W':2,'YKL141W':0.03125,'YLR231C':0,'YLR044C':32}	0.0173789097944988	0.9703640793962152	0.9385356004632687	0.17775977282683228
{'YDL093W':0,'YOL058W':4,'YGL125W':32,'YLR153C':0.125,'YKL120W':0.0625,'YKL141W':0.125,'YEL027W':0.5,'YLR044C':32}	0.0154064709090241	0.9719176178456308	0.9385356004632681	0.15692926614599578
{'YJR009C':0.03125,'YNR019W':0,'YLR081W':0,'YGL125W':32,'YLR044C':32,'YBR265W':0.5,'YKL141W':0,'YGR124W':8}	0.016286189584818	0.9702012213026154	0.9385356004632681	0.16610901365033642
{'YNR019W':0,'YLR081W':0,'YJR009C':0,'YGL125W':32,'YOR025W':0,'YBR265W':0.5,'YKL141W':0,'YLR044C':32}	0.0135748613214053	0.9750825181329564	0.9364499657955726	0.13820926847203607
{'YNR019W':0,'YLR081W':0,'YJR009C':0,'YGL125W':32,'YOR025W':0,'YDL090C':16,'YKL141W':0,'YLR044C':32}	0.0144040005742666	0.9741234074011608	0.9364499657955726	0.14671371250770082
{'YLR081W':0,'YJR009C':0,'YGL125W':32,'YER060W-A':0,'YOR025W':0,'YKL141W':0.125,'YLR044C':32}	0.0149181667989839	0.9724537446125052	0.9364499657955726	0.15216193566900385
{'YLR081W':0,'YJR009C':0,'YGL125W':32,'YER060W-A':0,'YOR025W':0,'YKL141W':0.125,'YLR044C':32}	0.0134844440024424	0.9759757062896536	0.9364499657955724	0.13693693921015132
{'YNR019W':32,'YAL038W':2,'YBR265W':0.5,'YGL125W':32,'YLR231C':0,'YOR025W':0,'YLR044C':8,'YER023W':0.5}	0.0117496727905446	0.9792647382066636	0.9364499657955722	0.11904451347773097
{'YNR019W':32,'YAL038W':2,'YBR265W':0.5,'YGL125W':32,'YLR231C':0,'YOR025W':0,'YLR044C':8,'YER023W':0.5}	0.0124533694333648	0.9778448747185208	0.9364499657955722	0.12654845464716 14
{'YNR019W':0,'YLR081W':0,'YJR009C':0,'YGL125W':32,'YER060WA':0,'YLR044C':16,'YER023W':0.5,'YKL141W':0}	0.0125255304961168	0.9773934870349932	0.9364499657955722	0.12707491252740 07
{'YLR081W':0,'YBR265W':0.5,'YGL125W':32,'YER060WA':0,'YLR044C':16,'YOR025W':0,'YER023W':0.5,'YKL141W':0}	0.0115563086546961	0.9792785247180182	0.9364499657955722	0.11702639933548079
{'YNR019W':0,'YAL038W':2,'YLR081W':0,'YGL125W':32,'YER060W':0,'YOR025W':0,'YLR044C':8,'YER023W':0.5}	0.0105144261353593	0.9810615287182513	0.9319061521964535	0.10657157333995466
{'YNR019W':0,'YLR081W':0,'YJR009C':0,'YGL125W':32,'YER060W:0,'YOR025W':0,'YER023W':0.5,'YKL141W':0}	0.0108075483202189	0.9810602904156014	0.9319061521964535	0.10929644559711633
{'YNR019W':0,'YLR081W':0,'YJR009C':0,'YGL125W':32,'YER060W-A':0,'YER023W':0.5,'YKL141W':0}	0.0101406910238044	0.9818926840149154	0.9290434319826707	0.10273253816120347

Appendix 4: *Continuation*

{'YNR019W':32,'YGL125W':32,'YLR044C':2,'YMR202W':2,'YKL141W':0.03125,'YIL125W':0,'YDR158W':2,'YBR265W':0.5}	0.010494076490769	0.9811009674884226	0.9290434319826707	0.10636243641449272
{'YNR019W':32,'YGL125W':32,'YLR044C':2,'YMR202W':2,'YKL141W':0.03125,'YIL125W':0,'YDR158W':2,'YBR265W':0.5}	0.010140688526439 1	0.9818926873696264	0.8394944595214344	0.10273253816120347
{'YLR081W':0,'YJR009C':0,'YGL125W':32,'YLR231C':0,'YKL085W':0.0625,'YDR158W':2,'YBR265W':0.5,'YKL141W':0}	0.009787766712165 2	0.9826666930254372	0.8348885730777442	0.09888458544771371
{'YGL125W':32,'YLR044C':2,'YLR231C':0,'YOR025W':0,'YIL125W':0,'YDR158W':2,'YBR265W':0.5,'YKL141W':0}	0.009725764813879 5	0.9828668184474766	0.8348885720788118	0.09820177375710151
{'YNR019W':0,'YLR081W':0,'YJR009C':0,'YGL125W':32,'YOR025W':0,'YLR044C':8,'YBR265W':0.5,'YKL141W':0}	0.009684735520596 9	0.9829447774247227	0.8342767013430179	0.09778104777930866
{'YNR019W':0,'YLR153C':4,'YLR231C':32,'YJR009C':0,'YGL125W':32,'YOR025W':0,'YBR265W':0.5,'YKL141W':0}	0.009460706118045 4	0.9805303380021526	0.8342202323849963	0.09574773295177848
{'YJR009C':0.03125,'YNR019W':0,'YLR153C':4,'YGL125W':32,'YLR231C':0,'YOR025W':0,'YBR265W':0.5,'YKL141W':0}	0.009540663733173 52	0.9831973713650 44	0.8342202323849963	0.09630489730062124
{'YNR019W':0,'YLR081W':0,'YGL125W':32,'YLR231C':0,'YKR097W':0,'YOR025W':0,'YBR265W':0.5,'YKL141W':0}	0.009455528489677 2	0.9805418499335176	0.8342202323849951	0.09569489433826489
{'YNR019W':0,'YLR153C':4,'YLR081W':0,'YGL125W':32,'YLR231C':0,'YOR025W':0,'YBR265W':0.5,'YKL141W':0}	-0.0	0.0216457882541274	0.0	0.6560109941244389
{'YNR019W':0,'YLR081W':0,'YJR009C':0,'YGL125W':32,'YOR025W':0,'YKL085W':0.0625,'YBR265W':0.5,'YKL141W':0}	-0.0	0.5386681365490052	0.0	0.11836746127673949
Frequency of the individual solutions: **YGL125W: 32 (93 times) - MET13**; YDR158W: 16 (39 times), 0.5 (25 times), 2 (6 times); YLR153C: 32 (55 times), 4 (1 time), 0.125 (4 times); YOL058W: 8 (29 times), 16 (8 times), 4 (3 times); YAL038W: 2 (38 times); YER023W: 2 (23 times), 4 (6 times); YLR044C: 32 (33 times), 2 (5 times); YKR097W: 0 (21 times); YKL141W: 0.03125 (11 times), 0 (17 times), 0.0625 (4 times), 0.125 (5 times), 0.5 (5 times), 0.25 (1 time); YHR002W: 32 (10 times); YMR208W: 0.5 (5 times); YKL085W: 0.0625 (8 times), 0.125 (7 times); YOR025W: 0 (16 times); YER060W-A: 0 (18 times); YJR009C: 0.03125 (6 times); YLR081W: 0 (10 times); YKL152C: 2 (13 times); YIL125W: 0 (3 times); YLR231C: 0.125 (3 times), 32 (2 times); YGR124W: 8 (9 times), 16 (8 times); YBR265W: 0.5 (21 times); YEL027W: 0.5 (4 times);YMR217W: 32 (2 times) YDR297W: 0.125 (2 times), 16 (2 times); YMR202W: 2 (3 times); YCR005C: 32 (3 times)				